12-2020

Hydraulic Analysis of Coupling a Labyrinth Weir with a Steep Stepped Chute

Tucker J. Jorgensen
Utah State University

HYDRAULIC ANALYSIS OF COUPLING A LABYRINTH WEIR WITH A STEEP STEPPED CHUTE

by

Tucker J. Jorgensen

A thesis submitted in partial fulfillment
of the requirements for the degree

of

MASTER OF SCIENCE

in

Civil and Environmental Engineering

Approved:

Blake P. Tullis, Ph.D.
Major Professor

Brian M. Crookston, Ph.D., P.E.
Committee Member

Austin Ball, M.S., S.E.
Committee Member

D. Richard Cutler, Ph.D.
Interim Vice Provost for Graduate Studies

UTAH STATE UNIVERSITY
Logan, Utah

2020

ABSTRACT

Hydraulic Analysis of Coupling a Labyrinth Weir with a Steep Stepped Chute

by

Tucker J. Jorgensen, Master of Science

Utah State University, 2020

Major Professor: Dr. Blake P. Tullis
Department: Civil and Environmental Engineering

There are many considerations involved in the design of a dam structure. A few of these include minimizing upstream flooding (and risk of embankment overtopping), economical construction, and downstream erosion. Addressing these concerns has, in part, led to a recent increase in the use of more efficient and economical hydraulic structures (e.g. nonlinear weirs, stepped chutes, etc.). Complex hydraulic structures such as nonlinear weirs and stepped chutes require extensive study to establish design methods. These design methods are typically dependent upon the geometry and flow conditions modeled. Combining two complex structures can result in dramatic changes in either geometry or flow characteristics. This is particularly true in the case of combing a nonlinear weir (labyrinth or piano key weirs) with a stepped chute. Flow from the labyrinth weir is typically turbulent and three-dimensional, which deviates significantly from the relatively uniform flow assumed in current design methods. A potential issue with this deviation is an underprediction in the flow depth experienced on the stepped

chute. This study was undertaken with the hope of understanding the flow conditions experienced by coupling a labyrinth weir with a stepped chute. A labyrinth weir with sidewall angle (α) of 10.67° was installed upstream of a relatively steep stepped chute [slope angle (ϕ) of 51.37°]. Preliminary testing found that the flow depths experienced on the stepped chute were significantly greater than expected, even at low flows. To help decrease the maximum flow depth on the stepped chute, sloping ramped floors were installed into the downstream cycle of the labyrinth weir. Various ramp configurations were tested to understand the impacts to both the labyrinth weir efficiency and the flow depth of the stepped chute. It was observed that increasing the ramp heights (p) resulted in both a reduction in the weir efficiency and the stepped chute flow depth. In particular, as the p approaches the height of the weir (P), the upstream water surface elevation was also raised for a given flow rate. The flow conditions on the stepped chute were highly variable, potentially due to the labyrinth weir. While the ramped floors did not directly decrease the overall variability, they did lower the maximum depth by ~13-15% depending on p.

(227 pages)

PUBLIC ABSTRACT

Hydraulic Analysis of Coupling a Labyrinth

Weir with a Steep Stepped Chute

Tucker J. Jorgensen

There are many considerations involved in the design of a dam structure. A few of these include minimizing upstream flooding (and risk of embankment overtopping), economical construction, and downstream erosion. Addressing these concerns has, in part, led to a recent increase in the use of more efficient and economical hydraulic. Complex hydraulic structures such as labyrinth weirs and stepped chutes require extensive study to establish design methods. Combining two complex structures can result in dramatic changes in flow characteristics. This is particularly true in the case of combining a labyrinth weir with a stepped chute. Flow from the labyrinth weir deviates significantly from the relatively uniform flow assumed in current design methods. A potential issue with this deviation is an underprediction in the flow depth experienced on the stepped chute. This study was undertaken with the hope of understanding the flow conditions experienced by coupling a labyrinth weir with a stepped chute. A labyrinth weir was installed upstream of a relatively steep stepped chute. Preliminary testing found that the flow depths experienced on the stepped chute were significantly greater than expected, even at low flows. To help decrease the maximum flow depth on the stepped chute, sloping ramped floors were installed into the downstream cycle of the labyrinth weir. It was observed that increasing the ramp heights (p) resulted in both a reduction in the weir efficiency and the stepped chute flow depth by ~13-15% depending on p.

ACKNOWLEDGMENTS

Even at a young age I had the desire to become a civil engineer. The support of others over the years has been crucial in my ability to reach this goal. Of paramount help has been the willingness of countless educators to accept my desire to move at my own pace. This led me to trust in my abilities to understand the complex and advanced subjects I would then tackle in later schooling. The guidance of my parents led me to recognize the opportunities to become a properly trained civil engineer by attending Utah State University (USU).

While at USU, I was still undecided upon the final subject to be studied with the discipline of civil engineering. Entering my Junior year this had not changed, until I took a course in Fluid Mechanics taught by Dr. Blake Tullis. Dr. Tullis' passion for the subject and the course brought out my desire to study the topic of hydraulics. His later willingness to hire me as an undergraduate research assistant has only increased my desire to better understand and design hydraulic systems and structures.

Working at the Utah Water Research Laboratory (UWRL) gave me the hands-on experience I needed. I would like to thank the many pioneers and innovators the preceded my work at the UWRL on labyrinth weirs and hydraulic structures. Especially the work of Dr. Blake Tullis and Dr. Brian Crookston. Their combined work laid a foundation for my own research work. In addition, I would also like to thank Dr. Zac Sharp for allowing me to come into the lab early and conduct my research. I would also like to thank Kade Flake and Taylor Vaughn. They often woke early or stayed late in an effort to increase the understandings of my research.

Most importantly, I would like to thank my dear wife, Eliza; our baby boy, KJ;

and God. Eliza put up with all of my extremely early mornings to go into work and perform research. Her unwavering support gave me the strength to push through challenging times. Welcoming KJ into life has only increased my desire to become a civil engineer. He gives me a greater desire to make the world an even better place for him to grow into. In closing I would like to thank God for the talents and skill necessary to overcome the challenges of this recent adventure I have accomplished.

- Tucker Jorgensen

CONTENTS

LIST OF TABLES

LIST OF FIGURES

NOMENCLATURE

A = inside apex width;

b = spillway width;

B = length of labyrinth weir (apron) in flow direction;

c_f = fluid friction factor;

C = weir discharge coefficient;

C_d = dimensionless discharge coefficient;

$C_{d(\alpha°)}$ = α dependent C_d;

$C_{d,B}$ = no ramp or baseline C_d;

$C_{d,R}$ = ramp C_d;

$C_{d\text{-}ramp}$ = dimensionless discharge coefficient with downstream ramp;

d_w = clear water depth;

D = outside apex width;

f = flow surging frequency;

g = acceleration constant of gravity;

h = depth of flow over weir crest, piezometric head;

h_s = vertical height of step;

h_c = critical flow depth;

h_i = flow depth at inception point;

H = total upstream head measured relative to the weir crest;

H/P = headwater ratio;

H_c = total upstream head measured relative to the stepped chute inlet;

H_{dam} = height of dam;

H_{max} = max design water elevation for stepped chute;

H_{res} = residual energy;

ΔH = change in head;

l_c = centerline length of weir sidewall;

L = total centerline length of labyrinth weir;

L_i = length of stepped chute to inception point;

L_s = length of chute step;

N = number of cycles;

p = ramp height;

P = weir height;

p/P = ramp height ratio;

PKW = Piano Key weir:

q = unit discharge;

Q = discharge over weir;

r = crest radius;

R = arc radius;

R^2 = correlation coefficient;

s = step height;

Tu = turbulence intensity;

t_w = weir thickness;

V = average cross-sectional velocity;

w = width of single labyrinth weir cycle;

W = width of channel;

w/P = cycle width ratio;

y_{90} = bulked flow depth;

α = sidewall angle;

β = approach flow angle;

ε = bulking coefficient;

θ = chute slope;

ϕ = spillway angle; and

ψ = ramp angle.

CHAPTER I

INTRODUCTION

As climate changes throughout the United States and the world, the way water is managed also changes. One major consideration is in the amount of flow that dams need to be able to pass through their outlets during flood events. For many dams, the design or required discharge capacities [probable maximum flood (PMF), 1,000-yr, or 100-yr, etc.] have increased over recent years. As the flood discharge requirement increases, so must the spillway capacity to avoid possible dam failure as a result of dam overtopping. Nonlinear weirs (including labyrinth weirs) are commonly used to increase spillway discharge capacity. As the discharge capacity increases, so does the need for energy dissipation. Stepped spillway chutes are often used to increase energy dissipation upstream of the stilling basin. This study evaluates the flow depth and propagation of variable flow depth when a stepped chute is preceded by a labyrinth weir crest.

A Labyrinth weir is used specifically to meet the need of increasing the discharge of a dam spillway. By replacing a linear weir system with a labyrinth weir, the discharge of the dam can be increased for the same upstream water elevation (increased hydraulic efficiency). This feature of labyrinth weirs is crucial in not only meeting flood flow discharge requirements, but also avoiding a need to increase the dam crest height (and thereby increasing reservoir storage for flood routing).

A stepped spillway chute does not necessarily increase the discharge of a dam, but it can be both economical and helpful in protecting the toe of a dam. For dams built using the modern construction technique of Roller Compacted Concrete (RCC) it is often cheaper to build a steep spillway chute using steps rather than a curved spillway invert.

While the economics of a stepped spillway chute are important, they also have allowed for an increase in energy dissipation upstream of the energy dissipation basin. In addition to allowing for a smaller energy dissipation basin, the operation of the energy dissipation basin will require less depth to dissipate the residual energy, making it less sensitive to tailwater elevation.

For cases where the benefits of labyrinth weirs and stepped chutes are to be combined in a spillway design, it's important to develop a better understanding of the effects of one on the other, specifically the labyrinth weir discharge pattern on the stepped chute hydraulics. It is important to be able to predict the depth of the water more accurately as it transitions from the horizontal weir apron to the steep spillway chute.

While much work has been done previously on understanding the hydraulics of each of these structures individually, no information was found in the literature describing the combined effects of these structures. This gap in knowledge leads to an increase in uncertainty when working on dam designs. This uncertainty can lead to overly conservative and more costly dam spillway structures. To provide a better understanding of the hydraulics related to labyrinth weir/stepped chute spillways, the following research objectives will be evaluated.

Research Objectives

The main objectives of this thesis are to:

- Examine the flow regime and conditions on a steep stepped spillway chute immediately downstream from a labyrinth weir. The depth of the water column at various points along the length of the chute is to be quantified from physical testing, including a discussion on the observed hydraulic

conditions throughout the combined system.

- Investigate the impact of placing sloping ramps of various heights in the downstream cycles with respect to the head-discharge relationship and downstream wave formation/splash heights.
- Evaluate the water surface profile fluctuations in the stepped chute as a function of upstream cycle ramp geometries with the goal being to minimize the chute wall heights to the greatest extent possible.

CHAPTER II

LITERATURE REVIEW

To optimize the economics of dam design, two structures commonly used are labyrinth weirs and stepped chutes. The labyrinth weir is used to increase discharge capacity relative to a linear weir design. Labyrinth weirs are particularly useful when the width of a spillway is limited. Stepped chutes can be more economical to construct then other types of steep chutes, particularly when using roller compacted concrete (RCC). In addition to the preferred economics of the construction, stepped chutes also increase energy dissipation. This is particularly needed since the increased discharge increases the kinetic energy of the water at the base of the spillway chute. Dissipating some of this energy can minimize the size and costs of the energy dissipation basin at the downstream end of the chute.

The purpose of this literature review is to discuss the previous research on both labyrinth weirs and stepped chutes. This includes a discussion on the current design practices of both types of structures as well as the governing equations used in their design. In addition, this literature review will discuss the challenges of using existing literature in combining a labyrinth weir with a steep stepped spillway by identifying the flow conditions created and required by the two structures, respectively.

Labyrinth Weirs

To help predict the head-discharge for labyrinth weir design, Hay and Taylor (1970) created discharge rating curves that were related to linear weirs. This method required discharge information from a linear weir of the same weir height (P), wall thickness (t_w), and crest shape. Using the information provided by Hay and Taylor

(1970), the Bureau of Reclamation (USBR) conducted a model study and found discrepancies between their results (Houston 1982) and the design recommendations from Hay and Taylor (1970). In part, the discrepancies were attributed to limited geometric data from Hay and Taylor. Additional research by Hinchliff and Lux (1985) and Lux (1989)further develop empirical equations for estimating head-discharge relationships using cycle width ratio of *w/P*.

Adding additional weir parameters into the weir equation only further complicates the design process. In addition, this leads to greater limitations on the applications of the equations based upon the experimental data. To help address this issue, Tullis et al. (1995) adopted the standard weir head-discharge relationship and applied it to labyrinth weirs, Equation. [1].

$$Q = \frac{2}{3} C_d L \sqrt{2g} H^{3/2} \qquad [1]$$

where C_d is the dimensionless discharge coefficient, L is the total weir length, g is the acceleration due to gravity, and H is the total upstream head. H is defined as $V^2/2g + h$ (V is the average cross-sectional velocity and h is piezometric head upstream of the weir measured relative to the weir crest elevation). The value of C_d is a complex relationship to many weir geometries including the side wall angle (α), weir thickness (t_w), weir crest height (P), and crest shape in addition to the approach flow conditions (Crookston and Tullis 2012a) As a result of this complexity, the C_d values for a labyrinth weir are often based on laboratory scale model data.

Crookston and Tullis (2013) established design equations for C_d based upon α and H/P using data collected by Crookston (2010). These design equations, combined with the design method proposed by Crookston and Tullis (2013) allow for greater confidence

in designing for labyrinth weirs. Crookston (2010) tested and Crookston and Tullis (2013) created design C_d equations for labyrinth weirs with α = 6°, 8°, 10°, 12°, 15°, 20° and 35° using both quarter-round (QR) and half-round (HR) crest shapes. Using the appropriate parameters for these equations creates a series of design curves related to the ratio of *H/P* (see **Figure. 1** and **Figure. 2**).

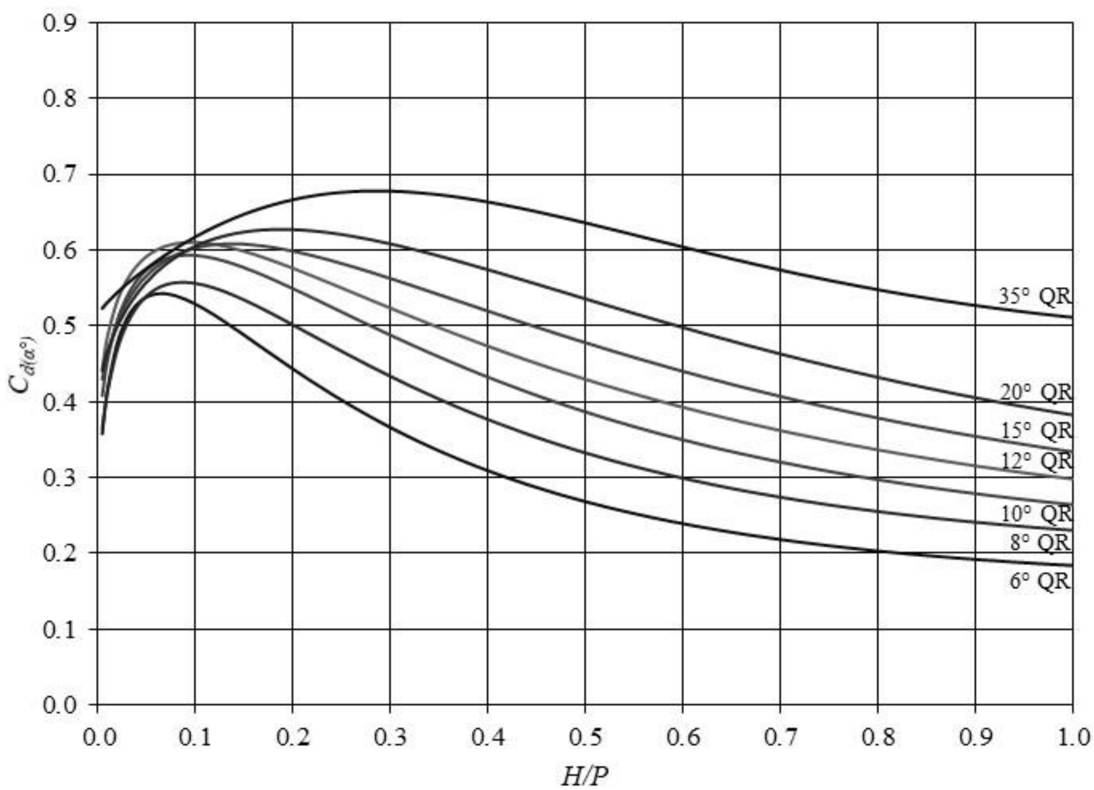

Figure. 1. Values of C_d versus *H/P* for quarter-round trapezoidal labyrinth weirs [from Crookston and Tullis (2013)]

There are two predominant trends between these sets of equations. First, the HR crest shape has a greater value for C_d for low heads compared to the QR crest shape. Crookston and Tullis (2013a and b) identified that the HR crest shape is more efficient at

lower heads due to the clinging nappe condition being maintained on the downstream side of the crest. Second, as the value of α is decreased so is the C_d value for the head-discharge relationship. This decrease in C_d value is offset by the increase in the crest length when decreasing the value of α for a given channel width (Crookston and Tullis 2013a).

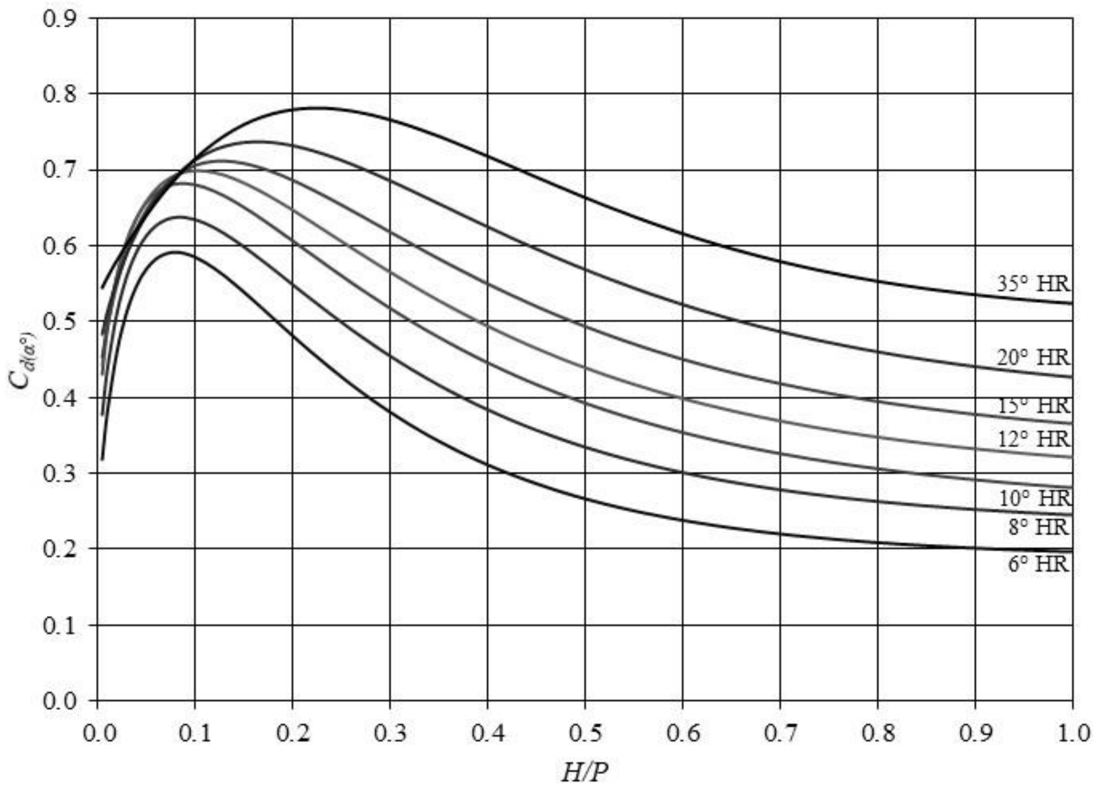

Figure. 2. Values of C_d versus *H/P* for half-rounded trapezoidal labyrinth weirs [from Crookston and Tullis (2013)].

While these design equations are very useful, they have their limitations. As discussed earlier, the value of C_d is dependent upon more parameters than just α, crest shape, and *H/P*. As additional geometric properties of the labyrinth weir are varied,

changes to the approximation of C_d can be required. Dabling et al. (2013), Seamons (2014), and Dabling and Tullis (2018) are a few examples of research done on varying labyrinth weir geometry and approach conditions. Dabling et al. (2013) noted that creating sections of the weir with varying crest heights (i.e., staged labyrinth weir) required additional variation to the flow prediction value beyond treating the separate sections as unique weirs. Seamons (2014) found that varying the cycle widths (w), Apex widths (A), and P can cause differences in the predicted vs observed C_d. Dabling and Tullis (2018) found that the approach flow conditions, or approach angle (β), begin to have an impact on the weir efficiency approach flow angles > 15°

Crookston et al. (2019) identified various construction reasons for why changes in a labyrinth weir geometry are made. Crookston et al. (2019) observed that the structural design of labyrinth weirs can result in changes to support the forces from the water experienced on the weir walls. Having already recognized the need for structural support within labyrinth weirs, San Mauro et al. (2016) installed various polyhedral bottoms (or ramps) into both the upstream and downstream cycles of labyrinth weirs. San Mauro et al. (2016) found that the installation of the ramps into the labyrinth weir decreased the weirs ability to discharge water. The studies done by San Mauro et al. (2016) only used a single maximum height for their polyhedral bottoms. As a result, little is known on the impacts to discharge by varying the height of the ramps. However, the work by San Mauro et al. (2016) as well as that by Dabling et al. (2013), Seamons (2014), and Dabling and Tullis (2018) confirm the discussion of Crookston et al. (2019) that the construction and design variations of labyrinth weirs can impact the head-discharge relationships previously established by Crookston and Tullis (2013a).

With the increase in the understanding of the head-discharge relationships for an increase in variation of geometries, labyrinth weirs are increasing in use (Crookston et al. 2019). This increase is particularly useful in addressing increased design floods for both existing and new dam construction. As labyrinth weirs are used, it is important to better understand how the flow conditions from the labyrinth weir might impact any downstream structures. Much of the research of labyrinth weir flow conditions focuses on how it can impact the head-discharge relationships and nappe conditions. Melo et al. (2002), Tullis et al. (2007), Crookston (2010), Crookston and Tullis (2013b), and San Mauro et al. (2016) are a few examples of this investigation.

Melo et al. (2002) created relationships based on converging the channel side walls. This relationship shows and impact on the convergence to the labyrinth weirs efficiency. Melo et al. (2002) did not work to describe the impact of labyrinth weirs on the flow within the converging channel. Tullis et al. (2007) explored the relationship between labyrinth weir discharge and downstream submergence. This research focused on whether dimensionless weir coefficient developed for linear weirs by Villemonte (1947) could be used in predicting submerged labyrinth weir discharge. Again, the discussion continued to focus on the labyrinth weir head-discharge relationship.

Regarding the flow conditions established by a labyrinth weir, much focus has been given to the nappe conditions. Crookston (2010) identified four different nappe conditions for labyrinth weirs; clinging, aerated, partially aerated, and drowned. This information lead to a greater understanding of the influence form the weir crest shape. Crookston (2010) found that when the napped condition is clinging, the weir has a higher relative value of C_d for a given value of H/P. As a result, Crookston and Tullis (2013a)

created the design equations for both QR and HR crest shapes, where HR has a higher value of C_d for low heads while the nappe is still experiencing a clinging condition. Once the nappe no longer clings to the weir side wall, Crookston (2010) found that there is no difference in the value for C_d.

San Mauro et al. (2016) found that when installing ramps or polyhedral bottoms into a labyrinth weir, the flow characteristics change in relation to the same labyrinth weir without any ramps. These changes include redistribution of the water velocity profile and a lowering of the downstream water surface. However, the changes of the flow characteristics where found to decrease the labyrinth weirs' discharge ability. San Mauro et al. (2016) also found structural advantages to using the installed ramps, such as a decrease in the hydrodynamic load on the labyrinth weir wall and an increase in structural stability (seen as a decrease in deflection). By increasing the stability of the structure and decreasing the load can potentially decrease the cost of construction labyrinth weirs.

Quantifying and understanding the change in a labyrinth weirs discharge efficiency is an important aspect of design for a PMF or similar design flood flow. Research has recognized the need to adjust established design values and relationship of C_d and H/P for changes in the design weir geometry. This study will investigate the relationship between the height of installed weir ramps and the changes to the value of C_d compared to a traditional flat bottom weir.

Stepped Spillway Chutes

Stepped spillway chutes have been used for an extremely long time. Schnitter (1994) compiled a list of some historical examples of using stepped spillway chutes or

stepped slopes in dam constructions. The earliest example mentioned by Schnitter (1994) is a dam in Iraq built around 700 BC. The use and interest in stepped spillway chutes has only increased in the last century (Chanson 1994 and Ruff and Ward 2002). This is in part attributed to the development of the construction technique called roller compacted concrete (RCC). RCC is not only a more popular construction method (Ruff and Ward 2002), but it also lends to a more economic dam design (Boes and Hager 2003). RCC is a construction technique that builds the dam face in lift of concrete, compacted using rollers. Each lift is then brought in at a design slope, creating the appearance of a large staircase up the side of the dam face. A layer of structural concrete is often placed onto of the RCC stepped chute surfaces for improved durability.

Stepped chute advantages aren't solely limited to construction economics compared to a traditional smooth chute; stepped spillway chutes also dissipate larger amounts of energy as water flows over the steps. Rajaratnma (1990) used a relationship called of the fluid friction factor, c_f, to estimate the energy dissipation along a stepped chute based on research done by Sorensen (1985). Rajaratnma (1990) used c_f to calculate the depth and velocity (allowing for energy calculations) at the toe of a spillway. Christodoulou (1993) continued the research of both Sorensen (1985) and Rajaratnma (1990). Christodoulou (1993) established that the number of steps in a stepped chute directly impacts the quantity of energy dissipated. As the number of steps decrease, so does the relative energy dissipation of the stepped chute. Chanson (1994) compiled much of the previous energy dissipation into one reference. By doing so, Chanson (1994) was able to establish guidelines based upon the various major geometric properties of a stepped spillway.

Increasing the relative energy dissipation by using stepped spillways has multiple benefits for dam economics as well as safety. Energy dissipation from stepped spillways has been found to decrease the water velocity at the toe of the spillway (Rice and Kadavy 1996). Increasing the energy dissipation along the spillway also allows for a decrease in the size of the stilling basin (Chanson 1994), this can increase the economic benefits already existing from using RCC in construction.

A major indicator on how energy dissipation happens is the flow regime of the water down the stepped spillway. Two major flow regimes are typically possible: nappe flow and skimming flow. Chanson (1994) describes nappe flow as a series of hydraulic jumps down single drop heights. The energy dissipation is then just the drop from one step to the next. Nappe flow typically only occurs when the unit discharge is low, the water depth is low, and the slope of the spillway is mild (Boes and Hager 2003 and Ruff and Ward 2002). Skimming flow is when the water acts as a single stream flowing over the steps of the spillway, resulting in a pseudo-bottom formed by the outermost edges of each of the steps (Rajaratnma 1990). This condition requires the contact of the stream of water with recirculating eddies within the steps to dissipate energy. Due to the crest heights and the high discharges related to design floods, dam stepped spillways typically experience skimming flow.

To expand the understanding of stepped spillway beyond just energy dissipation, Ruff and Ward (2002) built a near prototype scale model to be able calculate the energy dissipation along the spillway. In addition to establishing a relationship between relative energy dissipation and spillway station, Ruff and Ward (2002) created design charts that can be used in approximating the depth along a spillway for various geometric

relationships. In conjunction with these charts, Ruff and Ward (2002) created a series of steps with appropriate equations for calculating uniform depth or y_{90} for the spillway along with the energy dissipation. The steps from Ruff and Ward (2002) are limited in their geometric application. Ruff and Ward's (2002) physical data used stepped spillways with step heights of (s) 1.0 ft or 2.0 ft and spillway slope (ϕ) of 26.6°. Their specific steps involve:

Step1: Gathering the known design variables of Q, spillway width (b), ϕ, spillway height (H_{dam}), and s.

Step 2: Selecting an approximate friction factor (f) of ~0.25.

Step 3: Determining clear water depth (d_w) using a backwater computation (Ruff and Ward 2002 use an adaptation from Chow 1959).

Step 4: Determining the bulked flow depth (y_{90}) with ε = 1.75 designing for additional freeboard.

Step 5: Determining the energy dissipation along the spillway.

Ruff and Ward (2002) developed both a chart solution and an equation solution (see Eq. [2]) for y_{90}.

$$\varepsilon = \frac{y_{90}}{d_w} \qquad \text{Eq. [2]}$$

Where ε is the bulking coefficient found from chart solutions, y_{90} is the bulked flow depth, and d_w is the clear water depth. Due to empirical nature, the data from Ruff and Ward (2002) has limited application to only geometrically similar stepped spillways.

Independently, Boes and Hager (2003) also developed a series of equations and steps for stepped spillway design as well. This was done using model scale stepped spillways with a greater range in slopes (ϕ = 30, 40, and 50°). The 30° spillway slope was

tested using s = 23.1, 46.2, and 92.4 mm, the 40° spillway slope was tested only using s = 26.1 mm, and the 50° spillway slope was tested using s = 31.1 and 93.3 mm. The introduction of additional slope configurations greatly increases the complexities of the design process required. This process will not be covered here but can be seen in the research paper of Boes and Hager (2003). By increasing the variables tested, the applicability and complexity of the research increases. With an increase in complexity comes an increase in uncertainty and engineering judgment in designing for training wall heights (Ruff and Ward 2002). Despite this increase in complexity, the process outlined by Boes and Hager (2003) is relatively similar to that of Ruff and Ward (2002).

Both the work done by Ruff and Ward (2002) and Boes and Hager (2003) accounted for the training wall height, and by extension dam safety, based upon increasing the training wall height to a proportionate value of y_{90}. This proportionate value is often anywhere between 1.2 and 2.0 depending upon the erosion risk of the downstream face of the dam itself. This increase is to account for the splash that occurs during skimming flow not associated with the stream of water down the chute. To create maximum splash height and minimum training wall height guidelines, Hunt and Kadavy (2017) built a near prototype scale stepped spillway. Hunt and Kadavy (2017) found that to contain all the splash from the flow, the training wall heights could be as high as $5.5y_{90}$, which would be unrealistic and costly. Instead, Hunt and Kadavy (2017) suggested heights based upon the range of the ratio of step height to critical flow depth. The research done by Hunt and Kadavy (2017) however, is limited to spillway slopes of $10° \leq \phi \leq 30°$ but leads to an understanding that previous work on training wall height might not account for the entirety of flow at PMF or design flood flows. Hunt and

Kadavy (2017) give experimental data to justify the increase of training wall heights to a value greater than y_{90}.

The previous research done on stepped spillway chutes allows for a better understanding of the energy dissipation capabilities of stepped spillway chutes as well as the required training wall height for dam safety. The applicability of this research can be limited and impacted by the characteristics of the inflow water (Boes and Hager 2003). Chanson (2006) found that changing the inflow condition by changing the control structure greatly impacted skimming flow. The location and flow depth at the inception point changed greatly depending upon the type of structure in place. Simply stated, if the inflow conditions are changed, the ability to use previous research in designing wall height and energy dissipation is diminished. Chanson (2006) also summarized the use of control structures as almost exclusively ogee crest, broad-crested weirs, and pressurized intakes.

As stepped spillways are used to pass larger design floods, the opportunity of using a labyrinth weir as the control structure increases. With the minor changes of inflow conditions creating the large changes observed by Chanson (2006), it can be assumed that the drastically distinct flow conditions established by a labyrinth weir will even further change the required training wall heights for stepped spillways. This study aims to understand better the flow depths for stepped spillways when used in conjunction with a labyrinth weir. The design terminology and characteristics for this study will follow those outlined by Boes and Hager (2003) where their work is focused on steep spillways (see **Figure. 3**).

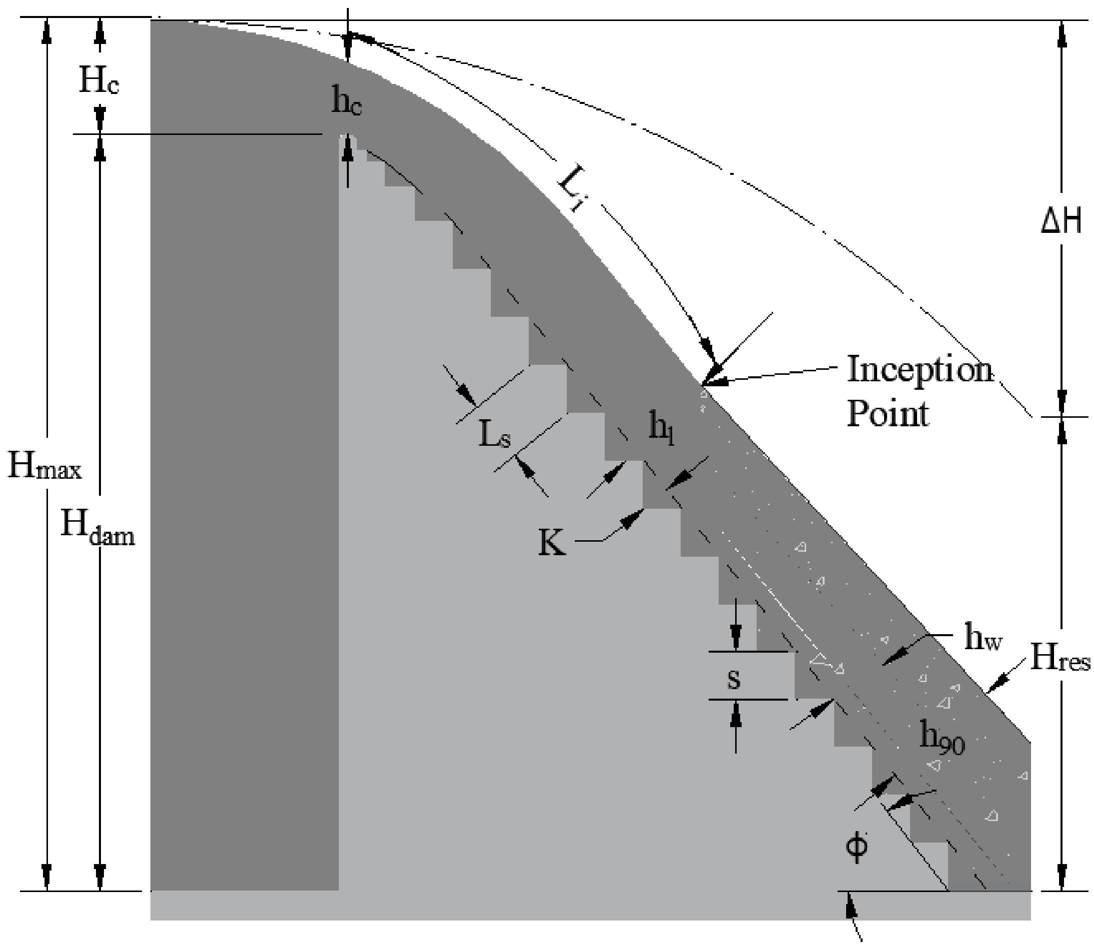

Figure. 3. Stepped chute terminology based on Boes and Hager (2003).

Combining Labyrinth Weirs with Stepped Spillway Chutes

Labyrinth weirs and stepped spillway chutes perform different functions when it comes to the safety of a dam. Due to their increased use and economical value, they have the potential for coupled use in further increasing the safety and economic benefits to dam constructions and rehabilitation. There are challenges in combining the two based upon their previous research. The flow conditions established by a labyrinth weir do not meet the requirements of the design for stepped chute, making traditional chute wall

height sizing methods non-applicable for this specific case. Further research is then needed to be able to confidently design training wall height when combining a labyrinth weir with a stepped chute.

This study will focus on using various ramp heights in the downstream cycle of the labyrinth weir to assist in transitioning the flow from the weir apron down the chute. The research will focus on two major aspects; first, the impacts of varying the ramp height relationship to the weir efficiency as calculated by relative changes in C_d and second, the changes in the water surface profile and the water surface depth using the various ramps heights.

CHAPTER III

EXPERIMENTAL SETUP

To generalize the results, a sectional spillway physical model was used, which included an upstream sloped approach, labyrinth weir and apron, steep stepped chute, and a downstream return channel. This section describes the testing facilities used, the weir materials and dimensions, the stepped spillway chute materials and dimensions, and the instrumentation used for both the labyrinth weir and stepped spillway chute data.

Testing Facilities

Physical modeling for this study was done at the Utah Water Research Laboratory (UWRL) at Utah State University in Logan, UT (https://uwrl.usu.edu/). A steel reinforced wooden headbox/reservoir (1.02 x 5.97 x 3.05 m) was constructed to represent a section of a gravity dam outlet structure (see **Figure. 4**). Included in the headbox is a sloped upstream approach ramp (0.8H:1V). Water was supplied by gravity from a reservoir adjacent to the laboratory via 60.96 cm (24-in) supply line pipe. The water is controlled using either a 30.48 cm (12-in) or 60.96 cm (24-in) butterfly valves installed in parallel supply lines of the same size. A baffle wall and wave suppressor pallet were installed just downstream of the pipe inlet to create a more uniform approach flow.

The downstream wall of the headbox was shortened to a height of 2.18 m. for the installation of a horizontal steel floor to act as the labyrinth weir apron. Connected to the weir apron was a stepped chute that terminated with a stilling basin and return channel (see **Figure. 4**). The stilling basin portion of the model system was not tested or observed as part of this study.

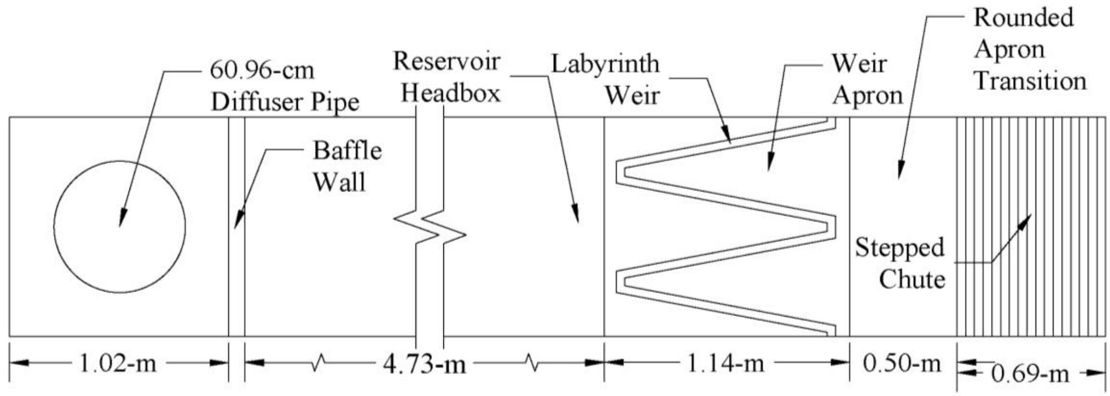

Figure. 4. Plane view of model with major components labeled.

Labyrinth Weir Fabrication and Installation

Test were performed on a single laboratory-scaled labyrinth weir using a total of six different downstream ramp heights. The labyrinth weir was constructed using high density polyethylene (HDPE) and polyvinyl chloride (PVC) sheeting with the weir wall height (P) of 33 cm and a nominal weir thickness (t_w) of 3.81 cm. The 2-cycle (N) labyrinth weir used the full width of the 1.02 m wide headbox, resulting in a cycle width (w) of 0.51 m and a crest length of 4.26 m. The crest shape of the weir consists of two different radii. The upstream radius was equal to 1/3 the weir thickness and the downstream radius is equal to 2/3, approximating an ogee crest weir profile. A schematic of the installed labyrinth weir is provided in **Figure. 5**.

There was a total of seven different downstream ramp configurations used, the first being the traditional labyrinth weir without a ramp installed. The triangular ramps, which were built using plywood, started at the downstream face of the upstream apex, and extended on a constant slope (slope varied with each configuration) to the edge of the downstream apex of the labyrinth weir. The tallest of the ramps was installed such that

the highest point was equal to the transition between the downstream crest curve and the downstream vertical face of the labyrinth weir, creating a ramp height (*p*) of 12 in. This was to allow for clinging nappe regime to be established at low heads and reach a higher level of efficiency (Crookston 2010). Each ramp is installed to reach from the inside of the upstream apex to the edge of the downstream apex (see **Figure. 6**). While the height of the ramp is the variable being tested, each ramp results in a unique angle from horizontal based upon the length of the ramp as well. Geometric information for the tested ramp configurations is included in **Table 1**.

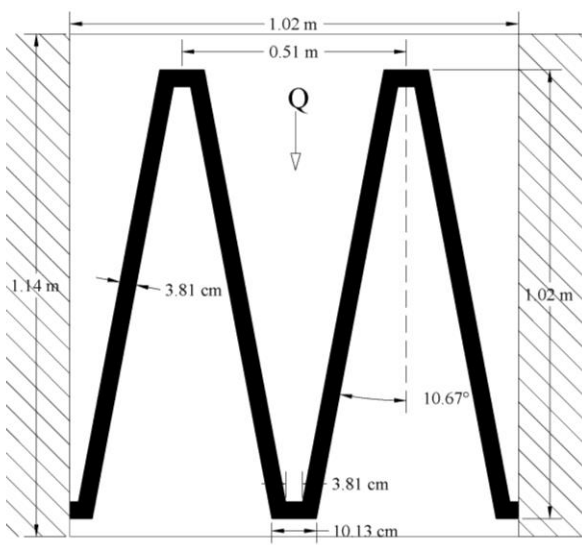

Figure. 5. Plan view layout schematic of the installed α = 10.67° labyrinth weir.

To ensure that the crest of the labyrinth weir was level, the weir apron was leveled prior to the installation of the labyrinth weir. The leveling was done using a surveying level and rod with a tolerance of ±0.8 mm. Nine elevation points of the weir apron were surveyed to level the apron. The labyrinth weir was then installed using PVC glue and

screws. Using the same leveling equipment, the weir crest elevation was measured in 9 locations to level the weir crest and metal shims were placed to raise the weir crest until level.

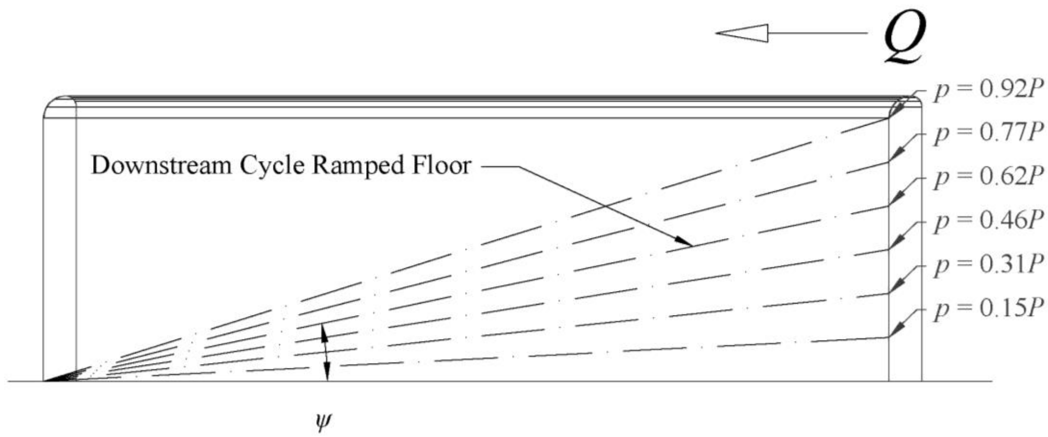

Figure. 6. Profile view schematic of installed downstream cycle ramp.

Table 1. The geometric design properties for the six tested ramp configurations.

p (cm)	(*p/P*) ()	Ramp Angle (ψ)
5.08	0.15	2.97°
10.16	0.31	5.93°
15.24	0.46	8.86°
20.32	0.62	11.74°
25.40	0.77	14.56°
30.48	0.92	17.31°

Stepped Chute Fabrication and Installation

The stepped spillway chute was constructed at a slope of 0.8H:1V or an angle (ϕ) of 51.3° from horizontal with the width the same as the labyrinth weir and headbox. Steps were built using plywood sheets first to a dimension of 10.16 cm in height and 8.13 cm in

depth. Secondary steps were built using wood pieces cut down to dimensions of 5.08-cm X 4.06-cm and installed on the plywood steps. One sidewall was built using clear acrylic plastic 1.91 cm thick to allow for viewing of the flow conditions and depth, with the other made from plywood sheeting painted light blue. The sidewalls were constructed to a height of 0.47 m. perpendicular to the pseudo-bottom of the chute represented by the outmost edge of each step. At the upstream edge of the stepped chute a curved transition section was installed to mimic the typical inflow conditions of research stepped spillway chutes (Chanson 2006). The stepped spillway terminated in a stilling basin and return channel. This portion is not considered as part of this project. Total length, drop height, and horizontal distance of the stepped spillway are as shown in **Figure. 7**. Due to the presence of bracing walls, the lowest portion of the stepped spillway chute is not visible. This results in a limit to the location where the perpendicular depths can be calculated. The bracing wall is labeled in Figure 8 to identify the lowest visible water surface elevation.

Instrumentation

Flow measurements were performed using calibrated venturi meters (±0.2%) installed into the parallel supply lines. Upstream and downstream pressure taps were connected via flexible plastic tubing to a pressure transducer. A multimeter was used to record 5-minute averages of the mA output from the pressure transducer. A spreadsheet was used to calculate the corresponding flow rate. Piezometric head values were measured using stilling basin hydraulically connected to the head box. The stilling basin was equipped with a precision point gauge (accurate to ±0.31 mm) referenced to the weir crest elevation using a survey level and rod. The point gauge was wetted prior to the

measurement of any data to ensure consistency. The tap location of the stilling basin was on the sidewall of the head box 1.06 m upstream and 0.15 m below the weir apron. The tap was on the sidewall rather than the bottom floor of the head box due to the bottom of the headbox being placed directly on a concrete floor. Due to this tap location, at high flows, secondary currents present along the side walls of the headbox creating a variable water surface in the stilling basin depth. This required closing a valve slightly at the stilling well to dampen out the variations due to the secondary flow patterns resulting in a stable water surface.

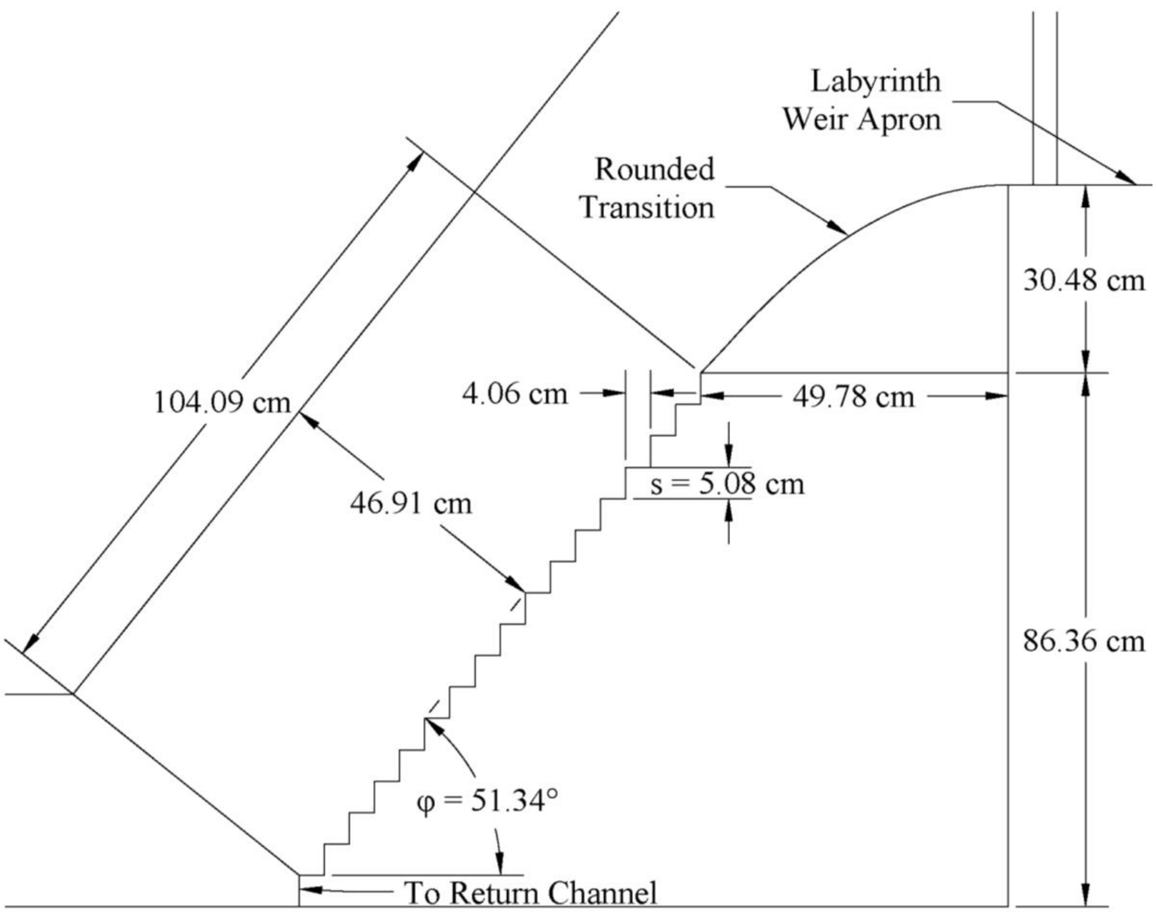

Figure. 7. Geometry and dimensions of the model stepped chute.

To assist in measuring the water surface coordinates, a transparent 2.54 X 2.54 cm grid was installed on the acrylic sidewall. Video records of the temporally fluctuating water surface conditions in the stepped chute were captured using three GoPro® cameras (2 Black 7 and 1 Black 6). Videos were recorded at a resolution of 2.7K with a frame rate of 30 fps. Videos were for a minimum of 10 seconds for reasonably steady flow conditions and the longer of either 15 seconds or three high surge waves for less steady flow conditions. Recorded videos were then processed by a series of software packages to extract still images and then water surface profiles. A maximum water surface elevation was also captured by hand to use as a verification of the photographic method.

The used software packages included Microsoft Office 360® for spreadsheets and data processing. GoPro Quik® was used as the preferred method to extract still images from the recorded videos. These images were than traced using AutoCAD®. The final software used for the water surface extraction was WebPlot Digitizer® to tabulate the water surfaces.

Data Management

All data management and calculations were done using a series of spreadsheets. Included within these spreadsheets was VBA Macro code programs to facilitate the ease of calculations. These codes are presented in Appendix A and should only be used with corresponding spreadsheets and the intended application. Data management includes the storage of collected data points and the aggregation of the various water surface profile coordinates into water surface levels representing the high-flow maximum and minimum for each flow and ramp height configuration.

CHAPTER IV

METHODOLOGY

The testing of the labyrinth weir and stepped spillway chute consists of two different processes. The first portion was to determine the C_d vs H/P curves for each of the seven unique ramp setups. The second portion was to determine the change in flow stability and depth for each of the seven unique ramp setups. In the calculation of C_d, the volumetric flow rate and upstream water elevation or head in addition to the geometric properties of the labyrinth weir must be known. Due to the unique parameters used in discussing the two aspects, the process involved was broken into two sections; impacts to labyrinth weir efficiency of varying ramp heights and increase of flow stability due to ramp installation.

Impacts to Labyrinth Weir Efficiency of Varying Ramp Heights

To better understand the impacts of variable downstream cycle ramp heights on discharge efficiency, the no-ramp baseline labyrinth weir discharge efficiency was determined. For this study, the efficiency of the labyrinth weir was evaluated using the C_d vs H/P relationship (Crookston and Tullis 2013a). Due to limitation in previous testing and research, the range for design is often limited to $H/P < 1.0$ (Crookston et al. 2019). In the application of design for increased PMF and design floods, the higher range of H/P will likely be what dominates the flow conditions experienced. As a result, the range of H/P to be tested will be $0.175 \leq H/P \leq 0.90$. The calculation of the value of C_d for each value of H/P was done using a rearrangement of the traditional labyrinth weir equation (see Eq. [3]).

$$C_d = \frac{3Q}{2L_c\sqrt{2g}H^{3/2}} \quad \text{Eq. [3]}$$

To allow for greater flow rate accuracy, the upstream flow control valve was adjusted to the approximate flow rate and then allowed to stabilize for between 5 and 10 minutes. This is especially important at higher flow rates when the presence of secondary currents along the side walls of the head box created additional variations in the water surface elevation. Once the flow rate had stabilized, a five-minute average of the multi-meter (discharge measurement) was taken. While the five-minute average was being taken, the point gauge was lowered to measure the water surface elevation. If during the five minutes the water surface had not changed (tolerance of ±0.0005 mm), equation 3 was used to calculate the value of C_d for that value of H/P. This calculation is done in the spreadsheet that also converts the multi-meter reading into a volumetric flow rate. Using the entire range of H/P, a 6th order polynomial function was developed to approximate the relationship between C_d and H/P for the installed labyrinth weir without any downstream ramps. A 6th order polynomial function was chosen due to establishing a correlation factor of $R^2 > 0.9991$ for all data sets. This process is then repeated for the ramp height ratios (p/P) of 0.15, 0.31, 0.46, 0.62, 0.77, and 0.92 to obtain C_d vs H/P curves for each of the six ramp heights. Using the established curves equations for the seven unique setups, the percent difference in C_d is calculated in the range of $0.175 \leq H/P \leq 0.90$ by using Eq. [4].

$$\%\text{ error in } C_d = \frac{C_{d,R} - C_{d,B}}{C_{d,B}} \quad \text{Eq. [4]}$$

Where $C_{d,R}$ is the value of C_d with the ramp and $C_{d,B}$ is the value of C_d at the same H/P for the no ramp labyrinth weir.

Minimizing Required Chute Training Wall Heights Due to Downstream Cycle Ramp Installation

To understand the resulting chute training wall height, the maximum flow depth on the stepped chute needs to be calculated. Prior to calculating flow depths, an aggregate maximum water level needs to be calculated. This water level represents the highest water level observable at a given chute location. The following process results in two distinct water surface levels: maximum and minimum. The maximum high-water level represents the absolute maximum water surface level for a given station, regardless of the location across the chute. A minimum high-water level represents only the lowest water level observed against the chute sidewall. It is possible that lower water surfaces exist, however, these two water levels will be used to approach the stability of the flow.

The process of determining the water surface level and corresponding flow depth requires multiple steps. The first step is to film different flow rates along the length of the stepped spillway chute using three cameras (chosen to optimize accuracy [see **Figure. 13**]). Next is to capture various photos of distinct frames during the video to capture the dynamic flow conditions along the stepped spillway. These photos are then used to traces the water surface profile. Exported .pdf files of the traced water surfaces are then imported into WebPlot Digitizer® to extract tabular data representing the water surface. These tabular data are then passed through a series of spreadsheets and macro code (Visual Basic) to combine the three separate camera images into the aggregated water surface maximum and minimum. This process constitutes a digital photographic extraction of the high-water levels observed on the stepped chute. Verification of the water surface levels extracted by the photographic method is done by using a single setup

and flow rate and tracing a maximum water surface by hand onto the acrylic side walls. Unlike a photographic method that has limits in data collection, it was assumed that the hand method found the true maximum value by observing a higher frame rates (>75 fps) and storing a significantly large number of "images" (Potter et al. 2013).

Three flow rates and their associated flow conditions were tested. The flow rates were chosen based upon the flow conditions experienced on the weir apron. To represent what is typically the design condition for labyrinth weirs, the highest flow condition observed resulted in $H/P \approx 0.878 \pm 0.028$ ($Q \approx 540$ l/s). At this flow rate the labyrinth weir experienced local submergence for all ramp configurations tested (see **Figure. 8**). A medium flow was selected based upon a transition from localized submergence to nappe interference for the labyrinth weir (see **Figure. 8**). The medium flow resulted in $H/P \approx 0.367 \pm 0.012$ ($Q \approx 230$ l/s). The low flow observed was based upon a condition with nearly no interference within the weir apron resulting in a near uniform flow at the inflow of the stepped chute (see **Figure. 8**). H/P for the low flow is $\approx 0.186 \pm 0.005$ ($Q \approx 116$ l/s).

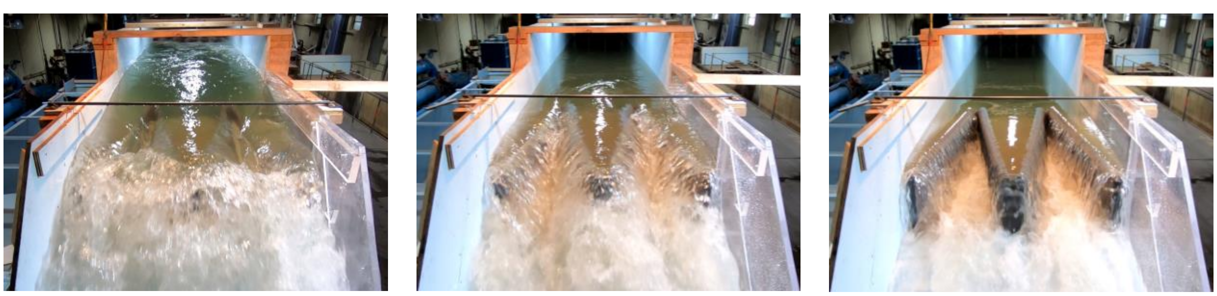

(a) (b) (c)

Figure. 8. Examples of flow interactions on weir apron for the three observed flow rates (a) $H/P \approx 0.878$, (b) $H/P \approx 0.367$, and (c) $H/P \approx 0.186$.

Tracing of Water Surface Profiles

Mapping of the water surface profiles starts by taking video recordings of the physical model with water running. In total, three cameras were used along the stepped chute to increase accuracy of data. After the labyrinth weir C_d was measured/calculated, the cameras were used to record videos of the flow conditions experienced throughout the model spillway. Videos were recorded at an approximate length of 10 seconds for relatively steady flow and 15 seconds, or for 3 surge waves, for non-stable high flows.

Still images were obtained from the videos using GoPro Quik® software. This software was used to import and edit video and photo files. The editing feature used in this study was capturing still images or “frames” from a recorded video. Each of these captured photos was used to represent a portion of the water surface at an instant of time. This study recorded the videos at a resolution of 2.7K with 30 fps, meaning for each second the video captures 30 unique still frames at a resolution of 2704 x 1520 pixels of the water flowing down the stepped spillway chute. The process of choosing the number of photos used from each second of video is described later.

Using still image photos captured from video recordings, the water surface profiles was traced. This study utilized AutoCAD® as a drafting software for the tracing of the water surface profiles. First, each sill photo was inserted into the drafting software. The water surface profile was traced, using a color that is not duplicated in the image. When tracing the water profiles, the transition from traced flow depth to water splash was identified by a change in transparency. It would be impractical to capture 100% of the splash, so this was assumed to represent the bulked flow depth.

In addition to the traced water surface, an axis is drawn on the still image. This

axis is positioned based upon the transparency installed and is used by the WebPlot Digitizer® software to extract water level data. The result of this process was a series of photos that represent instantaneous water surface profiles at individual points in time that can be exported as .pdf files (see **Figure. 9**).

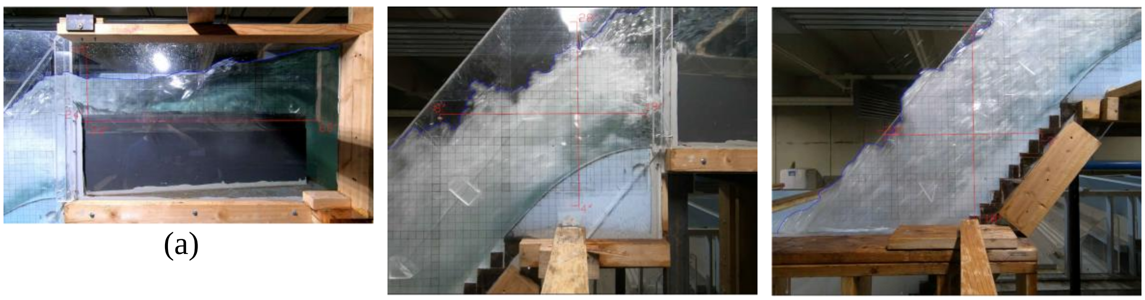

(a) (b) (c)

Figure. 9. Examples of traced water surfaces using still images from the videos recorded by; (a) camera 1, (b) camera 2, and (c) camera 3.

The traced .pdf water surfaces profiles were converted to tabular data using software called "WebPlot Digitizer" v 4.2. WebPlot digitizer is a program that converts charts to tabular data associated with them (see **Figure. 10**). WebPlot requires that the image has a solid unique colored line, in this case the water surface, and a four-point axis to calibrate. As an output, WebPlot creates a comma separated value (.csv) file that contains the coordinates along the entire length of the water surface line. The density of the extracted data is based upon Δx and Δy. This represents the change in the x and y direction as a number of pixels in the image. The default setting is to change data points by ~10 pixels in each direction, this was changed to 5 pixels to account for the dynamic flow observed. All other settings were left as defaults in running the WebPlot software. Prior to saving the .csv, it was very important to verify that all the data points were along

the line. Any erroneous data points from WebPlot Digitizer were removed prior to saving the .csv file.

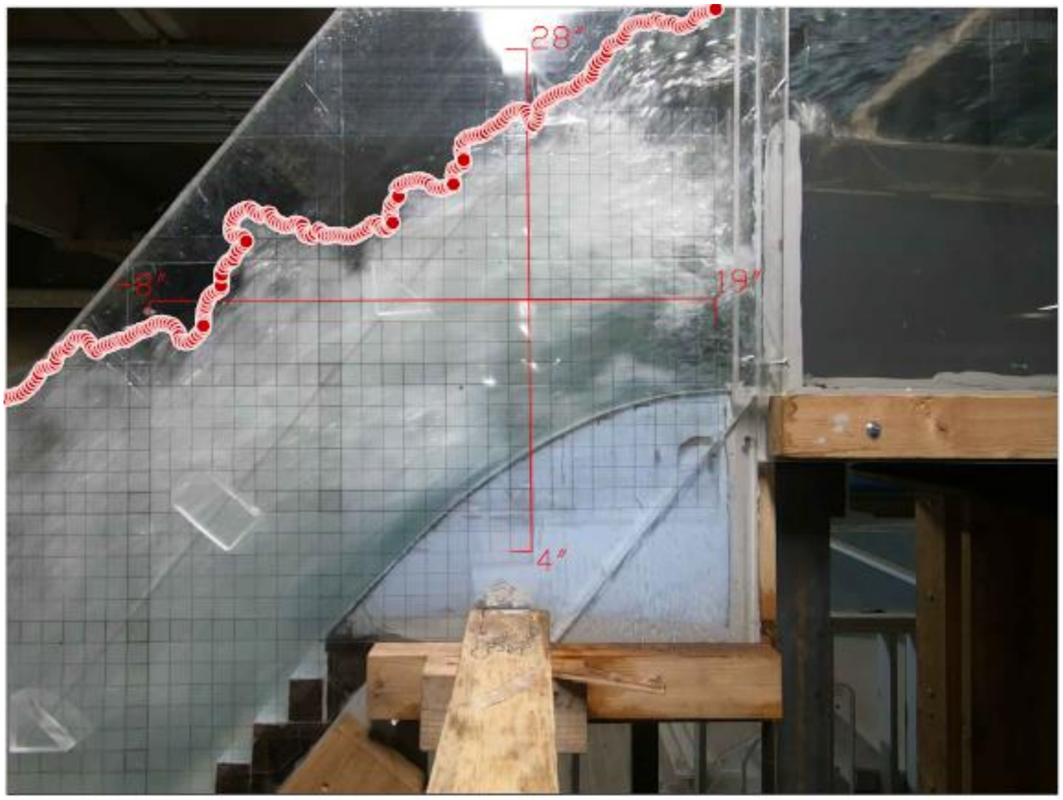

Figure. 10. Example of WebPlot Digitizer data points shown using camera 2.

The tabular coordinates of the water surface profiles have little meaning in stepped chute design. As such, this tabular data needed to be converted into water surface elevation profiles and both vertical and perpendicular water depths. This process was completed using a series of spreadsheets complete with VBA Macro codes (see Appendix A for code). The first spreadsheet was used to aggregate the water surfaces for each of the three cameras individually. This was done by adjusting the coordinates to a consistent

horizontal spacing of 0.64 cm using a linear interpolator. For each horizontal location, a maximum and minimum water elevation is calculated and turned into a unique dataset representing the entire length of the stepped spillway chute. These datasets do not represent the water surface at a given time, rather an aggregate of the water surfaces over the test. This process resulted in a set of aggregated water surfaces representing the maximum and minimum water surfaces levels observed during the course of the video recording.

To combine the three GoPro® camera location datasets into a single curve for the maximum and minimum elevations breakpoints between the cameras need to be identified. A simple method to do this is to graph the three GoPro® datasets and check intersection points between the various cameras (see **Figure. 11**). The intersection between the two camera datasets varies based upon the flow rate and setup. While the intersection between the two video lines is not a guarantee for the true water surface, it does create a starting region for combining the data into a single water surface.

Using the unique intersection point for the maximum and minimum water surfaces a combination dataset for each is created using the VBA code. This resulted in a single maximum and minimum water surface elevation for each flow and ramp condition (see **Figure. 12**). These curves represent the statistics of the high-water level at each point, with the maximum representing the highest elevation of the water regardless of the location across the stepped chute and the minimum representing the lowest elevation observed along the chute wall.

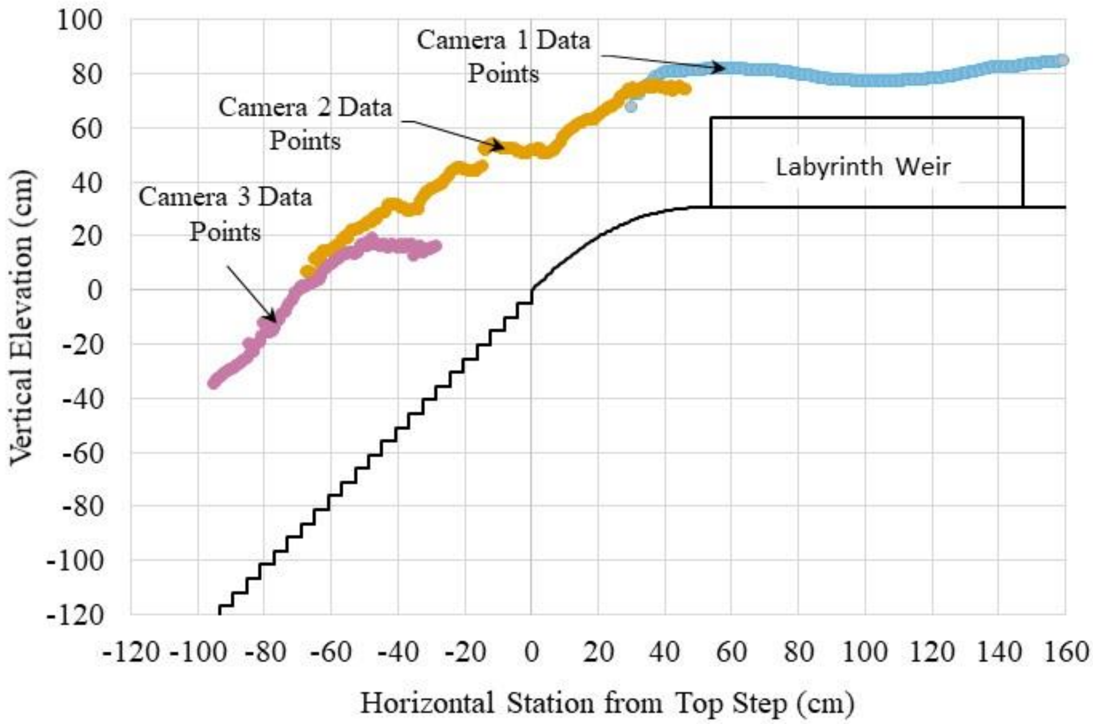

Figure. 11. Example of photographic extracted water surface data from the three camera locations, used to identify an intersection between data.

Calculating the perpendicular water depth for the water surface curves was done using an additional VBA code (see Appendix A). A perpendicular depth is also known as the shortest distance between two points. Calculating this distance between a known water surface elevation point and the dam structure required a recalculation of the horizontal stationing in addition to calculating the water depth. This resulted in a new dataset of both the "X" and the depth coordinate for both the maximum and the minimum water surface curves.

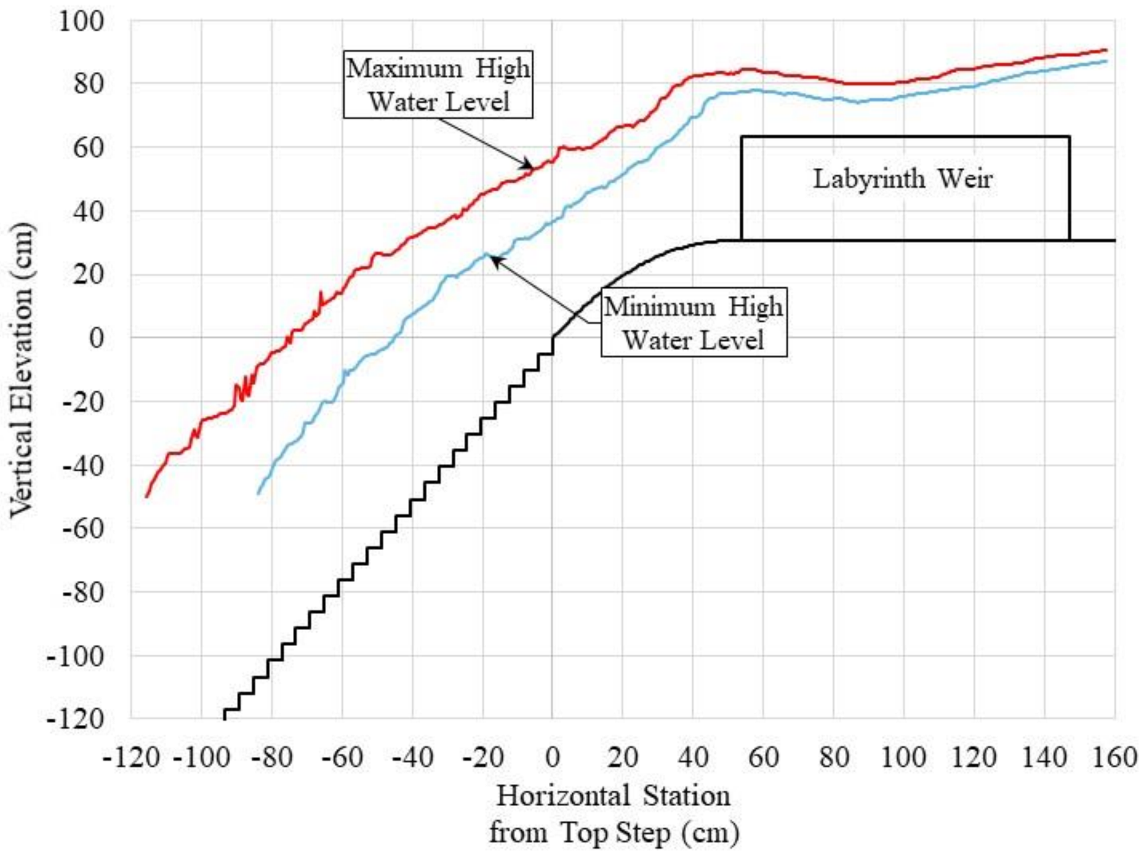

Figure. 12. Compilation of the representative high-water level approximations for $H/P \approx 0.878$ with no ramps installed in the labyrinth weir.

One concern of using cameras and photos to capture the water surfaces was the risk of distortion in the video resulting in inaccurate estimates. Distortions in the video can be caused by refraction through the acrylic side walls as well as "fisheye" effect due to increased distance from the lens of the camera. To address this issue, three cameras were used with the video setting on Linear field of view to minimize "fisheye" effect in the camera lens. Installing multiple cameras along the length of the spillway also helped to minimize the distance viewed by a single camera frame. Using too many cameras significantly increased the time for processing the images and combining the high-water data into a single dataset without any significant value added.

Initially, a single camera was used to capture the entire flow regime. It was hoped that by doing so the entire water surface profile would be captured in a single video and as a result a single photo. This would allow for a simple process to directly convert from photos to tabular water surface data. When using a single camera, the lens had to be a substantial distance back from the sidewalls to be able to capture the upstream and downstream most sections of the flow. By being so far back, the definition of the water surface was blurred. This resulted in distortions and increased difficulty in capturing the water surface that resulted in significantly variations from the hand extracted data. Using a single camera also created difficulties in capturing accurate stationing locations of the water surface points. As a result, using a single camera to capture the water surface profile information was abandoned.

It was thought that by adding an additional camera and spacing the two cameras out would result in greater resolution. Due to the method of constructing the stepped spillway chute, creating a location along the spillway to attach the two cameras would have required extensive rebuilds and potential interface in the flow regime along the stepped spillway chute. As a result, the possible locations for using two cameras were limited and did not allow for proper capturing of the water surface profile near either the upstream entrance to the chute, or the downstream end of the chute. This led to similar distortion as the single camera method and was also abandoned.

To capture the entire stepped spillway chute and the labyrinth weir flow, three cameras were used in the final data collection process. The upstream most camera was used to capture flow conditions across the labyrinth weir and onto the rounded transition. The second camera was stationed to capture the flow conditions over the rounded

transition to the inlet of the stepped spillway chute. The final camera was placed to capture the middle and bottom steps of the stepped chute (see **Figure. 13**).

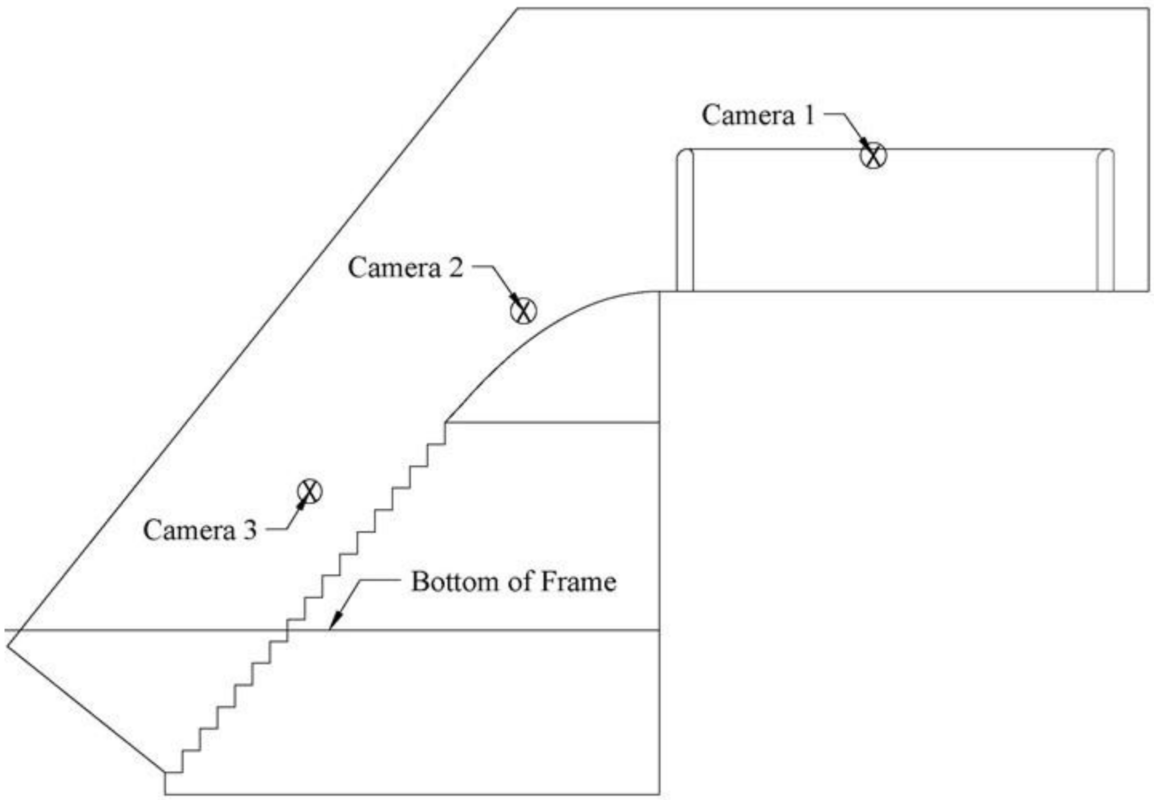

Figure. 13. Approximate center of frame locations for the three cameras (each camera was offset by ~ 0.61 m).

To ensure that the entire flow regime of the stepped spillway chute was captured, the three cameras were placed to ensure a small amount of overlap between their image location. This overlap was used to be able to inspect the distortion between the individual cameras as well as to assist in being able to create the transition between the three sets of flow. To verify the data between cameras, the extracted data (process discussed later) were plotted as statistical maximum for distortion and overlap comparison (see **Figure.**

14).

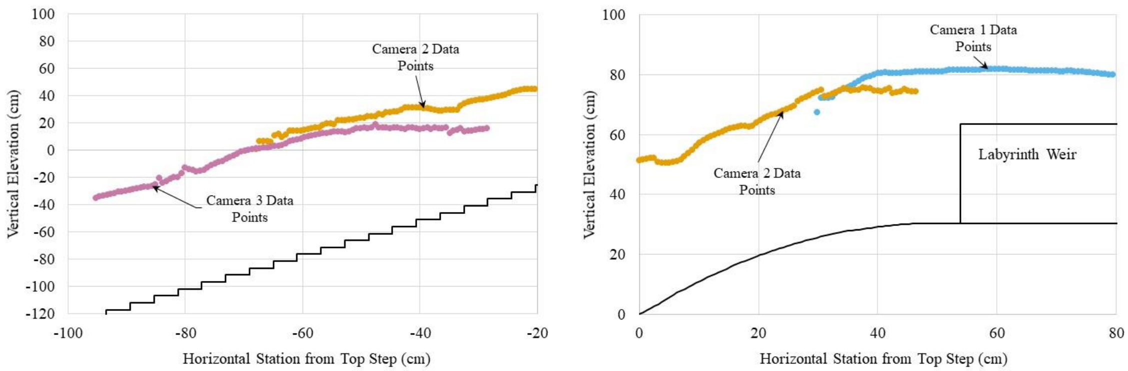

(a) (b)

Figure. 14. Display of overlap between the extracted high-water levels from different camera locations; (a) high-water level from cameras 2 and 3 and (b) high-water level from cameras 1 and 2.

Something of note is that the downstream camera's water surface (in each overlap scenario) reaches a maximum elevation as it moves upstream. This leveling of the water surface profile is due to the maximum elevation within the camera frame. For both the cameras 2 and 3 the flow entered along the top of the frame instead of along the side. As a result, as the water surface elevation changed the location of entering the frame shifts horizontally instead of vertically. Inspecting more closely the overlap between the cameras 2 and 3 showed that there are multiple intersection points between the two datasets. Observations found that the flow in this region varied the least due to already being in the stepped chute. The overlap between cameras 1 and 2 typically only had a single intersection point, this is possibly due to the dramatic changes experienced in the flow at the intersection between cameras 1 and 2. There exists a major difference in the flow conditions at the overlap of these sections. Camera 1 primarily captures the flow as

it passes over the labyrinth weir while camera 2 focus on the flow from the weir apron and the rounded transition. As a result, it was important to use sound judgment in choosing the intersection point between two cameras.

Capturing Photos from Recorded Videos

Compiling the water surface elevations from every single recorded frame would give a complete understanding of the range of water surface elevations at given locations along the stepped spillway chute. However, using every single frame recorded would be extremely time consuming and might not lend to an increase in information in using less photos spaced evenly during the video recording and only using a single frame would not be truly representative of the dynamic flow conditions. To understand the density of photos needed to no longer increase the acquired information, a frame rate convergence test was done. Like the overlap and distortion analysis, the frame rate convergence test compared the photographic method maximum water level to the hand measured water levels.

For the frame rate convergence study performed, the photographic maximum water levels were extracted with still images extracted at a spacing of 24, 18, 12, 9, and 7 frames at $H/P \approx 0.878$. These different spacings result in frequencies of 1.25, 1.67, 2.50, 3.33, and 4.35 frames/sec. This resulted in varying numbers of photos based on camera on camera (see **Table 2**). Increasing the still images extracted also increases the amount of work it takes to process the images. This means that minimizing the number of required still images while still maintain the accuracy was highly important.

Table 2. Number of still photos analyzed for each frame rate frequency tested during the performed frame rate sensitivity analysis.

Camera	**1.25 frames/sec**	**1.67 frames/sec**	**2.50 frames/sec**	**3.33 frames/sec**	**4.35 frames/sec**
Camera 1	16	21	31	41	53
Camera 2	17	22	32	43	55
Camera 3	16	21	31	41	53
Total	49	64	94	125	161

Visualizing the water surface elevations from each of the different frame rates resulted in a large amount of scatter (see **Figure. 15**). One pattern that can be gleaned was that for the largest frame spacings, the photographic method underestimates the water surface profile for a large extent of the stepped chute. This difference decreases until the frequency reaches 3.33 frames/sec, at which point there is minimal change to the water surface. For the frequencies less than 3.33 frames/sec, the increased time for processing does not correspond with an increase in data.

The result in the frame rate convergence analysis was that the spacing between the still images has an impact on the accuracy of the perpendicular water depths. For large spacings, the perpendicular water depths extracted by the photographic method underestimate the water surface compared to the hand measured water surface for the lowest frequencies tested. This was likely due to missing the waves of high water as they propagated down the stepped chute. It might be possible to capture these waves by changing the timing of the initial frames; however, this would lend to an inconsistent pattern of starting the still image processing. As the frame rate approaches 3.33 frames/sec, the high-water levels become increasingly more like the hand extracted water surface. However, once the frequency increases past this point, there is little to no

increase in perceived accuracy. This meant that further increasing the still images process would not result in an increase in accuracy of the water surface. While using a frequency of 4.35 frames/sec does not increase accuracy for the video length tested, it was used in this study to avoid effects due to shorter video lengths.

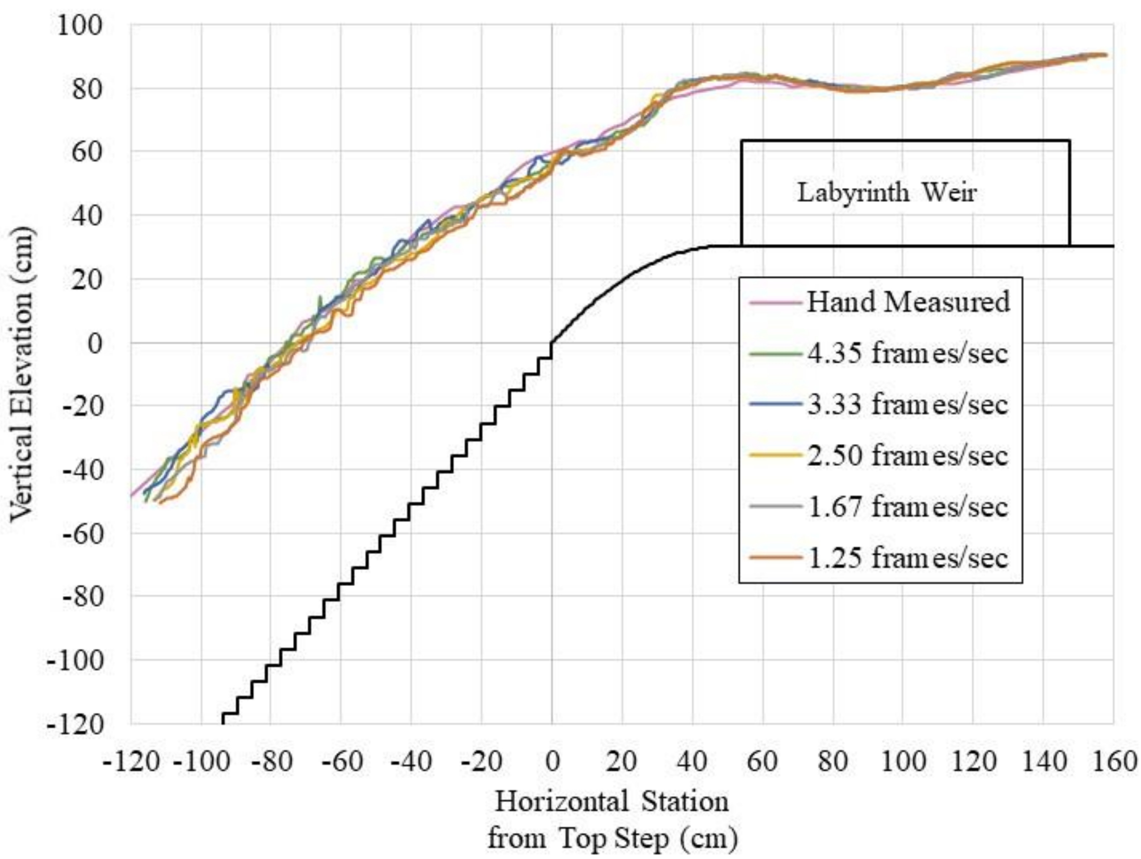

Figure. 15. Photographic extracted maximum high-level water profiles for each tested frame rate frequency tested.

CHAPTER V

THE INFLUENCE OF OUTLET RAMPS ON FLOW INSTABILITIES AND DISCHARGE EFFICIENCY OF LABYRINTH WEIRS FOR STEEP STEPPED CHUTE APPLICATIONS

Abstract

The installation of a labyrinth weir as the crest of a stepped chute significantly influences the downstream chute inflow conditions relative to published design standards for more traditional crest shapes. A current study at the Utah Water Research Laboratory (Utah State University) evaluated a 10.67º trapezoidal labyrinth weir crest discharging into a 0.8H:1.0V stepped chute. To better direct flows into the chute and mitigate flow instabilities (i.e., flow surging), sloped ramps were placed in the labyrinth weir outlet cycles. The influence of six different ramp geometries are reported herein relative to weir discharge efficiency, flow surging, and chute wall-height requirements based on splash and spray depths. The labyrinth weir increased the spillway wall height required for flow containment by 200 to 300 percent relative to linear weir wall height predictive methods. The addition of ramps provided better flow transition into the stepped chute and reduced the required chute wall heights by up to 15%. Furthermore, ramp heights taller than half the weir wall height effectively reduced flow surging but increased local submergence, which decreased discharge efficiency by up to 9%. Thus, an outlet cycle ramp geometry selection should be optimized by discharge efficiency, flow surging, and chute wall height requirements.

Keywords: dams, barrages, and reservoirs; floods and floodworks; hydraulics and hydrodynamics.

Introduction

Flood control and water supply projects often include diverse spillway geometries. For the rehabilitation of existing projects or for new projects, identifying a techno-economical solution is essential, and this objective has led to the selection of a nonlinear weir spillway crest for numerous recent projects (Crookston et al. 2019; Erpicum et al. 2017, 2013, 2011). Furthermore, the advancement of roller-compacted concrete has facilitated the use of stepped chutes for a variety of spillways at both gravity and embankment dams (Hunt et al. 2014, Ohtsu and Takahashi 2004, Chanson 2002, Ruff and Ward 2002).

Relative to more classical linear weir alternatives (e.g., broad crest, ogee, sharp crest) with a relatively uniform unit discharge (q), labyrinth weir discharges create complex three-dimensional flow conditions downstream (highly turbulent, unsteady, and nonuniform q) (Crookston and Tullis, 2013a), which can affect how flow transitions into downstream spillway components (spillway chute, stilling basin, river channel, etc.). A labyrinth weir followed by a steep stepped chute, for example, can present challenges to the hydraulic engineer in sizing stepped chute training wall heights based on current published design methods (e.g., Chanson, 2006). Indeed, stepped chute design guidance assumes the presence of a critical, laterally-uniform flow depth at the chute entrance (e.g., Boes and Hager, 2003; Hunt and Kadavy, 2017). Chute hydraulics are further complicated by a flow instability in labyrinth weirs known as flow surging (Crookston, 2010), which is described as an abrupt change in the nappe, including trajectory.

Previous Studies

As previously noted, stepped chutes have been extensively studied, yet limited information is available regarding a stepped chute with a crest that is a nonlinear weir. This lack of guidance has resulted in several project-specific physical model experiment studies focused on energy dissipation for stepped chutes with a piano key weir (PKW) crest.

For example, a physical model of Charmine Dam found a benefit to combining the PKW with a stepped chute (Loisel et al., 2014). The study reported that replacing a smooth chute with a stepped chute design both decreased the residual energy at the toe of the spillway (i.e., increased energy dissipation) and decreased the required chute wall height for flow containment. Similar project-specific studies were performed for Dakm 2 HPP and Vinh Son 3 HPP dams in Vietnam (Ho Ta Khanh et al. 2011). Rehabilitation of Gloriettes dam (France) also combined a PKW with a milder slope stepped chute (Bieri et al. 2011). Even though the original smooth chute for L'Etroit Dam was maintained, the newly added PKW featured steps in the outlet cycles (Vermeulen et al. (2011).

Erpicum et al. (2011) studied the energy dissipation of two different PKW geometries and an ogee crest followed by a relatively long, steep (chute slope angle θ = 52°), stepped chute and found negligible difference in residual energy entering the stilling basin between the alternatives. In contrast to the ogee/stepped chute configuration, which typically requires some finite length downstream from the crest before flow aeration is well developed, the flow conditions transitioning from the PKW to the stepped chute produced immediate air entrainment. Erpicum et al. (2011) hypothesized that this could potentially reduce the chute length needed to reach an also evaluated PKW and ogee crest

weir geometries followed by steep stepped chutes of varying lengths. The study found that PKW uniform flow conditions were achieved sooner (higher up in the chute) than with the ogee crest. Stepped chute uniform flow refers to a condition were the residual energy becomes constant (the energy increase due to gravitation effects in the falling flow column are balanced with turbulence-induced energy loss on the steps). The PKW uniform flow residual energy, however, was higher than the ogee crest weir (i.e., the highly aerated flow produced by the PKW experienced less energy dissipation than the ogee crest flow condition).

While the PKW is essentially a derivative of the labyrinth weir, the resulting flow conditions downstream can differ substantially between the two. First, the PKW typically includes ramps in the outlet cycles or keys that help direct flows into a chute, whereas labyrinth weirs are typically constructed on flat aprons. Second, a flow phenomenon known as flow surging has been observed with labyrinth weirs that results in nappe oscillations at moderate discharge levels (Crookston and Tullis, 2013b). Flow surging would be expected to increase required wall heights at the upstream end of the chute (i.e., near the labyrinth weir).

The authors performed a project-specific hydraulic model study at a geometric scale of 1:12 for a proposed new off-line pump-storage project in Texas (USA) where the auxiliary spillway included a labyrinth weir, a steep stepped chute, and a U.S. Bureau of Reclamation Type III stilling basin. Initial training wall heights were estimated by the designers using available linear weir-stepped chute design methods and then updated specifically for the project design using a RANS-based, RNG k-ε, single fluid computational fluid dynamics (CFD) model. Testing of the physical model revealed two

hydraulic concerns:

- the labyrinth weir increased flow depths in the chute relative to the CFD-based estimates (even at lower discharges), resulting in a need to raise the height of the chute wall, and
- flow (nappe) surging at the downstream side of the weir, which also influenced chute wall height requirements, was observed (see Figure. 16).

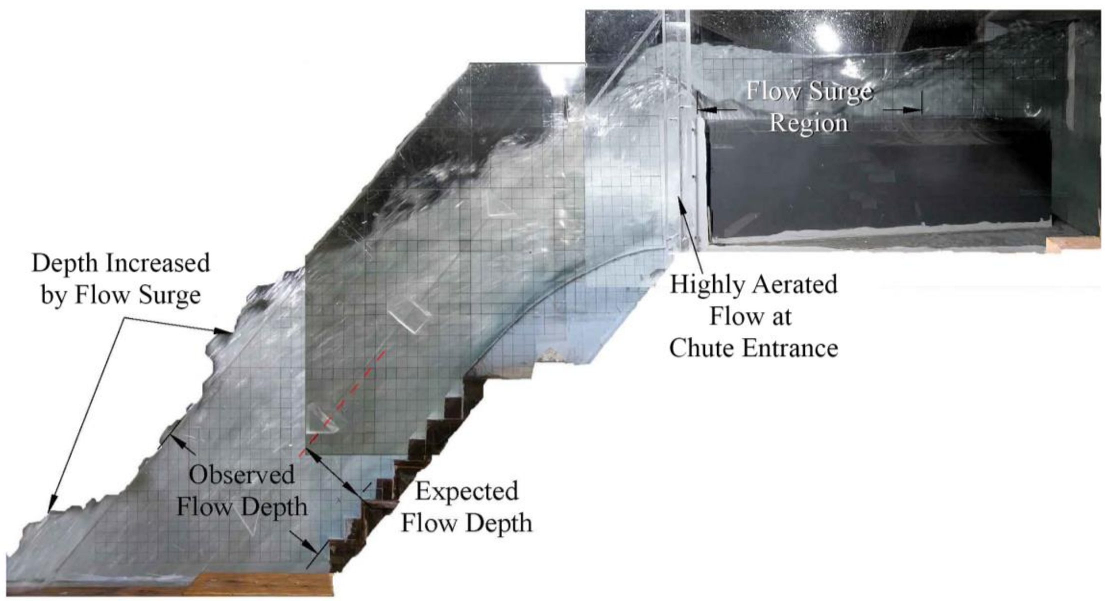

Figure. 16. Example of an instantaneous water surface profile for a labyrinth weir-stepped chute combination, weir height 330 mm and step height 51 mm (photo courtesy of Tucker Jorgensen)

The study found that placing sloping ramped floors (hereafter called ramps) in the downstream cycle of the labyrinth weir, similar to a PKW geometry, helped to direct flows downward into the chute, diminished flow surging, and reduced water levels

immediately downstream of the weir in the stepped chute.

As a result, the present systematic study was performed to investigate six different ramp configurations installed in the outlet cycles of a labyrinth weir and the corresponding effects on discharge capacity, flow surging, and flow depths in a steep stepped chute.

Experimental Method and Setup

As previously noted, the geometry of this study is based upon the proposed design for a new offline pumped storage reservoir formed with an embankment dam. A labyrinth weir made from high-density polyethylene (HDPE) sheeting was tested at the Utah Water Research Laboratory (UWRL); dimensions of the constructed weir are given in **Table 3**. The rounded crest of the labyrinth weir consisted of an upstream radius r = 1/3 wall thickness (t_w) and a downstream radius r = 2/3 t_w, forming a quasi-ogee crest shape (**Figure. 17**.).

The labyrinth weir was installed on an elevated flat apron 2.18 m above the floor of the upstream reservoir invert. The sectional weir model featured two labyrinth cycles and a stepped chute with θ = 51.3° (0.8H:1V) with a horizontal step length l = 4.06 cm and a vertical step height h_s of 5.08 cm, a total chute height H_{chute} of 3.05 m, and a length of 6.0 m. A 0.8H:1V sloping floor was placed in the headbox to represent a sloped reservoir approach selected by the designers of the embankment dam (see **Figure. 18**).

Calibrated venturi meters (±0.2%) installed in the supply piping were used to quantify discharge. For each data point, Q measurements were averaged for 5 minutes. A baffle wall and wave suppressor were installed at the upstream end of the reservoir to improve approach flow uniformity. A stilling well hydraulically connected to the side of

the head box and a precision point gauge (± 0.15 mm) were used to measure the reservoir water surface elevation. Piezometric head, *h*, relative to the weir crest could then be computed; an average velocity, *V*, was estimated at the stilling well measurement location to estimate total energy, $H=h+V^2/2g$ where g is gravity acceleration.

Table 3. Labyrinth weir geometry

Parameter	Dimension
α	10.67°
w	0.51 m
N	2
B	1.02 m
t_w	38.1 mm
A	38.1 mm
P	330.1 mm

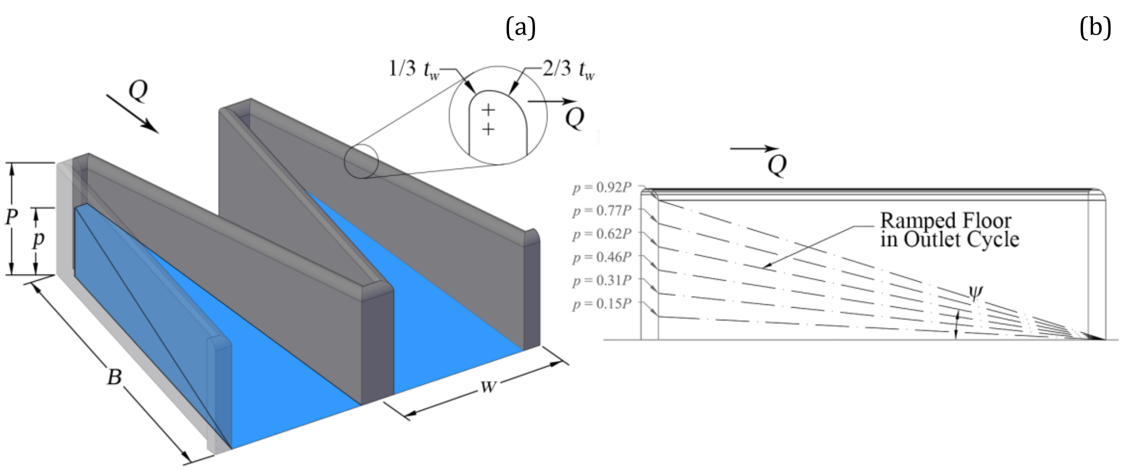

Figure. 17. Example of a sloping ramped floor installed in the downstream cycle of a labyrinth weir (a) isometric view and (b) profile view with all tested ramp configurations (Courtesy of B.M. Crookston)

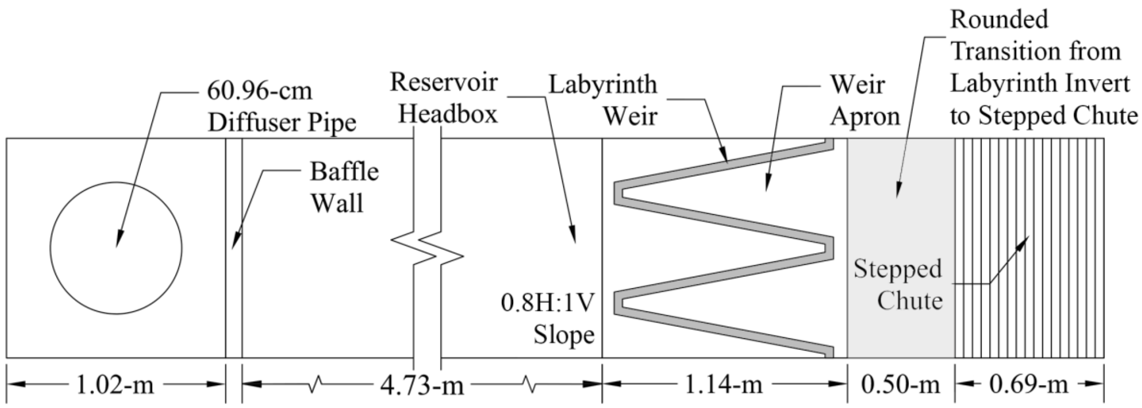

Figure. 18. Plan view schematic of the tested model setup

The ramped floors were installed in the downstream cycles of the labyrinth weir and extended to the downstream limits of the labyrinth weir (see **Figure. 17**.). Due to the rounded crest shape and corresponding hydraulic efficiency (Crookston, 2010), the ramp height, p, did not exceed the bottom edge of the downstream crest profile (92% of P). In total, six different ramp heights were tested (see **Figure. 17** [b]); the ramp heights, ramp/weir height ratios (p/P) and ramp angle, Ψ, are summarized in **Table 4**.

Table 4. Outlet cycle ramp configurations

p (cm)	p/P ( )	Ramp Angle (ψ)
5.08	0.15	2.97°
10.16	0.31	5.93°
15.24	0.46	8.86°
20.32	0.62	11.74°
25.40	0.77	14.56°
30.48	0.92	17.31°

Experimental Results

Overview

The placement of ramps in the outlet cycles may provide several advantages if balanced with head-discharge requirements. As discussed in the subsequent two sections, ramps may provide hydraulic benefits if configured to mitigate flow surging and reduce chute wall heights. However, larger ramp heights can increase local submergence and decrease the weir discharge efficiency and corresponding discharge coefficient C_d. In addition to hydraulic considerations, the ramps also influence the structural design by connecting adjacent walls and reduce cantilevered wall heights.

Flow Surging

The falling nappe at a labyrinth weir may transition from clinging to aerated, to partially aerated, and finally to drowned conditions as Q and H increase (Crookston, 2010). However, for certain labyrinth weir geometries, an unstable nappe condition may occur where the air cavity behind the nappe slowly reduces and the nappe trajectory approaches vertical. At a critical point and without observed perturbation, the air volume or size of the air cavity behind the nappe abruptly increases causing noise and the nappe trajectory to spring away from the weir (see **Figure. 19**.). This pattern occurs at a general or average oscillation frequency (f) of approximately 0.2 Hz, significantly different from nappe vibration or the thin nappe oscillations of 5.3–17.4 Hz (see Lodomez et al., 2018, 2019; Anderson and Tullis, 2017; Crookston and Tullis, 2013b). Undular linear weir flows, as noted by Chanson (1996) and Hager and Schwalt (1994), were not present. Furthermore, Crookston (2010) noted that venting of the nappe via a conduit or a flow

splitter did not mitigate flow surging but did reduce the range of flows within which surging occurred.

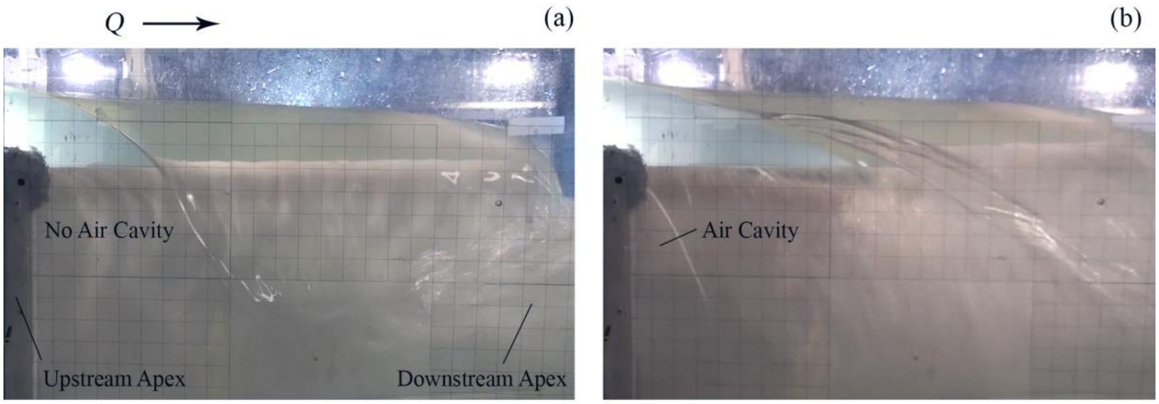

Figure. 19. Flow surging (profile view) in a labyrinth weir (Photos courtesy of B. M. Crookston)

Flow surging at the labyrinth weir caused an increase in flow depths in the upper portion of the stepped chute and produced waves that propagate down the chute and into the basin. Filling a portion of the outlet cycles reduced flow surging; increasing *p* decreased the flow surge on the apron, especially at the upper ranges of *H*/*P* where flow surging typically occurred. With downstream ramps in place, the water surface profile changed from a curved shape with a middle section that rises and lowers as the surge passes to a continuously downstream sloping profile that extended the full length of the labyrinth weir (see **Figure. 20**). The ramp-induced flow surge reduction increased with increasing p, but the flow surging was never fully eliminated.

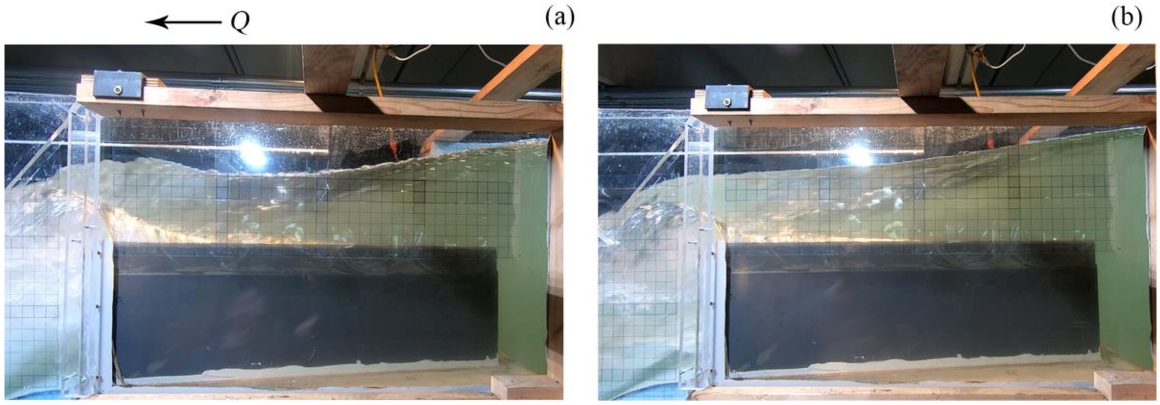

Figure. 20. Comparison of apron flow patterns at $H/P \approx 0.878$ for (a) non-ramped and (b) $p = 0.92P$ conditions (Photos courtesy of Tucker Jorgensen)

Impacts to Flow Conditions at Chute Entrance

In addition to the influences within the apron, the use of ramps in the downstream cycle of the labyrinth weir also impacted the flow depth in the stepped chute. A more complete analysis of stepped chute flow depths with labyrinth weir ramps is presented in Jorgensen et al. (2020). In general, the highest H/P evaluated resulted in a decrease in the flow depth (~15%) for $p \geq \sim 0.5P$ and an increase in the upstream flow depth required to pass the discharge, due to a loss in weir discharge efficiency (see **Figure. 21**).

Differences between laboratory experiments and field observations for air-water flows has been of high interest to researchers and practitioners (e.g., Valero and Bung 2018, Chanson 2013). These scale effects include turbulence intensities (Tu), air-water interface areas and aeration rates (e.g., bubble size distributions and bubble count rates), and splash and spray (Pfister and Chanson 2014, Chanson and Gonzalez 2005). Thus, laboratory-scaled experiments do not adequately represent flow bulking and potential water surface elevations, which should be considered when selecting an appropriate chute

wall height. Additional research and prototype data for labyrinth weirs with steep stepped chutes is needed to consider air-water flow scale effects that are present in this study and cannot be overcome in the laboratory.

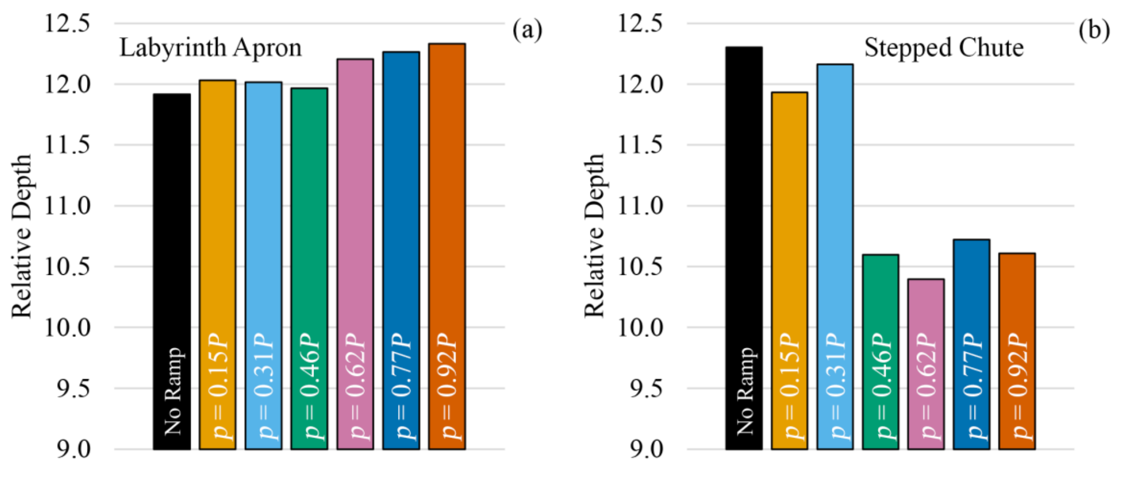

Figure. 21. Maximum relative flow depths observed in (a) apron of the labyrinth weir and (b) in the stepped chute downstream of a labyrinth weir crest for tested values of p at $H/P \approx 0.878$

Flow efficiency impacts from installation of ramps

While the installation of the ramps helped mitigate flow surging and reduced flow depths in the chute entrance, in some cases, ramps did have a negative impact on discharge efficiency by increasing the localized submergence near the upstream end of the downstream cycle of the labyrinth weir. When $p \leq 0.46P$, the increase in localized submergence was minimal and discharge efficiency was relatively unaffected. Both $p = 0.62P$ and $0.77P$ resulted in an observed increase in the localized submergence for H/P >~ 0.25. The increase in localized submergence was reduced at higher H/P, likely due to

a corresponding increase in local submergence for the no-ramps condition. In the case of the tallest ramp height tested ($p = 0.92P$), the increase to localized submergence was observed for even the lowest H/P values tested (see **Figure. 22**). Increases in localized submergence with increasing p was associated with losses in the weir efficiency.

Figure. 22. Example of jumping jets for low (<~0.25) H/P with $p = 0.92P$

The impacts to discharge efficiency were determined empirically using a standard form of the weir head-discharge relationship [Eq (1)].

$$Q = \frac{2}{3} C_d L \sqrt{2g} H^{3/2} \qquad 1.$$

In Eq 1, Q is the discharge, C_d is the dimensionless discharge coefficient, L is the weir length, g is the gravitational constant, and H is the total upstream head. C_d values for a dimensionless upstream head range of $0.20 \le H/P \le 0.85$ were calculated for the labyrinth weir no-ramped (baseline) condition and the six ramped floor configurations (see **Table 4**). These data are presented in **Figure. 1** with a trendline used to represent the Cd data for the no-ramp condition.

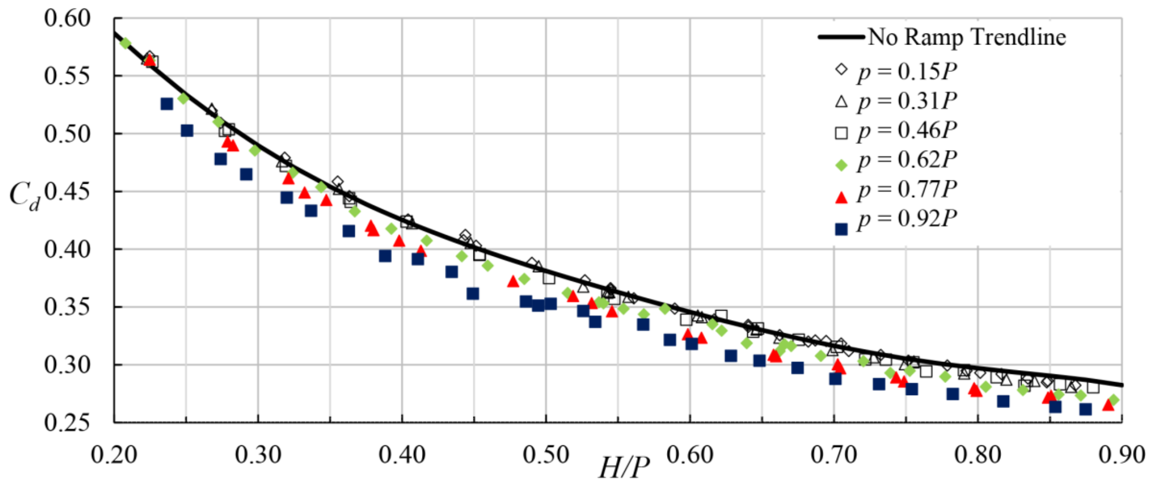

Figure. 23. Ramped C_d vs. H/P for all ramp and the no-ramp configurations

To further illustrate the influence of the ramped floors on hydraulic efficiency (C_d), the ramped to no-ramp (baseline) C_d ratios are presented in **Figure. 24** as a function of H/P ($0.20 \leq H/P \leq 0.85$, with the experimental data presented as trendlines (average correlation coefficient = 0.9994). The $C_{d\text{-}ramp}/C_d$ data for $p \leq 0.46P$ were consistently in the ~ ± 2% range (comparable with the accuracy of the experimental method), indicating that the ramps had essentially no impact on discharge efficiency. For the taller ramps, the C_d response follows various trends. Excluding $p = 0.92P$, discharge efficiency was essentially unaffected for $H/P \leq 0.30$. For $0.30 \leq H/P \leq 0.45$, local submergence increased relative to the no-ramp condition, and discharge efficiency decreased. As H/P increased further, only modest reductions in discharge efficiency were observed. For $p = 0.92P$, discharge efficiency reduction occurred over the entire range of H/P tested.

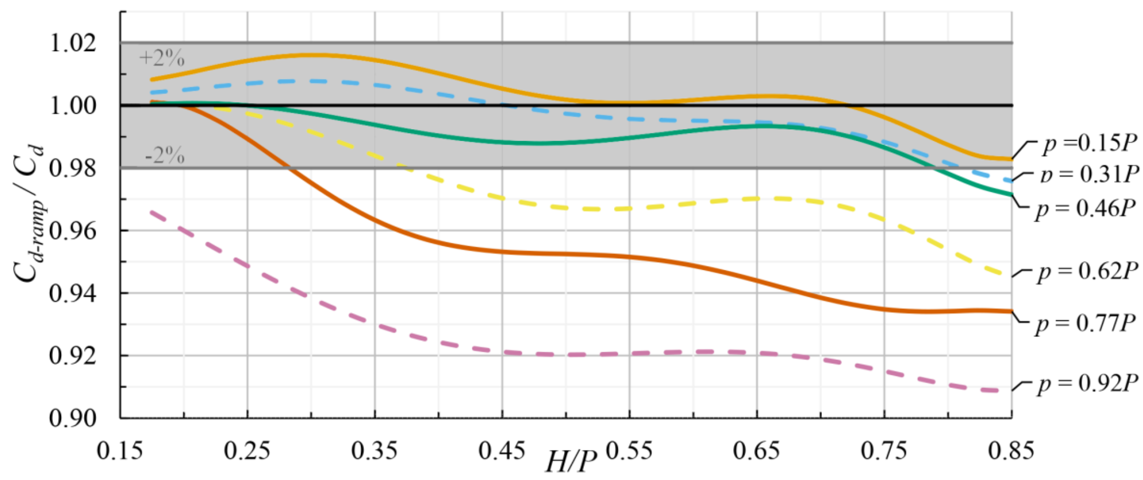

Figure. 24. Ratio of $C_{d\text{-}ramp}/C_d$ for labyrinth weir (gray highlighting identifies the ±2% limit)

Installing ramps into the downstream cycle of a labyrinth weir has multiple consequences. Optimizing the hydraulic influences (e.g., discharge efficiency and downstream chute wall heights) of ramped floors in the downstream cycles of labyrinth weirs that precede steep stepped chutes requires additional understanding of the flow depth impact discussed by Jorgensen et al. (2020).

Conclusions

Using a labyrinth weir as the control structure in a stepped chute spillway can change flow conditions entering the stepped chute and thus introduce potential design and performance uncertainty. Chute wall height requirements, as predicted by standard design methods, for example, will likely be undersized. In this study, sloping ramped floors were installed in the downstream cycle of a labyrinth weir in an effort to better transition weir discharge into the stepped chute and reduce chute wall height requirements. Installation of ramps has the potential to decrease hydraulic efficiency by increasing either the nappe

interference or localized submergence.

Six different ramp configurations were used to evaluate the effects on hydraulic efficiency relative to the no-ramp labyrinth weir (baseline) configuration over a wide range of dimensionless upstream heads ($0.175 \leq H/P \leq 0.90$). In general, as the ramp height (p) increased, the upstream head required to pass flow also increased (decreasing hydraulic efficiency). For $p < 0.5\,P$, the impact on hydraulic efficiency, as illustrated by response of C_d, was minimal. Major conclusions from this study include the following:

Installing ramped floors in the downstream cycles of a labyrinth weir can impact the hydraulic efficiency of the labyrinth weir. As the ramped floors increase in height, C_d decreases along with hydraulic efficiency relative to the no-ramp configuration (~9% reduction for the tallest ramped floor at higher H/P values).

When the ramped floors are less than approximately ½ of the weir crest height, the impact on C_d and discharge efficiency are negligible.

Increasing ramp height (p) leads to a reduction in labyrinth weir (nappe) flow surging and a decrease in stepped chute flow depth.

When considering ramped floors in the design of a labyrinth weir/steep stepped chute spillway, factors such as additional material and construction costs, structural benefits, and the sensitivity of flood routing requirements and consequences associated with small decreases in hydraulic efficiency should be evaluated.

It is important to note that the results of this ramped floor study are specific to the labyrinth weir/steep stepped chute spillway geometry tested. Future research should include variations in labyrinth weir and chute designs (e.g., milder sloping stepped chutes. Additional research is also needed to develop a better understanding regarding the

influence of scale effects on the hydraulic behavior of labyrinth weir/stepped chute spillway hydraulics.

Data Availability Statement

Some or all data, models, or code generated or used during the study are available from the corresponding author by request.

Acknowledgments

This study was funded by the State of Utah and the Utah Water Research Laboratory at Utah State University.

CHAPTER VI

STUDYING THE HYDRAULIC EFFECTS OF A LABYRINTH WEIR ON A STEEP STEPPED CHUTE

Abstract

Labyrinth weirs are commonly used to maximize spillway discharge efficiency. Stepped chutes represent a common spillway element used to help dissipate kinetic energy, thus reducing the size requirement of the downstream energy dissipation basin. This highly turbulent flow process can produce significant wave activity. When stepped chute spillways are placed on earthen embankment dams, it's important that the chute wall heights be sized adequately to contain the bulk flow, waves, and splash as much as possible to minimize the risk of erosion-induced embankment damage. This study evaluated some of the hydraulic impacts of coupling a labyrinth weir with a steep stepped chute at the laboratory scale.

Test results showed that required training wall heights for bulked flow containment were significantly higher than traditional stepped chute design predictions without a labyrinth weir. Placing ramped floors in the labyrinth weir downstream cycles, in some cases, reduced maximum chute water levels. To better understand this phenomenon and provide design guidance toward the use of ramped floors to reduce chute flow depths and training wall height requirements, a hydraulic behaviors of various ramped floor configurations were systematically evaluated. The results for the geometries tested ranged from no effect to an appreciable reduction in chute water levels. The ramp effectiveness at reducing chute water levels jumps once the ramps reach a certain height compared to the weir crest (~1/2).

Introduction

Spillway design can benefit from the combination of various highly efficient components such as nonlinear weirs for discharge efficiency and stepped chutes to aid with kinetic energy dissipation. The increased spillway discharge capacity of nonlinear weirs, such as labyrinth weirs, help to safely meet design floods discharge requirements while allowing water storage and supply to be maximized. Stepped chutes, which can increase spillway chute energy dissipation relative to smooth chutes (Rajaratnam 1990), can decrease the required size of a downstream energy dissipation structure. Relative to smooth chutes, stepped chutes can also be more economical to construct [e.g., formwork and roller compacted concrete (RCC) (Boes and Hager 2003)] relative to smooth chutes. Individually, these two spillway components can be of significant benefit, but it is unclear what hydraulic and economic impacts combining both into a single spillway might have.

At multiple locations in the USA, new reservoirs are in various stages of planning and completion in response to population growth and urbanization. For example, in 2017 construction began on the Cobbs Creek Reservoir (Virginia, USA), a new 18.2-billion-liter pumped storage impoundment for water supply. In the west, the Northern Integrated Supply Project (Colorado, USA) includes two new reservoirs to provide water to 11 rapid-growing communities and will incorporate an array of environmental and wildlife mitigations as well as recreational opportunities. Similarly, populations are rapidly increasing in the south-central region of the USA. In support of the design of a new dam in this region, a recent physical model study (1:12 geometric scale) was conducted at the Utah Water Research Laboratory (UWRL). This proposed embankment dam featured a

spillway with a labyrinth weir flow control structure coupled with a steep stepped chute. No specific hydraulic design guidance was available regarding the combination of these two structures. The physical model provided valuable insights regarding the influence of the labyrinth weir on flow bulking and surface waves to size the spillway chute walls, as initial wall heights, sized using results from a computational fluid dynamic (CFD) model were undersized. The flow entering the stepped chute from the labyrinth weir was nonuniform laterally, which contributed to increased surface waves propagating down the length of the stepped chute (see **Figure. 25**).

In an effort to reduce the flow depths and improve the flow transition from the labyrinth weir into the stepped chute, sloping ramped floors were installed in the downstream cycle of the labyrinth weir (Jorgensen 2020). The combination of the sloping ramped floors with a rounded downstream apron transition into stepped chute helped decreased the maximum water levels and wave action.

Previous Research

Stepped chutes

Stepped chute spillways of varying slope and step configuration, located downstream from a linear weir, have been studied extensively. For example, Ruff and Ward (2002) studied steps on a spillway chute with a chute angle (ϕ) of 26.6° (~2.0H:1.0V), utilizing step heights (s) of 0.305 m (1.00 ft) and 0.610 m (2.00 ft). Measured flow depths were representative of the estimate of a clear water or non-air entrained/air entrained flow boundary. The resulting clear water flow depth was then adjusted using various factors to estimate a training wall height with additional freeboard

as required. The primary focus of Ruff and Ward (2002) was to quantify the energy dissipation obtained by using a stepped chute instead of a smooth spillway. and limited their study to the one-stepped chute geometry.

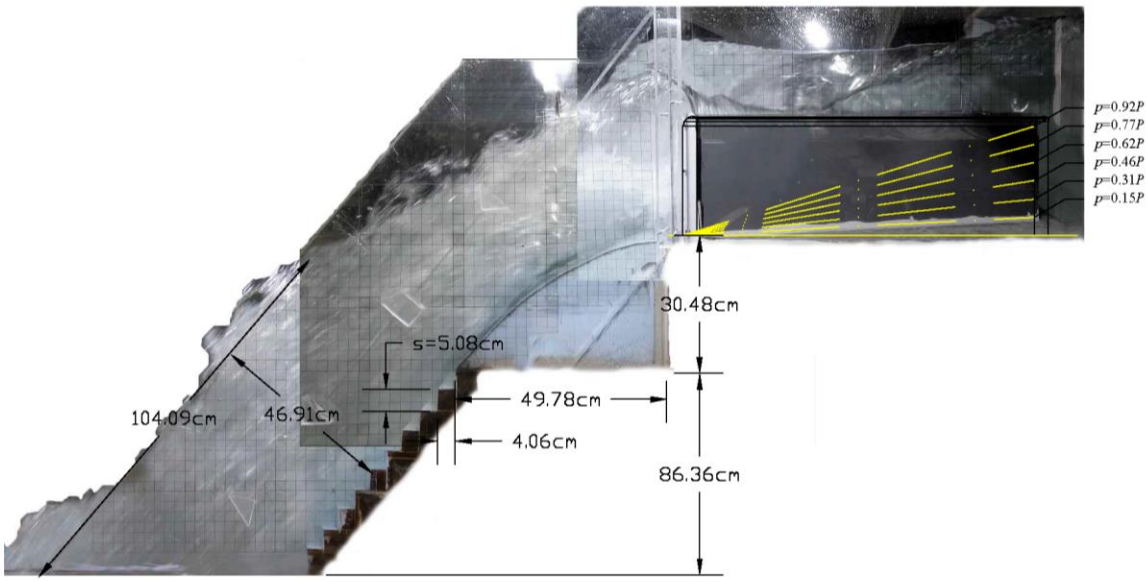

Figure. 25. Instantaneous water surface profile on a stepped chute downstream of a labyrinth weir with dimensions and ramp floor heights shown.

Boes and Hager (2003) evaluated the flow depth on a stepped chute utilizing various values of ϕ [30°, 40°, and 50° or 1.73:1, 1.19:1, and 0.84:1 (H: V)]. Analysis of the tests results found that the flow depth was related to the uniform critical flow depth for a smooth chute and the Froude number. Boes and Hager (2003) reported that, as might be expected, the maximum flow depth decreased with increasing ϕ. When designing a training wall height based on the maximum flow depth, a safety factor should be included to account for splash and other phenomena. Boes and Hager (2003) suggested that the factor of safety should be based, in part, on the potential for negative

impact (e.g., embankment erosion) if the chute walls are periodically overtopped. If the adjacent materials are non-erodible, a safety factor of 1.2 is suggested; if the embankment is highly erosive and the chute is stepped, a multiplier of 1.5 is recommended.

Chanson (2006), investigating the impacts of inflow conditions on stepped chute flow depth, reported that a pressurized inlet condition (e.g., jet box) led to greater downstream chute flow depths, relative to free-surface inflow. Flow over a stepped chute represents a complex two-phase flow condition, which makes it difficult to identify a single root cause for the varied, inlet-dependent flow depths. Seeing a change in flow depth corresponding to inflow conditions could represent a challenge when using stepped chutes in connection with non-linear weirs (such as labyrinth weirs). One such challenge is the added uncertainty associated with identifying an appropriate factor of safety for training wall heights (Boes and Hager 2003) associated with the corresponding three-dimensional flow condition.

Stepped chute flow depth uncertainties are typically handled by multiplying the maximum flow depth (actual or predicted) by a factor of safety. To validate the recommended safety factors in training wall design, Hunt and Kadavy (2017) built a near prototype scale stepped chute at ϕ = 18.4° (3H:1V). The reported maximum splash height was 5.5 times the maximum flow depth (defined as y_{90} by Hunt and Kadavy 2017). Building training wall heights to capture the entirety of splash would likely be cost prohibitive, so Hunt and Kadavy (2017) suggest a factor of safety for chute walls ranging from about 1.2 to 2.0.

Air-water flow uncertainty

A detailed review of air-water flows, including published literature and the

mechanics of air entrainment, is presented in Valero 2018 who clearly demonstrates current limitations regarding the understanding of the air-water flow structure. The aforementioned studies of stepped chutes based upon experimental data from laboratories provide significant practical and scientific insight, but as with this study, share a common limitation due to the challenge of scaling air-water flows from hydraulic models. This scaling challenge introduces uncertainty in all aspects of the self-aeration process including aspects that receive more attention by academics such as the complexities of turbulence, free-surface fluctuations, Taylor and Hinze scale lengths, the boundary layer, bubble formation and movement, etc. to more project-focused hydraulic parameters such as flow depths, air concentration profiles, and energy dissipation at each step in the chute. Scale effects in stepped chutes and more generally in high-speed flows in hydraulic structures, have been discussed, for example, by Kobus (1984), Chanson 2009, Felder and Chanson (2009, 2017), and Heller (2011). Detailed measurements from existing structures in the field remains an urgent need. The authors hope that an opportunity to collect such data for the proposed labyrinth-stepped chute structure may occur in the future and acknowledge that future work is needed to address scale effects related to flow depths in stepped chutes with a labyrinth crest.

Stepped chutes with nonlinear weirs

As described previously, there are various benefits in using both stepped chutes and non-linear weirs in dam design. The benefits of using these two structures in combination can be greatly reduced if the designed chute walls are undersized, which could lead to an increased risk of erosion due to overtopping (Hunt and Kadavy 2017) and, in extreme cases, dam failure and loss of life. Typically, research, hydraulic

modeling, and previous designs are used to limit this risk. In this particular case, however, limited information is available regarding stepped chutes in combination with nonlinear weirs. As a result, physical models for project-specific designs are conducted to verify the hydraulic performance of the spillway.

One such study related to the Charmine Dam in France, found a potentially significant benefit from combing a stepped chute with a Piano Key Weir (PKW) (Loisel et al., 2014). It was reported that for the geometry tested, replacing the existing smooth chute with a stepped chute resulted in both decreased flow depth (reduced chute wall height requirements) and residual energy (reduced stilling basin size). Similar studies have been conducted for dams in both Vietnam (Dakm 2 HPP and Vinh Son 3 HPP [Ho Ta Khanh et al. 2011]) and France (Gloriettes [Bieri et al. 2011]), highlighting the potential benefits of utilizing both structures in combination.

Regarding research specific to nonlinear weirs in combination with stepped chutes, Epricum et al. (2011) compared the hydraulic behaviors of PKW and ogee crest weir structures in conjunction with a relatively long, steep, stepped chute (slope angle θ = 52°) versus a smooth chute. Reported results found little to no difference in residual energy at the entrance of the downstream stilling basin between the various alternatives. However, Epricum et al. (2011) reported that the inception point of air in the flow for PKW geometries was immediate and hypothesized that this could result in a potential spillway length decrease and cost savings.

In an effort to expand the nonlinear weir and stepped chute research to include labyrinth weirs, the current study investigated the hydraulic behavior of a two-cycle labyrinth weir follow by a steep stepped chute (0.8H:1V) in a sectional model

configuration. The laboratory-scale spillway structure was a 1:12 scale model of a prototype dam in Texas (USA). The spillway was initially designed based on computational fluid dynamics (CFD) modeling, using a RANS-based, RNG k-ε, single fluid approach. Based on the findings of the physical model, two issues were identified that warranted further analysis (Jorgensen 2020):

- flow depths in the chute were significantly greater than predicted by the CFD model, requiring an increase in the required chute wall height
- the presence of water surface (nappe) fluctuations caused by flow surging downstream of the weir

Both issues were mitigated to some degree by incorporating ramps into the downstream cycle of the labyrinth weir (somewhat similar to the PKW geometry). The redirection of the flow entering the stepped chute by the ramps decreased both the flow surge and the stepped chute flow depth. The current study systematically evaluated the hydraulic behavior of various ramped (outlet cycle) labyrinth weir configurations on flow surging and water surface levels and fluctuations in a steep stepped chute.

Methodology and Experimental setup

All tests were conducted in a laboratory-scale spillway at the UWRL at Utah State University. The physical model consisted of three main components: a two-dimensional (sectional) upstream reservoir head box (1.02 x 5.97 x 3.05 m), a 2-cycle labyrinth weir with a sidewall angle (α) of 10.67° on a horizontal apron, and a steep stepped spillway with a rounded upstream apron transition (consisting of three arcs [R = 44 cm, 70cm, and 116 cm] with arc lengths of 20, 20 and 15 cm respectively).

Water was supplied from a nearby reservoir via gravity to the headbox through a

system of pipes (61-cm in diameter) that included calibrated venturi meters (±0.2%). Upon entering the headbox, flow passed through a baffle wall and surface wave suppressor to improve reservoir approach flow uniformity. The main chamber of the headbox was 4.73-m long and led to a 0.8H:1.0V (ϕ = 51.34°) ramped approach leading to the horizonal spillway apron. The labyrinth weir upstream apexes were located 15-cm downstream from the leading edge of the horizontal apron.

The dimensions of the 2-cycle labyrinth weir are presented in Table 1 and were developed based on the design method by Crookston and Tullis (2013). The rounded crest of the labyrinth weir was ogee-like with the upstream and downstream radii equal to 1/3 and 2/3 the weir wall thickness (t_w), respectively (see **Figure. 25** and **Figure. 26**). One wall of the model was made of transparent acrylic sheet to facilitate flow visualization.

Table 5. As-Built Labyrinth Weir Geometry

Parameter	Dimension
α	10.67°
w	0.51 m
W	1.02 m
B	1.02 m
t_w	3.81 cm
A	3.81 cm
P	33.01 cm

A schematic of the relatively steep [0.8H:1V (ϕ= 51.34°)] stepped spillway chute is presented in **Figure. 25** along with details of the rounded upstream transition. The intersection of the rounded transition and the top step was used as the cartesian coordinates origin reference. To facilitate documenting the water surface data, a

transparency grid (2.54 x 2.54 cm mesh size) was installed on the acrylic sidewall of the spillway and weir apron.

In total, seven different labyrinth weir configurations were tested: a no-ramp configuration consistent with Crookston and Tullis 2013, and six alternatives featuring the same weir but with sloping ramped floors of varying heights installed in the downstream cycles. Each ramped floor extends from the downstream side of the upstream apex to a line tangent with the most distal point of the downstream apexes. (see **Figure. 26**). The edges of the ramped floors were sealed to ensure that all flow was redirected along the ramped floor. The upstream ramp heights (*p*), measured vertically from the apron, equaled 0.15, 0.31, 0.46, 0.62, 0.77, and 0.92*P*, where *P* represents the weir height. The ramped floor height of 0.92 *P* tied into the tangent point between the downstream vertical weir face and the rounded crest (i.e., maximum ramp height permissible without distorting the crest profile).

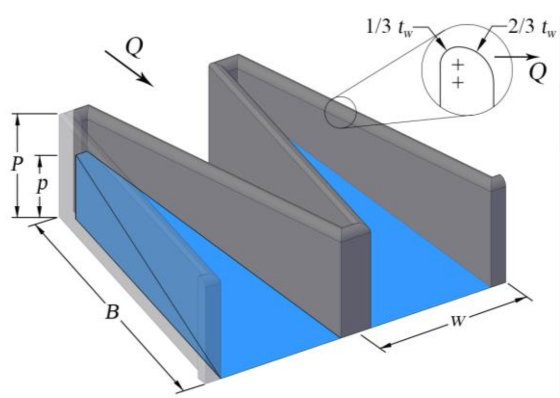

Figure. 26. Example of a sloping ramped floor installed in the downstream cycle of a labyrinth weir (isometric view).

To capture the flow behavior and extract maximum water level data, three digital

video cameras (GoPro, 30 frames/second)) were installed along the length of the spillway and flow. The three cameras were spaced sufficiently far apart to provide a continuous view from the apron transition through the majority of the stepped chute, and close enough to minimize optical distortion in the resulting images. Video data were used to approximate the maximum temporal water levels along the weir, the rounded transition, and the stepped chute. Every 7th frame was captured from the videos for evaluation, resulting in an image frequency of ~4.3/sec. The water surface profiles from the still images were evaluated and ultimately combined to produce a representative minimum and maximum water surface profile (i.e., the minimum and maximum water elevations at each interrogation point were determined from the capture images selected and plotted).

Water surface profiles were documented and processed for three different discharges (low, medium, and high). These discharges also corresponded to specific flow conditions at the labyrinth weir; namely no, moderate, and significant local submergence. (see **Figure. 27**). The discharge conditions are characterized as a function of the dimensionless upstream head, *H/P*, were *H* is the upstream total head (piezometric head plus average velocity head) measured relative to the crest elevation, as well as unit discharge (*q*).

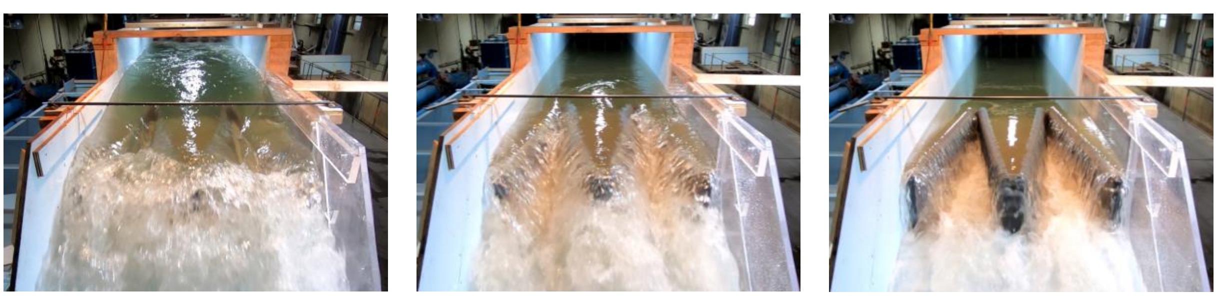

(a) (b) (c)

Figure. 27. Examples of flow interactions on weir apron for the three observed flow rates

(a) $H/P \approx 0.878$ (b) $H/P \approx 0.367$ and (c) $H/P \approx 0.186$ (photos courtesy of Tucker Jorgensen).

For the largest discharge condition with $H/P \approx 0.878 \pm 0.028$ [$q \approx 0.53$ m^3/(s·m)], the upstream apexes experienced local submergence (see **Figure. 27a**). For the medium discharge $H/P \approx 0.367 \pm 0.012$ [$q \approx 0.23$ m^3/(s·m)], the upstream apexes experienced local submergence but to a lesser extent (see **Figure. 27b)**. Nappe interference occurred along the full length of the weir, which also influenced discharge patterns. For these two discharges, flow exiting the labyrinth weir, though highly turbulent and temporally variable, consisted primarily of two different patterns, the nearly horizontal jet exiting the downstream cycles and the vertically plunging jet passing over the downstream apexes. These complicated, three-dimensional flow patterns converge at the rounded apron transition. For the smallest discharge $H/P \approx 0.186 \pm 0.005$ [$q \approx 0.11$ m^3/(s·m)], local submergence did not occur, minimal nappe interference was present, and in contrast to the two larger flow rates, a nearly uniform flow profile (laterally) entering the rounded apron transition was observed (see **Figure. 27c**).

For each test, the reported flow rate corresponds to an averaged value monitored over a 5-7-minute period. Once the appropriate discharge was set, videos were recorded with each of the three GoPro cameras. Video recordings had a duration of 10 seconds or the time required to capture three major waves propagating the length of the spillway, which ever was longer. Processing of the video data to obtain water surface levels and flow depths consisted of the following steps (verification of the method follows).

- Extracting still images at a frequency of 4.3/sec for a minimum of ~ 7 seconds (i.e., 30 images).
- Tracing of instantaneous water surface level in each still image using

AutoCAD.

- Tabularizing the water surface level data using WebPlot Digitizer.
- Aggregating the water surface level data at fixed stationing with 0.64 cm spacings.
- Identifying the maximum and minimum water level at each station from the tabular data.
- Compilating aggregated maximum and minimum water surface profiles for each discharge and ramp configuration.
- Calculating of perpendicular water depth based on the representative maximum water surface profile.

Experimental Results

To verify the described method of extracting the water surface for the various tests, a baseline condition needed to be verified. This was done by extracting the maximum water surface level using both the described photographic extraction method and by hand for the $H/P \approx 0.878$ flow condition. The hand method included marking the maximum water surface onto the acrylic side wall at a spacing of 2.54 cm. The offset from the 2.54 cm grid was quantified using a ruler and the transparent grid. Unlike the photographic method, there are no limitations in the number of "images" the human eye can process at each point to obtain a maximum water surface. This leads to a greater reliability in capturing the true maximum water surface. While there is some variation, it is important to remember that the chute wall height is suggested to be anywhere from 1.2 to 2.0 times the maximum water depth to be appropriately conservative (Chanson and Toombes 2002 and Hunt and Kadavy 2017).

Overall, the hand traced, and computer traced maximum water levels compare quite favorably. One region of concern is directly over the rounded apron transition. Assuming the hand traced surface to be more accurate, the digitized photographic method underestimated the flow depth over the rounded transition. Observations found a significant amount of splash at the location, for the high-flow conditions, associated with the nappes colliding together. As a result, in highly aerated regions of the spillway (e.g., the rounded apron transition), the photographic method often underestimated the water depth by misidentifying this boundary. The maximum water surface locations for both methods produced very similar results near the labyrinth weir and through most of the stepped chute. The comparison between the hand-drawn and photographic methods overall showed sufficient accuracy (see **Table 6**) to validate the photographic method as viable and representative for estimating the maximum water surface for this spillway configuration.

Table 6. Percent Difference of hand measured, and photo extracted perpendicular flow depths.

Spillway Location	Average % Diff. in Depth
Stepped Chute	0.20
Rounded Transition	-6.05
Horizontal Apron	2.21

Aggregated Maximum Chute Water Level Results for *H*/*P* ≈ 0.878.

Observations during testing showed temporal and spatial variations in the spillway water surface profile both longitudinally and laterally (see **Figure. 25**) caused by high turbulence levels and wave propagation. Data from the photographic extraction

methodology was used to produce aggregated maximum and minimum water surface profiles. The aggregated maximum water level represents the highest water level at each interrogation point along the spillway, the maximum water level was documented regardless of where it occurred along the lateral flow cross section at each measurement location. The aggregated minimum water level was produced in a similar fashion and represents the minimum water level occurring along the observable sidewall of the stepped chute. Statistics for the aggregated maximum and minimum water surface profiles for the $H/P \approx 0.878$, no-ramp and the six ramped configurations are shown in **Figure. 28**.

The data in **Figure. 28** show that as flow traverses through the spillway (e.g., from the downstream end of the labyrinth weir and into the stepped chute), the magnitude of the water surface fluctuation increases, which may be attributed in part to the high turbulence levels associated with stepped chutes as well as the flow conditions created by the labyrinth weir discharge, including air bulking.

The impact of adding ramped floors to the downstream labyrinth weir cycles on the aggregated maximum water surface profiles varied from no effect to appreciable, depending on ramp height. Ramps with $p \leq 0.31P$ had minimal effect on the water surface profile while ramps with $p \geq 0.46P$ were effective in reducing the aggregated maximum water surface profile (see **Figure. 28**). In general, the amount of decrease in the spillway water levels fell under two categories, no change for $p \leq 0.31P$ and a significant decrease once $p \geq 0.62P$ (changes are quantified in the following sections).

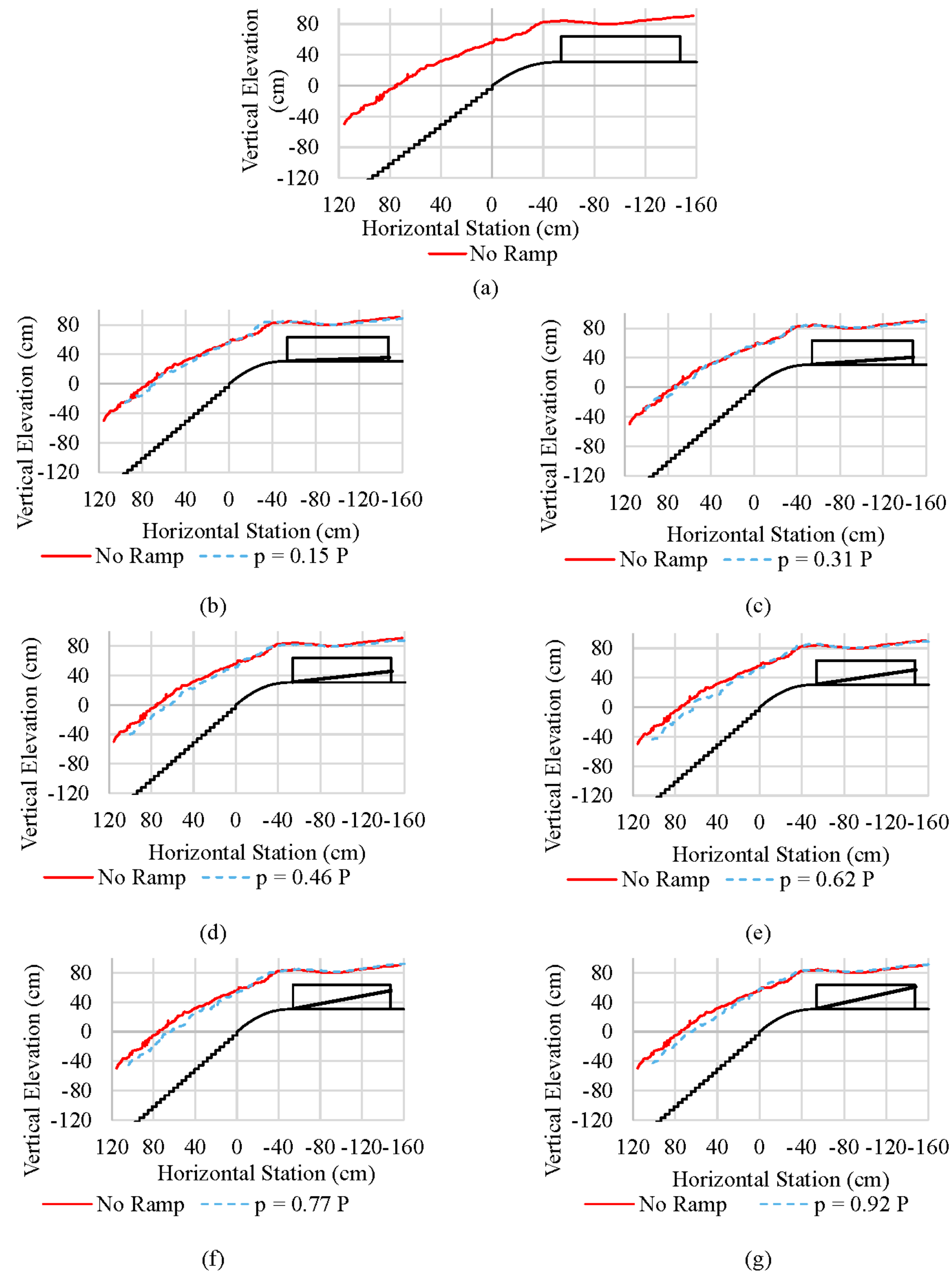

Figure. 28. Comparisons of aggregated maximum water surface profiles for various ramped and no-ramp labyrinth weir configurations (a) p = 0.15P, (b) p = 0.31P, (c) p = 0.46P, (d) p = 0.62P, (e) p = 0.77P, and (f) p = 0.92P.

To create a dimensionless relative flow depth, the perpendicular flow depth along the spillway (y_p) is divided by the *s*. With the different structural components of the spillway, the flow behaved differently based upon the location.

The flow depth decreases as it passes over the labyrinth weir and then increases as it approaches the downstream apexes. The rounded apron transition represents a region of dramatic change in flow depth. Once the flow reaches the stepped chute, the depth continues to increase until a quasi-uniform depth is reached. The quasi-uniform flow corresponds to a condition where water surface profiles are solely a function of the discharge and stepped chute geometry, the inlet flow conditions no longer being a factor.

Figure. 29 consolidates the relative perpendicular flow depth data, segregated by ramp height, for the $H/P \approx 0.878$ flow condition. Because of the minimal reduction in water level associated $p \leq 0.31P$, ramps within this height range are not recommended for chute wall height reduction. Installing ramped floors with $p \geq 0.46P$ resulted in a more appreciable reduction in the aggregated maximum water surface profile (~15%). Because of the relatively consistent results for $p \geq 0.46P$ and because shorter ramps are likely more economical, ramps with $p \approx 0.5P$ are recommended over taller ramps for reducing chute wall height requirements for labyrinth weirs followed by a relatively steep stepped chute.

Table 7 provides a comparison of the maximum apron relative flow depth and the quasi-uniform relative flow depth. There are two trends observed; an increase in the maximum weir apron flow depth with an increase in $p \geq 0.77P$ and a decrease in the quasi-uniform flow depth once $p \geq 0.62P$. Since the chute training wall height is associated with the quasi-uniform flow depth, maximizing the decrease in chute training

wall height is obtained for any $p \geq 0.62P$. The maximum weir apron relative flow depth is associated with the hydraulic efficiency of the labyrinth weir (Jorgensen 2020). Thus, to maximize the hydraulic efficiency of the labyrinth weir, p should be $\leq 0.62P$. Combining the two recommendation, ramps with $p \approx 0.5P$ is recommended for the geometry tested. While the intended purpose of the study was to study the decrease in the required chute wall height, it was also noticed that at certain flows the variability of the flow was decreased (see **Figure. 30**). However, this was not the case for $H/P \approx 0.878$.

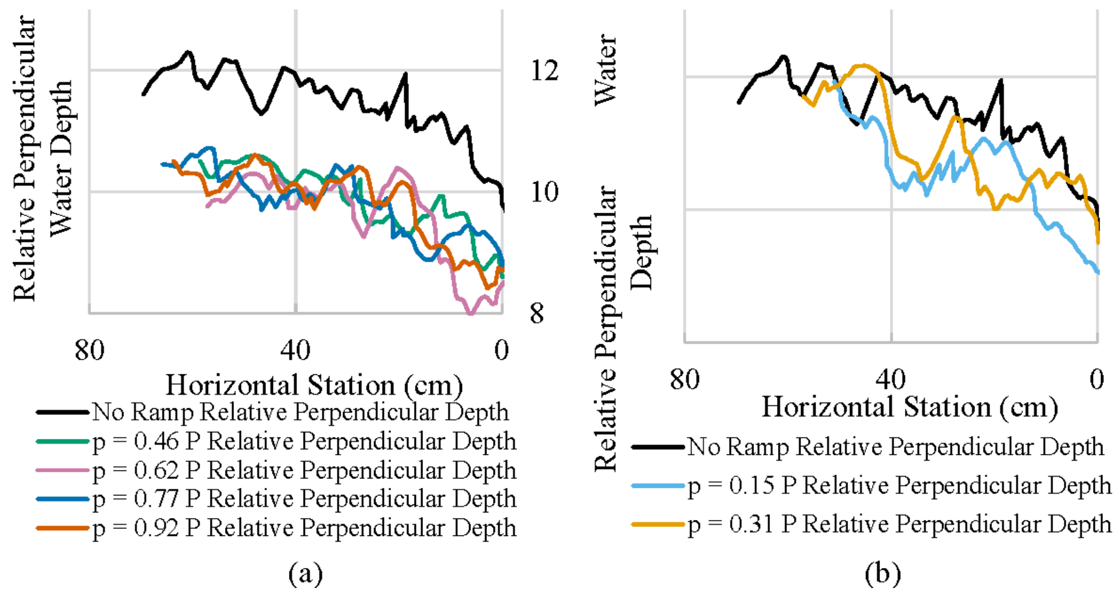

Figure. 29. Spillway relative flow depths measured perpendicular to the spillway profile and normalized by the vertical step height ($H/P \approx 0.878$) for the no-ramp configuration and: (a) $p = 0.15P$ and $0.31P$ and (b) $p = 0.46P$, $0.62P$, $0.77P$, and $0.92P$. (Negative station represents distance from transition of rounded transition to stepped chute).

Table 7. Quasi-uniform relative flow depths on spillway for *H*/*P* ≈ 0.878.

Ramp Scenario	Weir Apron Relative Depth	Chute Quasi-Unifrom Relative Depth
No Ramp	11.81	12.30
$p = 0.15\,P$	11.48	11.93
$p = 0.31\,P$	11.51	12.16
$p = 0.46\,P$	11.15	10.60
$p = 0.62\,P$	11.52	10.40
$p = 0.77\,P$	12.12	10.72
$p = 0.92\,P$	11.99	10.61

Aggregated Maximum Chute Water Level Results for *H*/*P* ≈ 0.367.

The use of ramps with a mid-range discharge (*H/P* ≈ 0.367) had no appreciable or consistent impact on the maximum relative flow depth on the stepped chute (see **Table 8**). Comparing the data presented in **Table 7** and **Table 8**, there are changes in the impacts on the quasi-uniform chute depth. Instead of creating a decrease in the chute depth, there is a decrease and then an increase in chute flow depth as *p* increases. This is not of major concern in chute wall height depth since lower values of *H*/*P* are not used for design. Potential benefits from the ramps at *H*/*P* ≈ 0.878 stems from decreasing the temporal fluctuations in flow depth. **Figure. 30** shows the difference between the maximum and minimum water surface levels with all tested *p*/*P* values. Though water surfaces still fluctuated temporally as shown in **Figure. 30**, observations for all ramped floors configurations at *H/P* ≈ 0.367 revealed that the fluctuations increase until $p = 0.31$ and then decreased. Further testing would be needed to verify any benefits gained in either safety or energy dissipation from this change.

Table 8. Quasi-uniform relative flow depths on spillway for *H*/*P* ≈ 0.367.

Ramp Scenario	Weir Apron Relative Depth	Chute Quasi-Uniform Relative Depth
No Ramp	8.91	7.18
p = 0.15 *P*	8.49	7.07
p = 0.31 *P*	8.69	6.67
p = 0.46 *P*	8.69	6.77
p = 0.62 *P*	8.58	6.93
p = 0.77 *P*	8.80	7.53
p = 0.92 *P*	8.78	7.20

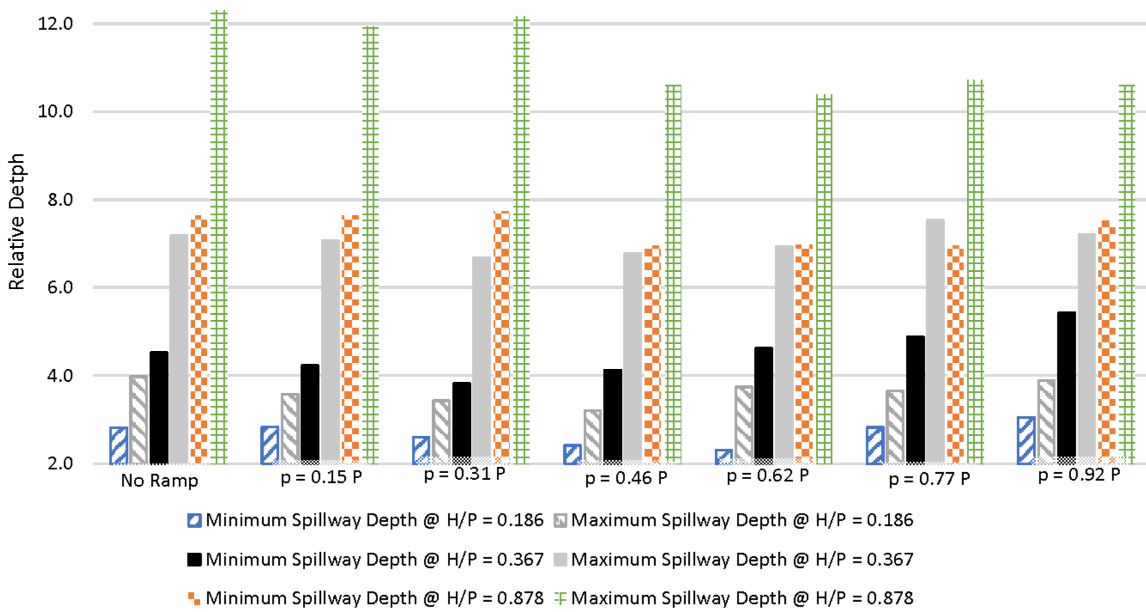

Figure. 30. Flow variation from maximum to minimum quasi uniform chute depths at *H*/*P* ≈ 0.878, *H*/*P* ≈ 0.367, and *H*/*P* ≈ 0.186 for all tested values of *p*.

Aggregated Maximum Chute Water Level Results for *H*/*P* ≈ 0.186

Testing of the ramps at H/*P* ≈ 0.186 (low discharge) found no appreciable impacts on the flow depths experienced throughout the spillway. The maximum relative depth on the stepped chute was nearly the same, independent of *p*, as was the apron water surface

(see **Table 9** and **Figure. 30.** Flow variation from maximum to minimum quasi uniform chute depths at $H/P \approx 0.878$, $H/P \approx 0.367$, and $H/P \approx 0.186$ for all tested values of *p*.). Observations during testing found that the flow at the inlet of the stepped chute reached the quasi-uniform flow depth almost immediately downstream of the rounded transition. Despite this, there was still variability in the flow depth based in *p* (see **Figure. 30**). While this is similar to the other *H*/*P* tested, the ramps associated with the lowest quasi uniform chute depth was $p = 0.46P$. These ramps were not associated with a decrease in flow depth for the other *H*/*P* tested. However, using $H/P \approx 0.187$ as the design value would be impractical, therefore this range should not be used to determine the use or not of sloping ramped floors in coupling a labyrinth weir with a steep stepped chute. Similar to ramps with $H/P \approx 0.367$, ramps with $H/P \approx 0.186$ sees similar change in temporal surface fluctuations.

Table 9. Quasi-uniform relative flow depths on spillway for $H/P \approx 0.186$.

Ramp Scenario	Weir Apron Relative Depth	Chute Quasi-Uniform Relative Depth
No Ramp	7.68	3.98
$p = 0.15\,P$	7.65	3.58
$p = 0.31\,P$	7.65	3.42
$p = 0.46\,P$	7.64	3.20
$p = 0.62\,P$	7.64	3.74
$p = 0.77\,P$	7.72	3.65
$p = 0.92\,P$	7.68	3.89

Conclusions

Economic benefits of combing both a labyrinth weir and a stepped chute are, in part, dependent upon the coupled hydraulic performance. Of concern in coupling labyrinth weir with a steep stepped chute is the drastic change to the inflow conditions compared to that required for existing design methods. Changing the inflow conditions to

the stepped chute can lead to an increase in flow depth and variability. The installation of sloping ramped floors into labyrinth weir downstream cycle can help to redirect the flow down the chute, potentially minimizing the flow depth (and the required chute training wall height). Ramps of various geometries were tested to observe the impacts to the flow depth in the stepped chute. In particular, the maximum flow depth was calculated to understand the required chute training wall heights.

Ramped floors with heights (p) of 0.15, 0.31, 0.46, 0.62, 0.77, and 0.92 the weir crest height (P), were installed and tested. The testes were performed using a steep stepped chute with a chute angle (ϕ) of 51.34° (0.8H:1.0V) and steps with a height (s) of 2.05 cm. The flow conditions on the model stepped chute were observed for flow rates corresponding to $H/P \approx 0.878$, 0.367, and 0.187 to represent different inflow conditions from the labyrinth weir. Testing the model spillway with no-ramp found that for $H/P \approx$ 0.878 and 0.367 the water surface level in the stepped chute was both spatially and temporally variable. Once flow reached the inlet to the stepped chute for $H/P \approx 0.187$ the flow established a quasi-uniform condition.

Test with the various ramp heights at $H/P \approx 0.878$ found an impact to the flow depth in the stepped chute. This impact was negligible for $p \leq 0.31P$ and increased drastically once $p \geq 0.46P$. If $p \geq 0.46P$ the perpendicular flow depth in the stepped chute was reduced by ~13-15%. While this can help with the economics of the dam spillway, installation of ramps with $p \geq 0.62P$ raised the apron flow depth. This results in an increased upstream water surface elevation, decreasing available water storage and potentially negatively impacting the economics of the dam spillway. The flow impacts observed at $H/P \approx 0.878$ where no longer observed for $H/P \approx 0.367$ and 0.187.The

economic impact of using ramped floors at lower values of H/P would be entirely dependent upon investigating any changes to energy dissipation. However, it is recommended that sloping ramped floors be designed with $p \approx 0.5P$ when coupling a labyrinth weir with steep stepped chutes, especially for high head dams.

It was found that utilizing sloping ramped floors in the downstream cycle of a labyrinth weir can reduce the maximum flow depth on a coupled steep stepped chute. The reduction in flow depth would lead to a similar reduction in the required training wall heights. However, the exact results are specific to the labyrinth weir and stepped chute geometries tested with the given flow conditions. Understanding the exact impact ramps would have on other systems would require further testing. Physical testing is suggested by the author at this time due to a lack of calibration data, increasing the uncertainty of parameter selection for any CFD model. As physical model studies of couple labyrinth weirs and stepped chutes increases, the potential for CFD modeling should then be explored more thoroughly.

Acknowledgments

This study was funded by the State of Utah and the Utah Water Research Laboratory at Utah State University.

CHAPTER VII

CONCLUSION

Studying and understanding how dam structures interact can be important in predicting their combined dam safety. This is particularly true when combing non-linear weirs (such as a labyrinth weir) with stepped spillways that traditional employ a simple linear weir. By using a labyrinth weir instead of a traditional linear weir, the expected flow conditions can vary drastically. This variation is of concern since the design guidelines are dependent upon the incoming flow condition. A recent study done at the Utah Water Research Laboratory (UWRL) found that the combination of a labyrinth weir with side wall angle $\alpha = 10.67°$ and a stepped spillway with a slope of 0.8H:1.0V resulted in depths significantly deeper than predicted using computation fluid dynamics modeling (CFD) and traditional design methods. As a direct result of these observations, this study was conducted to find a method to minimize the flow depth experienced on the stepped spillway while minimizing negative impacts to the hydraulic efficiency of the labyrinth weir.

Overview of Study Setup and Tests

This study addressed the challenge of minimizing flow depth in the stepped spillway by installing sloping ramped floors into the downstream cycles of the labyrinth weir. Including a baseline non-ramped labyrinth weir, a total of seven different configurations were tested. The ramps were classified by the relationship between the maximum height of the ramp and the weir crest height (P). Tested relationships were 2/13, 4/13, 6/13, 8/13, 10/13, and 12/13 of P. A maximum height of the ramps is located at the base of any crest shape to minimize hydraulic impacts particularly at low

relationships of upstream head (H/P). The effects on hydraulic efficiency was calculated by the changes caused to the dimensionless discharge coefficient (C_d) of the labyrinth weir compared to the non-ramped weir. This was done over a range of flows and H/P to observe trends. Flow depths were calculated at three different flow rates Q ≈ 19.21, 8.20, and 4.14 cfs.

Impacts to Hydraulic Efficiency of a Labyrinth Weir with Sloping Ramped Floors in Downstream Cycle.

The installation of ramped floors into the downstream cycles of a labyrinth weir had varying impacts to the hydraulic efficiency depending the ramp height and the value of H/P. For instance, at low values of H/P (~ < 0.250) only the tallest ramp height of 12/13 P impacted the hydraulic efficiency of the labyrinth weir. As H/P is increased above 0.250, more of the ramp heights begin to have an impact on the hydraulic efficiency. Ramp heights of 8/13, 10/13, and 12/13 P have the greatest impact. The observed decrease in hydraulic efficiency increases with both ramp height and with H/P. When the ramp is lowered to 6/13 P or less, the decrease in hydraulic efficiency becomes minimal even at the highest values of H/P tested (~ 2-3%).

Impacts to flow depth on a steep stepped spillway with a labyrinth weir upstream.

Using a labyrinth weir in conjunction with a steep stepped spillway resulted in 3d non-uniform flow conditions the length of the stepped spillway. Observations during testing found that without installing the sloping ramped floors a wave of varying flow depth propagates down the spillway. This wave is a potential cause of the significant increase in flow depth compare to what was predicted prior to the previous model study.

By understanding and minimizing the expected flow depth on the spillway, training wall heights can be lowered and designed with greater confidence.

Testing at the maximum flow found that for the non-ramped labyrinth weir and the labyrinth weir with ramp heights of 2/13 and 4/13 P the maximum flow depths observed on the stepped spillway were approximately equal to or greater than the flow depth over the labyrinth weir apron at the highest flow. A second lower maximum flow depth was observed for all ramp heights of 6/13 P and greater. Using the higher ramp heights lowered the maximum flow depth experienced on the stepped spillway significantly (~13-15%). For lower flows, the result of varying the ramp heights did little to vary the maximum flow depth on the stepped spillway. The observed flow depth at the lower flow rates for all ramp heights was also found to be less than the flow depth over the weir apron.

Observations during testing identified that the propagating wave height was decreased for the taller ramps, at the highest flow rate tested. Minimizing the wave height is potentially the cause of the decreased flow depth for the maximum flow rate. Further observations identified that for the higher ramp heights the flow seemed to remain in greater contact with the stepped spillway. This was identified as the at a point variation in flow depth over time decreased based upon the ramp height. It is anticipated, and requires further validation through testing, that this increased contact with the spillway could also increase energy dissipation by the stepped spillway.

While ramp heights of 6/13 P and greater had little effect on the flow depths at the two lower flows, it did significantly lower the flow depth at the maximum flow. Since the maximum design flood for a spillway is used sizing training wall heights, the use of a

ramp height of 6/13 P for the geometry tested in this study. Further physical model testing should be done on various spillway and labyrinth weir geometries to further validate the observations. Physical testing is preferred over CFD due to the major discrepancies found at the UWRL.

Recommendations for Coupling a Labyrinth Weir with a Steep Stepped Spillway

Coupling a labyrinth weir with a steep stepped spillway requires consideration of both the hydraulic efficiency of the weir and the flow depth on the stepped spillway. It is recommended for the geometry tested that a sloping ramped floor be installed in the downstream cycle of the labyrinth weir at a height equal to 6/13 the weir crest height (P). The tests of this scenario showed both a minimal impact to the hydraulic efficiency while still minimizing the spillway wall height to the maximum extent possible. It is also recommended, due to the complex 3D nature and poor CFD approximations, that further tests be first done using physical laboratory scaled modeling for additional geometries not tested as part of this study.

Lessons Learned and Future Research

In the process of this study, various things were learned beyond the original scope of the work. One major thing learned was the challenge associated with extracting the aggregated water surface level information. With the goal to understand more than just the maximum surface the combination of videos and photos were used. This effort was significantly more difficult due to the setup used. The background and varying surfaces made it difficult to use computer learning programs to be able to extract the water surface data automatically. Potential fixes to this issue include adjusting the background wall

height to be significantly higher than necessary to ensure that it is always beyond frame. This would help to create a solid background color to assist in extraction of the aggregated water surfaces. In addition to helping speed up the process of extracting the water surface data, it would potentially allow for an increase in the number of photos that could then be processed. This might allow for smoother aggregated water surfaces allowing for easier comparison of the different setups tested.

Another lesson learned was the importance of using the proper visual recording equipment for the goal of the study. The use of GoPro cameras was useful in being able to record the flow conditions, however, limitations in the focal length made it difficult to capture the entire model spillway in a single image. This essentially tripled the required data collection and even further increased the time to aggregate the water surface levels. Using a camera with a longer focal length would allow for capturing the entire model in a single frame, thus potentially decreasing the required number of frames as well as allowing for a greater understanding of the instantaneous flow rate.

Utilizing these lessons, further research should be done. A few of the options include adjusting the slope of the stepped chute or adjusting the height of the steps. This would allow for understanding how the various ramps impact a variety of embankment slopes, increasing the applicability of the research. An additional option is to adjust the geometry of the labyrinth weir. This can be done by altering the sidewall angle or the length of the sidewalls. Since labyrinth weirs are often designed to the available space, this gives a greater variety of ramp geometries and their impacts. An additional parameter that can be adjusted is the approach flow conditions. Altering the flow conditions could change the flow behavior within the labyrinth weir altering the impacts caused by the

ramps, both for the labyrinth weir efficiency and the chute flow depth.

REFERENCES

Anderson A and Tullis B (2017) Weir-flow nappe oscillation: causes & potential mitigation techniques. Journal of Hydraulic Engineering 144(6), 04018020: 1–9.

Bieri M, Fererspiel M, and Boillat J-L (2011) Energy dissipation downstream of piano key weirs-case study of Gloriettes Dam (France). In *Labyrinth and Piano Key Weirs – PKW 2011*. Taylor & Francis, London, UK, pp. 123–130.

Boes, R. M., and Hager, W. H. (2003). "Hydraulic design of stepped spillways." *Journal of Hydraulic Engineering*, 129(9), 671–679.

Chanson, H. (1994). *Hydraulic design of stepped cascades, channels, weirs, and spillways*. Pergamon, Oxford, England.

Chanson H (1996) Free-Surface Flows with Near-Critical Flow Conditions. Canadian Journal of Civil Engineering 23(6): 1272–1284.

Chanson H (2002) *The hydraulics of stepped chutes and spillways*. AA Balkema, Lisse, Netherlands.

Chanson, H. (2006). "Hydraulics of skimming flows on stepped chutes: The effects of inflow conditions?" *Journal of Hydraulic Research*, 44(1), 51–60.

Chanson, H. (2009). "Current knowledge in hydraulic jumps and related phenomena. A suvery of experimetnal results." *European J. of Mechanics*, 28(2), 191-210, https://doi.org/10.1016/j.euromechflu.2008.06.004

Chanson H and Gonzalez CA (2005) Physical Modelling and Scale Effects of Air-Water Flows on Stepped Spillways. Journal of Zhejiang University SCIENCE, 6A(3), March: pp. 243–250.

Chanson, H., and Toombes, L. (2002). "Experimental investigations of air entrainment in

transition and skimming flows down a stepped chute." *Canadian Journal of Civil Engineering*, 29(1), 145–156.

Christodoulou, G. C. (1993). "ENERGY DISSIPATION ON STEPPED SPILLWAYS By George C. Christodouiou, 1 Member, ASCE." *Journal of Hydraulic Engineering*, 119(5), 644–650.

Crookston, B. M. (2010). "LABYRINTH WEIRS." Ph.D. dissertations. Dept. of Civil and Environmental Engineering, Utah State Universtiy, Logan, UT, USA.

Crookston, B. M., Erpicum, S., Tullis, B. P., and Laugier, F. (2019). "Hydraulics of Labyrinth and Piano Key Weirs: 100 Years of Prototype Structures, Advancements, and Future Research Needs." *Journal of Hydraulic Engineering*, 145(12), 1–7. https://doi.org/0.1061/(ASCE)HY.1943-7900.0001646

Crookston, B. M., and Tullis, B. P. (2012a). "Discharge Efficiency of Reservoir-Application-Specific Labyrinth Weirs." *Journal of Irrigation and Drainage Engineering*, 138(6), 564–568.

Crookston, B. M., and Tullis, B. P. (2012b). "Labyrinth weirs: Nappe interference and local submergence." *Journal of Irrigation and Drainage Engineering*, 138(8), 757–765.

Crookston, B. M., and Tullis, B. P. (2013a). "Hydraulic Design and Analysis of Labyrinth Weirs. I: Discharge Relationships." *Journal of Irrigation and Drainage Engineering*, 139(5), 363–370. https://doi.org/10.1061/(ASCE)IR.1943-4774.0000558

Crookston, B. M., and Tullis, B. P. (2013b). "Hydraulic design and analysis of labyrinth weirs. II: Nappe aeration, instability, and vibration." *Journal of Irrigation and*

Drainage Engineering, 139(5), 371–377. https://doi.org/10.1061/(ASCE)IR.1943-4774.0000553

Dabling, M. R., and Tullis, B. P. (2018). “Labyrinth weirs with angled approach flow.” *Journal of Hydraulic Engineering*, 144(12), 1–5.

Dabling, M. R., Tullis, B. P., and Crookston, B. M. (2013). “Staged labyrinth weir hydraulics.” *Journal of Irrigation and Drainage Engineering*, 139(11), 955–960.

Erpicum S, Laugier F, Boillat JL, Pirotton M, Reverchon B, and Schleiss AJ (2011) *Labyrinth and Piano Key Weirs – PKW 2011.* CRC Press, London, UK.

Erpicum S, Laugier F, Ho Ta Khanh M, and Pfister M (2017) *Labyrinth and Piano Key Weirs III – PKW 2017.* CRC Press, London, UK.

Erpicum S, Laugier F, Pfister M, Pirotton M, Cicero G, and Schleiss AJ (2013) *Labyrinth and Piano Key Weirs II – PKW 2013.* CRC Press, London, UK.

Erpicum S, Machiels O, Archambeau P, Dewals B, Pirotton M, and Daux C (2011) Energy dissipation on a stepped spillway downstream of a Piano Key Weir – Experimental study. In *Labyrinth and Piano Key Weirs - PWK 2011*, by Erpicum Sébastian, CRC Press, pp. 105–111.

Felder, S. and Chanson, H. (2009). "Turbulence, dynamic similarity and scale effects in high-velocity free-surface flows above a stepped chute", *Exp Fluids*, 47, 1-18, DOI 10.1007/s00348-009-0628-3

Felder, S. and Chanson, H. (2017). "Scale effects in microscopic air-water flow properties in high-velocity free-surface flows", *Exp Thermal and Fluid Sci*, 83(5), 19-36, *https://doi.org/10.1016/j.expthermflusci.2016.12.009*

Hager WH and Schwalt M (1994) Broad-Crested Weir. Journal of Irrigation and

Drainage Engineering, American Society of Civil Engineers, 120 (1): 13–26.

Heller, V. (2011), "Scale effects in physical hydraulic engineering models". *J. of Hydr. Research*, 49(3) 293-306. https://doi.org/10.1080/00221686.2011.578914

Ho Ta Kahn M, Sy Quat D, and Xuan Thuy D (2011) P.K. weirs under design and construction in Vietnam. In *Labyrinth and Piano Key Weirs – PKW 2011*. Taylor & Francis, London, UK, pp 225–232.

Hunt SL, Kadavy KC, and Hanson GJ (2014) Simplistic design methods for moderate-sloped stepped chutes. *Journal of Hydraulic Engineering,* https://doi.org/10.1061/(ASCE)HY.1943-7900.0000938

Hunt SL and Kadavy KC (2017) Estimated splash and training wall height requirements for stepped chutes applied to embankment dams. *Journal of Hydraulic Engineering* 143(11), 1–6

Hay, N., and Taylor, G. (1970). “Performance and design of labyrinth weirs.” *Journal of Hydraulic Engineering1*, 96(11), 2337–2357.

Hinchliff, D., and Lux, F. (1985). “Design and construction of labyrinth spillways.” *15th ICOLD Congress*, IV, 249–274.

Houston, K. (1982). *Hydraulic model study of Ute Dam labyrinth spillway*. Denver, CO.

Hunt, S. L., and Kadavy, K. C. (2017). “Estimated splash and training wall height requirements for stepped chutes applied to embankment dams.” *Journal of Hydraulic Engineering*, 143(11), 1–6.

Lodomez M, Pirotton M, Dewals B, Archambeau P, and Erpicum S (2018) Nappe oscillations on free-overfall structures: An experimental analysis. *Journal of Hydraulic Engineering* 144 (3): 04018001.

https://doi.org/10.1061/(ASCE)HY.1943-7900.0001420.

Lodomez M, Crookston BM, Tullis BP, and Erpicum S (2019) Mitigation techniques for nappe oscillations on free-overfall structures. *Journal of Hydraulic Engineering* 145(2): 04018086. https://doi.org/10.1061/(ASCE)HY.1943-7900.0001558

Loisle PE, Valley P, and Laugier F (2014) Hydraulic physical model of Piano Key Weirs as additional flood spillways on the Charmine dam. In *Labyrinth and Piano Key Weirs II: PKW 2013*, by Sébastian Erpicum, CRC Press, pp. 195–202.

Lux, F. (1989). "Design and application of labyrinth weirs." *Design of Hydraulic Structures 89*, 1989.

Melo, J., Ramos, C., and Magalhaes, A. (2002). "Descarregadors com soleira em labirinto de um ciclo em canais convergentes. Dereminação da capcidad de vazão." *Proc., 6° Congreso da Água*, APRH, Lisboa, Portugal.

Ohtsu I, Yasuda Y, and Takahashi M (2004) Flow characteristics of skimming flows in stepped channels. *Journal of Hydraulic Engineering* 130(9): 860–869 https://doi.org/10.1061/(ASCE)0733-9429(2004)130:9(860) .

Pfister M and Chanson H (2014) Two-phase air-water flows: Scale effects in physical modeling. *Journal of Hydrodynamics, Series B* 26(2): 291–298. https://doi.org/10.1016/S1001-6058(14)60032-9

Potter, M. C., Wyble, B., Hagmann, C. E.,, and McCourt, E. S. (2013). "Detecting Meaning in RSVP at 13 Ms Per Picture." *Attention, Perception, & Psychophysics* 76, no. 2 (December 28, 2013): 270–279.

Rajaratnma, R. (1990). "Skimming Flow in Stepped Spillways." *Journal of Hydraulic Engineering*, 116(4), 587–591.

Rice, C. E., and Kadavy, K. C. (1996). "Model study of a roller compacted concrete stepped spillway." *Journal of Hydraulic Engineering*, 122(6), 292–297.

Ruff, J. F., and Ward, J. P. (2002). "Hydraulic design of stepped spillways." *Rsearch Project 99FC80156*.

San Mauro, J., Salazar, F., Toledo, M. Á., Caballero, F. J., Ponce-Farfán, C., and Ramos, T. (2016). "Modelación física y numérica de aliviaderos en laberinto con fondo poliédrico." *Ingeniería del agua*, 20(3), 127.

Schnitter, N. J. (1994). *A history of dams: the useful pyramids*. Balkema Publications, Rotterdam, The Netherlands.

Seamons, T. R. (2014). "LABYRINTH WEIRS: A LOOK INTO GEOMETRIC VARIATION AND ITS EFFECT ON EFFICIENCY AND DESIGN METHOD PREDICTIONS." *USU Thesis*.

Silvestri A, Archambeua P, Pirotton M, Dewals B, and Erpicum S (2014) Comparative analysis of the energy dissipation on a stepped spillway downstream of a Piano Key Weir. In *Labyrinth and Piano Key Weirs II: PKW 2013,* by Erpicum Sébastian, CRC Press, pp. 111–120.

Sorensen, R. M. (1985). "Stepped spillway hydraulic model investigation." *Journal of Hydraulic Engineering*, 111(12), 1461–1472.

Tullis, B. P., Young, J. C., and Chandler, M. A. (2007). "Head-discharge relationships for submerged Labyrinth Weirs." *Journal of Hydraulic Engineering*, 133(3), 248–254.

Tullis, J. P., Amanian, N., and Waldron, D. (1995). "By J . Paul Tullis , I Member , ASCE , Nosratollah Amanian , 2 and." *Journal of Hydraulic Engineering*, 121(3), 247–255.

Valero D and Bung DB (2018) Reformulating self-aeration in hydraulic structures: Turbulent growth of free surface perturbations leading to air entrainment. International Journal of Multiphase Flow 100(2018): 127–142, https://doi.org/10.1016/j.ijmultiphaseflow.2017.12.011.

Villemonte, J. R. (1947). “Submerged weir discharge studies.” *Engineering News Record*, 139, 54–57.

APPENDICES

APPENDIX A – VBA MACRO CODE FOR WATER SURFACE PROCESSING

VBA code for calculating water depths

```
Option Explicit
Option Base 1

Sub Depth()

'This Module calculates the perpendicular water depth for a given water surface.
'Code within this module is specific to the spreadsheet interface and the physical
'model used within the study.

'Perpendicular water depths refers to the distance between the water surface level
'and the elevation of the model taken with a line perpendicular between a point on
'the water surface and a line representing the model structure. This is also the
'shortest distance between the water surface and the model structure.

'The depths calculated represent the distance to the highest point of the water
'surface at a location. The statistical breakdown of a maximum, average, and
'minimum water depths only the statics of the high point of the water surface over
'time. They do not represent the lowest depths seen within the spillway at any given
'time.


'Note: The stepped spillway is represented as a line tangent to the outmost edge of
'the steps. This is done to be consistent with existing literature on stepped spillways.

'Note: All dimensions are in inches.

'++++++++++++++++++++++++
'Dimensioning of Variables
'++++++++++++++++++++++++

'Length Variables
Dim low As Double, High As Double, nn As Integer

'Counting Variables
Dim i As Integer, J As Integer

'Input Data Variables
Dim X() As Double, Cmin() As Double, Cmax() As Double, Cave() As Double

'Calculated Data Variables
Dim S() As Double, DVmin() As Double, DVmax() As Double, DVave() As Double
Dim DPmin() As Double, DPmax() As Double, DPave() As Double
Dim XXmin() As Double, XXmax() As Double, XXave() As Double
```

```
Dim M As Double, B As Double, MM As Double
Dim BBmin As Double, BBmax As Double, BBave As Double

'+++++++++++++++++++++++++++++++++++
'Inputting Water Surface Data Arrays
'+++++++++++++++++++++++++++++++++++

'Calculating the length of all arrays

low = Worksheets("Combined WS Data").Range("D2").Value
High = Worksheets("Combined WS Data").Range("D3").Value
nn = (High - low) / 0.25 + 1

'Redimensioning the arrarys for the Water Surface Profiles - NOTE: The array
'representing X is the same For Each Of the three water surface profiles.

ReDim X(nn) As Double, Cmin(nn) As Double, Cmax(nn) As Double, Cave(nn) As
Double

'Inputting the water surface elevation arrarys and creating an array representing X

For i = 1 To nn
   X(i) = low + (i - 1) * 0.25
   Cmin(i) = Worksheets("Combined WS Data").Cells(i + 8, 3).Value
   Cmax(i) = Worksheets("Combined WS Data").Cells(i + 8, 4).Value
   Cave(i) = Worksheets("Combined WS Data").Cells(i + 8, 5).Value
Next i

'++++++++++++++++++++++++++++
'Calculation of Dam Structure
'++++++++++++++++++++++++++++

'Redimensioning of Structure Array

ReDim S(nn) As Double

'Calculation of Structure Elevation Array in relation to X arrary from water surface
profiles.

For i = 1 To nn
   If X(i) <= 0 Then
      'Creation of Stepped Spillway Chute
      S(i) = X(i) * (1 / 0.8)
   Else
      If X(i) < 19.75 Then
```

```
            J = J + 1
            'Creation of Ogee crest from measured data points
            S(i) = Worksheets("Dam Structure").Range("B7").Cells(J, 1).Value
        Else
            'Creation of Labyrinth Weir Apron
            S(i) = 12#
        End If
    End If
Next i

'++++++++++++++++++++++++++++++++++
'Calculation of Vertical Water Depth
'++++++++++++++++++++++++++++++++++

'Calculation of vertical water depth is done by taking the elevation of the Water
Surface
'Profile - the Structure Elevation for each pt. (X)

'Re-dimensioning of vertical water depth arrays to match the input dataset lengths

ReDim DVmin(nn) As Double, DVmax(nn) As Double, DVave(nn) As Double

For i = 1 To nn
    DVmin(i) = Cmin(i) - S(i)
    DVmax(i) = Cmax(i) - S(i)
    DVave(i) = Cave(i) - S(i)
Next i

'+++++++++++++++++++++++++++++++++++++++
'Calculation of Perpendicular Water Depth
'+++++++++++++++++++++++++++++++++++++++

'This Loop Calculates the Perpendicular Water Depth for the max, min, and ave
water
'surface profiles.

'Within the loop are three series of if-then statements that allow for calculating the
'perpendicular water depths.

'The Loop first calculates the new (X,Y) based upon assuming the water surface is
over the
'stepped spillway chute.

'The if-then statements then check the assumed location of X to verify the structural
'portion it applies to. If the X is part of a different structural location, a new (X,Y)
```

```
'assuming the water surface is upstream one structural section.

'All perpendicular water depths are calculated using geometric relationships
between a 'point (X,Y) and a straight line with a cartesian coordinate system. This
requires 'approximating all structural features of the model as a series of liner
segments that can 'be defined by the equation of a line.

'Re-dimensioning of the Perpendicular Water Depth and X coordinate arrays

ReDim DPmin(nn) As Double, DPmax(nn) As Double, DPave(nn) As Double
ReDim XXmin(nn) As Double, XXmax(nn) As Double, XXave(nn) As Double

'Establishing Initial Structural Conditions (Downstream end of the Stepped Spillway
'Chute)

i = 1
M = 1.25: B = 0
MM = -1 / M

Do While i < nn + 1

'This series of if-then statements calculates the Min. Perpendicular Water Depth

  DPmin(i) = Abs(1.25 * X(i) - Cmin(i)) / (Sqr(1.25 * 1.25 + 1))
  BBmin = Cmin(i) - X(i) * MM
  XXmin(i) = -(BBmin - B) / (MM - M)
  If XXmin(i) >= 0 Then
    M = 1.0592: B = 0: MM = -1 / M
    DPmin(i) = Abs(M * X(i) - Cmin(i) + B) / (Sqr(M * M + 1))
    BBmin = Cmin(i) - X(i) * MM
    XXmin(i) = -(BBmin - B) / (MM - M)
    If XXmin(i) >= 1.75 Then
      M = 0.9947: B = 0.3283: MM = -1 / M
      DPmin(i) = Abs(M * X(i) - Cmin(i) + B) / (Sqr(M * M + 1))
      BBmin = Cmin(i) - X(i) * MM
      XXmin(i) = -(BBmin - B) / (MM - M)
      If XXmin(i) >= 6.25 Then
        M = 0.7338: B = 1.9037: MM = -1 / M
        DPmin(i) = Abs(M * X(i) - Cmin(i) + B) / (Sqr(M * M + 1))
        BBmin = Cmin(i) - X(i) * MM
        XXmin(i) = -(BBmin - B) / (MM - M)
        If XXmin(i) >= 9.75 Then
          M = 0.5287: B = 3.8584: MM = -1 / M
          DPmin(i) = Abs(M * X(i) - Cmin(i) + B) / (Sqr(M * M + 1))
          BBmin = Cmin(i) - X(i) * MM
```

```
                XXmin(i) = -(BBmin - B) / (MM - M)
                If XXmin(i) >= 13 Then
                    M = 0.2176: B = 7.2409: MM = -1 / M
                    DPmin(i) = Abs(M * X(i) - Cmin(i) + B) / (Sqr(M * M + 1))
                    BBmin = Cmin(i) - X(i) * MM
                    XXmin(i) = -(BBmin - B) / (MM - M)
                    If XXmin(i) >= 17 Then
                        M = 0.0915: B = 10.231: MM = -1 / M
                        DPmin(i) = Abs(M * X(i) - Cmin(i) + B) / (Sqr(M * M + 1))
                        BBmin = Cmin(i) - X(i) * MM
                        XXmin(i) = -(BBmin - B) / (MM - M)
                        If XXmin(i) > 19.5 Then
                            DPmin(i) = Cmin(i) - S(i)
                            XXmin(i) = X(i)
                        End If
                    End If
                End If
            End If
        End If
    End If
End If

'This series of if-then statements calculates the Max. Perpendicular Water Depth

DPmax(i) = Abs(1.25 * X(i) - Cmax(i)) / (Sqr(1.25 * 1.25 + 1))
BBmax = Cmax(i) - X(i) * MM
XXmax(i) = -(BBmax - B) / (MM - M)
If XXmax(i) >= 0 Then
    M = 1.0592: B = 0: MM = -1 / M
    DPmax(i) = Abs(M * X(i) - Cmax(i) + B) / (Sqr(M * M + 1))
    BBmax = Cmax(i) - X(i) * MM
    XXmax(i) = -(BBmax - B) / (MM - M)
    If XXmax(i) >= 1.75 Then
        M = 0.9947: B = 0.3283: MM = -1 / M
        DPmax(i) = Abs(M * X(i) - Cmax(i) + B) / (Sqr(M * M + 1))
        BBmax = Cmax(i) - X(i) * MM
        XXmax(i) = -(BBmax - B) / (MM - M)
        If XXmax(i) >= 6.25 Then
            M = 0.7338: B = 1.9037: MM = -1 / M
            DPmax(i) = Abs(M * X(i) - Cmax(i) + B) / (Sqr(M * M + 1))
            BBmax = Cmax(i) - X(i) * MM
            XXmax(i) = -(BBmax - B) / (MM - M)
            If XXmax(i) >= 9.75 Then
                M = 0.5287: B = 3.8584: MM = -1 / M
                DPmax(i) = Abs(M * X(i) - Cmax(i) + B) / (Sqr(M * M + 1))
```

```
              BBmax = Cmax(i) - X(i) * MM
              XXmax(i) = -(BBmax - B) / (MM - M)
              If XXmax(i) >= 13 Then
                M = 0.2176: B = 7.2409: MM = -1 / M
                DPmax(i) = Abs(M * X(i) - Cmax(i) + B) / (Sqr(M * M + 1))
                BBmax = Cmax(i) - X(i) * MM
                XXmax(i) = -(BBmax - B) / (MM - M)
                If XXmax(i) >= 17 Then
                  M = 0.0915: B = 10.231: MM = -1 / M
                  DPmax(i) = Abs(M * X(i) - Cmax(i) + B) / (Sqr(M * M + 1))
                  BBmax = Cmax(i) - X(i) * MM
                  XXmax(i) = -(BBmax - B) / (MM - M)
                  If XXmax(i) > 19.5 Then
                    DPmax(i) = Cmax(i) - S(i)
                    XXmax(i) = X(i)
                  End If
                End If
              End If
            End If
          End If
        End If
      End If

    'This series of if-then statements calculates the Ave. Perpendicular Water Depth

     DPave(i) = Abs(1.25 * X(i) - Cave(i)) / (Sqr(1.25 * 1.25 + 1))
      BBave = Cave(i) - X(i) * MM
      XXave(i) = -(BBave - B) / (MM - M)
      If XXave(i) >= 0 Then
        M = 1.0592: B = 0: MM = -1 / M
        DPave(i) = Abs(M * X(i) - Cave(i) + B) / (Sqr(M * M + 1))
        BBave = Cave(i) - X(i) * MM
        XXave(i) = -(BBave - B) / (MM - M)
        If XXave(i) >= 1.75 Then
          M = 0.9947: B = 0.3283: MM = -1 / M
          DPave(i) = Abs(M * X(i) - Cave(i) + B) / (Sqr(M * M + 1))
          BBave = Cave(i) - X(i) * MM
          XXave(i) = -(BBave - B) / (MM - M)
          If XXave(i) >= 6.25 Then
            M = 0.7338: B = 1.9037: MM = -1 / M
            DPave(i) = Abs(M * X(i) - Cave(i) + B) / (Sqr(M * M + 1))
            BBave = Cave(i) - X(i) * MM
            XXave(i) = -(BBave - B) / (MM - M)
            If XXave(i) >= 9.75 Then
              M = 0.5287: B = 3.8584: MM = -1 / M
```

```
                DPave(i) = Abs(M * X(i) - Cave(i) + B) / (Sqr(M * M + 1))
                BBave = Cave(i) - X(i) * MM
                XXave(i) = -(BBave - B) / (MM - M)
                If XXave(i) >= 13 Then
                   M = 0.2176: B = 7.2409: MM = -1 / M
                   DPave(i) = Abs(M * X(i) - Cave(i) + B) / (Sqr(M * M + 1))
                   BBave = Cave(i) - X(i) * MM
                   XXave(i) = -(BBave - B) / (MM - M)
                   If XXave(i) >= 17 Then
                      M = 0.0915: B = 10.231: MM = -1 / M
                      DPave(i) = Abs(M * X(i) - Cave(i) + B) / (Sqr(M * M + 1))
                      BBave = Cave(i) - X(i) * MM
                      XXave(i) = -(BBave - B) / (MM - M)
                      If XXave(i) > 19.5 Then
                         DPave(i) = Cave(i) - S(i)
                         XXave(i) = X(i)
                      End If
                   End If
                End If
             End If
          End If
       End If
   End If
   i = i + 1
Loop

'+++++++++++++++++++++++++++++++++++++++++++
'Printing Calculated Depths Into Spreadsheet
'+++++++++++++++++++++++++++++++++++++++++++

'Printing the Vertical Water Depth

For i = 1 To nn
   Worksheets("Water Depth").Range("B8").Cells(i, 1).Value = X(i)
   Worksheets("Water Depth").Range("B8").Cells(i, 2).Value = DVmin(i)
   Worksheets("Water Depth").Range("B8").Cells(i, 3).Value = DVmax(i)
   Worksheets("Water Depth").Range("B8").Cells(i, 4).Value = DVave(i)
Next i

'Printing the Perpendicular Water Depth and Corresponding X Coordinates

For i = 1 To nn
   Worksheets("Water Depth").Range("G8").Cells(i, 1).Value = XXmin(i)
   Worksheets("Water Depth").Range("G8").Cells(i, 2).Value = DPmin(i)
   Worksheets("Water Depth").Range("G8").Cells(i, 3).Value = XXmax(i)
```

```
  Worksheets("Water Depth").Range("G8").Cells(i, 4).Value = DPmax(i)
  Worksheets("Water Depth").Range("G8").Cells(i, 5).Value = XXave(i)
  Worksheets("Water Depth").Range("G8").Cells(i, 6).Value = DPave(i)
Next i

End Sub
```

VBA code for combining photographic extracted water surfaces

```
Sub Combine()

'This module automates the process of compiling the Raw Water Surface profile
'from three separate profiles Into a Single comprehensive profile. The break points
'between using the three different profiles Is identified visually and passed into
'program.

'The process to combine the raw water surface profiles includes identifying visually
'the intersection points between the three GoPro camera locations. These points are
'then tracked and located within the raw water surface data to calculate the array
'location to splice the data that is than compiled into a single water surface level
'representation.

'+++++++++++++++++++++
'Dimensioning Variables
'+++++++++++++++++++++

'Counter Variables

Dim nn As Integer, i As Integer, n As Integer, Z As Integer
Dim Q As Integer, R As Integer

'Break Point Variables

Dim low As Double, High As Double
Dim COmin As Double, COmax As Double, COave As Double
Dim OWmin As Double, OWmax As Double, OWave As Double

'Break Point Counter Variables

Dim K As Integer, KK As Integer, KKK As Integer, KKKK As Integer, KKKKK As
Integer
Dim L As Integer, LL As Integer, LLL As Integer, LLLL As Integer, LLLLL As Integer
Dim M As Integer, MM As Integer, MMM As Integer, MMMM As Integer, MMMMM As
Integer
```

```
'Input Water Surface Variables

Dim X() As Double, Wym() As Double, Wyx() As Double, Oya() As Double
Dim Oym() As Double, Oyx() As Double, Oyz() As Double
Dim Cym() As Double, Cyx() As Double, Cyz() As Double
Dim WX() As Double, OX() As Double, CX() As Double

'Calculated Water Surface Variables

Dim Cmin() As Double, Cmax() As Double, Cave() As Double

'+++++++++++++++++++++++++++++++++++++++++++
'Inputting of Water Surfaces and Parameters
'+++++++++++++++++++++++++++++++++++++++++++

'Break point values for changing Water Surface Profiles

low = Worksheets("Combined WS Data").Range("D2").Value
High = Worksheets("Combined WS Data").Range("D3").Value
COmin = Worksheets("Combined WS Data").Range("H2").Value
COmax = Worksheets("Combined WS Data").Range("H3").Value
COave = Worksheets("Combined WS Data").Range("H4").Value
OWmin = Worksheets("Combined WS Data").Range("L2").Value
OWmax = Worksheets("Combined WS Data").Range("L3").Value
OWave = Worksheets("Combined WS Data").Range("L4").Value

  '*************************
  'Weir Water Surface Profile
  '*************************

'Count of the number of data points in the Weir array data set

n = 0
Do While Worksheets("Raw WS Data").Range("A5").Cells(n, 1).Value <> ""
  n = n + 1
Loop
n = n - 1

'Re-Dimensioning the Weir Arrays

ReDim WX(n) As Double, Wym(n) As Double, Wyx(n) As Double, Wya(n) As Double

'Creating of Weir water surface arrays
```

```
For i = 1 To n
   WX(i) = Worksheets("Raw WS Data").Range("A5").Cells(i, 1).Value
   Wym(i) = Worksheets("Raw WS Data").Range("A5").Cells(i, 2).Value
   Wyx(i) = Worksheets("Raw WS Data").Range("A5").Cells(i, 3).Value
   Wya(i) = Worksheets("Raw WS Data").Range("A5").Cells(i, 4).Value
Next i

   '**************************
   'Ogee Water Surface Profile
   '**************************

'Count of the number of data points in the Ogee array data set

n = 0
Do While Worksheets("Raw WS Data").Range("F5").Cells(n, 1).Value <> ""
   n = n + 1
Loop
n = n - 1

'Redimensioning the Ogee Arrays

ReDim OX(n) As Double, Oym(n) As Double, Oyx(n) As Double, Oya(n) As Double

'Creating of Ogee water surface arrays

For i = 1 To n
   OX(i) = Worksheets("Raw WS Data").Range("F5").Cells(i, 1).Value
   Oym(i) = Worksheets("Raw WS Data").Range("F5").Cells(i, 2).Value
   Oyx(i) = Worksheets("Raw WS Data").Range("F5").Cells(i, 3).Value
   Oya(i) = Worksheets("Raw WS Data").Range("F5").Cells(i, 4).Value
Next i

   '**************************
   'Chute Water Surface Profile
   '**************************

'Count of the number of data points in the Chute array data set

n = 0
Do While Worksheets("Raw WS Data").Range("K5").Cells(n, 1).Value <> ""
   n = n + 1
Loop
n = n - 1

'Re-dimensioning the Chute Arrays
```

```
ReDim CX(n) As Double, Cym(n) As Double, Cyx(n) As Double, Cya(n) As Double

'Creating of Chute water surface arrays

For i = 1 To n
   CX(i) = Worksheets("Raw WS Data").Range("K5").Cells(i, 1).Value
   Cym(i) = Worksheets("Raw WS Data").Range("K5").Cells(i, 2).Value
   Cyx(i) = Worksheets("Raw WS Data").Range("K5").Cells(i, 3).Value
   Cya(i) = Worksheets("Raw WS Data").Range("K5").Cells(i, 4).Value
Next i

'++++++++++++++++++++++++++++++++++++++++++++++++
'Calculation of break point locations within arrays
'++++++++++++++++++++++++++++++++++++++++++++++++

'Count till Min Break Values

K = 1
Do While CX(K) < COmin
   K = K + 1
Loop

KK = 1
Do While OX(KK) < COmin
   KK = KK + 1
Loop

KKK = 1
Do While OX(KKK) < OWmin
   KKK = KKK + 1
Loop

KKKK = 1
Do While WX(KKKK) < OWmin
   KKKK = KKKK + 1
Loop

KKKKK = 1
Do While WX(KKKKK) < High
   KKKKK = KKKKK + 1
Loop

'Count till Max Break Values
```

```
L = 1
Do While CX(L) < COmax
   L = L + 1
Loop

LL = 1
Do While OX(LL) < COmax
   LL = LL + 1
Loop

LLL = 1
Do While OX(LLL) < OWmax
   LLL = LLL + 1
Loop

LLLL = 1
Do While WX(LLLL) < OWmax
   LLLL = LLLL + 1
Loop

LLLLL = 1
Do While WX(LLLLL) < High
   LLLLL = LLLLL + 1
Loop

'Count till Ave Break Values

M = 1
Do While CX(M) < COave
   M = M + 1
Loop

MM = 1
Do While OX(MM) < COave
   MM = MM + 1
Loop

MMM = 1
Do While OX(MMM) < OWave
   MMM = MMM + 1
Loop

MMMM = 1
Do While WX(MMMM) < OWave
   MMMM = MMMM + 1
```

```
Loop

MMMMM = 1
Do While WX(MMMMM) < High
   MMMMM = MMMMM + 1
Loop
'++++++++++++++++++++++++++++++++++++++++++++++++++++++++++++++++++
'Creation of Single Array to represent each statistical Water Surface Profile
'++++++++++++++++++++++++++++++++++++++++++++++++++++++++++++++++++

'X Coordinate Array

nn = (High - low) / 0.25 + 1
ReDim X(nn) As Double
For i = 1 To nn
   X(i) = low + (i - 1) * 0.25
   Worksheets("Combined WS Data").Cells(i + 8, 2).Value = X(i)
Next i

'Min Water Surface Profile Array

ReDim Cmin(nn) As Double, Cmax(nn) As Double, Cave(nn) As Double

For Z = 1 To K
   Cmin(Z) = Cym(Z)
Next Z

Q = K - KK

For Z = KK + 1 To KKK
   Cmin(Z + Q) = Oym(Z)
   R = Z + Q
Next Z

R = R - KKKK

For Z = KKKK To KKKKK
   Cmin(Z + R) = Wym(Z)
Next Z

'Max Water Surface Profile Array

For Z = 1 To L
   Cmax(Z) = Cyx(Z)
Next Z
```

```
Q = L - LL

For Z = LL + 1 To LLL
   Cmax(Z + Q) = Oyx(Z)
   R = Z + Q
Next Z

R = R - LLLL

For Z = LLLL To LLLLL
   Cmax(Z + R) = Wyx(Z)
Next Z

'Ave Water Surface Profile Array

For Z = 1 To M
   Cave(Z) = Cya(Z)
Next Z

Q = M - MM

For Z = MM + 1 To MMM
   Cave(Z + Q) = Oya(Z)
   R = Z + Q
Next Z

R = R - MMMM

For Z = MMMM To MMMMM
   Cave(Z + R) = Wya(Z)
Next Z

'++++++++++++++++++++++++++++++++++++++++++++++++++++++++++++++++
'Printing of the Combined Water Surface Arrays to the Spreadsheet Tables
'++++++++++++++++++++++++++++++++++++++++++++++++++++++++++++++++

'Printing of the three Combined Water Surface Arrays

For Z = 1 To nn
   Worksheets("Combined WS Data").Range("C9").Cells(Z, 1).Value = Cmin(Z)
   Worksheets("Combined WS Data").Range("C9").Cells(Z, 2).Value = Cmax(Z)
   Worksheets("Combined WS Data").Range("C9").Cells(Z, 3).Value = Cave(Z)
Next Z
```

```
End Sub
```

APPENDIX B – PHYSICAL DATA RESULTS

Table B1. Data for no ramp installed in labyrinth weir downstream cycle.

P	13.00	(in)	t_w	1.5	(in)
L	167.67	(in)	W	40.0	(in)
α	10.67	(°)	p	0.0	(in)

Run (#)	Q (cfs)	h (ft)	H (ft)	H/P ()	C_d ()
1	2.073	0.117	0.117	0.108	0.701
2	4.213	0.203	0.204	0.188	0.601
3	7.121	0.342	0.345	0.318	0.476
4	9.594	0.455	0.460	0.425	0.413
5	13.173	0.634	0.643	0.594	0.348
6	2.101	0.118	0.118	0.109	0.699
7	3.088	0.159	0.159	0.147	0.651
8	4.123	0.202	0.203	0.187	0.602
9	5.128	0.246	0.247	0.228	0.556
10	6.108	0.291	0.293	0.271	0.515
11	7.135	0.342	0.345	0.318	0.476
12	8.117	0.385	0.389	0.359	0.448
13	9.112	0.435	0.440	0.406	0.422
14	10.146	0.474	0.480	0.443	0.405
15	11.233	0.530	0.537	0.496	0.383
16	0.879	0.062	0.062	0.057	0.761
17	2.961	0.152	0.152	0.141	0.659
18	4.520	0.221	0.222	0.205	0.810
19	5.490	0.263	0.265	0.244	0.539
20	6.613	0.317	0.320	0.295	0.494
21	7.523	0.358	0.361	0.333	0.465
22	8.614	0.403	0.407	0.376	0.438
23	9.661	0.451	0.456	0.421	0.415
24	10.616	0.497	0.503	0.465	0.395
25	12.110	0.567	0.575	0.531	0.370
26	13.192	0.620	0.629	0.581	0.352
27	14.120	0.676	0.687	0.634	0.335
28	15.146	0.715	0.727	0.387	0.324
29	15.650	0.753	0.766	0.707	0.315
30	16.821	0.796	0.810	0.748	0.306
31	17.362	0.829	0.844	0.779	0.300
32	18.370	0.871	0.888	0.819	0.294
33	19.152	0.903	0.921	0.850	0.290
34	20.147	0.946	0.966	0.891	0.284

Table B2. Data for p = 0.15 P ramp installed in labyrinth weir downstream cycle.

P	13.00	(in)	t_w	1.5	(in)
L	167.67	(in)	W	40.0	(in)
α	10.67	(°)	p	2.0	(in)

Run (#)	Q (cfs)	h (ft)	H (ft)	H/P ()	C_d ()
1	2.266	0.124	0.124	0.115	0.693
2	3.083	0.156	0.156	0.144	0.667
3	4.137	0.201	0.202	0.186	0.610
4	5.088	0.242	0.243	0.225	0.567
5	6.069	0.288	0.290	0.268	0.520
6	7.257	0.342	0.345	0.319	0.479
7	8.179	0.381	0.385	0.355	0.458
8	9.215	0.433	0.438	0.404	0.426
9	10.278	0.475	0.481	0.444	0.412
10	10.294	0.483	0.489	0.451	0.403
11	11.226	0.524	0.531	0.490	0.388
12	12.368	0.582	0.590	0.545	0.365
13	12.653	0.599	0.608	0.561	0.357
14	13.29	0.629	0.638	0.589	0.349
15	12.025	0.563	0.571	0.527	0.373
16	13.843	0.658	0.668	0.617	0.339
17	14.374	0.683	0.694	0.641	0.333
18	14.783	0.706	0.717	0.662	0.326
19	15.197	0.727	0.739	0.682	0.320
20	15.73	0.757	0.769	0.710	0.312
21	15.4	0.732	0.744	0.687	0.321
22	16.292	0.780	0.794	0.732	0.308
23	16.667	0.800	0.814	0.752	0.304
24	15.877	0.751	0.764	0.705	0.318
25	17.333	0.828	0.844	0.779	0.299
26	17.714	0.853	0.868	0.802	0.293
27	18.145	0.868	0.884	0.816	0.292
28	18.51	0.887	0.904	0.835	0.288
29	18.731	0.901	0.918	0.848	0.285
30	19.219	0.922	0.940	0.868	0.282
31	4.175	0.205	0.206	0.190	0.599
2	6.157	0.295	0.297	0.274	0.509
33	8.229	0.390	0.394	0.363	0.446
34	10.121	0.474	0.480	0.443	0.408
35	12.409	0.582	0.590	0.545	0.366
36	14.446	0.683	0.694	0.640	0.335
37	15.634	0.740	0.752	0.695	0.321
38	17.510	0.843	0.858	0.792	0.295
39	18.840	0.902	0.919	0.848	0.286
40	20.325	0.980	0.999	0.923	0.272

Table B3. Data for p = 0.31 P ramp installed in labyrinth weir downstream cycle.

P	13.00	(in)	t_w	1.5	(in)
L	167.67	(in)	W	40.0	(in)
α	10.67	(°)	p	4.0	(in)

Run (#)	Q (cfs)	h (ft)	H (ft)	H/P ()	C_d ()
1	1.058	0.070	0.070	0.064	0.767
2	2.133	0.119	0.119	0.110	0.694
3	3.069	0.157	0.157	0.145	0.658
4	4.003	0.195	0.196	0.181	0.618
5	5.008	0.240	0.241	0.223	0.565
6	6.091	0.288	0.290	0.268	0.522
7	7.144	0.340	0.343	0.317	0.476
8	8.096	0.382	0.386	0.356	0.452
9	9.240	0.436	0.441	0.407	0.422
10	10.228	0.479	0.485	0.448	0.405
11	11.300	0.529	0.536	0.495	0.385
12	12.266	0.580	0.588	0.543	0.364
13	13.598	0.646	0.656	0.605	0.343
14	14.464	0.689	0.700	0.646	0.331
15	15.400	0.745	0.757	0.699	0.313
16	16.022	0.775	0.788	0.727	0.306
17	12.571	0.595	0.604	0.557	0.359
18	13.636	0.649	0.659	0.608	0.341
19	16.759	0.804	0.818	0.755	0.303
20	17.960	0.872	0.888	0.820	0.287
21	19.030	0.919	0.937	0.865	0.281
22	11.808	0.562	0.570	0.526	0.368
23	12.259	0.581	0.589	0.544	0.363
24	14.677	0.706	0.717	0.662	0.323
25	16.418	0.798	0.812	0.749	0.300
26	17.318	0.841	0.856	0.790	0.292
27	18.524	0.892	0.909	0.839	0.286
28	20.287	0.975	0.994	0.918	0.274
29	6.130	0.293	0.295	0.272	0.512
30	12.252	0.580	0.588	0.543	0.364
31	14.571	0.691	0.702	0.648	0.332
32	12.426	0.588	0.596	0.550	0.361
33	13.445	0.638	0.647	0.598	0.345
34	16.805	0.805	0.819	0.756	0.303
35	17.772	0.855	0.870	0.803	0.293

Table B4. Data for p = 0.46 P ramp installed in labyrinth weir downstream cycle.

P	13.00	(in)	t_w	1.5	(in)
L	167.67	(in)	W	40.0	(in)
α	10.67	(°)	p	6.0	(in)

Run (#)	Q (cfs)	h (ft)	H (ft)	H/P ()	C_d ()
1	0.934	0.065	0.065	0.060	0.757
2	2.061	0.116	0.116	0.107	0.697
3	3.058	0.158	0.158	0.146	0.649
4	4.104	0.200	0.201	0.185	0.610
5	5.108	0.244	0.245	0.227	0.562
6	6.174	0.298	0.300	0.277	0.502
7	7.177	0.343	0.346	0.319	0.472
8	8.175	0.391	0.395	0.364	0.441
9	9.141	0.432	0.437	0.403	0.424
10	10.195	0.486	0.492	0.454	0.396
11	11.241	0.537	0.544	0.502	0.375
12	12.183	0.585	0.593	0.547	0.357
13	13.192	0.638	0.647	0.598	0.339
14	16.559	0.814	0.828	0.764	0.294
15	14.138	0.663	0.674	0.622	0.342
16	14.535	0.690	0.701	0.647	0.331
17	15.043	0.720	0.732	0.675	0.322
18	15.634	0.748	0.761	0.702	0.315
19	16.197	0.784	0.797	0.736	0.304
20	16.698	0.804	0.818	0.755	0.302
21	17.481	0.841	0.856	0.790	0.295
22	17.859	0.865	0.881	0.813	0.289
23	18.356	0.887	0.904	0.834	0.286
24	18.922	0.911	0.928	0.857	0.283
25	19.511	0.935	0.953	0.880	0.281
26	20.095	0.968	0.987	0.911	0.274
27	6.277	0.301	0.303	0.280	0.504
28	8.192	0.390	0.394	0.363	0.444
29	10.171	0.486	0.492	0.454	0.395
30	12.204	0.580	0.588	0.543	0.362
31	14.302	0.687	0.698	0.644	0.329
32	15.730	0.769	0.782	0.722	0.304
33	18.031	0.886	0.902	0.832	0.282

Table B5. Data for p = 0.62 P ramp installed in labyrinth weir downstream cycle.

P	13.00	(in)	t_w	1.5	(in)
L	167.67	(in)	W	40.0	(in)
α	10.67	(°)	p	8.0	(in)

Run (#)	Q (cfs)	h (ft)	H (ft)	H/P ()	C_d ()
1	1.259	0.080	0.080	0.074	0.746
2	2.168	0.121	0.121	0.112	0.688
3	2.564	0.137	0.137	0.127	0.675
4	3.102	0.159	0.159	0.147	0.652
5	3.558	0.178	0.179	0.165	0.631
6	4.104	0.200	0.201	0.185	0.610
7	4.616	0.224	0.225	0.208	0.578
8	5.055	0.242	0.243	0.225	0.563
9	5.521	0.267	0.269	0.248	0.530
10	6.113	0.293	0.295	0.272	0.510
11	6.643	0.320	0.323	0.298	0.485
12	7.243	0.348	0.351	0.324	0.466
13	7.705	0.369	0.372	0.344	0.454
14	8.113	0.394	0.398	0.367	0.433
15	8.657	0.421	0.425	0.393	0.418
16	9.247	0.447	0.452	0.417	0.407
17	9.739	0.473	0.478	0.442	0.394
18	10.121	0.492	0.498	0.459	0.386
19	10.648	0.519	0.525	0.485	0.374
20	11.278	0.551	0.558	0.515	0.362
21	11.732	0.574	0.582	0.537	0.354
22	12.100	0.592	0.600	0.554	0.348
23	12.395	0.607	0.615	0.568	0.344
24	13.055	0.622	0.631	0.583	0.348
25	13.636	0.657	0.667	0.616	0.335
26	14.624	0.715	0.726	0.670	0.316
27	13.617	0.664	0.674	0.622	0.329
28	14.535	0.710	0.721	0.666	0.318
29	15.617	0.768	0.780	0.720	0.303
30	16.729	0.828	0.842	0.777	0.290
31	17.758	0.885	0.900	0.831	0.278
32	18.744	0.927	0.944	0.871	0.274
33	19.799	0.982	1.001	0.924	0.265
34	19.205	0.951	0.969	0.894	0.270
35	18.300	0.911	0.927	0.856	0.274
36	17.109	0.858	0.873	0.805	0.281
37	16.213	0.802	0.815	0.753	0.295
38	14.887	0.737	0.748	0.691	0.308
39	14.157	0.707	0.717	0.662	0.312
40	11.804	0.577	0.585	0.540	0.353

41	13.730	0.683	0.693	0.639	0.319
42	15.681	0.788	0.801	0.739	0.293

Table B6. Data for *p* = 0.77 *P* ramp installed in labyrinth weir downstream cycle.

P	13.00	(in)	t_w	1.5	(in)
L	167.67	(in)	*W*	40.0	(in)
α	10.67	(°)	*p*	10.0	(in)

Run (#)	*Q* (cfs)	*h* (ft)	*H* (ft)	*H/P* ()	C_d ()
1	2.105	0.119	0.119	0.110	0.686
2	3.064	0.159	0.159	0.147	0.644
3	4.034	0.198	0.199	0.184	0.609
4	5.062	0.242	0.243	0.225	0.564
5	6.119	0.300	0.302	0.279	0.493
6	7.248	0.357	0.360	0.332	0.449
7	8.225	0.408	0.412	0.380	0.416
8	10.342	0.511	0.517	0.477	0.372
9	11.318	0.555	0.562	0.519	0.359
10	6.201	0.304	0.306	0.283	0.490
11	7.073	0.345	0.348	0.321	0.461
12	7.635	0.373	0.376	0.347	0.443
13	8.241	0.406	0.410	0.378	0.420
14	8.621	0.427	0.431	0.398	0.407
15	8.917	0.443	0.448	0.413	0.399
16	11.765	0.584	0.591	0.546	0.346
17	12.734	0.640	0.648	0.599	0.326
18	13.880	0.705	0.715	0.660	0.307
19	14.783	0.752	0.763	0.704	0.297
20	15.584	0.799	0.811	0.749	0.286
21	16.698	0.852	0.866	0.799	0.277
22	17.888	0.904	0.919	0.849	0.272
23	18.990	0.961	0.978	0.903	0.263
24	11.543	0.569	0.576	0.532	0.353
25	12.915	0.650	0.659	0.608	0.323
26	13.880	0.703	0.713	0.658	0.309
27	14.905	0.750	0.761	0.703	0.300
28	15.601	0.793	0.805	0.743	0.289
29	16.775	0.850	0.864	0.797	0.280
30	18.060	0.906	0.922	0.851	0.273
31	18.786	0.948	0.965	0.890	0.265

Table B7. Data for p = 0.92 P ramp installed in labyrinth weir downstream cycle.

P	13.00	(in)	t	1.5	(in)
L	167.67	(in)	W	40.0	(in)
α	10.67	(°)	p	12.0	(in)

Run (#)	Q (cfs)	h (ft)	H (ft)	H/P ()	C_d ()
1	2.073	0.118	0.118	0.109	0.684
2	3.096	0.162	0.162	0.150	0.633
3	4.061	0.207	0.208	0.192	0.573
4	5.102	0.255	0.256	0.237	0.526
5	6.174	0.314	0.316	0.292	0.465
6	7.135	0.362	0.365	0.337	0.433
7	8.033	0.417	0.421	0.388	0.394
8	9.171	0.482	0.487	0.449	0.361
9	10.129	0.521	0.527	0.486	0.355
10	11.090	0.572	0.579	0.534	0.337
11	12.155	0.627	0.635	0.586	0.322
12	0.951	0.066	0.066	0.061	0.753
13	1.945	0.113	0.113	0.104	0.685
14	2.929	0.155	0.155	0.143	0.640
15	4.227	0.214	0.215	0.198	0.568
16	5.315	0.270	0.272	0.251	0.503
17	5.778	0.295	0.297	0.274	0.478
18	6.780	0.344	0.347	0.320	0.445
19	7.661	0.390	0.393	0.363	0.416
20	8.688	0.441	0.445	0.411	0.391
21	9.178	0.466	0.471	0.435	0.380
22	10.608	0.539	0.545	0.503	0.353
23	11.135	0.563	0.570	0.526	0.346
24	12.058	0.607	0.615	0.568	0.335
25	10.292	0.530	0.536	0.495	0.351
26	12.488	0.643	0.651	0.601	0.318
27	12.915	0.672	0.681	0.628	0.308
28	13.348	0.693	0.702	0.648	0.304
29	13.880	0.721	0.731	0.675	0.297
30	14.230	0.749	0.759	0.701	0.288
31	14.922	0.781	0.792	0.731	0.283

32	15.383	0.805	0.817	0.754	0.279
33	16.022	0.835	0.848	0.783	0.275
34	16.713	0.872	0.886	0.818	0.268
35	17.510	0.910	0.925	0.854	0.263
36	18.0167	0.932	0.948	0.875	0.261
37	18.81293	0.972	0.989	0.913	0.256

APPENDIX C – STATISTICAL REPRESENTATIONS OF HIGH-WATER LEVEL ON STEEP STEPPED SPILLWAY CHUTE FOR $H/P \approx 0.186$, 0.367, AND 0.878.

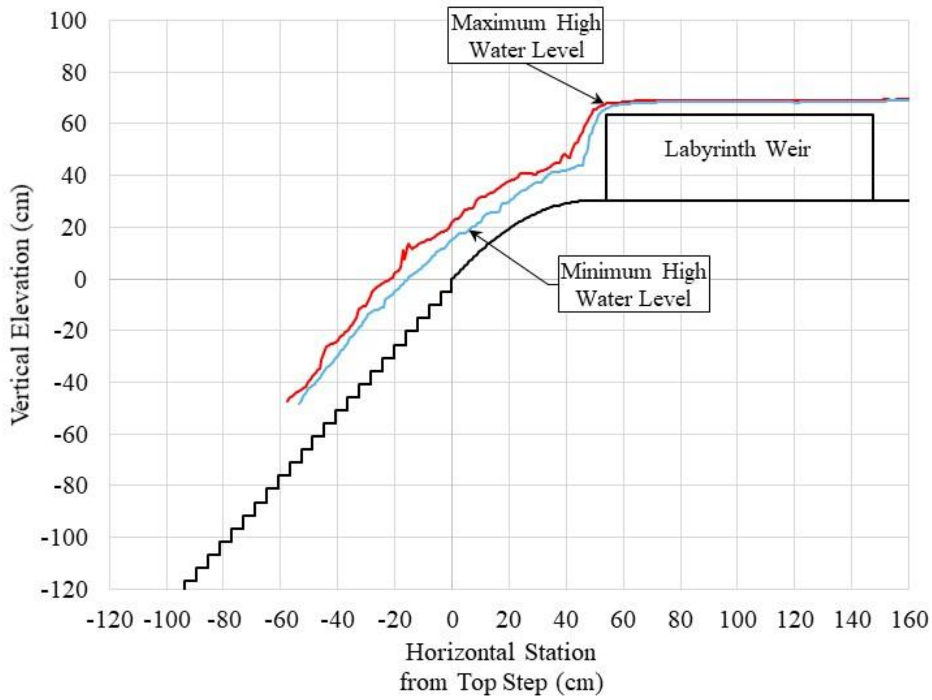

Figure. C1. Statistical representation of high-water levels with no ramp and $H/P \approx 0.186$ ($Q \approx 116$ l/s).

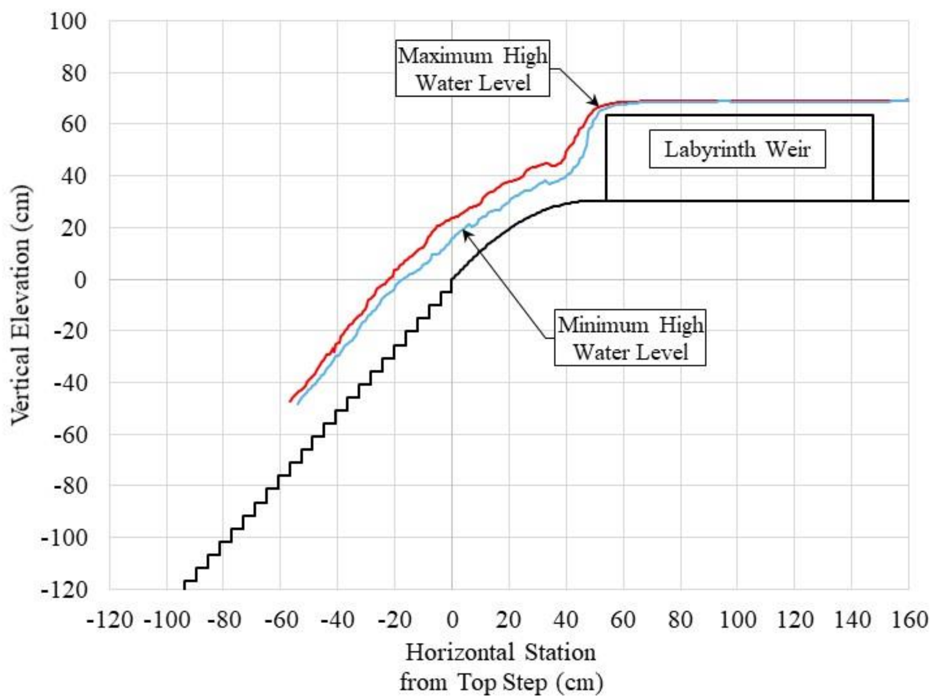

Figure. C2. Statistical representation of high-water levels with $p = 0.15\ P$ and H/P ≈ 0.186 (Q ≈ 116 l/s).

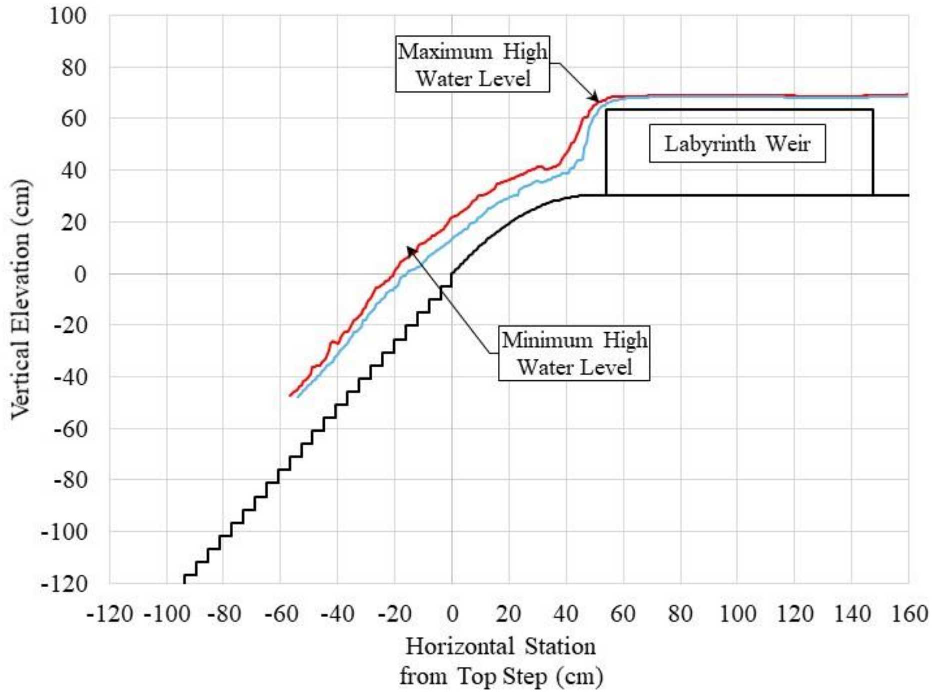

Figure. C3. Statistical representation of high-water levels with p = 0.31 P and H/P ≈ 0.186 (Q ≈ 116 l/s).

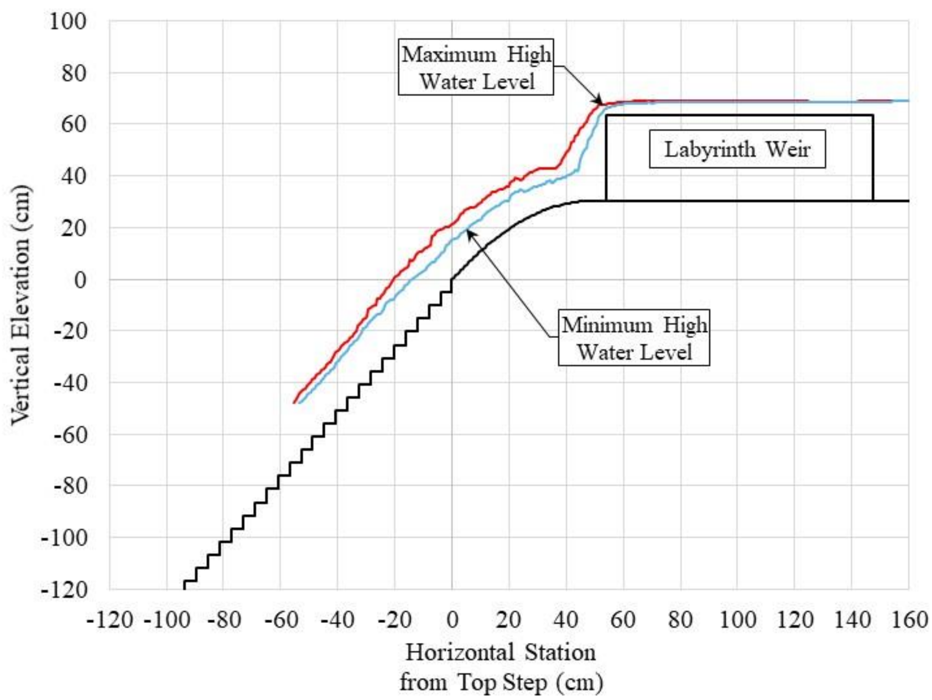

Figure. C4. Statistical representation of high-water levels with p = 0.46 P and H/P ≈ 0.186 (Q ≈ 116 l/s).

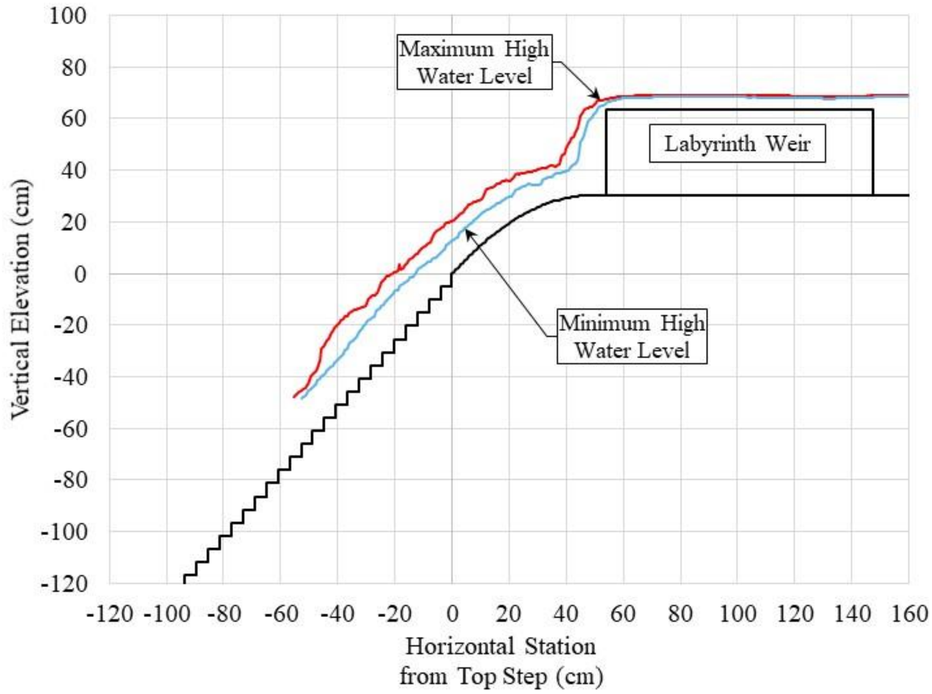

Figure. C5. Statistical representation of high-water levels with p = 0.62 P and H/P ≈ 0.186 (Q ≈ 116 l/s).

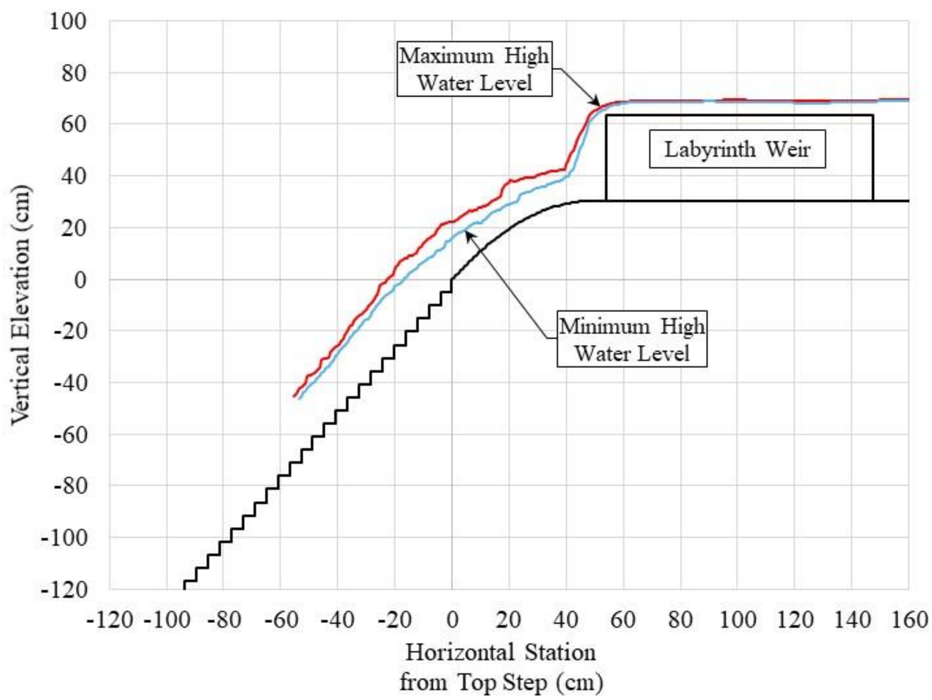

Figure. C6. Statistical representation of high-water levels with p = 0.77 P and H/P ≈ 0.186 (Q ≈ 116 l/s).

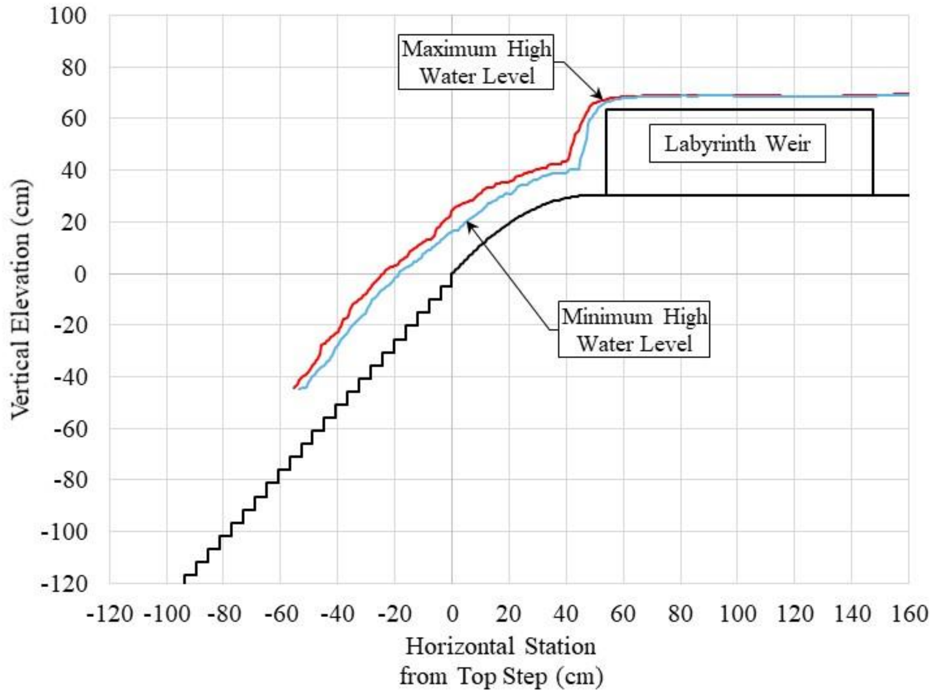

Figure. C7. Statistical representation of high-water levels with $p = 0.92\ P$ and H/P ≈ 0.186 (Q ≈ 116 l/s).

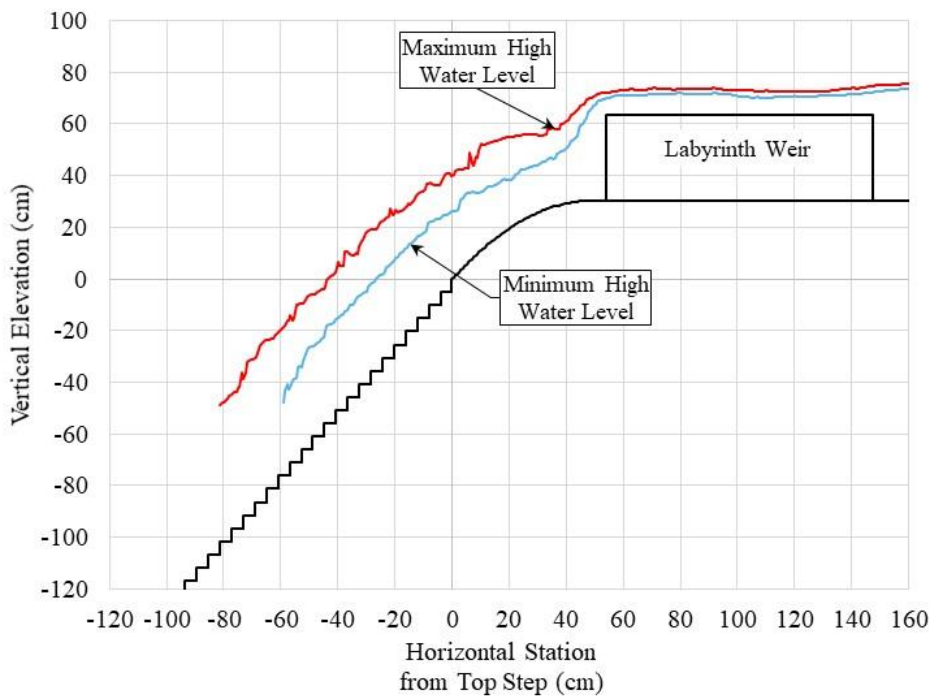

Figure. C8. Statistical representation of high-water levels with no ramp and H/P ≈ 0.367 (Q ≈ 230 l/s).

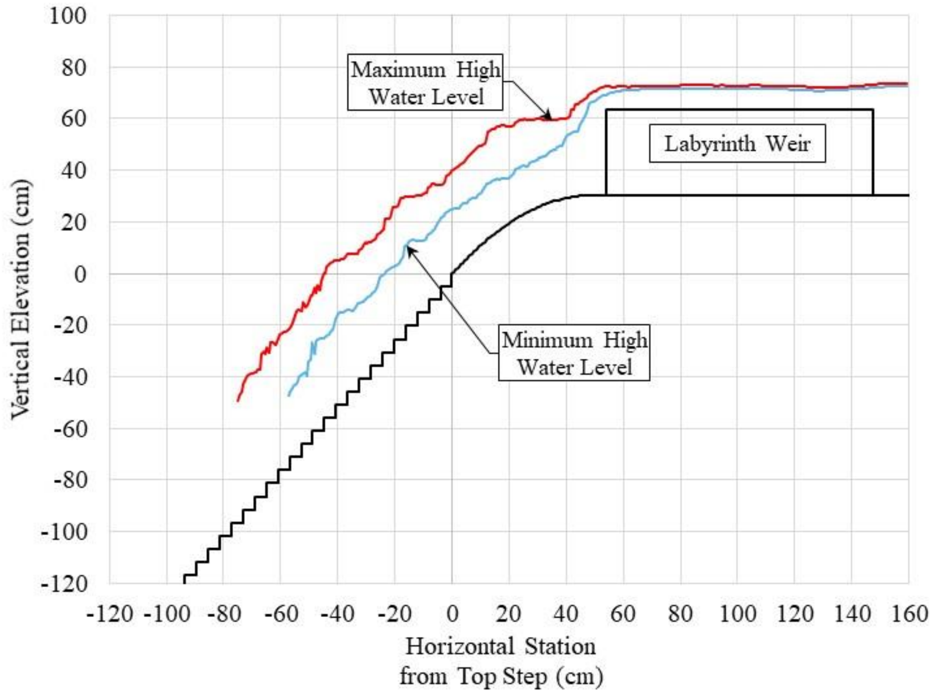

Figure. C9. Statistical representation of high-water levels with $p = 0.15\ P$ and H/P ≈ 0.367 (Q ≈ 230 l/s).

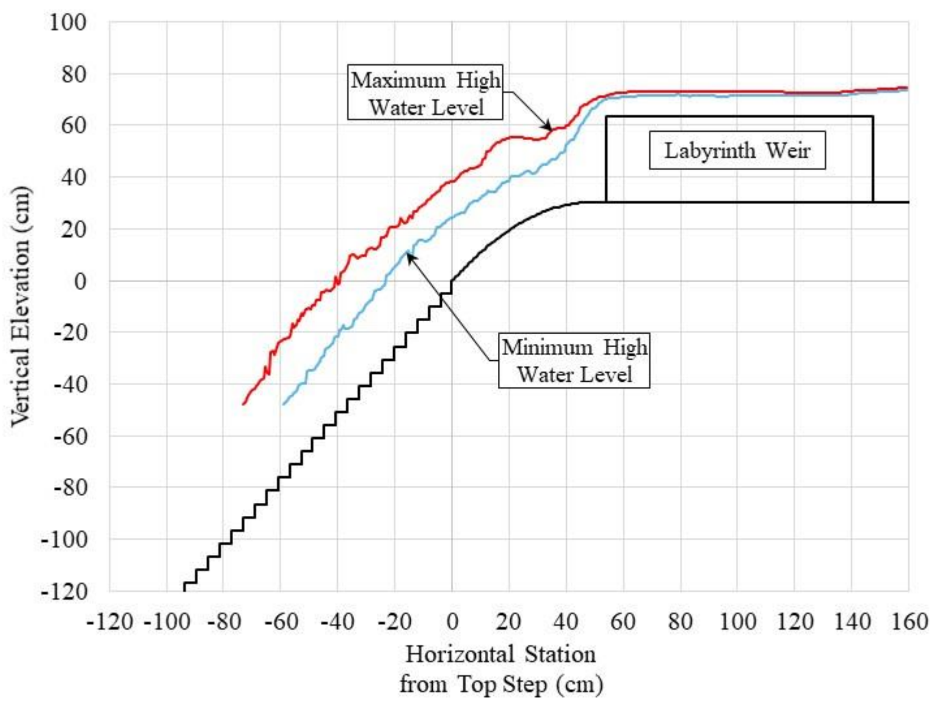

Figure. C10. Statistical representation of high-water levels with $p = 0.31\ P$ and H/P ≈ 0.367 (Q ≈ 230 l/s).

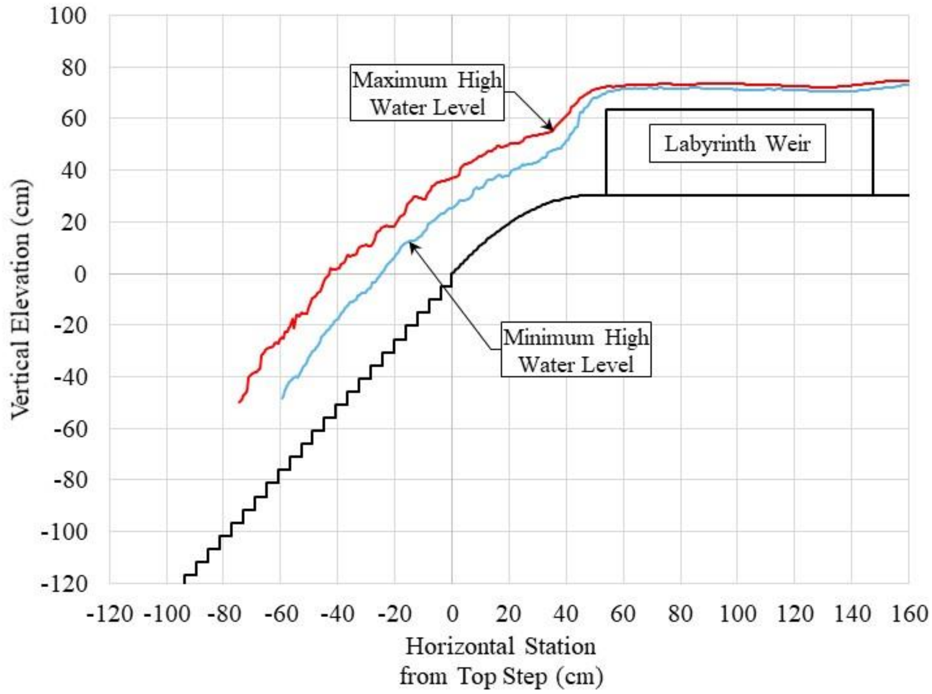

Figure. C11. Statistical representation of high-water levels with $p = 0.46\ P$ and H/P ≈ 0.367 (Q ≈ 230 l/s).

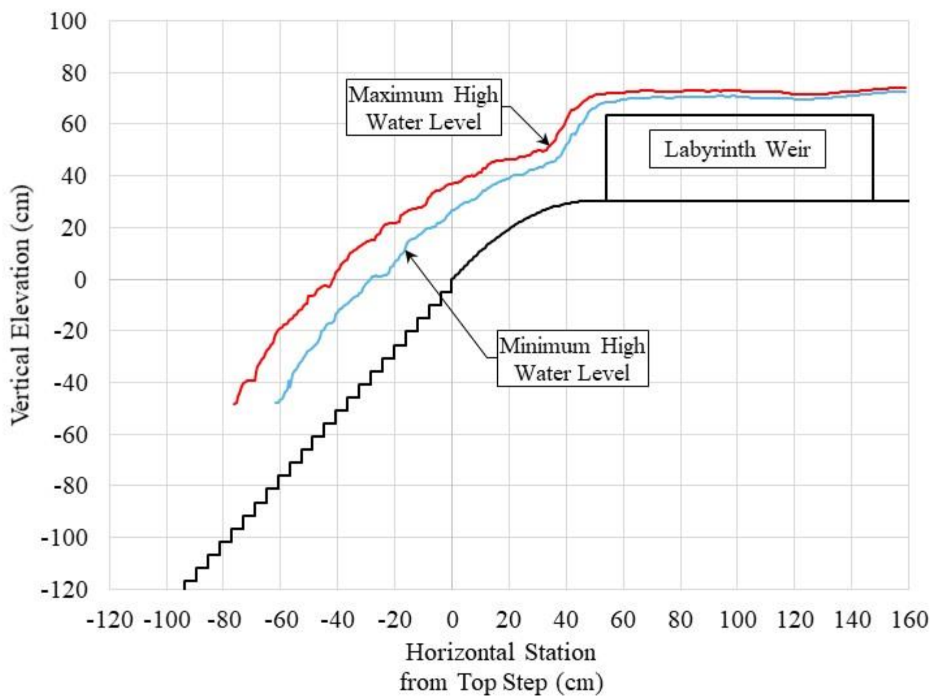

Figure. C12. Statistical representation of high-water levels with $p = 0.62\ P$ and H/P ≈ 0.367 (Q ≈ 230 l/s).

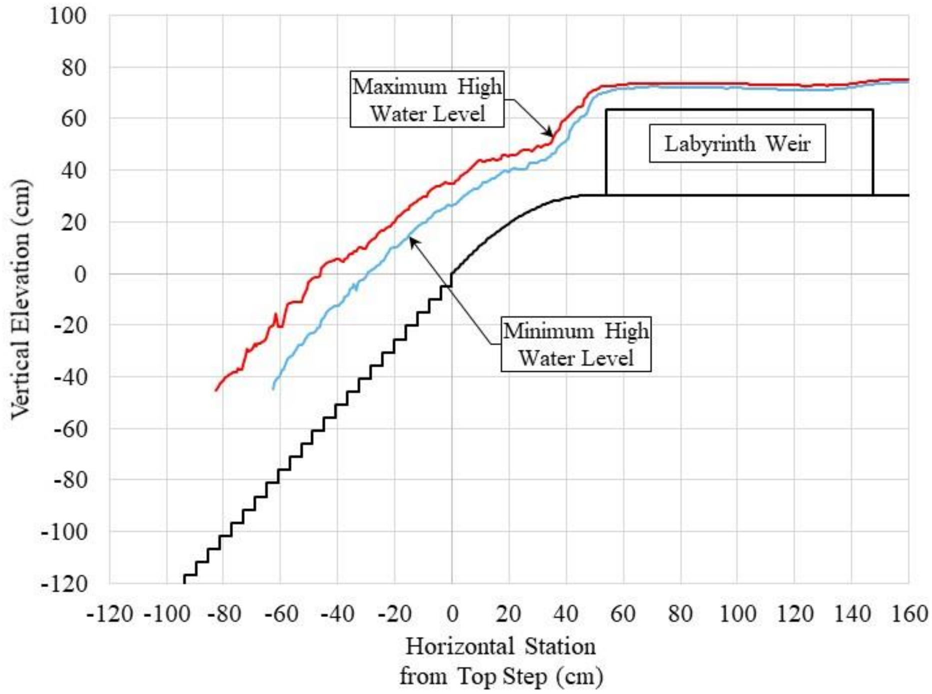

Figure. C13. Statistical representation of high-water levels with p = 0.77 P and H/P ≈ 0.367 (Q ≈ 230 l/s).

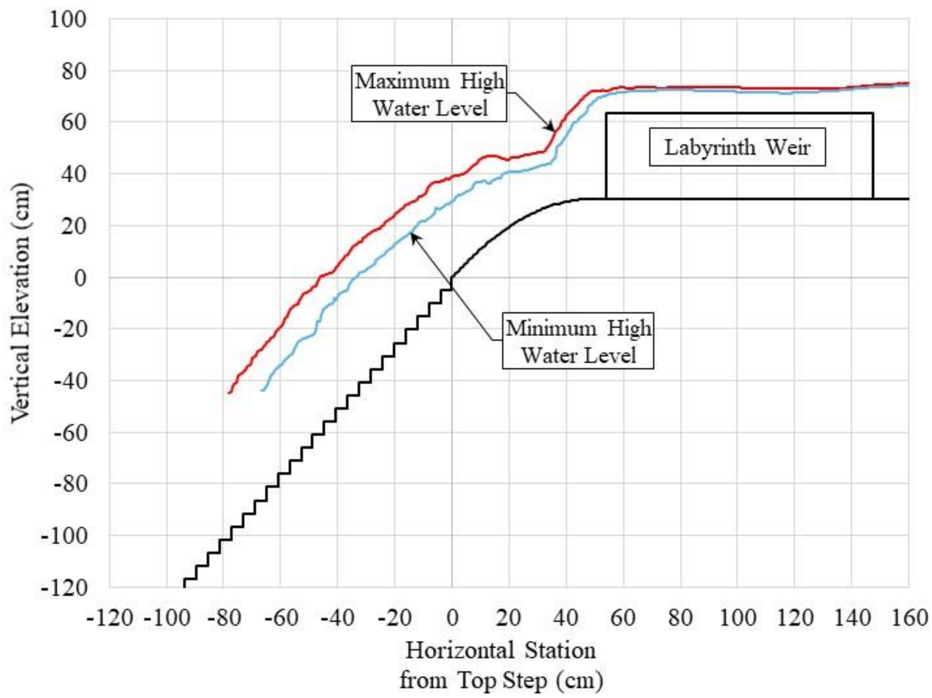

Figure. C14. Statistical representation of high-water levels with p = 0.92 P and H/P ≈ 0.367 (Q ≈ 230 l/s).

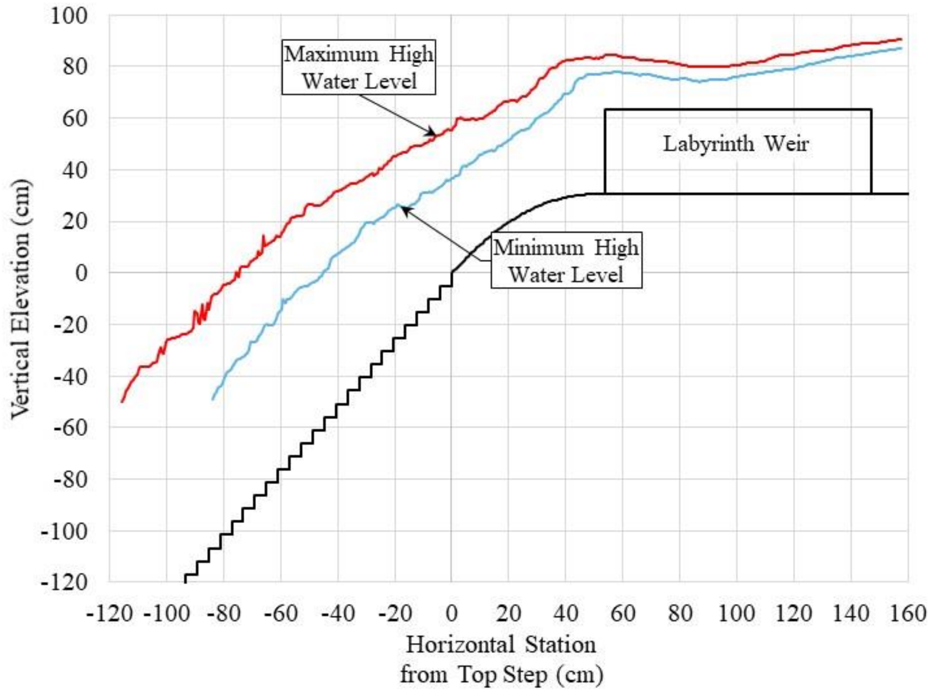

Figure. C15. Statistical representation of high-water levels with no ramp and H/P ≈ 0.878 (Q ≈ 540 l/s).

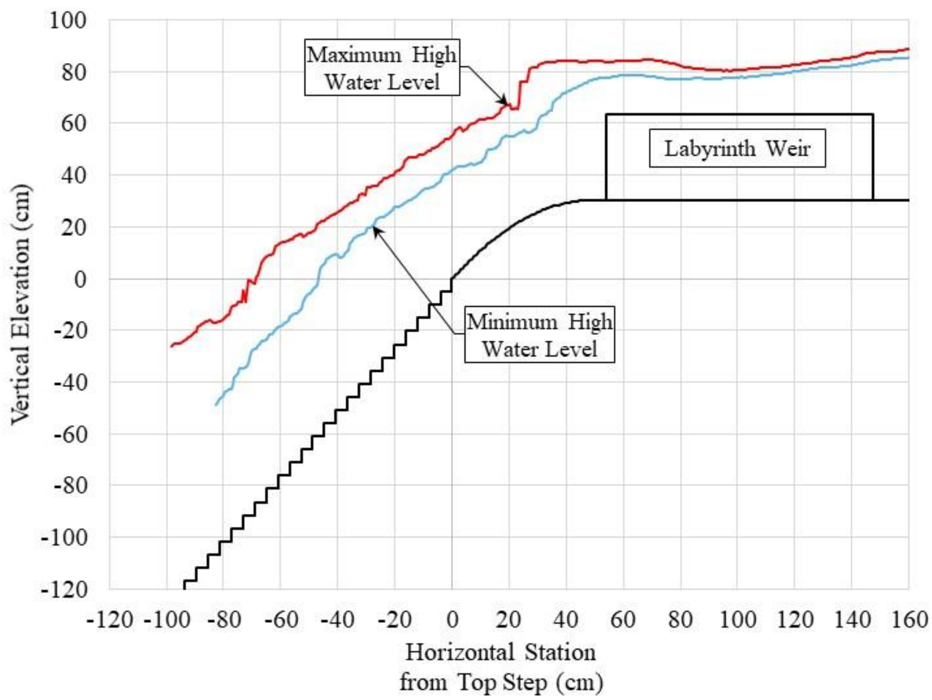

Figure. C16. Statistical representation of high-water levels with p = 0.15 P and H/P ≈ 0.878 (Q ≈ 540 l/s).

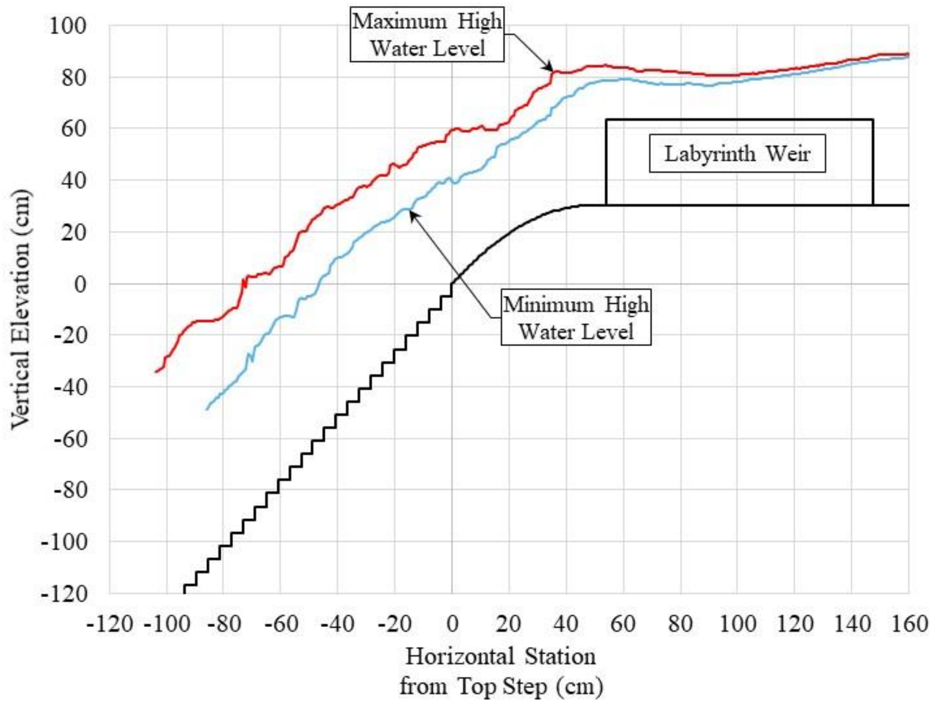

Figure. C17. Statistical representation of high-water levels with p = 0.31 P and H/P ≈ 0.878 (Q ≈ 540 l/s).

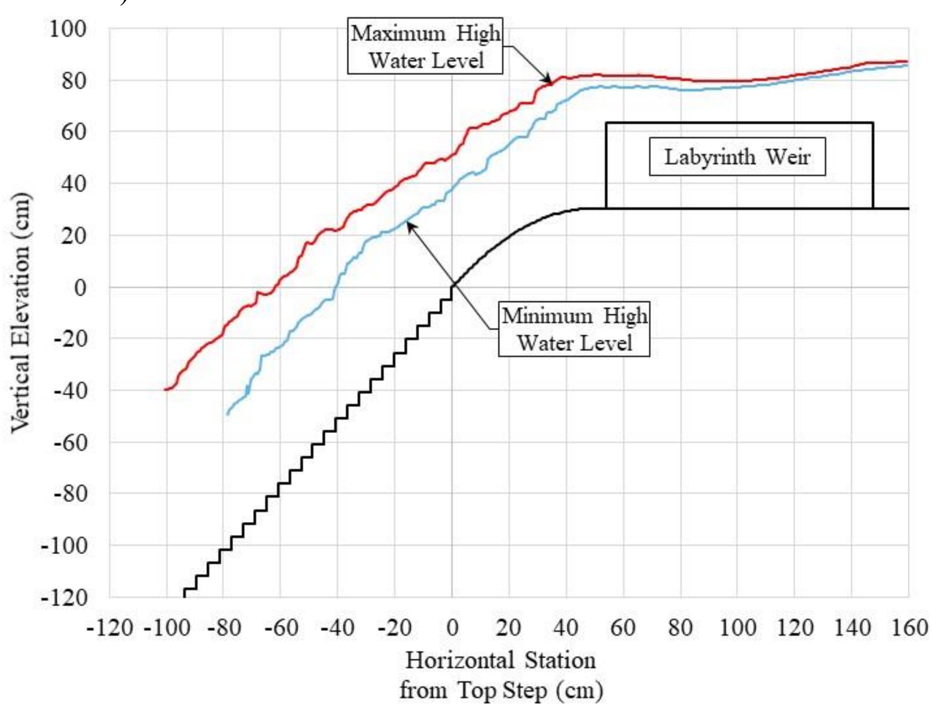

Figure. C18. Statistical representation of high-water levels with p = 0.46 P and H/P ≈ 0.878 (Q ≈ 540 l/s).

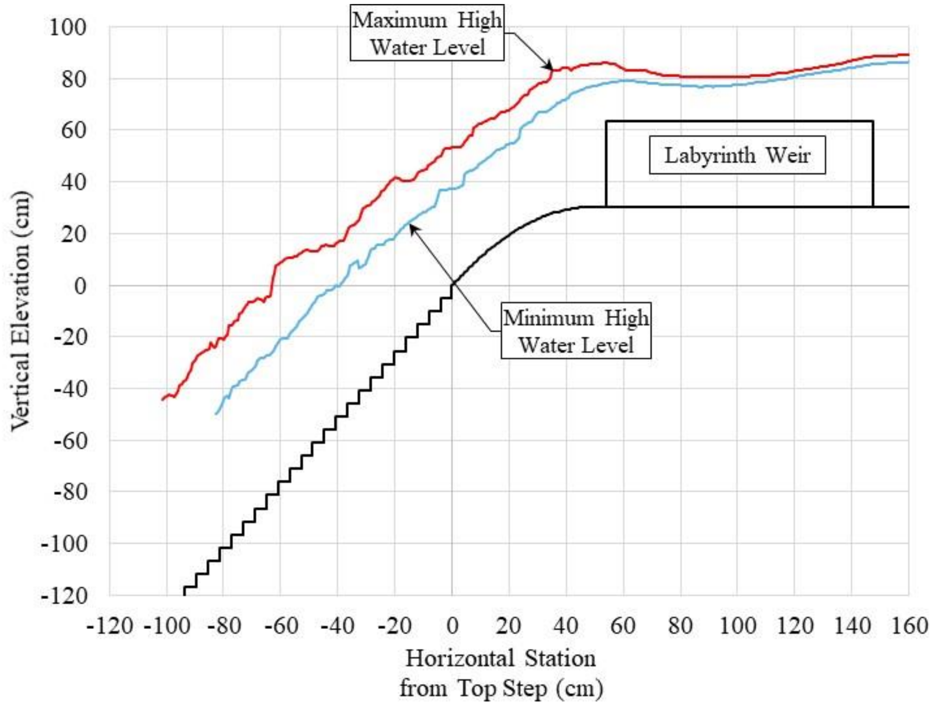

Figure. C19. Statistical representation of high-water levels with *p* = 0.62 *P* and H/P ≈ 0.878 (Q ≈ 540 l/s).

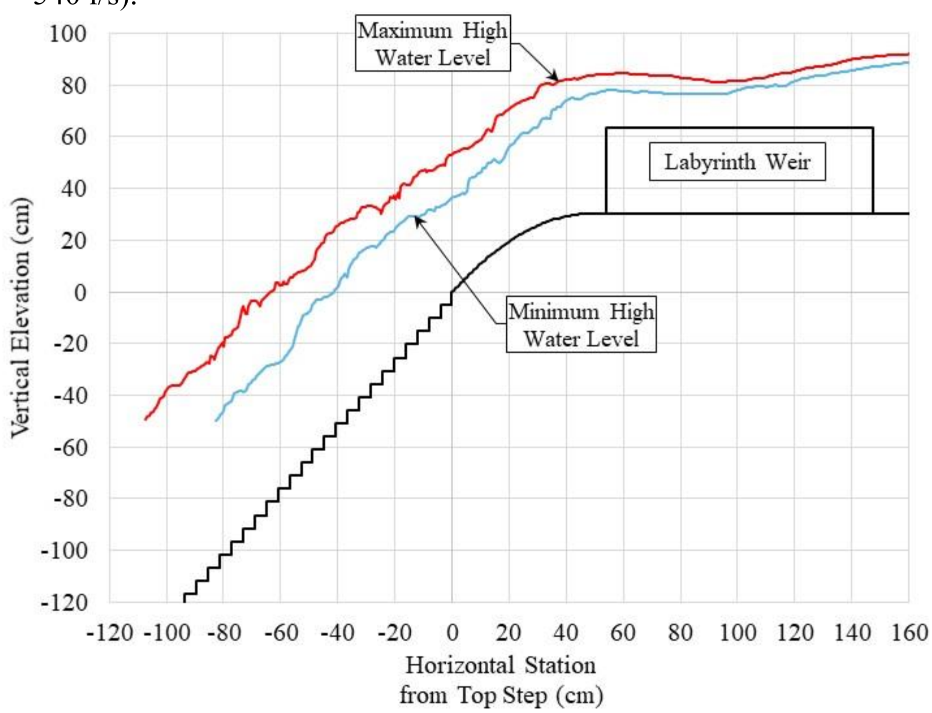

Figure. C20. Statistical representation of high-water levels with *p* = 0.77 *P* and H/P ≈ 0.878 (Q ≈ 540 l/s).

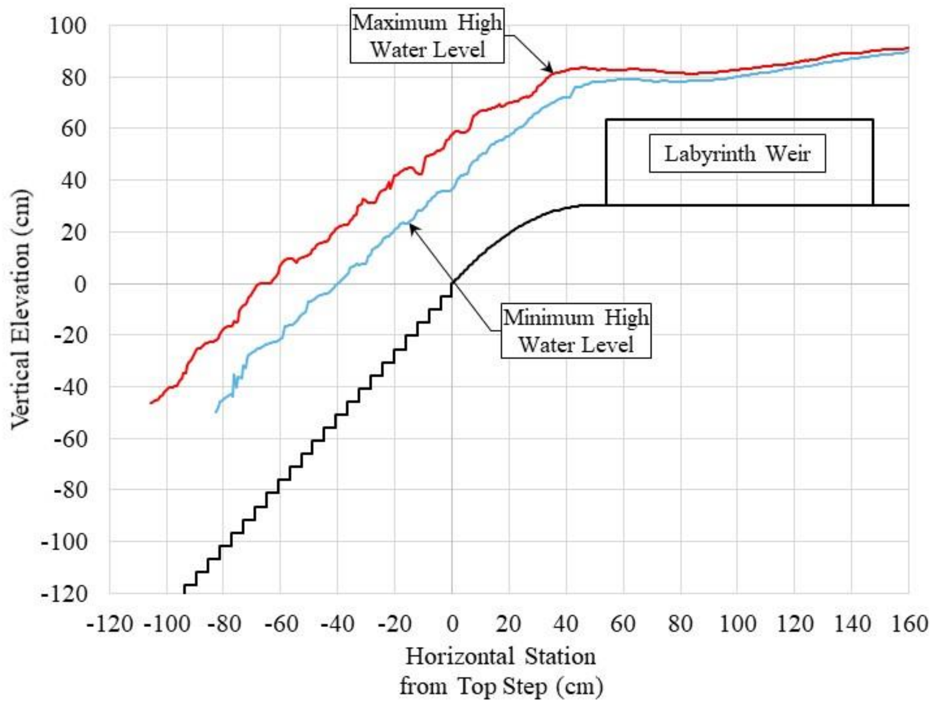

Figure. C21. Statistical representation of high-water levels with $p = 0.92\ P$ and H/P ≈ 0.878 (Q ≈ 540 l/s).

APPENDIX D – HIGH-WATER SURFACE DATA FOR $H/P \approx 0.878$ ($Q \approx 540$ L/S).

Table D1. High-Water statistics for H/P ≈ 0.878 (Q ≈ 540 L/S) and with no ramp, p = 0.15 P, and p = 0.31 P (units in inches).

High-Water Statistics for H/P ≈ 0.878 and no ramp			High-Water Statistics for H/P ≈ 0.878 and p = 0.15 P			High-Water Statistics for H/P ≈ 0.878 and p = 0.31 P		
X	Y Min.	Y Max.	X	Y Min.	Y Max.	X	Y Min.	Y Max.
62.00	34.21	35.62	63.00	33.65	34.96	63.00	34.48	34.98
61.75	34.18	35.59	62.75	33.63	34.89	62.75	34.47	35.03
61.50	34.15	35.56	62.50	33.61	34.82	62.50	34.44	34.98
61.25	34.13	35.53	62.25	33.58	34.76	62.25	34.41	34.94
61.00	34.10	35.49	62.00	33.56	34.72	62.00	34.38	34.89
60.75	34.07	35.45	61.75	33.53	34.67	61.75	34.39	34.84
60.50	34.02	35.41	61.50	33.51	34.62	61.50	34.39	34.85
60.25	33.97	35.37	61.25	33.48	34.57	61.25	34.37	34.88
60.00	33.92	35.33	61.00	33.45	34.52	61.00	34.33	34.91
59.75	33.88	35.28	60.75	33.45	34.49	60.75	34.23	34.93
59.50	33.84	35.23	60.50	33.43	34.48	60.50	34.23	34.94
59.25	33.79	35.16	60.25	33.41	34.48	60.25	34.20	34.93
59.00	33.76	35.08	60.00	33.39	34.48	60.00	34.21	34.93
58.75	33.71	35.08	59.75	33.37	34.48	59.75	34.21	34.93
58.50	33.67	35.07	59.50	33.33	34.48	59.50	34.20	34.91
58.25	33.62	35.05	59.25	33.30	34.50	59.25	34.17	34.91
58.00	33.57	35.04	59.00	33.27	34.50	59.00	34.10	34.91
57.75	33.52	35.02	58.75	33.23	34.49	58.75	34.05	34.84
57.50	33.48	35.00	58.50	33.18	34.45	58.50	34.01	34.75
57.25	33.43	34.99	58.25	33.12	34.42	58.25	33.96	34.69
57.00	33.38	34.97	58.00	33.09	34.39	58.00	33.91	34.64
56.75	33.33	34.96	57.75	33.08	34.36	57.75	33.88	34.58
56.50	33.32	34.95	57.50	33.01	34.32	57.50	33.83	34.48
56.25	33.31	34.93	57.25	32.94	34.28	57.25	33.78	34.39
56.00	33.28	34.89	57.00	32.86	34.23	57.00	33.75	34.36
55.75	33.22	34.84	56.75	32.82	34.17	56.75	33.72	34.33
55.50	33.15	34.80	56.50	32.78	34.10	56.50	33.69	34.30
55.25	33.11	34.76	56.25	32.73	34.02	56.25	33.66	34.25
55.00	33.07	34.73	56.00	32.69	33.92	56.00	33.63	34.22
54.75	33.04	34.71	55.75	32.64	33.81	55.75	33.56	34.18
54.50	32.98	34.66	55.50	32.56	33.74	55.50	33.48	34.18
54.25	32.93	34.60	55.25	32.49	33.70	55.25	33.45	34.19
54.00	32.89	34.55	55.00	32.44	33.65	55.00	33.46	34.15
53.75	32.87	34.46	54.75	32.40	33.57	54.75	33.40	34.10
53.50	32.85	34.35	54.50	32.36	33.52	54.50	33.37	34.08
53.25	32.81	34.23	54.25	32.34	33.48	54.25	33.28	33.97
53.00	32.76	34.15	54.00	32.32	33.45	54.00	33.20	33.86
52.75	32.70	34.12	53.75	32.28	33.43	53.75	33.11	33.81
52.50	32.62	34.08	53.50	32.25	33.40	53.50	33.05	33.77
52.25	32.54	34.04	53.25	32.23	33.37	53.25	33.00	33.69
52.00	32.47	34.00	53.00	32.21	33.33	53.00	32.95	33.59
51.75	32.43	33.99	52.75	32.20	33.30	52.75	32.88	33.56

51.50	32.34	33.93	52.50	32.21	33.26	52.50	32.84	33.53
51.25	32.25	33.89	52.25	32.21	33.24	52.25	32.80	33.51
51.00	32.18	33.87	52.00	32.21	33.21	52.00	32.75	33.52
50.75	32.11	33.83	51.75	32.17	33.18	51.75	32.72	33.51
50.50	32.04	33.80	51.50	32.14	33.15	51.50	32.69	33.47
50.25	31.98	33.83	51.25	32.12	33.12	51.25	32.65	33.41
50.00	31.88	33.84	51.00	32.09	33.09	51.00	32.60	33.34
49.75	31.83	33.83	50.75	32.08	33.06	50.75	32.53	33.26
49.50	31.83	33.78	50.50	32.06	33.03	50.50	32.48	33.23
49.25	31.78	33.72	50.25	32.01	33.02	50.25	32.46	33.24
49.00	31.69	33.66	50.00	31.97	32.97	50.00	32.44	33.21
48.75	31.60	33.61	49.75	31.93	32.92	49.75	32.38	33.17
48.50	31.53	33.59	49.50	31.89	32.83	49.50	32.32	33.11
48.25	31.47	33.56	49.25	31.85	32.78	49.25	32.27	33.05
48.00	31.37	33.52	49.00	31.79	32.77	49.00	32.22	33.00
47.75	31.28	33.44	48.75	31.73	32.75	48.75	32.18	32.96
47.50	31.20	33.38	48.50	31.70	32.73	48.50	32.14	32.90
47.25	31.15	33.32	48.25	31.67	32.68	48.25	32.08	32.84
47.00	31.09	33.27	48.00	31.64	32.63	48.00	32.02	32.81
46.75	31.02	33.23	47.75	31.59	32.60	47.75	31.96	32.83
46.50	30.99	33.20	47.50	31.53	32.56	47.50	31.92	32.84
46.25	30.98	33.24	47.25	31.49	32.53	47.25	31.91	32.82
46.00	30.98	33.33	47.00	31.45	32.49	47.00	31.89	32.76
45.75	30.98	33.31	46.75	31.41	32.45	46.75	31.87	32.73
45.50	30.96	33.26	46.50	31.36	32.42	46.50	31.82	32.72
45.25	30.95	33.17	46.25	31.31	32.38	46.25	31.77	32.62
45.00	30.92	33.05	46.00	31.27	32.34	46.00	31.73	32.51
44.75	30.86	32.96	45.75	31.24	32.31	45.75	31.69	32.52
44.50	30.80	32.90	45.50	31.22	32.26	45.50	31.66	32.51
44.25	30.74	32.82	45.25	31.21	32.21	45.25	31.62	32.45
44.00	30.71	32.72	45.00	31.19	32.17	45.00	31.57	32.44
43.75	30.67	32.60	44.75	31.15	32.14	44.75	31.51	32.38
43.50	30.64	32.44	44.50	31.12	32.13	44.50	31.47	32.37
43.25	30.59	32.32	44.25	31.09	32.12	44.25	31.43	32.30
43.00	30.53	32.28	44.00	31.05	32.11	44.00	31.38	32.27
42.75	30.48	32.22	43.75	31.01	32.09	43.75	31.34	32.30
42.50	30.44	32.17	43.50	30.99	32.08	43.50	31.33	32.28
42.25	30.42	32.13	43.25	30.98	32.06	43.25	31.34	32.24
42.00	30.34	32.10	43.00	30.95	32.05	43.00	31.29	32.19
41.75	30.30	32.07	42.75	30.91	32.05	42.75	31.28	32.10
41.50	30.30	32.05	42.50	30.87	32.04	42.50	31.23	32.07
41.25	30.34	32.03	42.25	30.82	32.03	42.25	31.20	32.06
41.00	30.33	32.02	42.00	30.79	32.00	42.00	31.16	32.02
40.75	30.24	31.99	41.75	30.76	31.97	41.75	31.13	32.03
40.50	30.18	31.95	41.50	30.74	31.94	41.50	31.11	32.05
40.25	30.14	31.91	41.25	30.71	31.91	41.25	31.09	32.03
40.00	30.08	31.84	41.00	30.68	31.89	41.00	31.07	31.94
39.75	30.01	31.77	40.75	30.66	31.87	40.75	31.05	31.95
39.50	29.95	31.69	40.50	30.65	31.83	40.50	30.97	31.95

39.25	29.93	31.65	40.25	30.65	31.79	40.25	30.87	31.90
39.00	29.93	31.62	40.00	30.66	31.75	40.00	30.83	31.86
38.75	29.82	31.59	39.75	30.66	31.72	39.75	30.81	31.85
38.50	29.70	31.58	39.50	30.64	31.69	39.50	30.80	31.83
38.25	29.62	31.55	39.25	30.62	31.68	39.25	30.73	31.78
38.00	29.58	31.52	39.00	30.60	31.67	39.00	30.66	31.80
37.75	29.53	31.51	38.75	30.58	31.65	38.75	30.66	31.80
37.50	29.49	31.53	38.50	30.53	31.64	38.50	30.63	31.80
37.25	29.44	31.53	38.25	30.50	31.64	38.25	30.57	31.80
37.00	29.47	31.52	38.00	30.49	31.66	38.00	30.56	31.80
36.75	29.49	31.48	37.75	30.48	31.65	37.75	30.62	31.78
36.50	29.50	31.47	37.50	30.49	31.63	37.50	30.56	31.76
36.25	29.47	31.47	37.25	30.46	31.66	37.25	30.52	31.73
36.00	29.45	31.46	37.00	30.43	31.69	37.00	30.50	31.73
35.75	29.45	31.46	36.75	30.40	31.70	36.75	30.49	31.76
35.50	29.45	31.46	36.50	30.39	31.71	36.50	30.42	31.77
35.25	29.35	31.49	36.25	30.37	31.72	36.25	30.34	31.77
35.00	29.28	31.51	36.00	30.36	31.76	36.00	30.25	31.77
34.75	29.23	31.49	35.75	30.38	31.78	35.75	30.21	31.76
34.50	29.20	31.47	35.50	30.41	31.76	35.50	30.20	31.71
34.25	29.19	31.46	35.25	30.43	31.80	35.25	30.19	31.74
34.00	29.21	31.47	35.00	30.45	31.84	35.00	30.23	31.81
33.75	29.27	31.50	34.75	30.46	31.88	34.75	30.25	31.87
33.50	29.32	31.54	34.50	30.47	31.90	34.50	30.26	31.86
33.25	29.37	31.55	34.25	30.48	31.91	34.25	30.27	31.88
33.00	29.46	31.56	34.00	30.48	31.92	34.00	30.31	31.93
32.75	29.54	31.56	33.75	30.48	31.94	33.75	30.38	31.95
32.50	29.61	31.61	33.50	30.48	31.98	33.50	30.42	32.00
32.25	29.66	31.66	33.25	30.47	32.02	33.25	30.46	32.04
32.00	29.69	31.70	33.00	30.45	32.05	33.00	30.50	32.07
31.75	29.65	31.77	32.75	30.44	32.12	32.75	30.48	32.11
31.50	29.59	31.84	32.50	30.42	32.17	32.50	30.47	32.14
31.25	29.55	31.89	32.25	30.41	32.19	32.25	30.46	32.16
31.00	29.54	31.93	32.00	30.41	32.24	32.00	30.43	32.17
30.75	29.53	31.97	31.75	30.42	32.33	31.75	30.41	32.17
30.50	29.54	32.03	31.50	30.42	32.42	31.50	30.38	32.18
30.25	29.57	32.08	31.25	30.42	32.51	31.25	30.41	32.21
30.00	29.60	32.13	31.00	30.43	32.59	31.00	30.41	32.25
29.75	29.64	32.19	30.75	30.43	32.66	30.75	30.38	32.27
29.50	29.73	32.24	30.50	30.44	32.70	30.50	30.37	32.29
29.25	29.77	32.30	30.25	30.44	32.74	30.25	30.37	32.31
29.00	29.81	32.35	30.00	30.43	32.79	30.00	30.37	32.34
28.75	29.84	32.33	29.75	30.43	32.89	29.75	30.36	32.40
28.50	29.90	32.31	29.50	30.44	32.96	29.50	30.40	32.41
28.25	29.99	32.29	29.25	30.48	33.02	29.25	30.43	32.41
28.00	30.08	32.33	29.00	30.51	33.07	29.00	30.47	32.43
27.75	30.18	32.43	28.75	30.55	33.11	28.75	30.47	32.47
27.50	30.22	32.52	28.50	30.59	33.17	28.50	30.45	32.51
27.25	30.20	32.54	28.25	30.62	33.20	28.25	30.45	32.54

27.00	30.19	32.54	28.00	30.66	33.23	28.00	30.45	32.57
26.75	30.21	32.53	27.75	30.69	33.25	27.75	30.49	32.53
26.50	30.22	32.51	27.50	30.71	33.30	27.50	30.52	32.52
26.25	30.19	32.53	27.25	30.74	33.36	27.25	30.54	32.53
26.00	30.13	32.55	27.00	30.78	33.38	27.00	30.60	32.52
25.75	30.24	32.56	26.75	30.82	33.38	26.75	30.68	32.54
25.50	30.31	32.62	26.50	30.86	33.36	26.50	30.76	32.52
25.25	30.33	32.80	26.25	30.89	33.29	26.25	30.81	32.42
25.00	30.41	32.85	26.00	30.93	33.19	26.00	30.85	32.39
24.75	30.38	32.90	25.75	30.98	33.08	25.75	30.89	32.42
24.50	30.41	32.94	25.50	31.02	33.13	25.50	30.91	32.43
24.25	30.43	32.94	25.25	31.00	33.14	25.25	30.94	32.55
24.00	30.41	32.93	25.00	31.01	33.19	25.00	31.01	32.64
23.75	30.45	32.92	24.75	31.03	33.22	24.75	31.08	32.72
23.50	30.53	32.92	24.50	31.04	33.21	24.50	31.10	32.80
23.25	30.64	33.06	24.25	31.03	33.18	24.25	31.13	32.86
23.00	30.68	33.15	24.00	31.02	33.16	24.00	31.16	32.92
22.75	30.69	33.20	23.75	31.01	33.16	23.75	31.20	32.98
22.50	30.66	33.23	23.50	30.98	33.16	23.50	31.22	32.99
22.25	30.59	33.22	23.25	30.94	33.18	23.25	31.23	32.93
22.00	30.55	33.27	23.00	30.89	33.18	23.00	31.15	32.87
21.75	30.55	33.34	22.75	30.83	33.16	22.75	30.98	32.92
21.50	30.55	33.30	22.50	30.77	33.12	22.50	30.96	32.99
21.25	30.54	33.19	22.25	30.73	33.00	22.25	30.98	33.03
21.00	30.49	33.06	22.00	30.69	32.88	22.00	30.94	33.08
20.75	30.43	32.89	21.75	30.65	32.86	21.75	30.88	33.14
20.50	30.34	32.77	21.50	30.62	32.86	21.50	30.88	33.19
20.25	30.33	32.75	21.25	30.60	32.90	21.25	30.87	33.24
20.00	30.34	32.79	21.00	30.57	32.97	21.00	30.87	33.25
19.75	30.36	32.76	20.75	30.56	33.05	20.75	30.91	33.22
19.50	30.35	32.75	20.50	30.54	33.16	20.50	30.86	33.18
19.25	30.37	32.77	20.25	30.49	33.22	20.25	30.82	33.15
19.00	30.38	32.81	20.00	30.43	33.22	20.00	30.78	33.12
18.75	30.18	32.86	19.75	30.37	33.22	19.75	30.69	33.11
18.50	30.02	32.86	19.50	30.29	33.21	19.50	30.58	33.09
18.25	29.83	32.80	19.25	30.20	33.20	19.25	30.53	33.10
18.00	29.74	32.70	19.00	30.09	33.17	19.00	30.46	33.22
17.75	29.72	32.61	18.75	29.98	33.13	18.75	30.37	33.18
17.50	29.68	32.65	18.50	29.86	32.98	18.50	30.30	33.06
17.25	29.27	32.66	18.25	29.80	32.93	18.25	29.88	32.93
17.00	29.19	32.61	18.00	29.64	32.88	18.00	29.73	32.76
16.75	27.86	32.53	17.75	29.45	32.95	17.75	29.69	32.62
16.50	27.66	32.52	17.50	29.30	33.03	17.50	29.76	32.56
16.25	27.48	32.50	17.25	29.16	33.10	17.25	29.63	32.52
16.00	27.32	32.47	17.00	29.03	33.16	17.00	29.18	32.40
15.75	27.31	32.42	16.75	28.90	33.18	16.75	28.81	32.30
15.50	27.29	32.35	16.50	28.80	33.19	16.50	28.66	32.22
15.25	26.97	32.26	16.25	28.65	33.20	16.25	28.51	32.07
15.00	26.51	32.09	16.00	28.50	33.20	16.00	28.48	32.08

14.75	26.25	31.84	15.75	28.34	33.20	15.75	28.46	32.19
14.50	26.00	31.43	15.50	28.20	33.19	15.50	28.39	32.24
14.25	25.77	31.22	15.25	28.08	33.17	15.25	28.11	32.22
14.00	25.39	31.28	15.00	27.86	33.15	15.00	27.75	32.19
13.75	25.13	31.21	14.75	27.64	33.11	14.75	27.67	32.27
13.50	24.67	31.04	14.50	27.47	33.07	14.50	27.24	32.29
13.25	24.50	30.74	14.25	27.17	33.02	14.25	26.92	32.25
13.00	24.37	30.01	14.00	26.88	33.00	14.00	26.77	32.16
12.75	24.24	29.90	13.75	25.66	32.98	13.75	26.69	32.01
12.50	24.08	29.78	13.50	25.58	32.96	13.50	25.57	30.48
12.25	23.97	29.67	13.25	25.35	32.91	13.25	25.57	30.35
12.00	23.83	29.44	13.00	25.09	32.85	13.00	25.33	30.16
11.75	23.61	28.52	12.75	25.02	32.84	12.75	25.08	30.07
11.50	23.34	28.30	12.50	24.89	32.81	12.50	24.95	29.97
11.25	23.01	28.07	12.25	24.79	32.73	12.25	24.73	29.86
11.00	22.59	27.84	12.00	24.12	32.47	12.00	24.72	29.72
10.75	22.25	27.51	11.75	23.41	32.20	11.75	24.66	29.55
10.50	21.88	27.11	11.50	22.90	32.11	11.50	24.41	29.40
10.25	21.88	26.93	11.25	22.54	32.12	11.25	24.04	29.26
10.00	21.70	26.89	11.00	22.37	32.08	11.00	23.86	28.55
9.75	21.71	26.86	10.75	22.27	31.97	10.75	23.65	27.91
9.50	21.66	26.79	10.50	22.19	30.78	10.50	23.43	27.52
9.25	21.59	26.43	10.25	22.25	29.94	10.25	23.18	27.25
9.00	21.44	26.21	10.00	22.70	29.95	10.00	23.12	27.14
8.75	21.23	26.27	9.75	22.45	29.97	9.75	22.98	27.00
8.50	20.98	26.32	9.50	22.29	29.93	9.50	22.64	26.87
8.25	20.66	26.29	9.25	22.14	26.73	9.25	22.34	26.73
8.00	20.35	26.24	9.00	22.01	25.89	9.00	22.20	26.58
7.75	20.12	26.12	8.75	21.86	25.98	8.75	22.16	26.41
7.50	19.92	26.07	8.50	21.71	25.76	8.50	22.11	25.57
7.25	19.74	26.06	8.25	21.61	25.76	8.25	22.00	25.33
7.00	19.59	25.94	8.00	21.58	26.58	8.00	21.76	24.92
6.75	19.41	25.76	7.75	21.57	26.36	7.75	21.63	24.61
6.50	19.33	25.56	7.50	21.79	26.34	7.50	21.47	24.44
6.25	19.13	25.30	7.25	21.67	26.20	7.25	21.30	24.37
6.00	18.68	24.82	7.00	21.49	26.06	7.00	21.25	24.13
5.75	18.67	24.66	6.75	21.14	25.87	6.75	21.19	24.18
5.50	18.71	24.58	6.50	20.38	25.18	6.50	21.11	24.16
5.25	18.67	24.43	6.25	20.06	24.97	6.25	20.83	23.51
5.00	18.54	24.22	6.00	19.87	24.76	6.00	19.80	23.49
4.75	18.46	23.98	5.75	19.77	24.55	5.75	19.31	23.49
4.50	18.41	23.76	5.50	19.71	24.35	5.50	19.21	23.50
4.25	18.20	23.59	5.25	19.68	24.32	5.25	19.12	23.49
4.00	18.04	23.60	5.00	19.64	24.33	5.00	18.91	23.40
3.75	17.89	23.52	4.75	19.32	24.31	4.75	18.41	23.33
3.50	17.37	23.37	4.50	18.49	24.29	4.50	18.05	23.32
3.25	17.26	23.41	4.25	18.03	24.27	4.25	17.75	24.04
3.00	17.06	23.50	4.00	17.73	24.24	4.00	17.41	24.02
2.75	16.78	23.50	3.75	17.58	24.13	3.75	17.28	23.90

2.50	16.64	23.43	3.50	17.45	23.99	3.50	17.19	23.65
2.25	16.52	23.37	3.25	17.37	23.83	3.25	17.10	23.62
2.00	16.19	23.36	3.00	17.36	23.68	3.00	17.01	23.60
1.75	16.35	23.36	2.75	17.40	23.53	2.75	16.93	23.58
1.50	16.20	23.59	2.50	17.38	23.37	2.50	16.85	23.22
1.25	15.71	23.73	2.25	17.32	23.18	2.25	16.78	23.19
1.00	15.10	23.44	2.00	17.22	22.85	2.00	16.72	23.21
0.75	14.90	23.58	1.75	17.17	22.66	1.75	16.65	23.18
0.50	14.76	22.46	1.50	17.14	22.38	1.50	16.53	23.21
0.25	14.48	22.16	1.25	17.11	23.07	1.25	16.32	23.45
0.00	14.35	21.73	1.00	17.10	23.08	1.00	15.77	23.61
-0.25	14.19	21.83	0.75	17.08	22.90	0.75	15.49	23.61
-0.50	14.09	21.92	0.50	16.96	22.54	0.50	15.28	23.59
-0.75	14.13	21.82	0.25	16.74	22.07	0.25	15.28	23.51
-1.00	13.63	21.60	0.00	16.50	21.63	0.00	15.66	23.33
-1.25	13.40	21.17	-0.25	16.25	21.40	-0.25	16.03	23.12
-1.50	13.24	21.10	-0.50	16.07	21.31	-0.50	16.05	22.91
-1.75	13.08	21.01	-0.75	15.97	21.19	-0.75	15.87	22.62
-2.00	12.89	20.91	-1.00	15.94	21.30	-1.00	15.42	21.73
-2.25	12.68	20.82	-1.25	15.85	20.80	-1.25	15.36	21.65
-2.50	12.45	20.46	-1.50	15.18	20.62	-1.50	15.38	21.60
-2.75	12.25	20.19	-1.75	14.65	20.41	-1.75	15.39	21.58
-3.00	12.36	20.33	-2.00	14.45	20.11	-2.00	15.31	21.57
-3.25	12.27	19.92	-2.25	14.28	20.03	-2.25	15.06	21.55
-3.50	12.26	19.85	-2.50	14.15	19.94	-2.50	14.76	21.52
-3.75	12.33	19.74	-2.75	13.93	19.81	-2.75	14.42	21.44
-4.00	12.21	19.60	-3.00	13.82	19.55	-3.00	14.15	21.34
-4.25	12.07	19.47	-3.25	13.74	19.45	-3.25	13.95	21.33
-4.50	11.21	19.36	-3.50	13.67	19.28	-3.50	13.57	21.24
-4.75	10.98	19.32	-3.75	13.69	19.05	-3.75	13.25	21.12
-5.00	10.74	19.36	-4.00	13.55	18.84	-4.00	13.19	20.95
-5.25	10.53	19.37	-4.25	13.24	18.90	-4.25	13.11	20.85
-5.50	10.36	19.27	-4.50	12.87	18.85	-4.50	12.98	20.75
-5.75	10.18	19.12	-4.75	12.66	18.68	-4.75	12.84	20.64
-6.00	10.01	18.85	-5.00	12.48	18.53	-5.00	12.70	20.11
-6.25	9.87	18.47	-5.25	12.31	18.51	-5.25	12.06	19.88
-6.50	9.98	18.39	-5.50	12.16	18.51	-5.50	11.59	19.24
-6.75	10.01	18.29	-5.75	12.01	18.53	-5.75	11.42	18.94
-7.00	10.14	18.20	-6.00	11.86	18.40	-6.00	11.29	18.71
-7.25	10.31	18.10	-6.25	11.72	18.24	-6.25	11.26	18.20
-7.50	10.45	17.98	-6.50	11.57	17.86	-6.50	11.27	18.10
-7.75	10.06	17.85	-6.75	11.34	17.13	-6.75	11.24	17.98
-8.00	9.89	17.71	-7.00	11.07	16.71	-7.00	11.16	17.80
-8.25	9.78	17.51	-7.25	10.93	16.56	-7.25	11.01	17.61
-8.50	9.68	17.27	-7.50	11.00	16.43	-7.50	10.73	17.96
-8.75	9.53	16.98	-7.75	11.01	16.31	-7.75	10.29	18.14
-9.00	9.08	16.68	-8.00	10.92	15.88	-8.00	10.09	18.21
-9.25	8.67	16.46	-8.25	10.49	15.72	-8.25	9.90	18.20
-9.50	8.46	15.96	-8.50	10.11	15.60	-8.50	9.69	18.08

-9.75	8.43	15.83	-8.75	10.00	15.48	-8.75	9.55	16.87
-10.00	8.34	15.95	-9.00	9.74	15.25	-9.00	9.45	16.45
-10.25	8.17	15.27	-9.25	9.53	15.32	-9.25	9.37	16.40
-10.50	7.86	15.05	-9.50	9.40	15.26	-9.50	9.30	16.40
-10.75	7.56	14.83	-9.75	9.36	14.75	-9.75	9.28	16.40
-11.00	7.71	15.31	-10.00	9.32	14.69	-10.00	9.22	16.38
-11.25	7.77	15.09	-10.25	9.13	14.15	-10.25	9.02	16.32
-11.50	7.74	14.87	-10.50	9.01	14.05	-10.50	8.84	16.11
-11.75	7.63	14.66	-10.75	8.27	14.03	-10.75	8.76	15.80
-12.00	7.42	14.44	-11.00	8.02	14.01	-11.00	8.38	15.52
-12.25	7.13	14.25	-11.25	7.75	13.99	-11.25	8.13	15.16
-12.50	6.70	14.08	-11.50	7.66	13.97	-11.50	7.95	14.83
-12.75	6.01	13.92	-11.75	7.52	13.91	-11.75	7.82	14.79
-13.00	5.65	13.80	-12.00	6.96	12.80	-12.00	7.79	14.83
-13.25	5.04	13.65	-12.25	6.83	12.82	-12.25	7.35	14.86
-13.50	4.69	13.66	-12.50	6.85	12.87	-12.50	7.18	14.79
-13.75	4.56	13.62	-12.75	6.64	12.81	-12.75	6.96	14.67
-14.00	4.28	13.56	-13.00	6.48	11.95	-13.00	6.68	14.55
-14.25	4.14	13.45	-13.25	6.34	11.99	-13.25	6.54	14.31
-14.50	3.95	13.31	-13.50	6.13	11.75	-13.50	6.42	13.60
-14.75	3.81	13.09	-13.75	5.80	11.60	-13.75	5.50	13.12
-15.00	3.58	12.90	-14.00	5.32	11.43	-14.00	4.99	13.01
-15.25	3.32	12.72	-14.25	4.44	11.26	-14.25	4.69	12.88
-15.50	3.08	12.58	-14.50	4.16	11.13	-14.50	4.52	12.72
-15.75	2.88	12.47	-14.75	3.82	10.99	-14.75	4.35	12.61
-16.00	2.72	12.36	-15.00	3.42	10.75	-15.00	4.18	12.48
-16.25	2.51	12.17	-15.25	3.24	10.42	-15.25	4.04	12.31
-16.50	2.40	11.92	-15.50	3.25	10.31	-15.50	3.96	12.18
-16.75	2.19	11.66	-15.75	3.63	10.16	-15.75	3.89	12.06
-17.00	0.83	11.41	-16.00	3.81	9.97	-16.00	3.83	11.91
-17.25	0.60	10.99	-16.25	3.66	9.80	-16.25	3.57	11.74
-17.50	0.38	10.82	-16.50	3.54	9.67	-16.50	3.13	11.59
-17.75	0.06	10.65	-16.75	3.40	9.51	-16.75	2.81	11.57
-18.00	-0.40	10.49	-17.00	3.13	9.34	-17.00	1.52	11.68
-18.25	-0.75	10.35	-17.25	2.91	9.12	-17.25	1.35	11.68
-18.50	-1.01	10.22	-17.50	2.38	8.88	-17.50	1.27	11.59
-18.75	-1.23	10.26	-17.75	2.15	8.71	-17.75	1.13	11.45
-19.00	-1.39	10.34	-18.00	1.88	8.65	-18.00	0.89	10.80
-19.25	-1.48	10.41	-18.25	1.38	8.46	-18.25	0.43	10.50
-19.50	-1.64	10.48	-18.50	-1.01	8.25	-18.50	-0.72	10.28
-19.75	-1.82	10.52	-18.75	-1.13	7.76	-18.75	-1.23	10.08
-20.00	-1.99	10.44	-19.00	-1.33	7.34	-19.00	-1.49	9.85
-20.25	-2.05	9.79	-19.25	-1.82	7.19	-19.25	-1.76	9.66
-20.50	-2.09	8.95	-19.50	-2.22	7.05	-19.50	-2.01	9.39
-20.75	-2.18	8.75	-19.75	-2.32	6.91	-19.75	-2.04	8.78
-21.00	-2.31	8.67	-20.00	-2.50	6.75	-20.00	-1.92	8.10
-21.25	-2.46	8.62	-20.25	-2.67	6.54	-20.25	-2.33	8.03
-21.50	-2.87	8.60	-20.50	-3.52	6.33	-20.50	-2.38	7.98
-21.75	-2.97	8.55	-20.75	-4.53	6.71	-20.75	-2.24	7.86

-22.00	-3.66	8.48	-21.00	-4.97	6.74	-21.00	-2.43	7.67
-22.25	-3.81	8.33	-21.25	-5.18	6.63	-21.25	-2.97	7.09
-22.50	-4.03	7.67	-21.50	-5.25	6.48	-21.50	-4.02	6.56
-22.75	-4.00	7.55	-21.75	-5.35	6.28	-21.75	-5.08	5.35
-23.00	-4.59	7.14	-22.00	-5.48	6.04	-22.00	-5.05	4.95
-23.25	-4.04	6.27	-22.25	-5.73	5.91	-22.25	-5.00	4.74
-23.50	-5.62	6.00	-22.50	-6.27	5.86	-22.50	-4.95	4.43
-23.75	-5.72	5.54	-22.75	-6.56	5.77	-22.75	-4.95	4.26
-24.00	-6.16	5.43	-23.00	-6.74	5.65	-23.00	-4.96	3.90
-24.25	-6.91	5.64	-23.25	-6.92	5.54	-23.25	-5.00	3.00
-24.50	-7.86	4.81	-23.50	-7.07	5.48	-23.50	-5.10	2.65
-24.75	-8.04	4.91	-23.75	-7.24	5.36	-23.75	-5.22	2.64
-25.00	-7.99	4.73	-24.00	-7.41	5.20	-24.00	-5.41	2.63
-25.25	-7.92	4.55	-24.25	-7.63	4.94	-24.25	-5.62	2.49
-25.50	-7.87	4.37	-24.50	-7.96	4.38	-24.50	-5.88	2.34
-25.75	-8.04	4.06	-24.75	-8.27	3.79	-24.75	-6.41	2.18
-26.00	-8.39	5.74	-25.00	-8.42	3.68	-25.00	-7.15	1.51
-26.25	-9.03	3.03	-25.25	-8.53	3.54	-25.25	-7.54	1.46
-26.50	-9.48	2.70	-25.50	-9.24	3.37	-25.50	-7.66	1.59
-26.75	-9.84	3.25	-25.75	-9.34	3.16	-25.75	-7.78	1.60
-27.00	-10.39	2.39	-26.00	-9.44	2.95	-26.00	-7.90	1.54
-27.25	-10.55	2.19	-26.25	-9.56	2.35	-26.25	-8.63	1.49
-27.50	-10.57	1.94	-26.50	-9.90	1.68	-26.50	-9.15	1.44
-27.75	-10.57	1.65	-26.75	-10.29	0.48	-26.75	-9.46	1.33
-28.00	-11.54	1.26	-27.00	-10.65	0.26	-27.00	-9.59	1.06
-28.25	-12.10	0.96	-27.25	-10.76	-0.68	-27.25	-9.71	1.00
-28.50	-12.51	0.89	-27.50	-10.97	-0.53	-27.50	-11.89	1.05
-28.75	-12.82	0.89	-27.75	-11.25	-0.37	-27.75	-11.07	1.11
-29.00	-12.99	0.94	-28.00	-12.85	-0.23	-28.00	-10.65	1.15
-29.25	-13.09	0.77	-28.25	-13.26	-1.83	-28.25	-11.70	1.05
-29.50	-13.14	-0.62	-28.50	-13.53	-3.56	-28.50	-13.07	-0.52
-29.75	-13.35	0.21	-28.75	-13.59	-1.75	-28.75	-13.40	0.53
-30.00	-13.75	-1.09	-29.00	-13.57	-3.55	-29.00	-13.75	-1.37
-30.25	-14.24	-1.26	-29.25	-13.76	-3.55	-29.25	-14.04	-2.59
-30.50	-14.72	-1.42	-29.50	-14.40	-3.65	-29.50	-14.35	-3.30
-30.75	-15.02	-1.60	-29.75	-14.66	-3.86	-29.75	-14.85	-3.73
-31.00	-15.16	-1.70	-30.00	-15.01	-4.08	-30.00	-15.14	-3.79
-31.25	-15.49	-1.76	-30.25	-16.28	-4.16	-30.25	-15.31	-3.81
-31.50	-16.50	-1.94	-30.50	-16.76	-4.35	-30.50	-15.48	-3.91
-31.75	-17.18	-2.14	-30.75	-16.86	-5.47	-30.75	-15.71	-4.16
-32.00	-17.35	-2.64	-31.00	-17.01	-5.51	-31.00	-15.95	-4.40
-32.25	-17.48	-3.07	-31.25	-17.25	-6.00	-31.25	-16.22	-4.65
-32.50	-18.17	-3.29	-31.50	-17.64	-6.20	-31.50	-16.56	-4.89
-32.75	-18.74	-3.30	-31.75	-18.07	-6.36	-31.75	-16.83	-5.15
-33.00	-19.31	-3.36	-32.00	-18.28	-6.47	-32.00	-16.78	-5.39
-33.25	N/A	-3.62	-32.25	-18.68	-6.54	-32.25	-17.39	-5.55
-33.50	N/A	-5.69	-32.50	-19.15	-6.66	-32.50	-17.51	-5.59
-33.75	N/A	-4.56	-32.75	N/A	-6.79	-32.75	-17.77	-5.63
-34.00	N/A	-7.10	-33.00	N/A	-6.67	-33.00	-18.00	-5.67

-34.25	N/A	-6.93
-34.50	N/A	-4.85
-34.75	N/A	-7.70
-35.00	N/A	-7.50
-35.25	N/A	-6.13
-35.50	N/A	-5.81
-35.75	N/A	-8.30
-36.00	N/A	-8.88
-36.25	N/A	-9.04
-36.50	N/A	-9.25
-36.75	N/A	-9.35
-37.00	N/A	-9.40
-37.25	N/A	-9.45
-37.50	N/A	-9.55
-37.75	N/A	-9.71
-38.00	N/A	-9.80
-38.25	N/A	-9.90
-38.50	N/A	-9.99
-38.75	N/A	-10.07
-39.00	N/A	-10.13
-39.25	N/A	-10.17
-39.50	N/A	-10.54
-39.75	N/A	-12.34
-40.00	N/A	-12.21
-40.25	N/A	-11.30
-40.50	N/A	-12.47
-40.75	N/A	-13.45
-41.00	N/A	-13.68
-41.25	N/A	-13.78
-41.50	N/A	-13.97
-41.75	N/A	-14.29
-42.00	N/A	-14.39
-42.25	N/A	-14.39
-42.50	N/A	-14.32
-42.75	N/A	-14.32
-43.00	N/A	-14.42
-43.25	N/A	-14.68
-43.50	N/A	-15.46
-43.75	N/A	-16.02
-44.00	N/A	-16.40
-44.25	N/A	-16.78
-44.50	N/A	-17.13
-44.75	N/A	-17.50
-45.00	N/A	-18.17
-45.25	N/A	-18.80
-45.50	N/A	-19.73

-33.25	N/A	-6.41
-33.50	N/A	-6.41
-33.75	N/A	-6.48
-34.00	N/A	-6.58
-34.25	N/A	-6.70
-34.50	N/A	-6.86
-34.75	N/A	-7.06
-35.00	N/A	-7.29
-35.25	N/A	-8.10
-35.50	N/A	-8.21
-35.75	N/A	-8.42
-36.00	N/A	-8.65
-36.25	N/A	-8.88
-36.50	N/A	-9.13
-36.75	N/A	-9.40
-37.00	N/A	-9.59
-37.25	N/A	-9.76
-37.50	N/A	-9.91
-37.75	N/A	-9.95
-38.00	N/A	-9.84
-38.25	N/A	-10.00
-38.50	N/A	-10.13
-38.75	N/A	-10.24

-33.25	-18.28	-5.71
-33.50	-18.60	-5.71
-33.75	-19.21	-5.69
-34.00	N/A	-5.67
-34.25	N/A	-5.66
-34.50	N/A	-5.64
-34.75	N/A	-5.64
-35.00	N/A	-5.70
-35.25	N/A	-5.79
-35.50	N/A	-5.89
-35.75	N/A	-6.02
-36.00	N/A	-6.25
-36.25	N/A	-6.48
-36.50	N/A	-6.72
-36.75	N/A	-7.00
-37.00	N/A	-7.33
-37.25	N/A	-7.65
-37.50	N/A	-7.98
-37.75	N/A	-8.70
-38.00	N/A	-9.06
-38.25	N/A	-9.82
-38.50	N/A	-10.19
-38.75	N/A	-10.58
-39.00	N/A	-11.00
-39.25	N/A	-11.02
-39.50	N/A	-11.22
-39.75	N/A	-12.66
-40.00	N/A	-12.86
-40.25	N/A	-13.06
-40.50	N/A	-13.27
-40.75	N/A	-13.47

Table D2. High-Water statistics for H/P ≈ 0.878 (Q ≈ 540 L/S) and with $p = 0.46\ P$, $p = 0.62\ P$, and $p = 0.77\ P$ (units in inches).

High-Water Statistics for H/P ≈ 0.878 and p = 0.46 P			High-Water Statistics for H/P ≈ 0.878 and p = 0.62 P			High-Water Statistics for H/P ≈ 0.878 and p = 0.77 P		
X	Y Min.	Y Max.	X	Y Min.	Y Max	X	Y Min.	Y Max.
62.75	33.79	34.29	63.00	34.07	35.03	63.75	34.92	36.24
62.50	33.71	34.29	62.75	34.00	35.03	63.50	34.91	36.23
62.25	33.67	34.29	62.50	33.99	35.03	63.25	34.91	36.23
62.00	33.63	34.29	62.25	33.98	35.03	63.00	34.89	36.22
61.75	33.59	34.28	62.00	33.95	35.02	62.75	34.88	36.20
61.50	33.56	34.26	61.75	33.92	35.02	62.50	34.87	36.20
61.25	33.51	34.23	61.50	33.89	35.02	62.25	34.84	36.18
61.00	33.51	34.20	61.25	33.92	35.00	62.00	34.80	36.17
60.75	33.49	34.15	61.00	33.96	35.00	61.75	34.76	36.17
60.50	33.49	34.11	60.75	33.96	34.99	61.50	34.74	36.14
60.25	33.47	34.13	60.50	33.94	34.99	61.25	34.72	36.14
60.00	33.43	34.15	60.25	33.89	34.98	61.00	34.70	36.11
59.75	33.42	34.15	60.00	33.85	34.95	60.75	34.68	36.09
59.50	33.39	34.09	59.75	33.77	34.94	60.50	34.64	36.07
59.25	33.35	34.11	59.50	33.71	34.91	60.25	34.61	36.04
59.00	33.31	34.13	59.25	33.69	34.91	60.00	34.58	36.02
58.75	33.27	34.16	59.00	33.69	34.88	59.75	34.53	35.99
58.50	33.24	34.18	58.75	33.69	34.87	59.50	34.47	35.97
58.25	33.20	34.19	58.50	33.68	34.86	59.25	34.41	35.95
58.00	33.18	34.19	58.25	33.65	34.83	59.00	34.41	35.93
57.75	33.16	34.19	58.00	33.65	34.82	58.75	34.41	35.90
57.50	33.10	34.17	57.75	33.65	34.80	58.50	34.38	35.86
57.25	33.08	34.14	57.50	33.61	34.79	58.25	34.34	35.83
57.00	33.09	34.09	57.25	33.57	34.76	58.00	34.29	35.81
56.75	33.06	34.02	57.00	33.52	34.73	57.75	34.25	35.77
56.50	33.03	33.94	56.75	33.47	34.65	57.50	34.20	35.74
56.25	33.00	33.85	56.50	33.43	34.58	57.25	34.15	35.71
56.00	32.98	33.78	56.25	33.38	34.53	57.00	34.10	35.68
55.75	32.96	33.70	56.00	33.30	34.47	56.75	34.05	35.65
55.50	32.92	33.63	55.75	33.25	34.38	56.50	33.98	35.63
55.25	32.86	33.55	55.50	33.23	34.30	56.25	33.92	35.60

55.00	32.81	33.48	55.25	33.23	34.25	56.00	33.88	35.57
54.75	32.78	33.43	55.00	33.16	34.21	55.75	33.85	35.53
54.50	32.75	33.40	54.75	33.12	34.15	55.50	33.80	35.48
54.25	32.68	33.38	54.50	33.09	34.04	55.25	33.74	35.43
54.00	32.63	33.35	54.25	33.02	33.98	55.00	33.68	35.38
53.75	32.58	33.31	54.00	32.95	33.93	54.75	33.64	35.33
53.50	32.53	33.25	53.75	32.86	33.77	54.50	33.60	35.28
53.25	32.43	33.19	53.50	32.78	33.70	54.25	33.56	35.20
53.00	32.37	33.14	53.25	32.73	33.67	54.00	33.53	35.11
52.75	32.33	33.09	53.00	32.73	33.63	53.75	33.48	35.02
52.50	32.28	33.04	52.75	32.71	33.54	53.50	33.44	34.92
52.25	32.25	32.97	52.50	32.64	33.48	53.25	33.41	34.86
52.00	32.25	32.94	52.25	32.60	33.47	53.00	33.38	34.81
51.75	32.23	32.91	52.00	32.64	33.46	52.75	33.35	34.73
51.50	32.19	32.88	51.75	32.61	33.41	52.50	33.32	34.64
51.25	32.13	32.84	51.50	32.57	33.36	52.25	33.26	34.59
51.00	32.06	32.79	51.25	32.52	33.33	52.00	33.15	34.56
50.75	32.04	32.75	51.00	32.47	33.29	51.75	33.05	34.53
50.50	32.03	32.71	50.75	32.42	33.26	51.50	32.97	34.49
50.25	32.00	32.67	50.50	32.35	33.23	51.25	32.95	34.40
50.00	31.97	32.63	50.25	32.30	33.21	51.00	32.93	34.32
49.75	31.89	32.58	50.00	32.27	33.16	50.75	32.92	34.29
49.50	31.86	32.53	49.75	32.24	33.09	50.50	32.90	34.29
49.25	31.85	32.51	49.50	32.21	33.02	50.25	32.89	34.28
49.00	31.80	32.48	49.25	32.18	32.96	50.00	32.85	34.24
48.75	31.77	32.43	49.00	32.13	32.93	49.75	32.80	34.18
48.50	31.70	32.36	48.75	32.08	32.90	49.50	32.76	34.13
48.25	31.63	32.35	48.50	32.01	32.87	49.25	32.71	34.10
48.00	31.59	32.32	48.25	31.97	32.83	49.00	32.64	34.08
47.75	31.57	32.29	48.00	31.94	32.79	48.75	32.59	34.03
47.50	31.55	32.25	47.75	31.93	32.74	48.50	32.59	33.95
47.25	31.48	32.21	47.50	31.79	32.70	48.25	32.47	33.87
47.00	31.41	32.17	47.25	31.70	32.65	48.00	32.36	33.80
46.75	31.37	32.11	47.00	31.65	32.59	47.75	32.28	33.72
46.50	31.33	32.05	46.75	31.61	32.52	47.50	32.20	33.63
46.25	31.28	32.01	46.50	31.57	32.46	47.25	32.12	33.56
46.00	31.24	31.98	46.25	31.50	32.42	47.00	32.03	33.48
45.75	31.19	31.95	46.00	31.42	32.35	46.75	31.86	33.40
45.50	31.14	31.92	45.75	31.36	32.31	46.50	31.69	33.35
45.25	31.09	31.86	45.50	31.33	32.34	46.25	31.53	33.35
45.00	31.05	31.80	45.25	31.31	32.43	46.00	31.44	33.36
44.75	31.02	31.79	45.00	31.28	32.40	45.75	31.40	33.34
44.50	30.97	31.78	44.75	31.25	32.32	45.50	31.38	33.31
44.25	30.92	31.76	44.50	31.23	32.23	45.25	31.40	33.28
44.00	30.88	31.74	44.25	31.20	32.13	45.00	31.43	33.22
43.75	30.83	31.71	44.00	31.20	32.05	44.75	31.47	33.16
43.50	30.82	31.66	43.75	31.18	32.02	44.50	31.47	33.09
43.25	30.79	31.59	43.50	31.13	31.98	44.25	31.44	33.02
43.00	30.75	31.56	43.25	31.04	31.95	44.00	31.39	32.93

42.75	30.70	31.54	43.00	31.02	31.94	43.75	31.29	32.84
42.50	30.68	31.53	42.75	31.01	31.94	43.50	31.19	32.76
42.25	30.66	31.51	42.50	30.95	31.93	43.25	31.17	32.69
42.00	30.66	31.49	42.25	30.92	31.93	43.00	31.28	32.63
41.75	30.63	31.48	42.00	30.90	31.93	42.75	31.39	32.61
41.50	30.62	31.46	41.75	30.89	31.92	42.50	31.38	32.58
41.25	30.60	31.45	41.50	30.83	31.90	42.25	31.36	32.56
41.00	30.59	31.43	41.25	30.73	31.87	42.00	31.35	32.52
40.75	30.57	31.42	41.00	30.70	31.84	41.75	31.29	32.49
40.50	30.57	31.42	40.75	30.66	31.81	41.50	31.19	32.45
40.25	30.53	31.43	40.50	30.62	31.78	41.25	31.11	32.36
40.00	30.47	31.44	40.25	30.58	31.75	41.00	31.09	32.29
39.75	30.45	31.44	40.00	30.56	31.72	40.75	31.07	32.26
39.50	30.45	31.42	39.75	30.56	31.70	40.50	31.06	32.22
39.25	30.45	31.41	39.50	30.58	31.72	40.25	31.00	32.18
39.00	30.44	31.42	39.25	30.59	31.75	40.00	30.92	32.15
38.75	30.41	31.42	39.00	30.53	31.76	39.75	30.83	32.13
38.50	30.39	31.42	38.75	30.46	31.76	39.50	30.76	32.11
38.25	30.36	31.42	38.50	30.43	31.78	39.25	30.69	32.11
38.00	30.35	31.41	38.25	30.40	31.81	39.00	30.63	32.11
37.75	30.36	31.42	38.00	30.38	31.80	38.75	30.55	32.10
37.50	30.32	31.43	37.75	30.38	31.78	38.50	30.43	32.09
37.25	30.28	31.43	37.50	30.35	31.77	38.25	30.30	32.08
37.00	30.24	31.40	37.25	30.34	31.76	38.00	30.22	32.07
36.75	30.21	31.38	37.00	30.31	31.76	37.75	30.20	32.03
36.50	30.18	31.36	36.75	30.27	31.71	37.50	30.17	32.01
36.25	30.15	31.32	36.50	30.26	31.67	37.25	30.16	32.02
36.00	30.12	31.28	36.25	30.26	31.66	37.00	30.13	32.02
35.75	30.13	31.28	36.00	30.26	31.68	36.75	30.11	32.02
35.50	30.15	31.30	35.75	30.26	31.68	36.50	30.10	32.02
35.25	30.12	31.31	35.50	30.28	31.72	36.25	30.08	32.00
35.00	30.10	31.33	35.25	30.32	31.74	36.00	30.08	32.00
34.75	30.07	31.34	35.00	30.34	31.74	35.75	30.10	32.04
34.50	30.05	31.34	34.75	30.30	31.73	35.50	30.12	32.09
34.25	30.03	31.34	34.50	30.23	31.73	35.25	30.10	32.15
34.00	30.00	31.35	34.25	30.20	31.73	35.00	30.09	32.21
33.75	30.00	31.36	34.00	30.25	31.80	34.75	30.07	32.27
33.50	30.01	31.39	33.75	30.27	31.83	34.50	30.07	32.32
33.25	30.00	31.43	33.50	30.27	31.83	34.25	30.07	32.37
33.00	29.95	31.46	33.25	30.28	31.80	34.00	30.07	32.41
32.75	29.95	31.49	33.00	30.34	31.79	33.75	30.09	32.42
32.50	29.95	31.52	32.75	30.39	31.78	33.50	30.12	32.43
32.25	29.98	31.55	32.50	30.40	31.77	33.25	30.16	32.43
32.00	30.02	31.58	32.25	30.43	31.78	33.00	30.19	32.45
31.75	30.02	31.64	32.00	30.44	31.84	32.75	30.23	32.46
31.50	30.02	31.69	31.75	30.44	31.84	32.50	30.24	32.49
31.25	30.03	31.72	31.50	30.47	31.84	32.25	30.21	32.56
31.00	30.07	31.75	31.25	30.49	31.85	32.00	30.19	32.60
30.75	30.12	31.75	31.00	30.53	31.87	31.75	30.17	32.62

30.50	30.17	31.75	30.75	30.52	31.89	31.50	30.15	32.63
30.25	30.22	31.76	30.50	30.51	31.92	31.25	30.13	32.68
30.00	30.26	31.80	30.25	30.50	31.92	31.00	30.11	32.75
29.75	30.28	31.83	30.00	30.50	31.93	30.75	30.10	32.80
29.50	30.30	31.86	29.75	30.49	31.96	30.50	30.11	32.84
29.25	30.32	31.89	29.50	30.49	31.97	30.25	30.15	32.86
29.00	30.35	31.90	29.25	30.50	31.99	30.00	30.16	32.87
28.75	30.40	31.93	29.00	30.54	32.04	29.75	30.18	32.87
28.50	30.46	31.98	28.75	30.60	32.09	29.50	30.18	32.87
28.25	30.55	32.03	28.50	30.66	32.16	29.25	30.21	32.89
28.00	30.52	32.04	28.25	30.72	32.23	29.00	30.27	32.91
27.75	30.50	32.06	28.00	30.78	32.31	28.75	30.34	32.94
27.50	30.48	32.10	27.75	30.81	32.33	28.50	30.37	32.95
27.25	30.46	32.12	27.50	30.81	32.43	28.25	30.35	32.98
27.00	30.44	32.12	27.25	30.81	32.53	28.00	30.37	32.99
26.75	30.44	32.07	27.00	30.81	32.63	27.75	30.37	33.00
26.50	30.44	32.06	26.75	30.86	32.71	27.50	30.38	33.01
26.25	30.45	32.10	26.50	30.93	32.75	27.25	30.41	33.03
26.00	30.47	32.18	26.25	30.96	32.78	27.00	30.46	33.07
25.75	30.49	32.26	26.00	30.98	32.78	26.75	30.50	33.15
25.50	30.52	32.23	25.75	31.01	32.81	26.50	30.50	33.22
25.25	30.50	32.19	25.50	31.05	32.81	26.25	30.49	33.22
25.00	30.44	32.13	25.25	31.06	32.77	26.00	30.46	33.21
24.75	30.41	32.14	25.00	31.06	32.73	25.75	30.42	33.20
24.50	30.41	32.18	24.75	31.05	32.73	25.50	30.39	33.19
24.25	30.40	32.16	24.50	31.07	32.73	25.25	30.39	33.19
24.00	30.37	32.15	24.25	31.08	32.74	25.00	30.45	33.19
23.75	30.38	32.18	24.00	31.15	32.77	24.75	30.52	33.21
23.50	30.39	32.19	23.75	31.16	33.02	24.50	30.62	33.22
23.25	30.41	32.20	23.50	31.15	33.16	24.25	30.61	33.25
23.00	30.44	32.24	23.25	31.13	33.19	24.00	30.59	33.27
22.75	30.49	32.23	23.00	31.09	33.36	23.75	30.55	33.31
22.50	30.53	32.21	22.75	31.01	33.56	23.50	30.58	33.34
22.25	30.53	32.23	22.50	30.96	33.66	23.25	30.62	33.33
22.00	30.49	32.24	22.25	30.91	33.75	23.00	30.64	33.32
21.75	30.45	32.21	22.00	30.89	33.79	22.75	30.66	33.30
21.50	30.43	32.19	21.75	30.89	33.81	22.50	30.73	33.27
21.25	30.38	32.22	21.50	30.85	33.83	22.25	30.75	33.21
21.00	30.39	32.23	21.25	30.79	33.86	22.00	30.78	33.15
20.75	30.54	32.22	21.00	30.74	33.86	21.75	30.77	33.12
20.50	30.60	32.25	20.75	30.66	33.84	21.50	30.76	33.14
20.25	30.52	32.28	20.50	30.59	33.82	21.25	30.68	33.16
20.00	30.42	32.29	20.25	30.46	33.80	21.00	30.62	33.16
19.75	30.40	32.28	20.00	30.42	33.77	20.75	30.57	33.15
19.50	30.38	32.26	19.75	30.38	33.75	20.50	30.49	33.15
19.25	30.35	32.22	19.50	30.34	33.71	20.25	30.39	33.14
19.00	30.31	32.18	19.25	30.28	33.68	20.00	30.30	33.12
18.75	30.23	32.11	19.00	30.21	33.65	19.75	30.25	33.06
18.50	30.15	32.08	18.75	30.15	33.62	19.50	30.20	32.99

18.25	30.07	32.12	18.50	30.08	33.58	19.25	30.15	32.98
18.00	30.00	32.12	18.25	29.97	33.55	19.00	30.09	32.98
17.75	29.93	32.09	18.00	29.86	33.50	18.75	29.98	32.94
17.50	29.78	32.05	17.75	29.74	33.46	18.50	29.89	32.86
17.25	29.54	31.96	17.50	29.61	33.41	18.25	29.78	32.77
17.00	29.34	31.92	17.25	29.47	33.35	18.00	29.62	32.69
16.75	29.15	31.88	17.00	29.36	33.13	17.75	29.45	32.57
16.50	28.90	31.84	16.75	29.28	33.04	17.50	29.35	32.48
16.25	28.73	31.75	16.50	29.21	32.81	17.25	29.32	32.40
16.00	28.60	31.74	16.25	28.92	33.01	17.00	29.34	32.45
15.75	28.47	31.91	16.00	28.63	33.10	16.75	29.47	32.45
15.50	28.35	32.00	15.75	28.44	33.16	16.50	29.51	32.44
15.25	28.21	31.95	15.50	28.27	33.13	16.25	29.41	32.43
15.00	28.01	31.85	15.25	28.10	33.07	16.00	29.33	32.40
14.75	27.93	31.70	15.00	27.96	32.95	15.75	29.24	32.39
14.50	27.68	31.54	14.75	27.86	32.76	15.50	29.05	32.33
14.25	27.04	31.44	14.50	27.69	32.70	15.25	28.65	32.23
14.00	26.73	31.21	14.25	27.34	32.67	15.00	28.23	32.15
13.75	26.66	30.83	14.00	27.11	32.64	14.75	28.19	32.06
13.50	26.66	30.81	13.75	26.93	32.63	14.50	28.19	31.87
13.25	26.66	30.77	13.50	26.76	31.54	14.25	27.86	31.70
13.00	26.47	30.70	13.25	26.51	31.20	14.00	27.71	31.52
12.75	25.65	30.63	13.00	26.46	31.04	13.75	27.60	31.62
12.50	25.57	30.53	12.75	26.43	31.01	13.50	26.41	31.75
12.25	25.57	30.41	12.50	26.40	30.92	13.25	26.48	31.76
12.00	25.56	30.25	12.25	26.38	30.83	13.00	26.54	31.74
11.75	25.49	30.00	12.00	26.30	30.71	12.75	26.44	31.69
11.50	25.32	29.72	11.75	26.17	30.59	12.50	26.30	31.60
11.25	24.71	28.25	11.50	25.99	30.42	12.25	26.10	31.48
11.00	24.27	28.06	11.25	25.45	30.24	12.00	25.32	31.12
10.75	23.82	27.94	11.00	25.07	30.04	11.75	24.99	30.61
10.50	23.15	27.99	10.75	24.90	29.67	11.50	24.92	30.44
10.25	22.89	28.05	10.50	24.76	29.23	11.25	24.96	29.66
10.00	22.87	28.05	10.25	24.62	29.04	11.00	24.84	29.60
9.75	22.84	27.98	10.00	24.45	28.91	10.75	24.48	29.53
9.50	22.80	27.89	9.75	24.18	28.72	10.50	24.28	29.46
9.25	22.84	27.70	9.50	23.79	28.38	10.25	24.26	29.38
9.00	22.81	27.36	9.25	22.50	28.03	10.00	24.24	29.26
8.75	22.70	27.02	9.00	22.13	27.71	9.75	24.19	29.12
8.50	22.44	26.94	8.75	21.86	27.38	9.50	24.01	28.99
8.25	22.12	26.88	8.50	21.69	27.18	9.25	23.67	28.85
8.00	21.81	26.77	8.25	21.58	26.98	9.00	23.34	28.71
7.75	21.59	26.62	8.00	21.54	26.77	8.75	23.02	28.57
7.50	21.32	26.46	7.75	21.52	26.61	8.50	22.71	28.43
7.25	21.03	26.30	7.50	21.36	26.54	8.25	22.49	28.25
7.00	20.88	26.15	7.25	21.02	26.42	8.00	22.24	28.05
6.75	20.73	25.96	7.00	20.90	26.31	7.75	21.93	27.84
6.50	20.59	25.69	6.75	20.81	26.34	7.50	21.17	27.62
6.25	20.48	25.46	6.50	20.74	26.29	7.25	20.63	27.31

6.00	20.34	25.32	6.25	20.69	25.70	7.00	20.06	27.00
5.75	20.16	25.21	6.00	20.53	25.54	6.75	19.83	27.05
5.50	19.97	25.11	5.75	20.16	25.45	6.50	19.70	26.96
5.25	19.75	24.97	5.50	19.85	25.45	6.25	19.89	26.82
5.00	19.40	24.78	5.25	19.57	25.44	6.00	20.12	26.46
4.75	18.18	24.73	5.00	19.40	25.29	5.75	20.17	25.65
4.50	17.87	24.76	4.75	19.27	25.09	5.50	19.93	24.48
4.25	17.67	24.72	4.50	19.15	24.93	5.25	19.70	24.59
4.00	17.47	24.59	4.25	18.93	24.80	5.00	19.56	24.74
3.75	17.32	24.43	4.00	18.75	24.67	4.75	19.30	24.67
3.50	17.22	24.28	3.75	18.54	24.53	4.50	18.81	24.14
3.25	17.16	24.25	3.50	18.12	24.36	4.25	18.79	23.52
3.00	17.49	24.31	3.25	17.80	24.16	4.00	18.26	23.13
2.75	17.53	24.26	3.00	17.65	23.97	3.75	18.12	23.01
2.50	17.34	24.16	2.75	17.54	22.80	3.50	18.00	22.90
2.25	17.30	24.01	2.50	17.44	22.74	3.25	17.72	22.76
2.00	17.08	23.46	2.25	17.32	22.64	3.00	17.53	22.43
1.75	16.89	22.66	2.00	17.22	22.17	2.75	17.43	22.16
1.50	16.74	21.74	1.75	16.94	21.76	2.50	17.33	22.10
1.25	16.55	21.63	1.50	15.23	21.37	2.25	16.72	21.85
1.00	16.22	21.44	1.25	15.03	21.10	2.00	15.27	21.80
0.75	15.80	20.94	1.00	14.93	21.02	1.75	14.92	21.75
0.50	15.52	20.18	0.75	14.84	21.01	1.50	15.02	21.73
0.25	15.29	20.16	0.50	14.72	20.99	1.25	14.84	21.65
0.00	14.77	20.11	0.25	14.63	20.97	1.00	14.71	21.52
-0.25	14.70	19.92	0.00	14.62	20.95	0.75	14.62	21.39
-0.50	14.55	19.67	-0.25	14.63	20.92	0.50	14.54	21.28
-0.75	14.22	19.44	-0.50	14.62	20.89	0.25	14.41	21.15
-1.00	13.52	19.33	-0.75	14.51	20.86	0.00	14.29	20.76
-1.25	13.16	19.36	-1.00	14.41	20.83	-0.25	14.11	20.77
-1.50	13.08	19.38	-1.25	14.44	20.74	-0.50	13.81	20.74
-1.75	13.07	19.37	-1.50	14.52	19.65	-0.75	13.48	20.21
-2.00	13.02	19.20	-1.75	14.45	19.58	-1.00	13.38	19.32
-2.25	12.83	19.01	-2.00	13.09	19.44	-1.25	13.23	19.41
-2.50	12.57	18.95	-2.25	12.53	19.21	-1.50	13.07	19.31
-2.75	12.47	18.91	-2.50	11.97	18.85	-1.75	12.86	19.21
-3.00	12.40	18.91	-2.75	11.88	18.67	-2.00	12.96	19.10
-3.25	12.14	18.91	-3.00	11.74	18.55	-2.25	12.96	18.90
-3.50	12.09	18.88	-3.25	11.57	18.31	-2.50	12.39	18.57
-3.75	12.10	18.76	-3.50	11.39	17.74	-2.75	12.48	18.51
-4.00	12.09	18.49	-3.75	11.22	17.63	-3.00	12.58	18.49
-4.25	11.96	17.98	-4.00	11.04	17.54	-3.25	12.54	18.38
-4.50	11.58	17.75	-4.25	10.85	17.41	-3.50	12.34	18.26
-4.75	11.15	17.49	-4.50	10.71	17.23	-3.75	12.00	18.63
-5.00	11.05	17.08	-4.75	10.60	17.04	-4.00	11.81	18.52
-5.25	10.90	16.87	-5.00	10.35	16.74	-4.25	11.72	18.40
-5.50	10.75	16.78	-5.25	10.12	16.17	-4.50	11.30	18.20
-5.75	10.59	16.70	-5.50	9.90	16.02	-4.75	11.59	17.95
-6.00	10.35	16.62	-5.75	9.70	15.90	-5.00	11.54	17.70

-6.25	10.08	16.53	-6.00	9.52	15.84	-5.25	11.54	17.42
-6.50	9.86	16.41	-6.25	9.34	15.88	-5.50	11.54	16.87
-6.75	9.67	16.25	-6.50	9.11	15.91	-5.75	11.54	16.21
-7.00	9.49	16.09	-6.75	8.84	15.90	-6.00	11.47	16.23
-7.25	9.31	15.94	-7.00	8.56	16.04	-6.25	11.25	16.38
-7.50	9.11	15.53	-7.25	8.24	16.18	-6.50	10.94	16.52
-7.75	8.92	15.24	-7.50	7.88	16.32	-6.75	10.68	16.44
-8.00	8.79	15.07	-7.75	7.49	16.39	-7.00	10.52	16.13
-8.25	8.67	14.90	-8.00	7.14	16.26	-7.25	10.36	14.25
-8.50	8.54	14.75	-8.25	6.99	16.11	-7.50	10.10	14.99
-8.75	8.41	14.61	-8.50	6.93	15.87	-7.75	9.80	14.17
-9.00	8.39	14.45	-8.75	6.86	15.44	-8.00	9.28	14.77
-9.25	8.42	14.28	-9.00	6.78	15.05	-8.25	9.23	14.29
-9.50	8.44	14.06	-9.25	6.53	14.75	-8.50	9.10	14.44
-9.75	8.43	13.77	-9.50	6.25	14.51	-8.75	8.93	13.66
-10.00	7.82	13.43	-9.75	6.17	14.23	-9.00	8.68	13.42
-10.25	7.67	13.07	-10.00	6.13	13.75	-9.25	8.35	13.23
-10.50	7.56	12.91	-10.25	6.07	13.25	-9.50	8.02	13.01
-10.75	7.51	12.72	-10.50	5.88	13.07	-9.75	7.72	11.99
-11.00	7.50	12.50	-10.75	5.67	12.98	-10.00	7.35	12.44
-11.25	7.39	12.56	-11.00	5.50	12.74	-10.25	6.98	12.70
-11.50	7.17	12.56	-11.25	5.43	12.41	-10.50	6.85	12.90
-11.75	7.03	12.48	-11.50	4.17	12.05	-10.75	6.90	12.99
-12.00	6.93	12.36	-11.75	3.79	12.02	-11.00	6.96	13.02
-12.25	5.98	12.11	-12.00	3.19	11.93	-11.25	6.95	13.05
-12.50	5.22	11.80	-12.25	3.09	11.80	-11.50	6.82	13.09
-12.75	5.09	11.72	-12.50	2.87	11.13	-11.75	6.69	13.06
-13.00	4.68	11.65	-12.75	2.64	9.86	-12.00	6.55	12.98
-13.25	4.35	11.57	-13.00	3.82	9.67	-12.25	6.36	12.90
-13.50	4.57	11.48	-13.25	3.68	9.57	-12.50	6.11	12.82
-13.75	4.09	11.30	-13.50	3.48	9.22	-12.75	5.93	12.06
-14.00	3.73	11.07	-13.75	3.25	9.07	-13.00	5.58	12.02
-14.25	3.56	10.82	-14.00	3.00	8.91	-13.25	5.15	11.29
-14.50	3.62	10.52	-14.25	1.98	8.68	-13.50	4.94	11.13
-14.75	1.91	9.80	-14.50	1.42	8.24	-13.75	4.50	11.10
-15.00	1.99	9.14	-14.75	1.00	7.13	-14.00	3.92	11.06
-15.25	1.98	8.94	-15.00	0.59	6.83	-14.25	3.47	11.00
-15.50	1.65	8.77	-15.25	0.21	6.75	-14.50	2.24	10.90
-15.75	0.62	8.67	-15.50	-0.14	6.67	-14.75	2.74	10.77
-16.00	-0.05	8.58	-15.75	-0.18	6.58	-15.00	2.47	10.62
-16.25	-0.62	8.64	-16.00	-0.07	6.35	-15.25	1.90	10.45
-16.50	-1.74	8.70	-16.25	-0.33	6.05	-15.50	1.47	10.28
-16.75	-1.94	8.76	-16.50	-0.65	5.97	-15.75	0.81	10.10
-17.00	-1.95	8.76	-16.75	-0.69	6.00	-16.00	0.46	9.92
-17.25	-1.96	8.72	-17.00	-0.70	6.05	-16.25	0.19	9.45
-17.50	-2.01	8.66	-17.25	-0.75	6.10	-16.50	-0.11	9.15
-17.75	-2.09	8.60	-17.50	-1.19	6.13	-16.75	-0.44	9.01
-18.00	-2.53	8.37	-17.75	-1.30	6.06	-17.00	-0.63	8.86
-18.25	-3.02	8.06	-18.00	-1.57	5.88	-17.25	-0.72	8.69

-18.50	-3.30	7.70	-18.25	-1.60	5.65	-17.50	-0.76	8.33
-18.75	-3.33	7.32	-18.50	-1.84	5.16	-17.75	-0.72	7.64
-19.00	-3.46	6.94	-18.75	-2.16	5.11	-18.00	-1.09	7.31
-19.25	-4.01	6.64	-19.00	-2.52	5.11	-18.25	-1.10	6.97
-19.50	-4.15	6.65	-19.25	-2.88	5.11	-18.50	-1.12	6.59
-19.75	-4.27	6.73	-19.50	-3.33	5.27	-18.75	-1.25	6.08
-20.00	-4.38	6.80	-19.75	-3.89	5.35	-19.00	-1.51	5.04
-20.25	-4.52	6.48	-20.00	-4.30	5.40	-19.25	-1.95	4.33
-20.50	-4.67	5.36	-20.25	-4.63	5.40	-19.50	-2.71	4.06
-20.75	-4.97	4.77	-20.50	-4.90	5.25	-19.75	-3.20	3.76
-21.00	-5.31	4.48	-20.75	-5.15	5.05	-20.00	-3.33	3.55
-21.25	-5.44	3.91	-21.00	-5.50	4.85	-20.25	-3.45	3.39
-21.50	-6.18	2.94	-21.25	-5.88	4.64	-20.50	-3.56	3.18
-21.75	-6.45	2.63	-21.50	-6.26	4.44	-20.75	-4.09	3.10
-22.00	-6.64	2.37	-21.75	-6.64	4.31	-21.00	-5.14	3.04
-22.25	-6.79	2.18	-22.00	-7.01	4.27	-21.25	-5.42	2.93
-22.50	-7.28	1.99	-22.25	-7.40	4.25	-21.50	-6.15	2.79
-22.75	-8.17	1.83	-22.50	-7.77	4.23	-21.75	-7.60	2.57
-23.00	-8.23	1.69	-22.75	-8.02	4.16	-22.00	-8.39	2.21
-23.25	-8.79	1.55	-23.00	-8.16	4.00	-22.25	-8.82	2.25
-23.50	-8.91	1.41	-23.25	-8.18	3.82	-22.50	-9.20	1.71
-23.75	-9.06	0.96	-23.50	-8.18	3.64	-22.75	-9.57	1.16
-24.00	-9.22	0.40	-23.75	-8.30	3.44	-23.00	-9.96	1.21
-24.25	-9.28	0.13	-24.00	-8.66	3.21	-23.25	-10.31	1.51
-24.50	-9.79	-0.18	-24.25	-9.35	2.97	-23.50	-10.51	1.10
-24.75	-9.91	-0.67	-24.50	-9.68	1.77	-23.75	-10.69	1.00
-25.00	-9.99	-0.89	-24.75	-10.03	1.29	-24.00	-10.84	1.47
-25.25	-10.25	-1.00	-25.00	-10.51	-1.62	-24.25	-10.93	1.36
-25.50	-10.32	-1.09	-25.25	-10.77	-1.77	-24.50	-11.00	0.50
-25.75	-10.39	-1.11	-25.50	-10.77	-1.86	-24.75	-11.07	0.29
-26.00	-10.46	-1.10	-25.75	-10.90	-1.98	-25.00	-11.15	0.04
-26.25	-10.53	-1.07	-26.00	-11.02	-2.55	-25.25	-11.23	-0.23
-26.50	-12.42	-1.06	-26.25	-11.06	-2.21	-25.50	-11.33	-0.48
-26.75	-13.18	-0.77	-26.50	-11.06	-2.07	-25.75	-11.54	-0.72
-27.00	-13.01	-2.40	-26.75	-11.55	-2.01	-26.00	-11.78	-0.97
-27.25	-13.28	-2.56	-27.00	-12.01	-2.17	-26.25	-12.02	-1.32
-27.50	-13.85	-2.77	-27.25	-12.52	-2.37	-26.50	-12.31	-2.20
-27.75	-14.12	-2.86	-27.50	-12.85	-2.47	-26.75	-12.65	-1.56
-28.00	-16.15	-2.81	-27.75	-13.11	-2.50	-27.00	-12.96	-1.47
-28.25	-15.05	-2.86	-28.00	-13.33	-2.61	-27.25	-13.23	-1.38
-28.50	-16.71	-2.95	-28.25	-13.69	-2.86	-27.50	-13.50	-1.34
-28.75	-16.86	-3.15	-28.50	-14.24	-3.20	-27.75	-13.77	-1.33
-29.00	-17.01	-3.41	-28.75	-14.41	-3.80	-28.00	-14.05	-2.07
-29.25	-17.20	-3.71	-29.00	-14.52	-4.10	-28.25	-14.65	-3.27
-29.50	-17.43	-4.40	-29.25	-14.64	-4.42	-28.50	-15.11	-3.34
-29.75	-17.67	-4.48	-29.50	-15.19	-5.24	-28.75	-15.16	-2.23
-30.00	-17.93	-4.67	-29.75	-15.33	-5.41	-29.00	-15.12	-2.82
-30.25	-18.19	-4.92	-30.00	-15.42	-5.61	-29.25	-15.08	-4.57
-30.50	-18.45	-5.16	-30.25	-15.47	-5.89	-29.50	-15.19	-5.36

-30.75	-18.73	-5.41
-31.00	-19.36	-5.66
-31.25		-5.93
-31.50		-6.54
-31.75		-7.31
-32.00		-7.56
-32.25		-7.78
-32.50		-7.99
-32.75		-8.19
-33.00		-8.31
-33.25		-8.42
-33.50		-8.54
-33.75		-8.73
-34.00		-8.93
-34.25		-9.14
-34.50		-9.35
-34.75		-9.60
-35.00		-9.87
-35.25		-10.14
-35.50		-10.44
-35.75		-10.79
-36.00		-11.14
-36.25		-11.56
-36.50		-12.04
-36.75		-12.40
-37.00		-12.67
-37.25		-12.95
-37.50		-13.27
-37.75		-13.61
-38.00		-14.70
-38.25		-15.04
-38.50		-15.28
-38.75		-15.39
-39.00		-15.48
-39.25		-15.58
-39.50		-15.72

-30.50	-15.93	-6.12
-30.75	-17.30	-6.23
-31.00	-16.74	-7.59
-31.25	-17.00	-7.89
-31.50	-17.48	-8.22
-31.75	-17.98	-8.17
-32.00	-18.85	-8.12
-32.25	-19.23	-8.07
-32.50	-19.58	-9.27
-32.75		-9.52
-33.00		-9.35
-33.25		-8.71
-33.50		-9.68
-33.75		-9.83
-34.00		-9.91
-34.25		-10.03
-34.50		-10.26
-34.75		-10.49
-35.00		-10.79
-35.25		-11.10
-35.50		-11.45
-35.75		-11.92
-36.00		-12.80
-36.25		-13.44
-36.50		-14.09
-36.75		-14.46
-37.00		-14.66
-37.25		-14.97
-37.50		-15.34
-37.75		-15.95
-38.00		-16.41
-38.25		-16.94
-38.50		-16.90
-38.75		-16.80
-39.00		-16.71
-39.25		-16.84
-39.50		-17.00
-39.75		-17.20
-40.00		-17.40

-29.75	-15.29	-5.57
-30.00	-15.43	-5.74
-30.25	-16.10	-5.91
-30.50	-16.59	-6.59
-30.75	-16.88	-6.77
-31.00	-17.08	-6.89
-31.25	-17.28	-6.95
-31.50	-18.04	-8.30
-31.75	-18.40	-7.65
-32.00	-18.77	-8.37
-32.25	-19.13	-8.43
-32.50	-19.68	-9.41
-32.75		-10.36
-33.00		-9.95
-33.25		-9.79
-33.50		-10.83
-33.75		-10.78
-34.00		-10.87
-34.25		-11.05
-34.50		-11.30
-34.75		-11.44
-35.00		-11.63
-35.25		-11.82
-35.50		-11.99
-35.75		-12.14
-36.00		-12.24
-36.25		-12.34
-36.50		-12.53
-36.75		-12.93
-37.00		-13.41
-37.25		-13.89
-37.50		-14.30
-37.75		-14.30
-38.00		-14.28
-38.25		-14.23
-38.50		-14.17
-38.75		-14.18
-39.00		-14.42
-39.25		-14.75
-39.50		-15.20
-39.75		-15.78
-40.00		-16.10
-40.25		-16.33
-40.50		-16.83
-40.75		-17.60
-41.00		-17.91
-41.25		-18.20
-41.50		-18.48
-41.75		-18.76

-42.00	-19.05
-42.25	-19.35

Table D3. High-Water statistics for H/P ≈ 0.878 (Q ≈ 540 L/S) and with $p = 0.92\ P$ (units in inches).

High-Water Statistics for H/P ≈ 0.878 and p = 0.92 P		
X	Y Min.	Y Max.
63.00	35.72	35.97
62.75	35.25	35.90
62.50	35.23	35.82
62.25	35.20	35.79
62.00	35.16	35.75
61.75	35.07	35.74
61.50	35.04	35.73
61.25	35.04	35.71
61.00	35.03	35.70
60.75	35.02	35.68
60.50	34.92	35.65
60.25	34.89	35.64
60.00	34.89	35.63
59.75	34.89	35.64
59.50	34.86	35.64
59.25	34.86	35.63
59.00	34.85	35.61
58.75	34.80	35.58
58.50	34.75	35.55
58.25	34.72	35.50
58.00	34.67	35.46
57.75	34.64	35.42
57.50	34.62	35.39
57.25	34.60	35.35
57.00	34.56	35.31
56.75	34.54	35.26
56.50	34.51	35.20
56.25	34.46	35.19
56.00	34.42	35.16
55.75	34.37	35.13
55.50	34.35	35.13
55.25	34.31	35.13
55.00	34.28	35.13
54.75	34.23	35.15
54.50	34.17	35.15
54.25	34.11	35.15
54.00	34.06	35.12
53.75	34.00	35.07
53.50	33.97	35.02
53.25	33.95	34.97
53.00	33.92	34.92
52.75	33.88	34.87

52.50	33.84	34.82
52.25	33.80	34.78
52.00	33.78	34.72
51.75	33.76	34.65
51.50	33.73	34.57
51.25	33.67	34.50
51.00	33.61	34.43
50.75	33.55	34.35
50.50	33.47	34.28
50.25	33.40	34.20
50.00	33.32	34.20
49.75	33.25	34.19
49.50	33.18	34.16
49.25	33.11	34.09
49.00	33.07	34.01
48.75	33.05	34.03
48.50	33.04	33.97
48.25	33.02	33.90
48.00	33.02	33.83
47.75	33.02	33.77
47.50	32.98	33.72
47.25	32.93	33.66
47.00	32.87	33.61
46.75	32.82	33.55
46.50	32.78	33.51
46.25	32.77	33.48
46.00	32.73	33.43
45.75	32.65	33.39
45.50	32.59	33.35
45.25	32.53	33.32
45.00	32.48	33.30
44.75	32.41	33.28
44.50	32.35	33.26
44.25	32.30	33.25
44.00	32.24	33.22
43.75	32.21	33.20
43.50	32.20	33.17
43.25	32.20	33.12
43.00	32.18	33.09
42.75	32.13	33.05
42.50	32.08	33.02
42.25	32.07	32.98
42.00	32.02	32.94
41.75	31.97	32.90
41.50	31.92	32.85
41.25	31.87	32.81
41.00	31.81	32.78
40.75	31.77	32.75
40.50	31.74	32.75

40.25	31.70	32.73
40.00	31.65	32.69
39.75	31.60	32.64
39.50	31.56	32.60
39.25	31.52	32.56
39.00	31.47	32.52
38.75	31.41	32.50
38.50	31.35	32.47
38.25	31.31	32.45
38.00	31.27	32.42
37.75	31.23	32.38
37.50	31.20	32.35
37.25	31.16	32.32
37.00	31.13	32.28
36.75	31.13	32.26
36.50	31.10	32.23
36.25	31.08	32.18
36.00	31.04	32.13
35.75	30.99	32.09
35.50	30.99	32.08
35.25	31.00	32.08
35.00	30.99	32.08
34.75	30.96	32.08
34.50	30.95	32.08
34.25	30.94	32.07
34.00	30.94	32.05
33.75	30.94	32.03
33.50	30.94	32.02
33.25	30.95	31.99
33.00	30.93	31.99
32.75	30.90	31.99
32.50	30.87	31.99
32.25	30.85	31.99
32.00	30.84	32.07
31.75	30.83	32.14
31.50	30.83	32.16
31.25	30.83	32.18
31.00	30.85	32.17
30.75	30.83	32.14
30.50	30.80	32.13
30.25	30.80	32.13
30.00	30.82	32.15
29.75	30.86	32.17
29.50	30.87	32.23
29.25	30.88	32.29
29.00	30.88	32.34
28.75	30.86	32.36
28.50	30.84	32.38
28.25	30.82	32.40

28.00	30.83	32.45
27.75	30.85	32.50
27.50	30.86	32.53
27.25	30.88	32.53
27.00	30.93	32.53
26.75	30.97	32.54
26.50	30.99	32.55
26.25	31.03	32.56
26.00	31.08	32.60
25.75	31.13	32.66
25.50	31.13	32.68
25.25	31.13	32.69
25.00	31.14	32.70
24.75	31.13	32.70
24.50	31.13	32.69
24.25	31.16	32.66
24.00	31.21	32.63
23.75	31.21	32.59
23.50	31.21	32.56
23.25	31.19	32.56
23.00	31.16	32.57
22.75	31.10	32.59
22.50	31.00	32.62
22.25	30.94	32.63
22.00	30.93	32.64
21.75	30.93	32.62
21.50	30.93	32.62
21.25	30.86	32.69
21.00	30.79	32.73
20.75	30.75	32.74
20.50	30.74	32.66
20.25	30.74	32.61
20.00	30.75	32.64
19.75	30.75	32.67
19.50	30.72	32.70
19.25	30.74	32.73
19.00	30.60	32.78
18.75	30.43	32.83
18.50	30.35	32.88
18.25	30.28	32.89
18.00	30.17	32.89
17.75	30.03	32.86
17.50	29.95	32.80
17.25	29.91	32.73
17.00	29.87	32.71
16.75	29.62	32.71
16.50	28.87	32.70
16.25	28.31	32.67
16.00	28.28	32.63

15.75	28.36	32.50
15.50	28.35	32.36
15.25	28.31	32.30
15.00	28.23	32.25
14.75	28.14	32.20
14.50	27.94	32.14
14.25	27.81	32.06
14.00	27.66	31.98
13.75	27.48	31.88
13.50	27.32	31.67
13.25	27.18	31.39
13.00	27.06	31.28
12.75	26.95	30.90
12.50	26.83	30.64
12.25	26.55	30.29
12.00	26.28	30.11
11.75	26.08	29.96
11.50	25.91	29.36
11.25	25.73	29.11
11.00	25.49	28.74
10.75	25.23	28.62
10.50	24.94	28.45
10.25	24.60	28.60
10.00	24.12	28.38
9.75	23.98	28.41
9.50	23.91	28.24
9.25	23.82	28.06
9.00	23.68	27.84
8.75	23.36	27.76
8.50	23.07	27.71
8.25	22.80	27.67
8.00	22.61	27.65
7.75	22.51	27.60
7.50	22.39	27.42
7.25	22.19	27.17
7.00	21.89	27.08
6.75	21.80	26.99
6.50	21.76	27.45
6.25	21.71	27.01
6.00	21.54	26.90
5.75	21.31	26.80
5.50	21.24	26.70
5.25	20.95	26.62
5.00	20.35	26.54
4.75	20.01	26.46
4.50	19.90	26.40
4.25	19.79	26.35
4.00	19.67	26.30
3.75	19.42	26.21

3.50	18.87	25.97
3.25	18.81	25.78
3.00	18.62	25.64
2.75	18.43	25.02
2.50	17.96	23.65
2.25	17.04	23.49
2.00	16.75	23.30
1.75	16.63	23.10
1.50	16.52	23.03
1.25	16.40	23.08
1.00	16.10	23.12
0.75	16.03	23.17
0.50	15.02	23.19
0.25	14.71	23.01
0.00	14.29	22.68
-0.25	14.08	22.36
-0.50	14.12	22.02
-0.75	14.18	21.75
-1.00	14.19	21.28
-1.25	14.14	20.67
-1.50	14.10	20.50
-1.75	14.00	20.34
-2.00	13.84	20.17
-2.25	13.47	20.02
-2.50	13.23	19.87
-2.75	13.10	19.72
-3.00	12.80	19.58
-3.25	12.47	19.50
-3.50	11.99	19.41
-3.75	11.67	19.25
-4.00	11.37	17.27
-4.25	11.20	16.73
-4.50	11.14	16.76
-4.75	11.08	16.78
-5.00	10.77	16.86
-5.25	9.93	17.39
-5.50	9.68	17.73
-5.75	9.47	17.67
-6.00	9.26	17.58
-6.25	9.16	17.49
-6.50	9.20	17.40
-6.75	9.25	17.31
-7.00	9.23	17.16
-7.25	8.89	16.95
-7.50	8.60	16.73
-7.75	8.37	16.53
-8.00	8.07	16.40
-8.25	7.67	15.60
-8.50	7.53	14.46

-8.75	7.15	15.49
-9.00	7.09	14.46
-9.25	7.05	14.35
-9.50	6.91	14.25
-9.75	6.19	14.14
-10.00	5.88	13.96
-10.25	5.66	13.06
-10.50	5.51	12.51
-10.75	5.46	12.37
-11.00	5.08	12.36
-11.25	4.30	12.36
-11.50	4.20	12.35
-11.75	3.30	12.49
-12.00	3.05	12.75
-12.25	3.01	12.90
-12.50	2.96	12.10
-12.75	2.86	11.95
-13.00	2.94	11.71
-13.25	3.04	10.55
-13.50	2.59	10.25
-13.75	2.51	9.96
-14.00	2.36	9.60
-14.25	1.69	9.10
-14.50	1.38	9.04
-14.75	1.09	8.96
-15.00	0.73	8.85
-15.25	0.45	8.80
-15.50	0.20	8.68
-15.75	-0.04	8.56
-16.00	-0.28	8.28
-16.25	-0.51	7.87
-16.50	-0.78	7.67
-16.75	-1.14	7.42
-17.00	-1.44	6.73
-17.25	-1.51	6.36
-17.50	-1.53	6.35
-17.75	-1.56	6.29
-18.00	-1.67	6.22
-18.25	-1.78	6.10
-18.50	-1.90	5.94
-18.75	-2.11	5.71
-19.00	-2.31	5.42
-19.25	-2.49	5.09
-19.50	-2.73	4.67
-19.75	-2.80	4.40
-20.00	-3.48	4.24
-20.25	-4.30	4.13
-20.50	-4.47	4.03
-20.75	-4.72	3.92

-21.00	-5.13	3.78
-21.25	-5.46	3.55
-21.50	-5.79	3.10
-21.75	-6.13	3.53
-22.00	-6.25	3.82
-22.25	-6.28	3.82
-22.50	-6.36	3.82
-22.75	-6.48	3.79
-23.00	-6.55	3.62
-23.25	-7.62	3.40
-23.50	-8.23	3.15
-23.75	-8.48	2.69
-24.00	-8.73	1.66
-24.25	-8.83	0.98
-24.50	-8.89	0.78
-24.75	-8.95	0.57
-25.00	-9.03	0.06
-25.25	-9.15	0.01
-25.50	-9.27	0.01
-25.75	-9.39	0.02
-26.00	-9.51	0.02
-26.25	-9.67	0.01
-26.50	-9.86	-0.05
-26.75	-9.94	-0.25
-27.00	-10.11	-0.46
-27.25	-10.28	-0.75
-27.50	-10.47	-1.38
-27.75	-10.70	-1.77
-28.00	-10.94	-2.20
-28.25	-11.41	-2.79
-28.50	-12.94	-3.07
-28.75	-12.42	-3.35
-29.00	-14.45	-3.65
-29.25	-14.19	-4.05
-29.50	-14.26	-5.76
-29.75	-15.77	-5.87
-30.00	-13.86	-5.83
-30.25	-17.21	-6.41
-30.50	-16.87	-6.47
-30.75	-16.98	-6.53
-31.00	-17.14	-6.60
-31.25	-17.36	-6.77
-31.50	-17.59	-6.97
-31.75	-17.81	-7.18
-32.00	-18.06	-7.67
-32.25	-18.89	-8.28
-32.50	-19.53	-8.63
-32.75		-8.76
-33.00		-8.85

-33.25	-8.94
-33.50	-9.00
-33.75	-9.03
-34.00	-9.05
-34.25	-9.32
-34.50	-9.64
-34.75	-9.83
-35.00	-9.97
-35.25	-10.14
-35.50	-10.41
-35.75	-11.32
-36.00	-11.60
-36.25	-12.03
-36.50	-12.38
-36.75	-13.62
-37.00	-13.69
-37.25	-14.51
-37.50	-14.86
-37.75	-15.25
-38.00	-15.67
-38.25	-15.71
-38.50	-15.76
-38.75	-15.81
-39.00	-15.90
-39.25	-16.13
-39.50	-16.40
-39.75	-16.71
-40.00	-17.00
-40.25	-17.31
-40.50	-17.67
-40.75	-17.82
-41.00	-17.92
-41.25	-18.06
-41.50	-18.24

APPENDIX E – HIGH-WATER SURFACE DATA FOR $H/P \approx 0.367$ ($Q \approx 230$ L/S).

Table E1. High-Water statistics for *H/*P ≈ 0.367 (*Q* ≈ 230 l/s) and with no ramp, *p* = 0.15 *P*, and *p* = 0.31 *P* (units in inches).

High-Water Statistics for H/P ≈ 0.367 and no ramp			High-Water Statistics for H/P ≈ 0.367 and *p* = 0.15 *P*			High-Water Statistics for H/P ≈ 0.367 and *p* = 0.31 *P*		
X	Y Min.	Y Max.	X	Y Min.	Y Max.	X	Y Min.	Y Max.
63.25	29.02	29.82	62.75	28.66	28.91	62.75	28.87	29.37
63.00	29.02	29.79	62.50	28.65	28.99	62.50	28.87	29.34
62.75	29.02	29.77	62.25	28.62	28.99	62.25	28.91	29.31
62.50	29.01	29.75	62.00	28.59	28.99	62.00	28.92	29.28
62.25	29.00	29.72	61.75	28.56	28.98	61.75	28.89	29.28
62.00	28.97	29.68	61.50	28.55	28.97	61.50	28.86	29.29
61.75	28.91	29.63	61.25	28.58	28.97	61.25	28.84	29.26
61.50	28.85	29.57	61.00	28.57	28.97	61.00	28.82	29.24
61.25	28.83	29.51	60.75	28.56	28.97	60.75	28.81	29.25
61.00	28.81	29.51	60.50	28.54	28.96	60.50	28.79	29.26
60.75	28.78	29.52	60.25	28.52	28.95	60.25	28.78	29.27
60.50	28.78	29.52	60.00	28.50	28.95	60.00	28.76	29.27
60.25	28.78	29.52	59.75	28.48	28.95	59.75	28.74	29.24
60.00	28.77	29.51	59.50	28.46	28.95	59.50	28.73	29.24
59.75	28.72	29.49	59.25	28.43	28.95	59.25	28.71	29.21
59.50	28.66	29.47	59.00	28.38	28.94	59.00	28.69	29.16
59.25	28.62	29.49	58.75	28.36	28.90	58.75	28.68	29.10
59.00	28.59	29.52	58.50	28.34	28.86	58.50	28.67	29.06
58.75	28.58	29.51	58.25	28.34	28.82	58.25	28.65	29.03
58.50	28.54	29.49	58.00	28.34	28.78	58.00	28.61	29.02
58.25	28.48	29.41	57.75	28.32	28.75	57.75	28.56	29.01
58.00	28.43	29.41	57.50	28.28	28.73	57.50	28.53	28.97
57.75	28.39	29.38	57.25	28.26	28.72	57.25	28.55	28.97
57.50	28.36	29.33	57.00	28.26	28.69	57.00	28.57	28.94
57.25	28.35	29.29	56.75	28.23	28.67	56.75	28.56	28.90
57.00	28.35	29.26	56.50	28.22	28.64	56.50	28.54	28.88
56.75	28.33	29.22	56.25	28.21	28.63	56.25	28.52	28.88
56.50	28.27	29.16	56.00	28.19	28.64	56.00	28.50	28.89
56.25	28.21	29.11	55.75	28.18	28.61	55.75	28.44	28.89
56.00	28.18	29.06	55.50	28.14	28.56	55.50	28.41	28.88
55.75	28.18	29.03	55.25	28.10	28.51	55.25	28.37	28.86
55.50	28.18	29.07	55.00	28.10	28.50	55.00	28.33	28.83
55.25	28.18	29.07	54.75	28.09	28.48	54.75	28.29	28.79
55.00	28.17	29.07	54.50	28.06	28.46	54.50	28.26	28.74
54.75	28.15	29.01	54.25	28.05	28.46	54.25	28.26	28.70
54.50	28.12	28.93	54.00	28.05	28.46	54.00	28.26	28.68
54.25	28.06	28.90	53.75	28.05	28.45	53.75	28.25	28.67
54.00	28.03	28.90	53.50	28.02	28.44	53.50	28.24	28.66
53.75	28.01	28.90	53.25	28.01	28.44	53.25	28.22	28.66
53.50	27.99	28.89	53.00	28.01	28.44	53.00	28.18	28.64
53.25	27.99	28.87	52.75	28.00	28.44	52.75	28.15	28.64
53.00	27.99	28.83	52.50	27.99	28.44	52.50	28.15	28.63

52.75	27.99	28.79	52.25	27.97	28.44	52.25	28.17	28.61
52.50	27.98	28.76	52.00	27.95	28.44	52.00	28.18	28.61
52.25	27.96	28.71	51.75	27.92	28.44	51.75	28.20	28.59
52.00	27.94	28.66	51.50	27.90	28.44	51.50	28.22	28.58
51.75	27.88	28.61	51.25	27.88	28.43	51.25	28.22	28.57
51.50	27.88	28.58	51.00	27.87	28.43	51.00	28.19	28.56
51.25	27.90	28.56	50.75	27.86	28.43	50.75	28.17	28.55
51.00	27.90	28.58	50.50	27.86	28.43	50.50	28.17	28.56
50.75	27.90	28.59	50.25	27.87	28.43	50.25	28.19	28.56
50.50	27.89	28.59	50.00	27.87	28.43	50.00	28.19	28.56
50.25	27.87	28.61	49.75	27.88	28.43	49.75	28.16	28.56
50.00	27.87	28.61	49.50	27.89	28.44	49.50	28.16	28.57
49.75	27.85	28.61	49.25	27.89	28.46	49.25	28.16	28.57
49.50	27.84	28.61	49.00	27.89	28.47	49.00	28.17	28.57
49.25	27.81	28.60	48.75	27.90	28.49	48.75	28.19	28.57
49.00	27.77	28.58	48.50	27.91	28.50	48.50	28.19	28.58
48.75	27.78	28.57	48.25	27.91	28.52	48.25	28.19	28.58
48.50	27.78	28.56	48.00	27.93	28.54	48.00	28.19	28.58
48.25	27.78	28.54	47.75	27.98	28.55	47.75	28.21	28.59
48.00	27.79	28.51	47.50	27.99	28.57	47.50	28.23	28.60
47.75	27.83	28.50	47.25	27.99	28.57	47.25	28.22	28.61
47.50	27.87	28.50	47.00	27.98	28.58	47.00	28.19	28.63
47.25	27.88	28.54	46.75	28.00	28.60	46.75	28.19	28.66
47.00	27.87	28.58	46.50	28.06	28.61	46.50	28.19	28.67
46.75	27.80	28.58	46.25	28.10	28.61	46.25	28.19	28.67
46.50	27.78	28.58	46.00	28.10	28.64	46.00	28.20	28.67
46.25	27.85	28.59	45.75	28.10	28.64	45.75	28.20	28.67
46.00	27.86	28.59	45.50	28.10	28.64	45.50	28.20	28.68
45.75	27.83	28.60	45.25	28.10	28.64	45.25	28.21	28.70
45.50	27.79	28.59	45.00	28.10	28.64	45.00	28.21	28.71
45.25	27.78	28.56	44.75	28.10	28.64	44.75	28.19	28.72
45.00	27.76	28.55	44.50	28.10	28.64	44.50	28.18	28.74
44.75	27.72	28.54	44.25	28.10	28.64	44.25	28.18	28.74
44.50	27.68	28.53	44.00	28.09	28.64	44.00	28.19	28.76
44.25	27.65	28.54	43.75	28.09	28.65	43.75	28.19	28.77
44.00	27.63	28.56	43.50	28.09	28.66	43.50	28.19	28.78
43.75	27.63	28.57	43.25	28.08	28.66	43.25	28.19	28.80
43.50	27.64	28.67	43.00	28.08	28.67	43.00	28.20	28.80
43.25	27.64	28.70	42.75	28.08	28.67	42.75	28.20	28.81
43.00	27.64	28.65	42.50	28.12	28.67	42.50	28.20	28.81
42.75	27.64	28.62	42.25	28.15	28.69	42.25	28.19	28.81
42.50	27.66	28.64	42.00	28.18	28.70	42.00	28.21	28.79
42.25	27.69	28.65	41.75	28.21	28.71	41.75	28.22	28.78
42.00	27.69	28.65	41.50	28.22	28.71	41.50	28.21	28.79
41.75	27.66	28.66	41.25	28.21	28.70	41.25	28.21	28.79
41.50	27.64	28.68	41.00	28.20	28.68	41.00	28.20	28.79
41.25	27.68	28.71	40.75	28.20	28.67	40.75	28.18	28.79
41.00	27.70	28.73	40.50	28.19	28.67	40.50	28.15	28.78
40.75	27.70	28.73	40.25	28.17	28.67	40.25	28.12	28.76

40.50	27.69	28.74	40.00	28.17	28.67	40.00	28.10	28.75
40.25	27.69	28.74	39.75	28.17	28.67	39.75	28.09	28.77
40.00	27.71	28.73	39.50	28.16	28.67	39.50	28.10	28.77
39.75	27.76	28.73	39.25	28.14	28.67	39.25	28.10	28.77
39.50	27.87	28.75	39.00	28.12	28.67	39.00	28.12	28.77
39.25	27.91	28.76	38.75	28.10	28.67	38.75	28.11	28.78
39.00	27.89	28.76	38.50	28.09	28.67	38.50	28.09	28.78
38.75	27.96	28.76	38.25	28.09	28.66	38.25	28.08	28.77
38.50	28.08	28.76	38.00	28.09	28.66	38.00	28.07	28.76
38.25	28.11	28.76	37.75	28.09	28.66	37.75	28.07	28.76
38.00	28.15	28.79	37.50	28.09	28.68	37.50	28.06	28.78
37.75	28.18	28.82	37.25	28.09	28.69	37.25	28.07	28.79
37.50	28.19	28.83	37.00	28.09	28.68	37.00	28.07	28.79
37.25	28.23	28.88	36.75	28.09	28.67	36.75	28.05	28.79
37.00	28.23	28.95	36.50	28.11	28.67	36.50	28.06	28.79
36.75	28.24	29.00	36.25	28.13	28.67	36.25	28.10	28.77
36.50	28.28	29.03	36.00	28.16	28.68	36.00	28.14	28.77
36.25	28.30	29.10	35.75	28.14	28.70	35.75	28.17	28.77
36.00	28.30	29.11	35.50	28.12	28.70	35.50	28.17	28.77
35.75	28.27	29.06	35.25	28.16	28.70	35.25	28.17	28.75
35.50	28.24	29.05	35.00	28.21	28.70	35.00	28.17	28.77
35.25	28.21	29.02	34.75	28.23	28.69	34.75	28.15	28.78
35.00	28.20	29.00	34.50	28.23	28.69	34.50	28.14	28.81
34.75	28.20	28.98	34.25	28.25	28.69	34.25	28.15	28.82
34.50	28.23	28.97	34.00	28.26	28.69	34.00	28.15	28.81
34.25	28.26	28.97	33.75	28.26	28.69	33.75	28.15	28.81
34.00	28.25	28.97	33.50	28.26	28.69	33.50	28.14	28.80
33.75	28.24	28.97	33.25	28.23	28.69	33.25	28.12	28.79
33.50	28.25	28.98	33.00	28.23	28.69	33.00	28.09	28.79
33.25	28.27	28.99	32.75	28.23	28.69	32.75	28.08	28.79
33.00	28.27	28.99	32.50	28.23	28.69	32.50	28.10	28.79
32.75	28.24	28.99	32.25	28.23	28.69	32.25	28.15	28.79
32.50	28.20	28.98	32.00	28.23	28.69	32.00	28.20	28.78
32.25	28.21	28.97	31.75	28.22	28.69	31.75	28.24	28.78
32.00	28.25	28.95	31.50	28.25	28.68	31.50	28.27	28.77
31.75	28.33	28.93	31.25	28.26	28.66	31.25	28.30	28.76
31.50	28.32	28.91	31.00	28.25	28.65	31.00	28.29	28.75
31.25	28.30	28.89	30.75	28.22	28.64	30.75	28.22	28.77
31.00	28.30	28.87	30.50	28.23	28.63	30.50	28.18	28.79
30.75	28.24	28.84	30.25	28.22	28.62	30.25	28.18	28.80
30.50	28.27	28.82	30.00	28.22	28.62	30.00	28.20	28.81
30.25	28.26	28.88	29.75	28.22	28.62	29.75	28.20	28.82
30.00	28.26	28.89	29.50	28.22	28.61	29.50	28.20	28.84
29.75	28.22	28.89	29.25	28.23	28.61	29.25	28.20	28.83
29.50	28.19	28.89	29.00	28.24	28.61	29.00	28.20	28.82
29.25	28.16	28.89	28.75	28.22	28.58	28.75	28.20	28.81
29.00	28.18	28.89	28.50	28.18	28.58	28.50	28.20	28.79
28.75	28.16	28.89	28.25	28.15	28.57	28.25	28.20	28.79
28.50	28.13	28.93	28.00	28.18	28.55	28.00	28.19	28.77

28.25	28.13	29.00	27.75	28.19	28.57	27.75	28.17	28.76
28.00	28.12	29.09	27.50	28.19	28.58	27.50	28.17	28.74
27.75	28.13	29.07	27.25	28.19	28.56	27.25	28.15	28.73
27.50	28.13	28.95	27.00	28.19	28.54	27.00	28.15	28.73
27.25	28.13	28.91	26.75	28.17	28.53	26.75	28.14	28.73
27.00	28.08	28.89	26.50	28.14	28.51	26.50	28.12	28.73
26.75	28.04	28.86	26.25	28.12	28.48	26.25	28.12	28.75
26.50	28.03	28.84	26.00	28.09	28.51	26.00	28.12	28.76
26.25	28.06	28.83	25.75	28.07	28.51	25.75	28.11	28.76
26.00	28.05	28.83	25.50	28.04	28.52	25.50	28.10	28.77
25.75	28.02	28.78	25.25	28.00	28.54	25.25	28.07	28.79
25.50	28.05	28.81	25.00	27.99	28.52	25.00	28.05	28.79
25.25	28.05	28.86	24.75	28.00	28.49	24.75	28.03	28.75
25.00	28.00	28.91	24.50	28.01	28.47	24.50	28.03	28.71
24.75	27.97	28.94	24.25	28.01	28.45	24.25	28.03	28.67
24.50	27.96	28.91	24.00	27.98	28.52	24.00	28.01	28.63
24.25	27.97	28.85	23.75	27.94	28.60	23.75	28.01	28.63
24.00	27.97	28.77	23.50	27.90	28.67	23.50	28.00	28.62
23.75	27.97	28.76	23.25	27.86	28.65	23.25	27.93	28.61
23.50	27.95	28.74	23.00	27.79	28.59	23.00	27.88	28.58
23.25	27.92	28.70	22.75	27.77	28.50	22.75	27.82	28.56
23.00	27.89	28.68	22.50	27.75	28.41	22.50	27.78	28.50
22.75	27.95	28.64	22.25	27.68	28.36	22.25	27.83	28.34
22.50	27.88	28.59	22.00	27.60	28.43	22.00	27.90	28.38
22.25	27.81	28.56	21.75	27.48	28.57	21.75	27.82	28.31
22.00	27.75	28.49	21.50	27.31	28.60	21.50	27.76	28.24
21.75	27.67	28.40	21.25	27.27	28.58	21.25	27.62	28.16
21.50	27.61	28.37	21.00	27.25	28.53	21.00	27.49	28.07
21.25	27.57	28.31	20.75	27.23	28.47	20.75	27.31	28.02
21.00	27.48	28.31	20.50	27.03	28.36	20.50	27.13	28.00
20.75	27.35	28.33	20.25	26.77	28.17	20.25	26.90	27.96
20.50	27.22	28.28	20.00	26.51	27.96	20.00	26.65	27.87
20.25	27.12	28.17	19.75	26.38	27.77	19.75	26.44	27.68
20.00	26.99	28.10	19.50	26.26	27.70	19.50	26.27	27.55
19.75	26.62	27.96	19.25	26.12	27.61	19.25	26.16	27.46
19.50	26.30	27.84	19.00	25.91	27.48	19.00	25.61	27.22
19.25	26.05	27.66	18.75	25.36	27.16	18.75	25.14	27.01
19.00	25.52	27.54	18.50	24.69	26.79	18.50	24.92	26.82
18.75	25.38	27.42	18.25	23.88	26.57	18.25	24.40	26.70
18.50	24.64	27.30	18.00	23.47	26.37	18.00	24.04	26.57
18.25	23.93	26.69	17.75	22.74	26.16	17.75	23.54	26.29
18.00	23.69	26.59	17.50	22.15	26.01	17.50	23.21	25.66
17.75	23.37	26.45	17.25	21.72	25.75	17.25	22.56	25.29
17.50	22.76	25.97	17.00	21.69	25.70	17.00	22.10	24.92
17.25	21.85	25.80	16.75	21.61	25.04	16.75	21.42	24.55
17.00	21.39	25.47	16.50	21.38	25.07	16.50	21.45	24.28
16.75	21.20	25.18	16.25	21.26	23.99	16.25	21.30	24.04
16.50	21.05	24.92	16.00	21.25	23.77	16.00	21.08	23.70
16.25	20.57	24.70	15.75	20.92	23.63	15.75	20.60	23.62

16.00	20.26	24.24	15.50	20.52	23.58	15.50	19.70	23.29
15.75	19.80	24.05	15.25	19.48	23.63	15.25	19.52	23.28
15.50	19.70	23.84	15.00	19.43	23.71	15.00	19.41	23.27
15.25	19.53	23.64	14.75	19.38	23.57	14.75	19.25	23.23
15.00	19.39	23.56	14.50	19.31	23.39	14.50	18.68	23.17
14.75	19.35	22.84	14.25	18.92	23.45	14.25	18.55	23.11
14.50	19.02	22.78	14.00	18.90	23.32	14.00	18.51	22.99
14.25	18.40	22.91	13.75	18.66	23.38	13.75	18.38	22.81
14.00	18.23	23.00	13.50	18.59	23.43	13.50	18.18	22.59
13.75	18.44	22.96	13.25	18.29	23.44	13.25	17.89	22.25
13.50	18.38	22.92	13.00	18.07	23.44	13.00	17.74	21.74
13.25	18.22	22.85	12.75	17.95	23.46	12.75	17.72	21.66
13.00	18.13	21.94	12.50	17.85	23.51	12.50	17.72	21.66
12.75	17.87	21.95	12.25	17.76	23.57	12.25	17.44	21.60
12.50	17.78	21.85	12.00	17.67	23.59	12.00	16.98	21.46
12.25	17.68	21.88	11.75	17.31	23.56	11.75	16.67	21.45
12.00	17.48	21.91	11.50	17.20	23.52	11.50	16.39	21.48
11.75	17.28	21.93	11.25	17.11	23.46	11.25	16.31	21.51
11.50	17.20	21.98	11.00	17.00	23.40	11.00	16.33	21.54
11.25	17.17	22.04	10.75	16.78	23.33	10.75	16.58	21.58
11.00	17.13	22.05	10.50	16.42	23.32	10.50	16.70	21.62
10.75	17.02	22.05	10.25	16.35	23.43	10.25	16.60	21.67
10.50	16.86	22.06	10.00	16.40	23.52	10.00	16.42	21.71
10.25	16.78	22.07	9.75	16.43	23.49	9.75	16.18	21.73
10.00	16.73	22.04	9.50	16.20	23.44	9.50	16.00	21.76
9.75	16.67	21.96	9.25	16.13	23.37	9.25	15.93	21.77
9.50	16.59	21.90	9.00	16.08	23.25	9.00	15.91	21.77
9.25	16.35	21.83	8.75	15.81	23.08	8.75	15.95	21.77
9.00	16.05	21.78	8.50	15.38	22.65	8.50	15.95	21.76
8.75	15.82	21.75	8.25	14.87	22.34	8.25	15.90	21.74
8.50	15.47	21.71	8.00	14.65	22.37	8.00	15.74	21.74
8.25	15.15	21.72	7.75	14.55	22.43	7.75	15.13	21.70
8.00	15.08	21.73	7.50	14.46	22.51	7.50	15.03	21.63
7.75	15.10	21.69	7.25	14.41	22.60	7.25	14.96	21.52
7.50	15.15	21.59	7.00	14.46	22.63	7.00	14.90	21.37
7.25	15.22	21.47	6.75	14.58	22.54	6.75	14.56	21.22
7.00	15.06	21.34	6.50	14.39	22.43	6.50	14.21	21.09
6.75	14.85	21.24	6.25	14.40	22.33	6.25	13.86	21.02
6.50	14.69	21.17	6.00	14.37	22.22	6.00	13.55	20.91
6.25	14.54	21.13	5.75	14.33	22.10	5.75	13.50	20.60
6.00	14.38	21.10	5.50	14.15	21.97	5.50	13.55	20.15
5.75	14.23	21.02	5.25	13.85	21.84	5.25	13.60	19.86
5.50	14.10	20.90	5.00	13.70	21.70	5.00	13.61	19.73
5.25	14.07	20.75	4.75	13.60	20.72	4.75	13.25	19.60
5.00	14.03	20.63	4.50	13.37	19.81	4.50	13.01	18.73
4.75	13.94	20.56	4.25	12.72	19.70	4.25	12.95	18.47
4.50	13.76	20.53	4.00	12.36	19.54	4.00	12.80	17.64
4.25	13.39	20.54	3.75	12.21	19.37	3.75	12.32	17.55
4.00	13.24	20.70	3.50	11.91	19.19	3.50	12.12	17.35

3.75	13.16	19.73	3.25	11.61	18.98	3.25	12.07	17.21
3.50	13.16	18.36	3.00	11.57	18.70	3.00	12.11	17.17
3.25	13.20	18.58	2.75	11.57	18.41	2.75	11.90	17.15
3.00	13.24	17.37	2.50	11.39	18.12	2.50	11.63	17.10
2.75	13.24	17.74	2.25	11.03	17.90	2.25	11.36	16.94
2.50	13.20	19.27	2.00	10.76	17.60	2.00	11.12	16.76
2.25	13.01	16.97	1.75	10.67	17.10	1.75	10.39	16.58
2.00	13.02	16.91	1.50	10.64	16.90	1.50	10.33	16.39
1.75	12.75	16.82	1.25	10.23	16.69	1.25	10.28	16.20
1.50	12.31	16.70	1.00	10.03	16.44	1.00	10.19	15.92
1.25	12.04	16.63	0.75	9.92	16.23	0.75	10.09	15.59
1.00	11.18	16.67	0.50	9.88	16.06	0.50	9.95	15.32
0.75	10.57	16.60	0.25	9.85	15.88	0.25	9.80	15.11
0.50	10.40	16.49	0.00	9.79	15.66	0.00	9.63	15.05
0.25	10.40	15.94	-0.25	9.66	15.37	-0.25	9.48	15.04
0.00	10.42	15.65	-0.50	9.49	15.08	-0.50	9.42	14.98
-0.25	10.18	16.13	-0.75	9.30	14.83	-0.75	9.11	14.88
-0.50	9.90	16.14	-1.00	9.04	14.14	-1.00	8.82	14.73
-0.75	9.79	16.02	-1.25	8.75	13.75	-1.25	8.68	14.50
-1.00	9.82	15.83	-1.50	8.46	13.56	-1.50	8.42	14.22
-1.25	9.67	15.53	-1.75	8.06	13.48	-1.75	8.18	13.69
-1.50	9.41	14.61	-2.00	7.61	13.45	-2.00	8.07	13.47
-1.75	9.13	14.33	-2.25	7.18	13.52	-2.25	7.79	13.26
-2.00	9.05	14.27	-2.50	6.76	13.67	-2.50	7.03	13.05
-2.25	9.08	14.22	-2.75	6.44	13.61	-2.75	6.70	12.81
-2.50	8.95	14.34	-3.00	6.20	13.27	-3.00	6.36	12.59
-2.75	8.78	14.54	-3.25	5.90	13.08	-3.25	6.08	12.37
-3.00	8.69	14.63	-3.50	5.55	12.35	-3.50	6.02	12.20
-3.25	8.57	14.57	-3.75	5.21	12.25	-3.75	6.04	11.75
-3.50	7.46	14.50	-4.00	5.04	12.08	-4.00	6.07	11.43
-3.75	7.24	13.73	-4.25	4.98	11.91	-4.25	6.10	11.35
-4.00	6.97	13.29	-4.50	4.92	11.89	-4.50	6.12	11.20
-4.25	6.75	13.27	-4.75	4.89	11.93	-4.75	5.96	10.65
-4.50	6.64	13.14	-5.00	5.06	11.85	-5.00	5.59	10.56
-4.75	6.47	12.96	-5.25	5.25	11.71	-5.25	5.39	10.46
-5.00	6.25	12.76	-5.50	5.18	11.66	-5.50	3.54	9.63
-5.25	5.84	11.91	-5.75	4.97	11.74	-5.75	3.87	9.98
-5.50	5.59	11.63	-6.00	4.75	11.78	-6.00	4.58	9.51
-5.75	5.36	11.41	-6.25	4.36	11.73	-6.25	4.32	8.96
-6.00	5.12	11.45	-6.50	4.18	11.66	-6.50	4.06	8.82
-6.25	4.82	11.14	-6.75	2.57	11.58	-6.75	3.79	8.85
-6.50	4.50	10.74	-7.00	1.94	11.46	-7.00	3.37	9.49
-6.75	4.20	10.58	-7.25	1.62	10.86	-7.25	2.89	8.54
-7.00	3.99	10.32	-7.50	1.32	10.23	-7.50	2.59	8.31
-7.25	3.74	10.42	-7.75	1.16	10.12	-7.75	2.29	8.19
-7.50	3.41	10.09	-8.00	1.05	10.16	-8.00	2.01	8.21
-7.75	3.09	10.54	-8.25	0.95	10.21	-8.25	1.72	8.22
-8.00	2.82	9.89	-8.50	0.84	8.51	-8.50	1.24	8.12
-8.25	2.57	9.78	-8.75	0.64	8.29	-8.75	1.01	8.01

-8.50	2.24	10.76	-9.00	0.37	8.31	-9.00	0.80	6.68
-8.75	2.02	9.54	-9.25	0.11	8.28	-9.25	-0.53	6.67
-9.00	1.71	9.43	-9.50	-0.10	6.77	-9.50	-0.85	6.64
-9.25	1.21	9.16	-9.75	-0.30	6.34	-9.75	-1.18	6.61
-9.50	0.87	8.99	-10.00	-0.50	6.19	-10.00	-1.32	5.39
-9.75	0.69	8.84	-10.25	-1.97	6.03	-10.25	-1.38	5.02
-10.00	0.54	8.58	-10.50	-2.32	5.36	-10.50	-1.47	4.81
-10.25	0.23	7.67	-10.75	-2.67	5.11	-10.75	-1.58	4.87
-10.50	-0.06	7.62	-11.00	-3.04	4.94	-11.00	-2.88	4.92
-10.75	-0.35	7.57	-11.25	-3.37	4.76	-11.25	-2.93	4.97
-11.00	-0.61	7.52	-11.50	-3.56	4.77	-11.50	-3.40	4.87
-11.25	-0.87	7.46	-11.75	-3.72	4.50	-11.75	-3.58	4.63
-11.50	-1.15	7.39	-12.00	-3.98	4.85	-12.00	-3.75	3.80
-11.75	-1.90	7.25	-12.25	-4.30	4.09	-12.25	-4.55	3.71
-12.00	-2.05	7.02	-12.50	-4.43	3.88	-12.50	-4.71	3.77
-12.25	-2.17	6.03	-12.75	-4.51	3.61	-12.75	-4.84	3.51
-12.50	-2.42	5.71	-13.00	-4.59	3.09	-13.00	-5.33	3.42
-12.75	-2.49	5.01	-13.25	-5.01	2.92	-13.25	-5.66	3.50
-13.00	-2.75	3.71	-13.50	-5.51	2.92	-13.50	-5.98	4.04
-13.25	-3.00	3.96	-13.75	-5.74	2.93	-13.75	-6.89	4.03
-13.50	-3.71	3.51	-14.00	-5.49	2.94	-14.00	-7.11	3.85
-13.75	-3.87	3.61	-14.25	-5.53	2.93	-14.25	-7.35	2.89
-14.00	-4.00	3.78	-14.50	-5.62	2.92	-14.50	-7.33	2.37
-14.25	-4.30	4.06	-14.75	-5.76	2.42	-14.75	-7.29	1.63
-14.50	-4.65	4.20	-15.00	-5.90	2.17	-15.00	-6.82	1.48
-14.75	-5.00	4.21	-15.25	-5.90	2.16	-15.25	-7.45	1.19
-15.00	-5.27	1.96	-15.50	-5.84	2.03	-15.50	-7.54	-0.36
-15.25	-5.55	1.96	-15.75	-6.16	1.93	-15.75	-8.48	-0.58
-15.50	-5.81	2.01	-16.00	-6.85	1.99	-16.00	-8.56	0.56
-15.75	-5.95	2.58	-16.25	-7.64	1.94	-16.25	-8.78	-0.91
-16.00	-6.09	0.98	-16.50	-8.45	1.76	-16.50	-9.44	-1.12
-16.25	-6.60	0.77	-16.75	-8.88	1.57	-16.75	-9.87	-1.53
-16.50	-6.79	0.58	-17.00	-9.25	1.35	-17.00	-10.15	-1.47
-16.75	-6.94	0.40	-17.25	-9.51	1.08	-17.25	-10.32	-1.47
-17.00	-7.01	0.21	-17.50	-9.76	0.06	-17.50	-10.45	-1.54
-17.25	-7.09	-0.16	-17.75	-9.87	0.01	-17.75	-11.56	-1.68
-17.50	-7.98	-1.09	-18.00	-9.93	-1.26	-18.00	-11.78	-1.86
-17.75	-8.92	-1.53	-18.25	-9.98	-2.49	-18.25	-12.34	-2.88
-18.00	-9.04	-1.61	-18.50	-10.08	-1.85	-18.50	-12.80	-2.86
-18.25	-9.54	-1.73	-18.75	-10.25	-2.95	-18.75	-13.15	-2.96
-18.50	-9.70	-1.95	-19.00	-12.33	-2.12	-19.00	-13.40	-3.65
-18.75	-9.86	-2.17	-19.25	-10.58	-3.33	-19.25	-13.62	-3.81
-19.00	-10.13	-2.31	-19.50	-13.13	-3.42	-19.50	-13.74	-4.31
-19.25	-10.29	-2.33	-19.75	-13.51	-4.49	-19.75	-13.76	-4.24
-19.50	-10.37	-2.36	-20.00	-15.63	-4.99	-20.00	-13.95	-4.42
-19.75	-10.51	-2.54	-20.25	-15.08	-5.12	-20.25	-15.56	-4.42
-20.00	-10.80	-2.81	-20.50	-15.26	-4.32	-20.50	-15.60	-5.34
-20.25	-11.54	-3.21	-20.75	-15.43	-5.73	-20.75	-15.68	-4.99
-20.50	-12.49	-3.66	-21.00	-15.60	-5.45	-21.00	-15.92	-6.12

-20.75	-13.42	-3.82
-21.00	-13.18	-3.82
-21.25	-13.56	-3.87
-21.50	-15.01	-4.04
-21.75	-15.26	-5.87
-22.00	-15.47	-6.30
-22.25	-16.51	-5.48
-22.50	-16.78	-6.34
-22.75	-16.13	-6.36
-23.00	-16.95	-7.20
-23.25	-18.80	-7.34
-23.50	N/A	-7.55
-23.75	N/A	-7.87
-24.00	N/A	-8.18
-24.25	N/A	-8.46
-24.50	N/A	-8.73
-24.75	N/A	-9.04
-25.00	N/A	-9.19
-25.25	N/A	-9.23
-25.50	N/A	-9.27
-25.75	N/A	-9.38
-26.00	N/A	-9.55
-26.25	N/A	-9.82
-26.50	N/A	-10.15
-26.75	N/A	-11.32
-27.00	N/A	-11.89
-27.25	N/A	-12.06
-27.50	N/A	-12.21
-27.75	N/A	-12.32
-28.00	N/A	-12.38
-28.25	N/A	-12.75
-28.50	N/A	-14.19
-28.75	N/A	-15.23
-29.00	N/A	-14.23
-29.25	N/A	-16.48
-29.50	N/A	-16.69
-29.75	N/A	-17.21
-30.00	N/A	-17.24
-30.25	N/A	-17.38
-30.50	N/A	-17.56
-30.75	N/A	-17.86
-31.00	N/A	-18.22
-31.25	N/A	-18.59
-31.50	N/A	-18.76
-31.75	N/A	-18.91
-32.00	N/A	-19.21

-21.25	-16.53	-5.53
-21.50	-16.85	-5.66
-21.75	-16.94	-6.94
-22.00	-17.45	-7.60
-22.25	-18.04	-8.24
-22.50	-18.55	-8.51
-22.75	N/A	-8.69
-23.00	N/A	-8.94
-23.25	N/A	-9.00
-23.50	N/A	-9.09
-23.75	N/A	-9.23
-24.00	N/A	-9.80
-24.25	N/A	-10.85
-24.50	N/A	-10.78
-24.75	N/A	-10.55
-25.00	N/A	-10.48
-25.25	N/A	-12.14
-25.50	N/A	-11.24
-25.75	N/A	-12.30
-26.00	N/A	-11.86
-26.25	N/A	-12.23
-26.50	N/A	-14.72
-26.75	N/A	-14.61
-27.00	N/A	-15.01
-27.25	N/A	-15.09
-27.50	N/A	-15.20
-27.75	N/A	-15.32
-28.00	N/A	-15.44
-28.25	N/A	-15.71
-28.50	N/A	-16.09
-28.75	N/A	-16.79
-29.00	N/A	-18.01
-29.25	N/A	-18.69
-29.50	N/A	-19.36

-21.25	-16.22	-5.97
-21.50	-16.84	-6.68
-21.75	-17.00	-7.11
-22.00	-17.42	-6.56
-22.25	-17.69	-8.47
-22.50	-17.91	-8.62
-22.75	-18.20	-8.72
-23.00	-18.58	-8.82
-23.25	-18.79	-8.93
-23.50	N/A	-9.09
-23.75	N/A	-9.25
-24.00	N/A	-9.50
-24.25	N/A	-10.77
-24.50	N/A	-11.21
-24.75	N/A	-10.73
-25.00	N/A	-10.94
-25.25	N/A	-14.28
-25.50	N/A	-13.88
-25.75	N/A	-13.06
-26.00	N/A	-14.91
-26.25	N/A	-15.00
-26.50	N/A	-15.34
-26.75	N/A	-15.78
-27.00	N/A	-16.12
-27.25	N/A	-16.38
-27.50	N/A	-16.64
-27.75	N/A	-16.91
-28.00	N/A	-17.34
-28.25	N/A	-17.81
-28.50	N/A	-18.35
-28.75	N/A	-18.83

Table E2. High-Water statistics for *H*/*P* ≈ 0.367 (*Q* ≈ 230 l/s) and with *p* = 0.46 *P*, *p* = 0.62 *P*, and *p* = 0.92 *P* (units in inches).

High-Water Statistics for H/P ≈ 0.367 and *p* = 0.46 *P*			High-Water Statistics for H/P ≈ 0.367 and *p* = 0.62 *P*			High-Water Statistics for H/P ≈ 0.367 and *p* = 0.77 *P*		
X	Y Min.	Y Max.	X	Y Min.	Y Max.	X	Y Min.	Y Max.
63.00	28.78	29.34	62.50	28.59	29.16	63.00	29.33	29.55
62.75	28.78	29.37	62.25	28.58	29.11	62.75	29.20	29.60
62.50	28.77	29.33	62.00	28.57	29.11	62.50	29.20	29.59
62.25	28.74	29.31	61.75	28.54	29.11	62.25	29.18	29.57
62.00	28.69	29.31	61.50	28.53	29.11	62.00	29.18	29.55
61.75	28.61	29.32	61.25	28.53	29.11	61.75	29.16	29.52
61.50	28.54	29.32	61.00	28.52	29.11	61.50	29.15	29.50
61.25	28.49	29.32	60.75	28.51	29.13	61.25	29.13	29.49
61.00	28.47	29.32	60.50	28.51	29.12	61.00	29.12	29.49
60.75	28.46	29.31	60.25	28.49	29.09	60.75	29.10	29.49
60.50	28.45	29.29	60.00	28.48	29.07	60.50	29.08	29.50
60.25	28.43	29.28	59.75	28.46	29.04	60.25	29.05	29.52
60.00	28.40	29.28	59.50	28.44	29.01	60.00	29.03	29.52
59.75	28.34	29.28	59.25	28.42	28.99	59.75	29.01	29.52
59.50	28.29	29.26	59.00	28.39	28.98	59.50	28.99	29.51
59.25	28.27	29.25	58.75	28.37	28.99	59.25	28.97	29.49
59.00	28.26	29.23	58.50	28.36	28.95	59.00	28.96	29.47
58.75	28.23	29.21	58.25	28.34	28.92	58.75	28.94	29.44
58.50	28.19	29.13	58.00	28.28	28.88	58.50	28.91	29.40
58.25	28.16	29.06	57.75	28.26	28.83	58.25	28.89	29.37
58.00	28.13	29.03	57.50	28.25	28.79	58.00	28.85	29.37
57.75	28.08	29.02	57.25	28.24	28.78	57.75	28.81	29.37
57.50	28.03	28.96	57.00	28.23	28.77	57.50	28.79	29.34
57.25	28.00	28.93	56.75	28.21	28.76	57.25	28.77	29.30
57.00	27.95	28.91	56.50	28.18	28.73	57.00	28.74	29.26
56.75	27.93	28.88	56.25	28.14	28.71	56.75	28.71	29.22
56.50	27.91	28.82	56.00	28.04	28.67	56.50	28.66	29.17
56.25	27.90	28.79	55.75	28.04	28.62	56.25	28.61	29.13
56.00	27.89	28.77	55.50	28.05	28.63	56.00	28.56	29.09
55.75	27.87	28.75	55.25	28.05	28.62	55.75	28.50	29.05
55.50	27.84	28.71	55.00	27.98	28.58	55.50	28.46	29.00
55.25	27.81	28.70	54.75	27.92	28.53	55.25	28.42	28.96
55.00	27.78	28.66	54.50	27.89	28.58	55.00	28.39	28.92
54.75	27.76	28.60	54.25	27.87	28.61	54.75	28.35	28.88
54.50	27.79	28.56	54.00	27.86	28.60	54.50	28.31	28.85
54.25	27.82	28.54	53.75	27.85	28.55	54.25	28.27	28.84

54.00	27.83	28.54	53.50	27.83	28.48	54.00	28.23	28.82
53.75	27.83	28.54	53.25	27.81	28.40	53.75	28.20	28.80
53.50	27.82	28.52	53.00	27.78	28.37	53.50	28.17	28.79
53.25	27.84	28.50	52.75	27.75	28.41	53.25	28.14	28.77
53.00	27.86	28.47	52.50	27.70	28.39	53.00	28.12	28.75
52.75	27.84	28.46	52.25	27.67	28.34	52.75	28.09	28.73
52.50	27.83	28.43	52.00	27.66	28.28	52.50	28.07	28.71
52.25	27.83	28.43	51.75	27.64	28.24	52.25	28.06	28.70
52.00	27.80	28.43	51.50	27.64	28.19	52.00	28.04	28.68
51.75	27.79	28.41	51.25	27.63	28.18	51.75	28.02	28.67
51.50	27.79	28.40	51.00	27.61	28.16	51.50	28.00	28.69
51.25	27.76	28.42	50.75	27.61	28.16	51.25	27.99	28.69
51.00	27.74	28.44	50.50	27.61	28.16	51.00	27.99	28.69
50.75	27.72	28.46	50.25	27.57	28.14	50.75	28.00	28.69
50.50	27.71	28.47	50.00	27.52	28.14	50.50	28.01	28.69
50.25	27.77	28.46	49.75	27.46	28.17	50.25	28.02	28.69
50.00	27.84	28.44	49.50	27.43	28.17	50.00	28.03	28.69
49.75	27.82	28.43	49.25	27.37	28.18	49.75	28.03	28.67
49.50	27.83	28.45	49.00	27.33	28.17	49.50	28.05	28.67
49.25	27.87	28.48	48.75	27.35	28.19	49.25	28.06	28.67
49.00	27.92	28.48	48.50	27.37	28.22	49.00	28.06	28.67
48.75	27.93	28.48	48.25	27.38	28.22	48.75	28.08	28.67
48.50	27.95	28.49	48.00	27.40	28.18	48.50	28.07	28.66
48.25	27.97	28.52	47.75	27.41	28.19	48.25	28.07	28.67
48.00	27.97	28.54	47.50	27.44	28.22	48.00	28.06	28.67
47.75	27.98	28.53	47.25	27.46	28.24	47.75	28.05	28.67
47.50	27.99	28.51	47.00	27.50	28.24	47.50	28.05	28.68
47.25	28.00	28.53	46.75	27.52	28.26	47.25	28.04	28.70
47.00	28.03	28.58	46.50	27.54	28.28	47.00	28.04	28.70
46.75	28.04	28.57	46.25	27.55	28.31	46.75	28.04	28.70
46.50	28.04	28.58	46.00	27.57	28.36	46.50	28.05	28.71
46.25	28.05	28.62	45.75	27.59	28.42	46.25	28.05	28.71
46.00	28.07	28.64	45.50	27.60	28.49	46.00	28.05	28.71
45.75	28.07	28.64	45.25	27.63	28.54	45.75	28.05	28.71
45.50	28.09	28.66	45.00	27.63	28.56	45.50	28.05	28.71
45.25	28.11	28.68	44.75	27.61	28.59	45.25	28.05	28.71
45.00	28.11	28.69	44.50	27.61	28.59	45.00	28.07	28.71
44.75	28.08	28.68	44.25	27.60	28.62	44.75	28.10	28.71
44.50	28.07	28.68	44.00	27.60	28.64	44.50	28.12	28.73
44.25	28.08	28.68	43.75	27.60	28.64	44.25	28.15	28.74
44.00	28.09	28.70	43.50	27.61	28.63	44.00	28.18	28.74
43.75	28.11	28.72	43.25	27.58	28.55	43.75	28.18	28.76
43.50	28.11	28.74	43.00	27.58	28.48	43.50	28.16	28.78
43.25	28.08	28.75	42.75	27.58	28.50	43.25	28.14	28.81
43.00	28.04	28.76	42.50	27.59	28.55	43.00	28.12	28.82
42.75	28.04	28.77	42.25	27.60	28.58	42.75	28.10	28.80
42.50	28.04	28.75	42.00	27.62	28.59	42.50	28.11	28.80
42.25	28.04	28.75	41.75	27.64	28.59	42.25	28.12	28.80
42.00	28.04	28.78	41.50	27.65	28.64	42.00	28.14	28.79

41.75	28.00	28.79	41.25	27.68	28.66	41.75	28.14	28.81
41.50	27.94	28.79	41.00	27.69	28.66	41.50	28.16	28.82
41.25	27.93	28.81	40.75	27.70	28.66	41.25	28.18	28.84
41.00	27.96	28.82	40.50	27.71	28.66	41.00	28.21	28.86
40.75	27.98	28.85	40.25	27.72	28.66	40.75	28.25	28.87
40.50	27.99	28.85	40.00	27.74	28.65	40.50	28.25	28.89
40.25	27.99	28.88	39.75	27.78	28.69	40.25	28.27	28.91
40.00	27.99	28.88	39.50	27.82	28.72	40.00	28.28	28.92
39.75	28.02	28.88	39.25	27.86	28.75	39.75	28.29	28.94
39.50	28.06	28.88	39.00	27.89	28.76	39.50	28.31	28.95
39.25	28.09	28.88	38.75	27.91	28.77	39.25	28.34	28.97
39.00	28.08	28.89	38.50	27.91	28.76	39.00	28.33	28.99
38.75	28.13	28.92	38.25	27.87	28.75	38.75	28.32	29.00
38.50	28.16	28.93	38.00	27.84	28.74	38.50	28.30	29.00
38.25	28.15	28.95	37.75	27.85	28.73	38.25	28.28	29.00
38.00	28.15	28.95	37.50	27.89	28.71	38.00	28.27	29.01
37.75	28.15	28.95	37.25	27.95	28.70	37.75	28.27	29.02
37.50	28.15	28.95	37.00	27.99	28.67	37.50	28.29	29.02
37.25	28.15	28.95	36.75	27.95	28.70	37.25	28.30	29.02
37.00	28.17	28.95	36.50	27.90	28.70	37.00	28.31	29.02
36.75	28.18	28.95	36.25	27.87	28.70	36.75	28.32	29.02
36.50	28.20	28.95	36.00	27.84	28.70	36.50	28.37	29.02
36.25	28.22	28.95	35.75	27.81	28.69	36.25	28.36	29.02
36.00	28.22	28.95	35.50	27.78	28.66	36.00	28.36	29.03
35.75	28.24	28.95	35.25	27.77	28.64	35.75	28.37	29.02
35.50	28.25	28.95	35.00	27.75	28.66	35.50	28.37	29.03
35.25	28.25	28.93	34.75	27.74	28.68	35.25	28.37	29.03
35.00	28.25	28.91	34.50	27.76	28.70	35.00	28.37	29.01
34.75	28.25	28.91	34.25	27.76	28.73	34.75	28.37	29.00
34.50	28.26	28.90	34.00	27.75	28.74	34.50	28.37	29.00
34.25	28.28	28.89	33.75	27.74	28.75	34.25	28.40	29.00
34.00	28.29	28.87	33.50	27.75	28.78	34.00	28.38	29.01
33.75	28.32	28.87	33.25	27.78	28.80	33.75	28.38	29.02
33.50	28.32	28.87	33.00	27.79	28.82	33.50	28.38	29.02
33.25	28.32	28.85	32.75	27.81	28.78	33.25	28.40	29.02
33.00	28.31	28.82	32.50	27.79	28.72	33.00	28.38	29.02
32.75	28.29	28.80	32.25	27.79	28.68	32.75	28.38	29.03
32.50	28.27	28.78	32.00	27.80	28.68	32.50	28.38	29.03
32.25	28.25	28.78	31.75	27.83	28.67	32.25	28.35	29.03
32.00	28.22	28.79	31.50	27.86	28.66	32.00	28.35	29.03
31.75	28.19	28.82	31.25	27.82	28.66	31.75	28.38	29.03
31.50	28.16	28.82	31.00	27.75	28.64	31.50	28.38	29.03
31.25	28.15	28.83	30.75	27.69	28.63	31.25	28.41	29.02
31.00	28.15	28.85	30.50	27.66	28.64	31.00	28.42	29.02
30.75	28.15	28.86	30.25	27.67	28.63	30.75	28.44	29.01
30.50	28.15	28.86	30.00	27.63	28.62	30.50	28.43	28.99
30.25	28.15	28.89	29.75	27.62	28.61	30.25	28.43	28.99
30.00	28.18	28.94	29.50	27.65	28.60	30.00	28.43	29.02
29.75	28.21	29.00	29.25	27.70	28.62	29.75	28.43	29.03

29.50	28.24	29.03	29.00	27.69	28.64	29.50	28.43	29.05
29.25	28.25	29.04	28.75	27.70	28.62	29.25	28.43	29.05
29.00	28.29	29.02	28.50	27.71	28.62	29.00	28.44	29.05
28.75	28.29	28.98	28.25	27.71	28.64	28.75	28.46	29.05
28.50	28.28	28.87	28.00	27.75	28.67	28.50	28.49	29.03
28.25	28.25	28.82	27.75	27.75	28.67	28.25	28.51	29.03
28.00	28.24	28.82	27.50	27.70	28.68	28.00	28.54	29.05
27.75	28.24	28.78	27.25	27.64	28.68	27.75	28.55	29.06
27.50	28.29	28.81	27.00	27.58	28.69	27.50	28.53	29.06
27.25	28.29	28.81	26.75	27.53	28.69	27.25	28.49	29.04
27.00	28.29	28.83	26.50	27.52	28.69	27.00	28.46	29.02
26.75	28.24	28.83	26.25	27.54	28.67	26.75	28.43	29.02
26.50	28.22	28.80	26.00	27.56	28.68	26.50	28.40	29.04
26.25	28.22	28.75	25.75	27.58	28.67	26.25	28.38	29.03
26.00	28.22	28.78	25.50	27.61	28.64	26.00	28.42	28.99
25.75	28.22	28.80	25.25	27.58	28.62	25.75	28.38	28.99
25.50	28.24	28.81	25.00	27.57	28.60	25.50	28.33	29.04
25.25	28.29	28.79	24.75	27.55	28.58	25.25	28.28	28.99
25.00	28.27	28.81	24.50	27.52	28.55	25.00	28.23	28.98
24.75	28.23	28.80	24.25	27.49	28.51	24.75	28.23	28.96
24.50	28.20	28.77	24.00	27.46	28.47	24.50	28.27	28.94
24.25	28.17	28.72	23.75	27.44	28.45	24.25	28.29	28.92
24.00	28.15	28.68	23.50	27.41	28.44	24.00	28.24	28.86
23.75	28.15	28.64	23.25	27.37	28.42	23.75	28.23	28.86
23.50	28.13	28.62	23.00	27.28	28.42	23.50	28.23	28.78
23.25	28.10	28.63	22.75	27.17	28.39	23.25	28.21	28.78
23.00	28.05	28.60	22.50	27.08	28.39	23.00	28.17	28.77
22.75	27.97	28.56	22.25	27.05	28.38	22.75	28.11	28.71
22.50	27.89	28.50	22.00	27.02	28.34	22.50	28.04	28.63
22.25	27.85	28.47	21.75	26.99	28.33	22.25	27.97	28.60
22.00	27.86	28.52	21.50	26.97	28.31	22.00	27.89	28.55
21.75	27.80	28.53	21.25	26.94	28.29	21.75	27.77	28.50
21.50	27.73	28.49	21.00	26.92	28.26	21.50	27.70	28.50
21.25	27.55	28.49	20.75	26.86	28.20	21.25	27.58	28.54
21.00	27.35	28.46	20.50	26.77	28.14	21.00	27.54	28.58
20.75	27.30	28.41	20.25	26.54	28.16	20.75	27.49	28.57
20.50	27.27	28.34	20.00	26.34	28.15	20.50	27.45	28.52
20.25	26.98	28.27	19.75	26.21	28.12	20.25	27.34	28.23
20.00	26.85	28.21	19.50	26.09	28.00	20.00	27.18	28.11
19.75	26.88	28.14	19.25	25.97	27.81	19.75	26.90	28.06
19.50	26.76	28.01	19.00	25.51	27.72	19.50	26.80	27.99
19.25	26.56	27.90	18.75	25.30	27.54	19.25	26.40	27.85
19.00	26.08	27.64	18.50	24.72	27.34	19.00	25.60	27.67
18.75	25.62	27.52	18.25	24.26	27.15	18.75	25.00	27.43
18.50	25.33	27.45	18.00	23.75	26.93	18.50	24.50	27.08
18.25	25.12	27.28	17.75	23.60	26.69	18.25	24.10	26.66
18.00	24.69	27.08	17.50	23.32	26.44	18.00	24.06	25.66
17.75	24.60	26.80	17.25	22.81	26.17	17.75	23.83	25.49
17.50	23.80	26.51	17.00	21.96	26.01	17.50	23.44	25.44

17.25	22.49	26.16	16.75	22.20	25.85	17.25	23.15	25.35
17.00	22.18	25.75	16.50	22.04	25.72	17.00	23.06	25.07
16.75	21.85	25.65	16.25	21.15	25.43	16.75	22.85	24.79
16.50	21.16	25.33	16.00	20.94	25.05	16.50	22.12	24.47
16.25	21.15	24.63	15.75	20.38	24.25	16.25	21.75	24.24
16.00	20.44	24.36	15.50	20.11	23.59	16.00	20.72	24.01
15.75	20.30	24.06	15.25	19.25	23.11	15.75	20.25	23.70
15.50	19.86	23.91	15.00	18.80	22.77	15.50	20.04	23.39
15.25	19.43	23.46	14.75	18.67	22.68	15.25	19.86	23.17
15.00	19.15	23.14	14.50	18.52	21.97	15.00	19.75	22.84
14.75	19.13	22.94	14.25	18.05	21.26	14.75	19.42	22.11
14.50	19.02	22.69	14.00	17.83	20.76	14.50	19.09	21.64
14.25	18.90	22.36	13.75	17.86	20.58	14.25	18.55	21.37
14.00	18.79	21.77	13.50	17.82	20.38	14.00	18.27	20.72
13.75	18.74	21.70	13.25	17.69	20.02	13.75	18.21	19.99
13.50	18.59	21.57	13.00	17.71	19.70	13.50	17.84	19.84
13.25	18.41	21.43	12.75	17.48	19.57	13.25	17.62	19.72
13.00	17.96	21.49	12.50	17.06	19.39	13.00	17.48	19.60
12.75	17.76	21.43	12.25	17.12	19.56	12.75	17.30	19.55
12.50	17.63	21.28	12.00	17.00	19.67	12.50	17.25	19.46
12.25	17.47	21.26	11.75	16.88	19.56	12.25	17.21	19.33
12.00	17.14	21.16	11.50	16.81	19.48	12.00	17.12	19.49
11.75	17.14	21.11	11.25	16.77	19.46	11.75	16.97	19.41
11.50	16.96	21.11	11.00	16.73	19.34	11.50	16.84	19.26
11.25	16.81	21.08	10.75	16.61	18.89	11.25	16.80	18.95
11.00	16.70	20.98	10.50	16.43	18.85	11.00	16.84	18.75
10.75	16.63	20.88	10.25	16.26	18.81	10.75	16.89	18.76
10.50	16.70	20.81	10.00	16.08	18.69	10.50	16.41	18.79
10.25	16.59	20.76	9.75	15.89	18.57	10.25	16.02	18.82
10.00	16.56	20.67	9.50	15.82	18.60	10.00	15.88	18.85
9.75	16.58	20.21	9.25	15.82	18.60	9.75	15.85	18.78
9.50	16.31	20.02	9.00	15.93	18.51	9.50	15.81	18.69
9.25	16.14	19.87	8.75	15.95	18.36	9.25	15.85	18.41
9.00	16.04	19.86	8.50	15.85	18.24	9.00	15.93	18.23
8.75	15.90	19.87	8.25	15.71	18.25	8.75	16.02	18.11
8.50	15.80	19.88	8.00	15.58	18.31	8.50	16.07	18.08
8.25	15.59	19.90	7.75	15.32	18.36	8.25	15.86	18.08
8.00	15.32	19.86	7.50	15.22	18.28	8.00	15.65	18.04
7.75	14.98	19.73	7.25	15.13	18.18	7.75	15.55	17.94
7.50	14.87	19.54	7.00	15.03	18.08	7.50	15.70	18.11
7.25	14.79	19.36	6.75	14.93	18.07	7.25	15.59	18.15
7.00	14.76	19.27	6.50	14.83	18.07	7.00	15.40	17.99
6.75	14.96	19.23	6.25	14.71	18.05	6.75	15.31	17.55
6.50	15.06	19.35	6.00	14.59	17.98	6.50	15.15	17.42
6.25	14.98	19.38	5.75	14.46	17.89	6.25	14.98	17.33
6.00	14.69	19.15	5.50	14.30	17.78	6.00	14.74	17.33
5.75	14.47	18.97	5.25	14.10	17.63	5.75	14.53	17.38
5.50	14.34	18.71	5.00	13.92	17.44	5.50	14.51	17.38
5.25	14.28	18.70	4.75	13.73	17.17	5.25	14.26	17.32

5.00	14.32	18.68	4.50	13.56	16.94	5.00	14.04	17.27
4.75	14.17	18.52	4.25	13.43	16.85	4.75	13.92	17.22
4.50	13.62	18.16	4.00	13.07	16.34	4.50	13.81	17.17
4.25	13.19	18.03	3.75	12.79	16.22	4.25	13.81	17.12
4.00	13.03	17.90	3.50	12.56	16.10	4.00	13.52	17.26
3.75	12.99	17.79	3.25	12.37	15.91	3.75	13.18	17.28
3.50	13.08	17.67	3.00	12.20	15.62	3.50	13.00	17.15
3.25	13.09	17.52	2.75	12.03	15.79	3.25	12.91	16.85
3.00	12.70	17.34	2.50	11.89	15.77	3.00	12.84	16.53
2.75	11.88	17.15	2.25	11.80	15.71	2.75	12.76	16.25
2.50	11.61	16.95	2.00	11.72	15.61	2.50	12.54	15.96
2.25	11.41	16.82	1.75	11.63	15.51	2.25	12.25	15.65
2.00	11.27	16.75	1.50	11.51	15.19	2.00	12.06	15.46
1.75	11.14	16.65	1.25	11.33	14.89	1.75	11.90	15.32
1.50	11.03	16.48	1.00	11.12	14.82	1.50	11.65	15.14
1.25	11.06	16.18	0.75	10.91	14.75	1.25	11.37	14.91
1.00	11.20	15.18	0.50	10.64	14.68	1.00	11.10	14.59
0.75	10.70	14.91	0.25	10.44	14.62	0.75	10.85	14.31
0.50	10.26	14.69	0.00	10.56	14.58	0.50	10.62	14.01
0.25	10.07	14.64	-0.25	10.09	14.54	0.25	10.44	13.78
0.00	9.92	14.56	-0.50	9.93	14.47	0.00	10.34	13.72
-0.25	9.97	14.48	-0.75	9.48	14.30	-0.25	10.39	13.72
-0.50	9.96	14.38	-1.00	9.18	14.03	-0.50	10.43	13.61
-0.75	9.51	14.27	-1.25	8.94	13.81	-0.75	10.35	13.85
-1.00	9.36	14.16	-1.50	8.74	13.64	-1.00	10.02	13.82
-1.25	9.23	14.16	-1.75	8.63	13.59	-1.25	9.86	13.66
-1.50	9.12	14.03	-2.00	8.56	13.54	-1.50	9.69	13.49
-1.75	9.02	13.89	-2.25	8.14	13.46	-1.75	9.56	13.30
-2.00	8.63	13.84	-2.50	7.91	13.30	-2.00	9.48	13.29
-2.25	8.33	13.72	-2.75	7.88	13.08	-2.25	9.42	13.26
-2.50	8.12	13.50	-3.00	7.84	12.71	-2.50	9.32	13.13
-2.75	7.91	13.22	-3.25	7.77	12.24	-2.75	8.84	12.96
-3.00	7.75	12.76	-3.50	7.68	11.72	-3.00	8.58	12.78
-3.25	7.62	12.27	-3.75	7.55	11.41	-3.25	8.32	12.29
-3.50	6.73	11.86	-4.00	7.21	11.15	-3.50	7.99	11.75
-3.75	6.53	11.39	-4.25	6.90	10.99	-3.75	7.76	11.74
-4.00	6.19	11.33	-4.50	6.73	10.87	-4.00	7.66	11.74
-4.25	5.84	11.44	-4.75	6.57	10.83	-4.25	7.59	11.58
-4.50	5.56	11.52	-5.00	6.41	10.75	-4.50	7.43	11.40
-4.75	5.32	11.64	-5.25	6.21	10.69	-4.75	7.21	11.17
-5.00	5.07	11.77	-5.50	6.10	10.63	-5.00	6.87	10.98
-5.25	4.94	11.72	-5.75	5.96	10.57	-5.25	6.62	10.82
-5.50	4.90	11.24	-6.00	5.83	10.48	-5.50	6.31	10.60
-5.75	4.89	10.90	-6.25	5.50	10.34	-5.75	6.01	10.30
-6.00	4.86	10.75	-6.50	4.40	10.17	-6.00	5.70	9.81
-6.25	4.82	10.58	-6.75	4.02	10.00	-6.25	5.47	9.66
-6.50	4.64	9.15	-7.00	3.70	9.77	-6.50	5.25	9.48
-6.75	4.39	8.91	-7.25	3.37	8.83	-6.75	4.97	9.25
-7.00	3.89	8.70	-7.50	3.04	8.75	-7.00	4.62	8.98

-7.25	3.59	8.46	-7.75	2.71	8.63	-7.25	4.34	8.83
-7.50	3.21	8.22	-8.00	2.39	8.53	-7.50	4.13	8.65
-7.75	2.80	7.55	-8.25	2.10	8.54	-7.75	3.94	8.07
-8.00	2.48	7.09	-8.50	1.74	8.60	-8.00	3.94	7.83
-8.25	2.12	7.07	-8.75	1.09	8.56	-8.25	3.98	7.70
-8.50	1.81	7.13	-9.00	0.65	8.44	-8.50	3.76	7.24
-8.75	1.52	7.20	-9.25	0.58	8.30	-8.75	3.34	7.07
-9.00	1.17	7.26	-9.50	0.53	8.10	-9.00	2.87	6.89
-9.25	0.79	7.24	-9.75	0.47	7.59	-9.25	2.36	6.77
-9.50	0.40	7.15	-10.00	0.42	7.00	-9.50	2.05	6.62
-9.75	0.01	6.99	-10.25	0.44	6.75	-9.75	1.75	6.46
-10.00	-0.35	6.65	-10.50	0.67	6.52	-10.00	1.45	6.31
-10.25	-0.76	6.28	-10.75	0.46	5.93	-10.25	1.21	6.02
-10.50	-1.17	5.94	-11.00	0.34	5.90	-10.50	1.07	5.57
-10.75	-1.29	5.12	-11.25	0.00	5.87	-10.75	0.78	5.29
-11.00	-1.38	4.41	-11.50	-0.29	5.83	-11.00	0.57	5.10
-11.25	-2.08	4.27	-11.75	-0.50	5.71	-11.25	0.42	4.90
-11.50	-2.29	4.24	-12.00	-0.76	5.55	-11.50	0.14	4.49
-11.75	-2.58	4.38	-12.25	-1.35	5.40	-11.75	-0.24	4.25
-12.00	-2.86	4.40	-12.50	-1.95	5.21	-12.00	-0.63	3.82
-12.25	-2.93	4.28	-12.75	-2.23	5.02	-12.25	-0.89	3.77
-12.50	-2.96	4.13	-13.00	-2.50	4.82	-12.50	-1.04	3.97
-12.75	-3.36	3.96	-13.25	-2.58	4.62	-12.75	-1.27	4.04
-13.00	-3.31	3.58	-13.50	-2.72	4.41	-13.00	-1.51	3.87
-13.25	-4.03	2.90	-13.75	-3.04	4.19	-13.25	-2.48	3.34
-13.50	-4.16	2.82	-14.00	-3.37	3.95	-13.50	-1.58	3.42
-13.75	-4.27	2.71	-14.25	-3.60	3.68	-13.75	-2.22	3.07
-14.00	-4.42	2.64	-14.50	-3.80	2.91	-14.00	-2.34	2.93
-14.25	-4.84	2.73	-14.75	-3.98	2.71	-14.25	-3.11	2.72
-14.50	-4.90	2.78	-15.00	-4.18	2.50	-14.50	-3.38	2.44
-14.75	-5.29	1.79	-15.25	-4.53	2.12	-14.75	-3.61	2.16
-15.00	-5.77	1.57	-15.50	-4.59	1.57	-15.00	-4.11	1.88
-15.25	-6.18	1.33	-15.75	-4.93	1.38	-15.25	-4.57	2.03
-15.50	-6.58	0.87	-16.00	-5.43	1.07	-15.50	-4.75	2.14
-15.75	-6.92	0.73	-16.25	-6.26	0.13	-15.75	-4.92	2.12
-16.00	-7.16	0.70	-16.50	-6.58	-0.06	-16.00	-4.99	2.11
-16.25	-7.39	0.60	-16.75	-6.65	-0.95	-16.25	-5.02	2.08
-16.50	-7.81	0.59	-17.00	-6.70	-1.13	-16.50	-5.06	2.00
-16.75	-8.09	0.74	-17.25	-6.95	-1.00	-16.75	-5.29	1.89
-17.00	-8.44	-0.28	-17.50	-7.34	-0.89	-17.00	-5.63	1.76
-17.25	-8.70	-0.55	-17.75	-7.62	-0.99	-17.25	-5.97	1.59
-17.50	-9.05	-0.87	-18.00	-7.90	-1.18	-17.50	-6.32	1.42
-17.75	-9.35	-1.26	-18.25	-8.95	-1.39	-17.75	-6.69	1.23
-18.00	-9.65	-2.39	-18.50	-9.68	-1.65	-18.00	-7.08	0.74
-18.25	-10.40	-2.69	-18.75	-9.93	-2.05	-18.25	-8.08	-0.47
-18.50	-11.03	-3.03	-19.00	-10.18	-2.41	-18.50	-8.39	-0.66
-18.75	-11.31	-3.27	-19.25	-10.42	-2.53	-18.75	-8.69	-0.60
-19.00	-11.59	-3.55	-19.50	-10.66	-2.52	-19.00	-8.96	-0.63
-19.25	-11.88	-3.81	-19.75	-10.91	-2.55	-19.25	-9.08	-0.81

-19.50	-12.37	-4.34	-20.00	-11.16	-3.75	-19.50	-9.17	-1.00
-19.75	-12.93	-5.31	-20.25	-11.41	-3.65	-19.75	-9.40	-1.29
-20.00	-13.41	-6.08	-20.50	-12.08	-4.21	-20.00	-9.61	-2.32
-20.25	-13.82	-6.21	-20.75	-12.39	-4.46	-20.25	-9.90	-2.80
-20.50	-14.21	-6.07	-21.00	-12.81	-4.71	-20.50	-10.68	-3.52
-20.75	-14.75	-5.91	-21.25	-13.33	-4.99	-20.75	-10.84	-4.29
-21.00	-15.40	-6.44	-21.50	-13.63	-5.28	-21.00	-10.92	-4.29
-21.25	-15.84	-6.30	-21.75	-14.09	-5.57	-21.25	-10.99	-4.31
-21.50	-15.71	-6.42	-22.00	-14.56	-5.86	-21.50	-11.57	-4.35
-21.75	-15.83	-8.39	-22.25	-16.39	-6.14	-21.75	-12.06	-4.40
-22.00	-16.13	-7.00	-22.50	-15.54	-6.42	-22.00	-12.49	-4.44
-22.25	-16.43	-8.10	-22.75	-16.78	-6.70	-22.25	-12.71	-4.47
-22.50	-16.72	-8.34	-23.00	-17.27	-6.91	-22.50	-12.89	-4.51
-22.75	-17.00	-8.89	-23.25	-17.84	-7.01	-22.75	-13.11	-4.65
-23.00	-17.77	-8.95	-23.50	-18.19	-7.37	-23.00	-14.10	-6.24
-23.25	-18.62	-9.96	-23.75	-18.51	-7.54	-23.25	-14.64	-7.42
-23.50	-19.05	-9.63	-24.00	-18.83	-7.80	-23.50	-14.75	-8.08
-23.75	N/A	-10.16	-24.25	-18.90	-8.21	-23.75	-15.73	-8.06
-24.00	N/A	-10.62	-24.50	N/A	-8.86	-24.00	-15.93	-8.04
-24.25	N/A	-10.58	-24.75	N/A	-9.68	-24.25	-16.31	-6.22
-24.50	N/A	-10.73	-25.00	N/A	-10.11	-24.50	-16.70	-7.25
-24.75	N/A	-11.01	-25.25	N/A	-10.50	-24.75	-17.60	-7.94
-25.00	N/A	-11.19	-25.50	N/A	-10.88	-25.00	N/A	-8.03
-25.25	N/A	-11.33	-25.75	N/A	-11.32	-25.25	N/A	-8.28
-25.50	N/A	-11.48	-26.00	N/A	-11.86	-25.50	N/A	-9.71
-25.75	N/A	-11.67	-26.25	N/A	-12.26	-25.75	N/A	-10.01
-26.00	N/A	-11.99	-26.50	N/A	-12.71	-26.00	N/A	-10.24
-26.25	N/A	-12.48	-26.75	N/A	-13.31	-26.25	N/A	-10.46
-26.50	N/A	-14.39	-27.00	N/A	-14.16	-26.50	N/A	-10.70
-26.75	N/A	-14.76	-27.25	N/A	-15.41	-26.75	N/A	-10.59
-27.00	N/A	-15.05	-27.50	N/A	-15.38	-27.00	N/A	-10.99
-27.25	N/A	-15.01	-27.75	N/A	-15.35	-27.25	N/A	-10.78
-27.50	N/A	-15.23	-28.00	N/A	-15.40	-27.50	N/A	-11.44
-27.75	N/A	-15.51	-28.25	N/A	-15.51	-27.75	N/A	-11.66
-28.00	N/A	-15.88	-28.50	N/A	-15.63	-28.00	N/A	-11.90
-28.25	N/A	-17.84	-28.75	N/A	-15.76	-28.25	N/A	-11.40
-28.50	N/A	-18.17	-29.00	N/A	-16.15	-28.50	N/A	-12.49
-28.75	N/A	-18.60	-29.25	N/A	-17.46	-28.75	N/A	-13.80
-29.00	N/A	-19.14	-29.50	N/A	-17.82	-29.00	N/A	-14.67
-29.25	N/A	-19.58	-29.75	N/A	-18.75	-29.25	N/A	-14.60
			-30.00	N/A	-18.97	-29.50	N/A	-14.54
						-29.75	N/A	-15.01
						-30.00	N/A	-15.08
						-30.25	N/A	-15.14
						-30.50	N/A	-15.22
						-30.75	N/A	-15.41
						-31.00	N/A	-15.67
						-31.25	N/A	-15.91
						-31.50	N/A	-16.17

-31.75	N/A	-16.42
-32.00	N/A	-16.75
-32.25	N/A	-17.26
-32.50	N/A	-17.83

Table E3. High-Water statistics for *H*/*P* ≈ 0.367 (*Q* ≈ 116 l/s) and with *p* = 0.92 *P* (units in inches).

High-Water Statistics for H/P ≈ 0.367 and *p* = 0.92 *P*		
X	Y Min.	Y Max.
63.25	29.31	29.31
63.00	29.28	29.57
62.75	29.21	29.54
62.50	29.25	29.51
62.25	29.22	29.47
62.00	29.20	29.46
61.75	29.17	29.47
61.50	29.14	29.47
61.25	29.11	29.46
61.00	29.09	29.46
60.75	29.06	29.43
60.50	29.06	29.43
60.25	29.04	29.42
60.00	29.01	29.40
59.75	28.98	29.39
59.50	28.95	29.39
59.25	28.95	29.38
59.00	28.96	29.36
58.75	28.96	29.35
58.50	28.96	29.32
58.25	28.95	29.29
58.00	28.94	29.26
57.75	28.92	29.22
57.50	28.88	29.19
57.25	28.85	29.16
57.00	28.84	29.13
56.75	28.81	29.11

56.50	28.78	29.08
56.25	28.74	29.07
56.00	28.73	29.05
55.75	28.71	29.03
55.50	28.69	29.01
55.25	28.66	28.97
55.00	28.64	28.93
54.75	28.59	28.90
54.50	28.55	28.88
54.25	28.54	28.86
54.00	28.52	28.85
53.75	28.50	28.85
53.50	28.47	28.84
53.25	28.44	28.82
53.00	28.42	28.80
52.75	28.41	28.79
52.50	28.39	28.79
52.25	28.37	28.78
52.00	28.36	28.75
51.75	28.34	28.73
51.50	28.33	28.73
51.25	28.31	28.73
51.00	28.30	28.73
50.75	28.28	28.73
50.50	28.26	28.73
50.25	28.23	28.72
50.00	28.21	28.70
49.75	28.18	28.69
49.50	28.16	28.70
49.25	28.13	28.72
49.00	28.10	28.74
48.75	28.08	28.73
48.50	28.08	28.73
48.25	28.09	28.76
48.00	28.09	28.76
47.75	28.09	28.76
47.50	28.09	28.76
47.25	28.10	28.76
47.00	28.09	28.76
46.75	28.08	28.76
46.50	28.06	28.76
46.25	28.05	28.76
46.00	28.04	28.76
45.75	28.03	28.76
45.50	28.05	28.76
45.25	28.07	28.76
45.00	28.09	28.76
44.75	28.10	28.76
44.50	28.13	28.76

44.25	28.16	28.76
44.00	28.19	28.74
43.75	28.22	28.73
43.50	28.23	28.71
43.25	28.22	28.70
43.00	28.21	28.70
42.75	28.21	28.70
42.50	28.21	28.71
42.25	28.21	28.75
42.00	28.21	28.76
41.75	28.21	28.76
41.50	28.19	28.77
41.25	28.18	28.79
41.00	28.18	28.79
40.75	28.17	28.80
40.50	28.16	28.80
40.25	28.15	28.83
40.00	28.15	28.86
39.75	28.17	28.88
39.50	28.21	28.90
39.25	28.27	28.91
39.00	28.33	28.91
38.75	28.36	28.90
38.50	28.36	28.94
38.25	28.38	28.98
38.00	28.40	28.99
37.75	28.42	28.98
37.50	28.42	28.98
37.25	28.40	28.98
37.00	28.39	29.00
36.75	28.39	29.01
36.50	28.39	29.01
36.25	28.39	29.01
36.00	28.39	29.03
35.75	28.39	29.04
35.50	28.39	29.04
35.25	28.39	29.04
35.00	28.39	29.04
34.75	28.39	29.03
34.50	28.40	29.01
34.25	28.41	28.99
34.00	28.42	29.00
33.75	28.44	29.00
33.50	28.47	29.00
33.25	28.49	28.97
33.00	28.50	28.95
32.75	28.51	28.93
32.50	28.51	28.90
32.25	28.51	28.88

32.00	28.51	28.88
31.75	28.51	28.89
31.50	28.53	28.89
31.25	28.55	28.89
31.00	28.56	28.89
30.75	28.56	28.88
30.50	28.54	28.88
30.25	28.50	28.88
30.00	28.50	28.88
29.75	28.50	28.88
29.50	28.50	28.87
29.25	28.50	28.85
29.00	28.49	28.85
28.75	28.48	28.85
28.50	28.48	28.85
28.25	28.48	28.86
28.00	28.47	28.88
27.75	28.46	28.91
27.50	28.45	28.93
27.25	28.43	28.94
27.00	28.43	28.95
26.75	28.45	28.95
26.50	28.43	28.95
26.25	28.43	28.96
26.00	28.40	28.95
25.75	28.39	28.91
25.50	28.37	28.91
25.25	28.35	28.89
25.00	28.33	28.86
24.75	28.31	28.85
24.50	28.30	28.84
24.25	28.30	28.82
24.00	28.27	28.83
23.75	28.26	28.92
23.50	28.22	28.92
23.25	28.18	28.92
23.00	28.12	28.90
22.75	28.08	28.82
22.50	28.05	28.80
22.25	28.03	28.71
22.00	27.99	28.61
21.75	27.89	28.54
21.50	27.79	28.47
21.25	27.70	28.39
21.00	27.62	28.44
20.75	27.55	28.48
20.50	27.47	28.42
20.25	27.37	28.33
20.00	27.11	28.35

19.75	26.97	28.39
19.50	26.71	28.36
19.25	26.46	28.30
19.00	26.27	28.18
18.75	26.01	27.98
18.50	25.26	27.74
18.25	24.79	27.55
18.00	24.67	27.18
17.75	24.43	27.05
17.50	24.16	26.61
17.25	23.78	26.36
17.00	23.68	25.93
16.75	23.52	25.72
16.50	22.91	25.40
16.25	22.51	25.16
16.00	22.13	24.97
15.75	21.36	24.58
15.50	21.16	24.03
15.25	20.63	23.75
15.00	20.29	23.22
14.75	20.24	22.75
14.50	19.88	22.44
14.25	18.16	22.16
14.00	17.79	21.29
13.75	17.67	20.80
13.50	17.28	20.50
13.25	17.25	19.91
13.00	17.23	19.70
12.75	17.15	19.22
12.50	17.07	19.14
12.25	17.05	19.05
12.00	16.93	19.00
11.75	16.84	18.97
11.50	16.77	18.88
11.25	16.66	18.81
11.00	16.50	18.76
10.75	16.39	18.72
10.50	16.35	18.68
10.25	16.35	18.63
10.00	16.31	18.58
9.75	16.24	18.52
9.50	16.17	18.40
9.25	16.11	18.30
9.00	16.09	18.30
8.75	16.06	18.30
8.50	16.08	18.28
8.25	16.06	18.19
8.00	16.05	17.98
7.75	16.00	17.82

7.50	15.94	17.87
7.25	15.87	17.99
7.00	15.69	18.11
6.75	15.18	18.26
6.50	15.10	18.35
6.25	15.03	18.40
6.00	14.96	18.45
5.75	14.85	18.49
5.50	14.70	18.52
5.25	14.38	18.50
5.00	14.35	18.46
4.75	14.58	18.41
4.50	14.65	18.31
4.25	14.63	18.17
4.00	14.58	18.04
3.75	14.54	17.83
3.50	14.55	17.51
3.25	14.43	17.33
3.00	14.13	17.12
2.75	13.57	16.82
2.50	13.33	16.46
2.25	13.19	16.25
2.00	13.12	16.05
1.75	12.82	15.84
1.50	12.67	15.66
1.25	12.57	15.64
1.00	12.47	15.55
0.75	12.46	15.48
0.50	12.16	15.45
0.25	11.73	15.47
0.00	11.48	15.34
-0.25	11.30	15.15
-0.50	11.19	14.93
-0.75	11.07	15.05
-1.00	10.91	14.95
-1.25	10.74	14.79
-1.50	10.55	14.63
-1.75	10.41	14.48
-2.00	10.43	14.45
-2.25	10.48	14.43
-2.50	9.68	14.40
-2.75	9.40	14.30
-3.00	9.14	14.15
-3.25	8.91	13.73
-3.50	8.70	13.16
-3.75	8.62	12.76
-4.00	8.62	12.49
-4.25	8.51	12.37
-4.50	8.28	12.23

-4.75	8.03	11.98
-5.00	7.76	11.71
-5.25	7.41	11.55
-5.50	7.03	11.43
-5.75	6.82	11.31
-6.00	6.62	11.19
-6.25	6.43	11.05
-6.50	6.23	10.83
-6.75	6.03	10.62
-7.00	5.83	10.41
-7.25	5.61	10.19
-7.50	5.43	9.97
-7.75	5.23	9.73
-8.00	5.05	9.41
-8.25	4.51	9.18
-8.50	4.37	8.99
-8.75	4.13	8.77
-9.00	3.90	8.53
-9.25	3.66	8.27
-9.50	3.38	8.01
-9.75	3.16	7.72
-10.00	2.92	7.44
-10.25	2.70	7.30
-10.50	2.50	7.19
-10.75	2.05	7.07
-11.00	1.73	6.92
-11.25	1.54	6.77
-11.50	1.36	6.60
-11.75	1.18	6.42
-12.00	1.02	6.23
-12.25	0.90	6.02
-12.50	0.82	5.47
-12.75	0.61	5.33
-13.00	0.31	5.14
-13.25	0.02	4.95
-13.50	-0.26	4.74
-13.75	-0.47	4.50
-14.00	-0.94	4.03
-14.25	-1.28	3.62
-14.50	-2.04	3.37
-14.75	-2.11	3.14
-15.00	-2.14	2.85
-15.25	-2.39	2.47
-15.50	-2.63	2.12
-15.75	-2.74	1.83
-16.00	-3.53	1.48
-16.25	-3.25	1.02
-16.50	-3.92	0.73
-16.75	-4.07	0.67

-17.00	-4.23	0.58
-17.25	-4.62	0.49
-17.50	-4.66	0.40
-17.75	-4.81	0.31
-18.00	-5.76	0.21
-18.25	-6.64	-0.01
-18.50	-6.75	-0.82
-18.75	-7.99	-1.28
-19.00	-8.43	-1.42
-19.25	-8.84	-1.64
-19.50	-8.96	-1.87
-19.75	-9.05	-2.09
-20.00	-9.15	-2.36
-20.25	-9.24	-2.44
-20.50	-9.33	-2.64
-20.75	-9.41	-2.88
-21.00	-9.66	-3.65
-21.25	-9.92	-4.05
-21.50	-10.30	-4.15
-21.75	-11.10	-4.37
-22.00	-11.61	-4.61
-22.25	-11.80	-4.98
-22.50	-12.07	-5.36
-22.75	-12.33	-5.85
-23.00	-12.61	-6.39
-23.25	-12.91	-6.89
-23.50	-13.32	-7.40
-23.75	-13.50	-7.64
-24.00	-13.68	-7.96
-24.25	-13.97	-8.39
-24.50	-14.34	-8.81
-24.75	-14.71	-9.13
-25.00	-15.08	-9.35
-25.25	-15.56	-9.63
-25.50	-16.66	-9.93
-25.75	-16.84	-10.24
-26.00	-17.16	-10.56
-26.25	-17.30	-11.00
-26.50	N/A	-11.09
-26.75	N/A	-11.24
-27.00	N/A	-11.94
-27.25	N/A	-12.15
-27.50	N/A	-12.29
-27.75	N/A	-13.33
-28.00	N/A	-13.54
-28.25	N/A	-13.76
-28.50	N/A	-14.15
-28.75	N/A	-14.37
-29.00	N/A	-14.60

-29.25	N/A	-14.84
-29.50	N/A	-15.12
-29.75	N/A	-15.95
-30.00	N/A	-16.30
-30.25	N/A	-16.64
-30.50	N/A	-17.34
-30.75	N/A	-17.58

APPENDIX F – HIGH-WATER SURFACE DATA FOR $H/P \approx 0.186$ ($Q \approx 116$ L/S).

Table F1. High-Water statistics for $H/P \approx 0.186$ ($Q \approx 116$ l/s) and with no ramp, $p = 0.15$ P, and $p = 0.31$ P (units in inches).

High-Water Statistics for H/P ≈ 0.186 and no ramp			High-Water Statistics for H/P ≈ 0.186 and *p* = 0.15 *P*			High-Water Statistics for H/P ≈ 0.186 and *p* = 0.31 *P*		
X	Y Min.	Y Max.	X	Y Min.	Y Max.	X	Y Min.	Y Max.
63.75	27.29	27.29	63.00	27.23	27.26	62.75	27.08	27.29
63.50	27.22	27.36	62.75	27.14	27.30	62.50	27.08	27.28
63.25	27.16	27.36	62.50	27.14	27.26	62.25	27.07	27.26
63.00	27.16	27.36	62.25	27.14	27.26	62.00	27.07	27.26
62.75	27.14	27.36	62.00	27.14	27.26	61.75	27.05	27.25
62.50	27.14	27.36	61.75	27.13	27.26	61.50	27.03	27.25
62.25	27.10	27.36	61.50	27.11	27.25	61.25	27.02	27.23
62.00	27.10	27.34	61.25	27.11	27.23	61.00	27.02	27.23
61.75	27.13	27.32	61.00	27.11	27.22	60.75	27.00	27.22
61.50	27.13	27.30	60.75	27.10	27.22	60.50	27.00	27.21
61.25	27.11	27.29	60.50	27.09	27.22	60.25	27.00	27.20
61.00	27.10	27.28	60.25	27.08	27.22	60.00	26.99	27.19
60.75	27.10	27.28	60.00	27.07	27.22	59.75	26.97	27.19
60.50	27.10	27.28	59.75	27.07	27.22	59.50	26.97	27.18
60.25	27.10	27.30	59.50	27.07	27.22	59.25	26.96	27.17
60.00	27.09	27.30	59.25	27.06	27.20	59.00	26.95	27.16
59.75	27.08	27.30	59.00	27.04	27.19	58.75	26.94	27.16
59.50	27.07	27.29	58.75	27.04	27.18	58.50	26.93	27.15
59.25	27.05	27.27	58.50	27.04	27.15	58.25	26.92	27.14
59.00	27.04	27.27	58.25	27.03	27.15	58.00	26.91	27.13
58.75	27.02	27.25	58.00	27.01	27.15	57.75	26.90	27.12
58.50	27.03	27.24	57.75	27.01	27.15	57.50	26.89	27.11
58.25	27.03	27.23	57.50	27.01	27.15	57.25	26.88	27.11
58.00	27.02	27.22	57.25	27.01	27.15	57.00	26.86	27.09
57.75	27.00	27.21	57.00	27.01	27.13	56.75	26.86	27.09
57.50	26.99	27.20	56.75	27.01	27.12	56.50	26.84	27.08
57.25	26.97	27.19	56.50	27.01	27.13	56.25	26.83	27.07
57.00	26.96	27.18	56.25	27.01	27.13	56.00	26.81	27.06
56.75	26.96	27.18	56.00	27.00	27.13	55.75	26.80	27.05
56.50	26.96	27.17	55.75	26.99	27.13	55.50	26.81	27.04
56.25	26.95	27.16	55.50	26.99	27.13	55.25	26.81	27.04
56.00	26.94	27.16	55.25	26.99	27.13	55.00	26.81	27.05
55.75	26.94	27.15	55.00	26.99	27.13	54.75	26.81	27.05
55.50	26.94	27.14	54.75	26.99	27.13	54.50	26.80	27.05
55.25	26.94	27.14	54.50	27.00	27.13	54.25	26.79	27.05
55.00	26.94	27.14	54.25	27.00	27.11	54.00	26.78	27.04
54.75	26.94	27.15	54.00	27.00	27.11	53.75	26.77	27.04
54.50	26.94	27.15	53.75	27.00	27.11	53.50	26.76	27.04
54.25	26.94	27.15	53.50	27.00	27.11	53.25	26.76	27.03
54.00	26.94	27.16	53.25	27.00	27.11	53.00	26.76	27.03
53.75	26.94	27.15	53.00	27.00	27.11	52.75	26.76	27.03
53.50	26.93	27.15	52.75	27.00	27.11	52.50	26.76	27.03

53.25	26.93	27.15	52.50	27.00	27.11	52.25	26.77	27.04
53.00	26.93	27.15	52.25	27.01	27.11	52.00	26.75	27.04
52.75	26.93	27.14	52.00	27.01	27.11	51.75	26.74	27.04
52.50	26.92	27.14	51.75	27.01	27.11	51.50	26.74	27.04
52.25	26.91	27.14	51.50	27.01	27.11	51.25	26.76	27.03
52.00	26.91	27.14	51.25	27.02	27.11	51.00	26.78	27.02
51.75	26.91	27.14	51.00	27.02	27.11	50.75	26.78	27.02
51.50	26.91	27.14	50.75	27.02	27.11	50.50	26.81	27.02
51.25	26.91	27.15	50.50	27.02	27.11	50.25	26.82	27.02
51.00	26.90	27.15	50.25	27.02	27.12	50.00	26.82	27.03
50.75	26.90	27.15	50.00	27.02	27.15	49.75	26.82	27.03
50.50	26.90	27.15	49.75	27.02	27.15	49.50	26.82	27.03
50.25	26.91	27.15	49.50	27.02	27.15	49.25	26.83	27.03
50.00	26.92	27.15	49.25	27.03	27.15	49.00	26.81	27.04
49.75	26.91	27.15	49.00	27.03	27.15	48.75	26.80	27.04
49.50	26.91	27.13	48.75	27.04	27.15	48.50	26.81	27.04
49.25	26.91	27.13	48.50	27.04	27.13	48.25	26.81	27.05
49.00	26.91	27.13	48.25	27.04	27.12	48.00	26.80	27.07
48.75	26.90	27.13	48.00	27.04	27.13	47.75	26.81	27.08
48.50	26.89	27.14	47.75	27.04	27.13	47.50	26.81	27.08
48.25	26.89	27.15	47.50	27.03	27.13	47.25	26.81	27.09
48.00	26.89	27.16	47.25	27.02	27.13	47.00	26.81	27.09
47.75	26.88	27.17	47.00	27.02	27.13	46.75	26.82	27.10
47.50	26.88	27.17	46.75	27.03	27.13	46.50	26.82	27.12
47.25	26.88	27.17	46.50	27.04	27.13	46.25	26.84	27.12
47.00	26.89	27.17	46.25	27.05	27.15	46.00	26.87	27.13
46.75	26.90	27.17	46.00	27.05	27.16	45.75	26.89	27.13
46.50	26.90	27.17	45.75	27.05	27.17	45.50	26.92	27.13
46.25	26.90	27.18	45.50	27.05	27.15	45.25	26.93	27.13
46.00	26.90	27.17	45.25	27.05	27.15	45.00	26.93	27.14
45.75	26.90	27.16	45.00	27.04	27.15	44.75	26.93	27.14
45.50	26.90	27.16	44.75	27.04	27.15	44.50	26.94	27.14
45.25	26.90	27.16	44.50	27.04	27.13	44.25	26.94	27.14
45.00	26.91	27.16	44.25	27.04	27.13	44.00	26.93	27.14
44.75	26.91	27.16	44.00	27.03	27.13	43.75	26.91	27.14
44.50	26.91	27.16	43.75	27.04	27.13	43.50	26.91	27.15
44.25	26.91	27.18	43.50	27.04	27.14	43.25	26.91	27.15
44.00	26.91	27.18	43.25	27.04	27.15	43.00	26.92	27.15
43.75	26.92	27.19	43.00	27.04	27.16	42.75	26.92	27.16
43.50	26.93	27.20	42.75	27.04	27.16	42.50	26.92	27.16
43.25	26.93	27.20	42.50	27.04	27.16	42.25	26.89	27.16
43.00	26.93	27.20	42.25	27.04	27.16	42.00	26.90	27.17
42.75	26.95	27.22	42.00	27.04	27.16	41.75	26.93	27.19
42.50	26.95	27.23	41.75	27.04	27.16	41.50	26.93	27.20
42.25	26.95	27.23	41.50	27.05	27.16	41.25	26.93	27.20
42.00	26.95	27.24	41.25	27.05	27.16	41.00	26.94	27.21
41.75	26.95	27.21	41.00	27.05	27.16	40.75	26.96	27.22
41.50	26.95	27.21	40.75	27.05	27.16	40.50	26.97	27.22
41.25	26.95	27.21	40.50	27.05	27.16	40.25	26.98	27.21

41.00	26.96	27.21	40.25	27.06	27.16	40.00	26.98	27.21
40.75	26.97	27.22	40.00	27.07	27.16	39.75	26.98	27.22
40.50	26.99	27.23	39.75	27.08	27.18	39.50	26.98	27.22
40.25	26.99	27.23	39.50	27.08	27.19	39.25	26.98	27.21
40.00	27.00	27.21	39.25	27.08	27.19	39.00	26.99	27.19
39.75	27.01	27.21	39.00	27.08	27.19	38.75	26.99	27.19
39.50	27.02	27.21	38.75	27.08	27.19	38.50	26.99	27.17
39.25	27.00	27.21	38.50	27.08	27.19	38.25	27.00	27.16
39.00	27.00	27.21	38.25	27.09	27.19	38.00	27.03	27.16
38.75	27.01	27.22	38.00	27.09	27.19	37.75	27.03	27.17
38.50	27.01	27.22	37.75	27.09	27.19	37.50	27.03	27.17
38.25	27.01	27.22	37.50	27.09	27.19	37.25	27.04	27.17
38.00	27.01	27.22	37.25	27.09	27.19	37.00	27.04	27.17
37.75	27.01	27.22	37.00	27.09	27.19	36.75	27.04	27.18
37.50	27.01	27.22	36.75	27.09	27.19	36.50	27.04	27.18
37.25	27.00	27.22	36.50	27.08	27.20	36.25	27.05	27.18
37.00	27.00	27.22	36.25	27.08	27.21	36.00	27.05	27.18
36.75	27.00	27.22	36.00	27.08	27.21	35.75	27.05	27.17
36.50	27.00	27.23	35.75	27.08	27.21	35.50	27.05	27.17
36.25	27.00	27.23	35.50	27.08	27.21	35.25	27.05	27.17
36.00	27.00	27.23	35.25	27.08	27.21	35.00	27.04	27.16
35.75	27.00	27.23	35.00	27.08	27.21	34.75	27.04	27.16
35.50	27.00	27.23	34.75	27.08	27.20	34.50	27.04	27.16
35.25	27.00	27.22	34.50	27.08	27.20	34.25	27.03	27.17
35.00	27.01	27.24	34.25	27.08	27.19	34.00	27.03	27.17
34.75	27.01	27.26	34.00	27.05	27.20	33.75	27.03	27.17
34.50	27.01	27.26	33.75	27.04	27.21	33.50	27.03	27.17
34.25	27.01	27.26	33.50	27.04	27.20	33.25	27.01	27.17
34.00	27.01	27.25	33.25	27.04	27.18	33.00	27.01	27.18
33.75	27.01	27.23	33.00	27.04	27.17	32.75	27.01	27.18
33.50	27.01	27.22	32.75	27.04	27.17	32.50	27.01	27.18
33.25	27.01	27.22	32.50	27.04	27.18	32.25	27.01	27.19
33.00	27.01	27.22	32.25	27.04	27.18	32.00	27.02	27.22
32.75	27.01	27.22	32.00	27.04	27.19	31.75	27.02	27.22
32.50	26.99	27.22	31.75	27.03	27.19	31.50	27.02	27.23
32.25	27.00	27.22	31.50	27.02	27.19	31.25	27.00	27.23
32.00	26.98	27.22	31.25	27.01	27.18	31.00	26.97	27.21
31.75	26.98	27.23	31.00	27.01	27.18	30.75	26.94	27.18
31.50	26.98	27.21	30.75	27.01	27.18	30.50	26.91	27.15
31.25	26.97	27.23	30.50	27.01	27.18	30.25	26.92	27.13
31.00	26.97	27.23	30.25	27.01	27.18	30.00	26.92	27.12
30.75	26.97	27.22	30.00	27.01	27.18	29.75	26.92	27.12
30.50	26.97	27.19	29.75	27.01	27.18	29.50	26.92	27.13
30.25	26.97	27.19	29.50	27.00	27.18	29.25	26.96	27.13
30.00	26.96	27.19	29.25	27.00	27.16	29.00	26.98	27.13
29.75	26.96	27.20	29.00	27.00	27.15	28.75	26.97	27.12
29.50	26.97	27.20	28.75	26.97	27.15	28.50	26.95	27.11
29.25	26.95	27.19	28.50	26.96	27.15	28.25	26.95	27.12
29.00	26.94	27.21	28.25	26.94	27.15	28.00	26.94	27.12

28.75	26.92	27.20	28.00	26.93	27.15	27.75	26.94	27.11
28.50	26.91	27.19	27.75	26.93	27.17	27.50	26.94	27.09
28.25	26.90	27.17	27.50	26.93	27.16	27.25	26.92	27.09
28.00	26.88	27.16	27.25	26.93	27.14	27.00	26.88	27.09
27.75	26.87	27.15	27.00	26.93	27.13	26.75	26.88	27.08
27.50	26.86	27.15	26.75	26.93	27.13	26.50	26.87	27.07
27.25	26.85	27.15	26.50	26.93	27.13	26.25	26.86	27.07
27.00	26.84	27.16	26.25	26.90	27.12	26.00	26.85	27.06
26.75	26.82	27.17	26.00	26.90	27.09	25.75	26.83	27.04
26.50	26.82	27.18	25.75	26.89	27.08	25.50	26.82	27.04
26.25	26.82	27.19	25.50	26.85	27.08	25.25	26.80	27.02
26.00	26.81	27.19	25.25	26.81	27.08	25.00	26.78	27.02
25.75	26.80	27.17	25.00	26.82	27.07	24.75	26.76	27.02
25.50	26.79	27.13	24.75	26.83	27.07	24.50	26.74	27.02
25.25	26.77	27.10	24.50	26.82	27.08	24.25	26.71	27.02
25.00	26.73	27.06	24.25	26.75	27.08	24.00	26.70	27.02
24.75	26.69	27.03	24.00	26.67	27.08	23.75	26.67	27.02
24.50	26.68	27.04	23.75	26.64	27.02	23.50	26.64	27.03
24.25	26.68	27.05	23.50	26.70	26.99	23.25	26.61	27.00
24.00	26.65	27.04	23.25	26.66	26.97	23.00	26.54	26.99
23.75	26.63	26.97	23.00	26.62	26.95	22.75	26.47	26.97
23.50	26.60	26.92	22.75	26.56	26.89	22.50	26.39	26.95
23.25	26.57	26.88	22.50	26.51	26.84	22.25	26.32	26.91
23.00	26.53	26.88	22.25	26.44	26.86	22.00	26.24	26.91
22.75	26.46	26.88	22.00	26.34	26.78	21.75	26.16	26.87
22.50	26.42	26.85	21.75	26.26	26.69	21.50	26.01	26.80
22.25	26.37	26.85	21.50	26.16	26.65	21.25	25.90	26.63
22.00	26.30	26.86	21.25	26.09	26.60	21.00	25.68	26.49
21.75	26.18	26.87	21.00	25.98	26.53	20.75	25.54	26.36
21.50	26.06	26.82	20.75	25.88	26.45	20.50	25.38	26.26
21.25	25.93	26.75	20.50	25.75	26.38	20.25	25.01	26.12
21.00	25.73	26.65	20.25	25.45	26.26	20.00	24.47	26.00
20.75	25.59	26.49	20.00	25.04	26.11	19.75	24.18	25.86
20.50	25.34	26.31	19.75	24.69	25.94	19.50	23.90	25.59
20.25	24.91	26.13	19.50	24.16	25.81	19.25	23.29	25.29
20.00	24.42	25.95	19.25	23.29	25.47	19.00	22.48	24.84
19.75	23.91	25.87	19.00	23.01	25.02	18.75	21.48	24.01
19.50	23.30	25.78	18.75	22.36	24.73	18.50	20.08	23.81
19.25	22.25	25.25	18.50	20.51	24.34	18.25	19.16	23.74
19.00	21.89	24.68	18.25	19.50	23.66	18.00	17.55	23.56
18.75	19.97	24.18	18.00	18.56	23.17	17.75	17.28	22.34
18.50	19.28	23.83	17.75	18.37	23.06	17.50	17.29	21.80
18.25	18.66	23.26	17.50	17.88	22.80	17.25	17.21	21.34
18.00	17.19	22.33	17.25	17.49	22.10	17.00	16.63	20.48
17.75	17.20	21.83	17.00	17.14	21.63	16.75	16.14	20.12
17.50	17.23	21.44	16.75	17.06	20.76	16.50	16.07	19.76
17.25	17.24	20.92	16.50	16.36	20.39	16.25	15.96	19.34
17.00	17.00	20.59	16.25	16.10	20.22	16.00	15.32	18.80
16.75	16.85	20.21	16.00	16.01	20.04	15.75	15.26	18.32

16.50	16.87	19.21	15.75	15.61	19.37	15.50	15.22	17.99
16.25	16.68	18.43	15.50	15.43	18.45	15.25	15.19	17.46
16.00	16.58	18.46	15.25	15.32	18.01	15.00	15.11	17.07
15.75	16.53	18.77	15.00	15.21	17.70	14.75	14.92	16.70
15.50	16.49	19.06	14.75	15.09	17.58	14.50	14.82	16.49
15.25	16.44	18.66	14.50	14.97	17.47	14.25	14.72	16.36
15.00	16.39	18.12	14.25	14.85	17.35	14.00	14.64	16.24
14.75	16.36	17.68	14.00	14.72	17.19	13.75	14.50	16.12
14.50	16.32	17.67	13.75	14.60	17.32	13.50	14.34	16.00
14.25	16.28	17.60	13.50	14.57	17.48	13.25	14.20	15.98
14.00	16.35	17.48	13.25	14.75	17.58	13.00	14.10	15.98
13.75	16.19	17.36	13.00	14.90	17.59	12.75	14.04	15.94
13.50	16.01	17.16	12.75	14.99	17.59	12.50	13.97	16.25
13.25	15.92	16.85	12.50	14.79	17.56	12.25	13.97	16.38
13.00	15.47	16.73	12.25	14.60	17.46	12.00	14.07	16.29
12.75	15.54	16.65	12.00	14.56	17.34	11.75	14.15	16.19
12.50	14.92	16.49	11.75	14.35	17.23	11.50	14.11	16.08
12.25	14.78	16.38	11.50	14.02	17.15	11.25	13.98	15.93
12.00	14.70	16.29	11.25	13.89	17.07	11.00	13.78	15.83
11.75	14.63	16.19	11.00	13.67	17.00	10.75	13.49	15.76
11.50	14.60	15.97	10.75	13.50	16.88	10.50	13.40	15.61
11.25	14.49	15.93	10.50	13.46	16.75	10.25	13.33	15.45
11.00	14.24	16.09	10.25	13.46	16.58	10.00	13.21	15.28
10.75	14.04	16.13	10.00	13.45	16.17	9.75	13.10	15.12
10.50	13.90	16.15	9.75	13.25	15.60	9.50	12.99	15.00
10.25	13.70	16.16	9.50	13.07	15.47	9.25	12.72	14.90
10.00	13.56	16.13	9.25	12.92	15.37	9.00	12.00	14.80
9.75	13.46	16.09	9.00	12.77	15.27	8.75	11.95	14.62
9.50	13.36	16.05	8.75	12.62	15.17	8.50	11.88	14.52
9.25	13.02	15.88	8.50	12.47	15.07	8.25	11.76	14.42
9.00	12.92	15.57	8.25	12.25	14.98	8.00	11.63	14.32
8.75	12.65	15.29	8.00	12.10	14.91	7.75	11.51	14.22
8.50	12.28	15.16	7.75	11.65	14.85	7.50	11.38	14.11
8.25	12.06	15.03	7.50	11.49	14.77	7.25	11.25	14.03
8.00	11.86	14.90	7.25	11.33	14.60	7.00	11.12	13.95
7.75	11.65	14.81	7.00	11.12	14.40	6.75	11.00	13.88
7.50	11.46	14.71	6.75	10.78	14.21	6.50	10.87	13.79
7.25	11.46	14.52	6.50	10.56	14.03	6.25	10.69	13.61
7.00	11.52	14.26	6.25	10.51	13.84	6.00	10.49	13.36
6.75	11.15	14.01	6.00	10.48	13.67	5.75	10.28	13.00
6.50	10.27	13.85	5.75	10.44	13.48	5.50	10.10	12.73
6.25	10.12	13.68	5.50	10.38	13.35	5.25	10.02	12.53
6.00	10.12	13.55	5.25	10.30	13.26	5.00	9.85	12.32
5.75	10.10	13.37	5.00	10.06	13.17	4.75	9.63	12.17
5.50	10.09	13.16	4.75	9.77	13.00	4.50	9.39	12.08
5.25	10.08	13.14	4.50	9.56	12.75	4.25	8.89	12.00
5.00	10.00	12.96	4.25	9.53	12.29	4.00	8.71	11.91
4.75	9.84	12.67	4.00	9.37	11.64	3.75	8.61	11.82
4.50	9.68	12.57	3.75	9.06	11.35	3.50	8.26	11.73

4.25	9.42	12.52	3.50	8.61	11.24	3.25	7.98	11.38
4.00	8.72	12.48	3.25	8.35	11.05	3.00	7.82	11.12
3.75	8.50	12.35	3.00	8.10	11.07	2.75	7.77	10.87
3.50	8.49	12.18	2.75	7.86	11.02	2.50	7.51	10.39
3.25	8.20	11.97	2.50	8.35	10.84	2.25	7.16	10.11
3.00	8.03	10.97	2.25	8.33	10.66	2.00	6.84	9.89
2.75	7.92	10.82	2.00	8.11	10.49	1.75	6.76	9.73
2.50	7.64	10.73	1.75	7.83	10.33	1.50	6.56	9.57
2.25	7.41	10.66	1.50	7.56	10.14	1.25	6.26	9.40
2.00	7.24	10.59	1.25	7.33	9.94	1.00	6.13	9.23
1.75	7.02	10.44	1.00	7.12	9.79	0.75	5.99	8.97
1.50	6.99	10.19	0.75	6.90	9.62	0.50	5.86	8.83
1.25	6.98	9.62	0.50	6.68	9.47	0.25	5.56	8.69
1.00	6.87	9.43	0.25	6.43	9.41	0.00	5.19	8.55
0.75	6.71	9.19	0.00	6.11	9.29	-0.25	4.96	8.35
0.50	6.42	9.04	-0.25	5.78	9.16	-0.50	4.75	8.00
0.25	6.22	8.89	-0.50	5.45	9.04	-0.75	4.58	7.44
0.00	6.03	8.56	-0.75	5.14	8.91	-1.00	4.39	7.08
-0.25	5.83	8.12	-1.00	4.83	8.79	-1.25	4.14	6.83
-0.50	5.64	7.70	-1.25	4.54	8.62	-1.50	3.90	6.60
-0.75	5.02	7.41	-1.50	4.29	8.43	-1.75	3.76	6.36
-1.00	4.83	7.30	-1.75	4.08	8.24	-2.00	3.58	6.11
-1.25	4.66	7.21	-2.00	3.87	8.05	-2.25	3.45	5.97
-1.50	4.49	7.11	-2.25	3.76	7.84	-2.50	3.19	5.83
-1.75	4.33	7.00	-2.50	3.76	7.52	-2.75	2.97	5.68
-2.00	4.17	6.81	-2.75	3.76	7.17	-3.00	2.84	5.47
-2.25	4.02	6.60	-3.00	3.04	6.74	-3.25	2.55	5.24
-2.50	3.65	6.40	-3.25	2.65	6.28	-3.50	2.25	5.00
-2.75	3.31	6.19	-3.50	2.48	5.82	-3.75	1.95	4.80
-3.00	2.99	6.02	-3.75	2.32	5.34	-4.00	1.64	4.64
-3.25	2.65	5.94	-4.00	2.17	4.87	-4.25	1.28	4.48
-3.50	2.35	5.87	-4.25	1.76	4.71	-4.50	1.09	4.31
-3.75	2.13	5.79	-4.50	1.48	4.55	-4.75	0.91	3.91
-4.00	1.91	5.66	-4.75	1.31	4.38	-5.00	0.73	3.33
-4.25	1.69	5.51	-5.00	1.14	4.15	-5.25	0.58	3.04
-4.50	1.47	5.35	-5.25	0.97	3.87	-5.50	0.56	2.96
-4.75	1.26	5.19	-5.50	0.81	3.58	-5.75	0.46	2.70
-5.00	1.04	5.04	-5.75	0.73	3.36	-6.00	0.32	2.58
-5.25	0.82	4.83	-6.00	0.67	3.16	-6.25	0.02	2.43
-5.50	0.60	4.68	-6.25	0.44	2.95	-6.50	-0.29	2.22
-5.75	0.38	5.02	-6.50	0.27	2.73	-6.75	-0.33	2.00
-6.00	0.16	5.31	-6.75	0.06	2.49	-7.00	-0.62	1.78
-6.25	-0.10	4.81	-7.00	-0.12	2.25	-7.25	-1.09	1.49
-6.50	-0.44	3.00	-7.25	-0.30	1.94	-7.50	-1.77	1.06
-6.75	-0.76	4.29	-7.50	-0.51	1.51	-7.75	-2.10	0.64
-7.00	-1.01	1.72	-7.75	-1.07	1.36	-8.00	-2.15	0.20
-7.25	-1.32	1.40	-8.00	-1.65	1.32	-8.25	-2.48	-0.33
-7.50	-1.59	1.12	-8.25	-1.83	0.47	-8.50	-2.62	-0.67
-7.75	-1.83	0.93	-8.50	-1.99	0.25	-8.75	-2.73	-0.91

-8.00	-2.06	0.72	-8.75	-2.17	0.09	-9.00	-2.96	-1.14
-8.25	-2.28	0.16	-9.00	-2.33	-0.45	-9.25	-3.52	-1.23
-8.50	-2.51	-0.04	-9.25	-2.50	-0.83	-9.50	-3.70	-1.56
-8.75	-2.75	-0.18	-9.50	-2.82	-0.86	-9.75	-3.98	-1.74
-9.00	-2.96	-0.32	-9.75	-3.25	-1.05	-10.00	-4.27	-1.91
-9.25	-3.19	-0.45	-10.00	-3.72	-1.25	-10.25	-4.58	-2.09
-9.50	-4.29	-0.61	-10.25	-4.18	-1.45	-10.50	-4.82	-2.26
-9.75	-4.43	-0.77	-10.50	-4.46	-1.67	-10.75	-5.38	-2.47
-10.00	-4.54	-0.93	-10.75	-4.72	-2.33	-11.00	-5.67	-3.28
-10.25	-4.65	-1.09	-11.00	-4.96	-2.72	-11.25	-5.99	-3.76
-10.50	-4.75	-1.29	-11.25	-5.28	-2.90	-11.50	-6.32	-4.15
-10.75	-4.81	-1.64	-11.50	-5.57	-3.16	-11.75	-6.76	-4.51
-11.00	-4.89	-2.02	-11.75	-5.85	-3.96	-12.00	-7.10	-5.04
-11.25	-5.12	-2.51	-12.00	-6.29	-4.48	-12.25	-7.19	-5.57
-11.50	-5.39	-3.43	-12.25	-6.56	-4.91	-12.50	-8.17	-6.11
-11.75	-5.78	-3.81	-12.50	-6.80	-5.24	-12.75	-8.44	-6.62
-12.00	-6.18	-4.08	-12.75	-7.44	-5.48	-13.00	-8.70	-6.80
-12.25	-6.62	-4.21	-13.00	-7.66	-5.74	-13.25	-8.85	-6.95
-12.50	-7.03	-4.41	-13.25	-8.45	-5.99	-13.50	-8.97	-7.09
-12.75	-7.34	-4.61	-13.50	-8.87	-6.28	-13.75	-9.54	-7.60
-13.00	-7.66	-5.05	-13.75	-9.26	-6.68	-14.00	-9.93	-8.26
-13.25	-8.01	-5.91	-14.00	-9.57	-6.94	-14.25	-10.30	-8.66
-13.50	-8.47	-6.61	-14.25	-9.75	-7.14	-14.50	-10.68	-8.87
-13.75	-8.73	-6.89	-14.50	-9.93	-7.48	-14.75	-11.00	-8.98
-14.00	-8.98	-7.30	-14.75	-10.11	-7.83	-15.00	-11.31	-9.11
-14.25	-9.24	-7.69	-15.00	-10.41	-8.27	-15.25	-11.63	-9.78
-14.50	-9.84	-7.99	-15.25	-11.02	-8.78	-15.50	-11.95	-10.31
-14.75	-10.36	-8.14	-15.50	-11.45	-9.74	-15.75	-12.25	-10.71
-15.00	-10.68	-8.46	-15.75	-11.65	-9.62	-16.00	-12.67	-10.56
-15.25	-10.95	-8.68	-16.00	-11.76	-9.94	-16.25	-12.91	-10.39
-15.50	-11.38	-8.92	-16.25	-12.10	-11.02	-16.50	-13.47	-10.37
-15.75	-11.71	-9.24	-16.50	-12.44	-10.56	-16.75	-13.69	-10.67
-16.00	-12.04	-9.64	-16.75	-13.15	-11.27	-17.00	-13.89	-11.68
-16.25	-12.36	-9.75	-17.00	-13.33	-11.39	-17.25	-14.14	-12.74
-16.50	-12.68	-9.86	-17.25	-13.69	-11.53	-17.50	-14.41	-13.03
-16.75	-13.12	-9.97	-17.50	-14.15	-11.85	-17.75	-14.72	-13.32
-17.00	-13.33	-10.08	-17.75	-14.41	-12.20	-18.00	-15.04	-13.58
-17.25	-13.54	-10.24	-18.00	-14.67	-12.66	-18.25	-15.43	-13.98
-17.50	-13.78	-10.68	-18.25	-14.99	-12.98	-18.50	-15.66	-14.06
-17.75	-14.13	-11.20	-18.50	-15.43	-13.58	-18.75	-16.02	-14.13
-18.00	-14.57	-12.31	-18.75	-15.76	-14.14	-19.00	-16.24	-14.20
-18.25	-15.04	-13.64	-19.00	-16.03	-14.36	-19.25	-16.46	-14.28
-18.50	-15.38	-13.94	-19.25	-16.32	-14.84	-19.50	-16.75	-15.26
-18.75	-15.66	-14.27	-19.50	-16.58	-15.09	-19.75	-17.04	-15.79
-19.00	-15.95	-14.52	-19.75	-16.82	-15.36	-20.00	-17.33	-15.95
-19.25	-16.25	-14.81	-20.00	-17.21	-15.65	-20.25	-17.63	-16.17
-19.50	-16.47	-15.27	-20.25	-17.42	-16.23	-20.50	-17.93	-16.54
-19.75	-16.67	-15.72	-20.50	-17.74	-16.64	-20.75	-18.25	-16.98
-20.00	-17.07	-16.14	-20.75	-18.12	-16.81	-21.00	-18.66	-17.28

-20.25	-17.39	-16.44
-20.50	-17.90	-16.72
-20.75	-18.38	-16.94
-21.00	-18.94	-17.04
-21.25	N/A	-17.16
-21.50	N/A	-17.29
-21.75	N/A	-17.54
-22.00	N/A	-17.80
-22.25	N/A	-18.07
-22.50	N/A	-18.32
-22.75	N/A	-18.68

-21.00	-18.55	-17.04
-21.25	-19.03	-17.18
-21.50	N/A	-17.47
-21.75	N/A	-17.78
-22.00	N/A	-18.12
-22.25	N/A	-18.58

-21.25	-18.90	-17.63
-21.50	N/A	-17.82
-21.75	N/A	-18.00
-22.00	N/A	-18.31
-22.25	N/A	-18.69

Table F2. High-Water statistics for *H*/*P* ≈ 0.186 (*Q* ≈ 116 l/s) and with *p* = 0.46 *P*, *p* = 0.62 *P*, and *p* = 0.77 *P* (units in inches).

High-Water Statistics for H/P ≈ 0.186 and *p* = 0.46 *P*			High-Water Statistics for H/P ≈ 0.186 and *p* = 0.62 *P*			High-Water Statistics for H/P ≈ 0.186 and *p* = 0.77 *P*		
X	Y Min.	Y Max.	X	Y Min.	Y Max.	X	Y Min.	Y Max.
63.25	27.11	27.24	63.00	27.23	27.23	63.00	27.26	27.33
63.00	27.14	27.27	62.75	27.05	27.15	62.75	27.26	27.32
62.75	27.14	27.26	62.50	27.05	27.14	62.50	27.26	27.31
62.50	27.13	27.26	62.25	27.04	27.13	62.25	27.24	27.30
62.25	27.13	27.25	62.00	27.02	27.12	62.00	27.22	27.29
62.00	27.11	27.24	61.75	27.00	27.12	61.75	27.22	27.28
61.75	27.11	27.22	61.50	27.00	27.11	61.50	27.22	27.27
61.50	27.11	27.22	61.25	27.00	27.10	61.25	27.20	27.26
61.25	27.11	27.22	61.00	27.00	27.10	61.00	27.19	27.25
61.00	27.10	27.22	60.75	26.99	27.09	60.75	27.18	27.24
60.75	27.10	27.19	60.50	26.98	27.08	60.50	27.17	27.23
60.50	27.08	27.19	60.25	26.98	27.08	60.25	27.16	27.22
60.25	27.07	27.18	60.00	26.97	27.07	60.00	27.15	27.21
60.00	27.07	27.18	59.75	26.96	27.06	59.75	27.14	27.20
59.75	27.06	27.17	59.50	26.96	27.05	59.50	27.13	27.19
59.50	27.04	27.17	59.25	26.96	27.05	59.25	27.11	27.18
59.25	27.03	27.17	59.00	26.94	27.04	59.00	27.10	27.17
59.00	27.03	27.15	58.75	26.93	27.03	58.75	27.09	27.16
58.75	27.02	27.15	58.50	26.91	27.02	58.50	27.08	27.15
58.50	27.00	27.13	58.25	26.89	27.01	58.25	27.07	27.14
58.25	26.99	27.13	58.00	26.87	27.00	58.00	27.05	27.13
58.00	26.99	27.13	57.75	26.86	26.99	57.75	27.05	27.12
57.75	26.99	27.13	57.50	26.85	26.98	57.50	27.04	27.11
57.50	26.98	27.13	57.25	26.85	26.97	57.25	27.03	27.10
57.25	26.96	27.12	57.00	26.85	26.96	57.00	27.01	27.10
57.00	26.95	27.12	56.75	26.85	26.96	56.75	27.00	27.09
56.75	26.95	27.11	56.50	26.84	26.95	56.50	27.00	27.08
56.50	26.95	27.10	56.25	26.84	26.94	56.25	27.00	27.07
56.25	26.96	27.10	56.00	26.84	26.94	56.00	27.00	27.07
56.00	26.96	27.09	55.75	26.82	26.93	55.75	26.99	27.06
55.75	26.95	27.08	55.50	26.81	26.93	55.50	26.97	27.06
55.50	26.95	27.08	55.25	26.79	26.92	55.25	26.97	27.05
55.25	26.95	27.08	55.00	26.77	26.91	55.00	26.97	27.04
55.00	26.95	27.08	54.75	26.76	26.91	54.75	26.97	27.04
54.75	26.94	27.08	54.50	26.73	26.90	54.50	26.97	27.03
54.50	26.94	27.08	54.25	26.73	26.90	54.25	26.96	27.03
54.25	26.93	27.07	54.00	26.74	26.89	54.00	26.95	27.02
54.00	26.93	27.07	53.75	26.73	26.88	53.75	26.95	27.02
53.75	26.93	27.07	53.50	26.71	26.88	53.50	26.94	27.01
53.50	26.93	27.07	53.25	26.71	26.87	53.25	26.93	27.01
53.25	26.93	27.07	53.00	26.69	26.87	53.00	26.92	27.00
53.00	26.92	27.07	52.75	26.68	26.87	52.75	26.92	27.00

52.75	26.92	27.07	52.50	26.67	26.86	52.50	26.90	26.99
52.50	26.92	27.07	52.25	26.66	26.86	52.25	26.89	26.99
52.25	26.92	27.07	52.00	26.65	26.86	52.00	26.89	26.99
52.00	26.93	27.06	51.75	26.65	26.86	51.75	26.88	26.99
51.75	26.94	27.06	51.50	26.66	26.85	51.50	26.86	26.98
51.50	26.93	27.06	51.25	26.67	26.86	51.25	26.85	26.98
51.25	26.93	27.07	51.00	26.69	26.86	51.00	26.85	26.99
51.00	26.94	27.08	50.75	26.71	26.86	50.75	26.85	26.99
50.75	26.95	27.08	50.50	26.70	26.86	50.50	26.85	26.99
50.50	26.95	27.08	50.25	26.71	26.86	50.25	26.85	26.99
50.25	26.95	27.08	50.00	26.72	26.86	50.00	26.85	26.99
50.00	26.95	27.08	49.75	26.72	26.86	49.75	26.85	26.99
49.75	26.96	27.07	49.50	26.73	26.86	49.50	26.85	26.99
49.50	26.96	27.07	49.25	26.73	26.86	49.25	26.85	27.00
49.25	26.96	27.08	49.00	26.74	26.87	49.00	26.85	27.00
49.00	26.96	27.09	48.75	26.73	26.87	48.75	26.85	27.00
48.75	26.96	27.10	48.50	26.73	26.87	48.50	26.86	27.00
48.50	26.96	27.10	48.25	26.73	26.88	48.25	26.87	27.00
48.25	26.96	27.10	48.00	26.73	26.88	48.00	26.87	27.00
48.00	26.96	27.10	47.75	26.74	26.89	47.75	26.87	27.00
47.75	26.96	27.10	47.50	26.74	26.89	47.50	26.87	27.01
47.50	26.96	27.11	47.25	26.75	26.89	47.25	26.88	27.01
47.25	26.96	27.12	47.00	26.74	26.90	47.00	26.89	27.01
47.00	26.96	27.13	46.75	26.73	26.91	46.75	26.89	27.01
46.75	26.95	27.13	46.50	26.74	26.91	46.50	26.91	27.01
46.50	26.95	27.13	46.25	26.74	26.92	46.25	26.91	27.02
46.25	26.95	27.13	46.00	26.75	26.93	46.00	26.91	27.02
46.00	26.95	27.13	45.75	26.75	26.94	45.75	26.92	27.03
45.75	26.95	27.13	45.50	26.75	26.94	45.50	26.93	27.03
45.50	26.95	27.13	45.25	26.75	26.95	45.25	26.93	27.04
45.25	26.95	27.12	45.00	26.78	26.96	45.00	26.93	27.04
45.00	26.95	27.14	44.75	26.78	26.97	44.75	26.93	27.05
44.75	26.95	27.14	44.50	26.79	26.97	44.50	26.93	27.05
44.50	26.95	27.14	44.25	26.79	26.98	44.25	26.93	27.06
44.25	26.95	27.15	44.00	26.80	26.99	44.00	26.93	27.06
44.00	26.95	27.15	43.75	26.81	27.00	43.75	26.92	27.07
43.75	26.95	27.15	43.50	26.81	27.00	43.50	26.92	27.07
43.50	26.95	27.17	43.25	26.83	27.01	43.25	26.92	27.08
43.25	26.96	27.18	43.00	26.85	27.02	43.00	26.92	27.08
43.00	26.98	27.18	42.75	26.87	27.03	42.75	26.94	27.09
42.75	26.99	27.19	42.50	26.88	27.04	42.50	26.95	27.09
42.50	27.01	27.21	42.25	26.88	27.04	42.25	26.95	27.10
42.25	27.02	27.22	42.00	26.89	27.05	42.00	26.95	27.10
42.00	27.02	27.23	41.75	26.89	27.06	41.75	26.95	27.11
41.75	27.02	27.25	41.50	26.90	27.06	41.50	26.94	27.11
41.50	27.01	27.25	41.25	26.87	27.07	41.25	26.96	27.12
41.25	27.01	27.27	41.00	26.86	27.08	41.00	26.96	27.12
41.00	27.01	27.28	40.75	26.87	27.08	40.75	26.96	27.13
40.75	27.01	27.28	40.50	26.91	27.09	40.50	26.96	27.14

40.50	27.01	27.28	40.25	26.95	27.10	40.25	26.95	27.14
40.25	27.01	27.28	40.00	26.99	27.10	40.00	26.95	27.15
40.00	27.01	27.28	39.75	27.01	27.11	39.75	26.95	27.15
39.75	27.02	27.26	39.50	26.99	27.11	39.50	26.97	27.16
39.50	27.03	27.24	39.25	26.99	27.11	39.25	26.97	27.16
39.25	27.04	27.24	39.00	26.99	27.11	39.00	26.99	27.17
39.00	27.04	27.24	38.75	26.99	27.11	38.75	26.99	27.17
38.75	27.04	27.23	38.50	26.98	27.11	38.50	27.01	27.17
38.50	27.04	27.23	38.25	26.99	27.11	38.25	27.02	27.17
38.25	27.03	27.21	38.00	27.01	27.11	38.00	27.03	27.18
38.00	27.03	27.21	37.75	27.01	27.12	37.75	27.05	27.18
37.75	27.03	27.21	37.50	27.00	27.12	37.50	27.05	27.18
37.50	27.03	27.21	37.25	27.01	27.12	37.25	27.07	27.18
37.25	27.03	27.21	37.00	27.00	27.12	37.00	27.07	27.18
37.00	27.03	27.22	36.75	27.00	27.12	36.75	27.07	27.18
36.75	27.03	27.22	36.50	26.99	27.12	36.50	27.07	27.18
36.50	27.05	27.22	36.25	27.00	27.12	36.25	27.09	27.18
36.25	27.06	27.22	36.00	26.99	27.12	36.00	27.10	27.18
36.00	27.06	27.22	35.75	26.99	27.13	35.75	27.09	27.18
35.75	27.06	27.22	35.50	27.00	27.12	35.50	27.09	27.18
35.50	27.06	27.19	35.25	26.99	27.12	35.25	27.10	27.18
35.25	27.06	27.18	35.00	26.99	27.12	35.00	27.11	27.18
35.00	27.05	27.18	34.75	27.00	27.12	34.75	27.10	27.17
34.75	27.05	27.18	34.50	27.01	27.12	34.50	27.08	27.17
34.50	27.05	27.18	34.25	27.01	27.12	34.25	27.07	27.17
34.25	27.05	27.17	34.00	27.02	27.12	34.00	27.05	27.16
34.00	27.05	27.18	33.75	27.02	27.12	33.75	27.04	27.16
33.75	27.05	27.17	33.50	27.03	27.12	33.50	27.04	27.16
33.50	27.05	27.17	33.25	27.04	27.12	33.25	27.04	27.15
33.25	27.05	27.17	33.00	27.04	27.11	33.00	27.05	27.14
33.00	27.04	27.17	32.75	27.03	27.11	32.75	27.06	27.14
32.75	27.01	27.17	32.50	27.02	27.11	32.50	27.07	27.14
32.50	27.01	27.17	32.25	27.03	27.11	32.25	27.07	27.13
32.25	27.02	27.17	32.00	27.03	27.10	32.00	27.07	27.13
32.00	27.02	27.16	31.75	27.03	27.10	31.75	27.08	27.12
31.75	27.02	27.15	31.50	27.01	27.10	31.50	27.07	27.12
31.50	27.01	27.15	31.25	27.00	27.09	31.25	27.07	27.12
31.25	27.01	27.14	31.00	27.00	27.09	31.00	27.05	27.11
31.00	27.01	27.14	30.75	26.99	27.09	30.75	27.04	27.10
30.75	27.01	27.14	30.50	26.98	27.09	30.50	27.04	27.10
30.50	27.01	27.13	30.25	27.00	27.09	30.25	27.04	27.09
30.25	27.00	27.12	30.00	27.01	27.08	30.00	27.04	27.09
30.00	27.00	27.14	29.75	27.01	27.09	29.75	27.03	27.09
29.75	26.98	27.15	29.50	27.00	27.08	29.50	27.02	27.08
29.50	26.98	27.15	29.25	27.00	27.08	29.25	27.01	27.07
29.25	26.93	27.15	29.00	26.99	27.07	29.00	27.00	27.07
29.00	26.89	27.15	28.75	26.99	27.07	28.75	27.00	27.07
28.75	26.91	27.14	28.50	26.98	27.06	28.50	27.00	27.06
28.50	26.92	27.14	28.25	26.96	27.06	28.25	27.00	27.06

28.25	26.92	27.14	28.00	26.93	27.06	28.00	27.00	27.05
28.00	26.90	27.14	27.75	26.90	27.05	27.75	26.99	27.05
27.75	26.88	27.13	27.50	26.87	27.04	27.50	26.98	27.05
27.50	26.88	27.13	27.25	26.84	27.03	27.25	26.96	27.04
27.25	26.90	27.11	27.00	26.83	27.03	27.00	26.95	27.04
27.00	26.89	27.11	26.75	26.84	27.02	26.75	26.95	27.04
26.75	26.88	27.11	26.50	26.84	27.01	26.50	26.96	27.04
26.50	26.87	27.11	26.25	26.85	27.00	26.25	26.96	27.04
26.25	26.87	27.13	26.00	26.86	27.00	26.00	26.95	27.03
26.00	26.86	27.15	25.75	26.86	26.99	25.75	26.93	27.02
25.75	26.83	27.17	25.50	26.83	26.98	25.50	26.91	27.02
25.50	26.82	27.14	25.25	26.80	26.96	25.25	26.90	27.02
25.25	26.80	27.13	25.00	26.77	26.95	25.00	26.90	27.01
25.00	26.78	27.09	24.75	26.77	26.94	24.75	26.90	27.00
24.75	26.76	27.05	24.50	26.80	26.94	24.50	26.89	26.98
24.50	26.74	27.02	24.25	26.82	26.93	24.25	26.89	26.96
24.25	26.74	27.00	24.00	26.82	26.92	24.00	26.88	26.94
24.00	26.73	26.99	23.75	26.76	26.89	23.75	26.85	26.93
23.75	26.70	26.96	23.50	26.70	26.87	23.50	26.82	26.91
23.50	26.66	26.95	23.25	26.67	26.84	23.25	26.75	26.88
23.25	26.64	26.95	23.00	26.65	26.81	23.00	26.68	26.83
23.00	26.59	26.95	22.75	26.57	26.78	22.75	26.61	26.78
22.75	26.53	26.89	22.50	26.48	26.73	22.50	26.57	26.72
22.50	26.48	26.86	22.25	26.39	26.68	22.25	26.52	26.65
22.25	26.42	26.85	22.00	26.31	26.63	22.00	26.42	26.57
22.00	26.35	26.82	21.75	26.25	26.56	21.75	26.30	26.49
21.75	26.27	26.78	21.50	26.10	26.47	21.50	26.15	26.40
21.50	26.17	26.72	21.25	25.98	26.38	21.25	26.00	26.29
21.25	26.07	26.65	21.00	25.77	26.27	21.00	25.85	26.11
21.00	25.90	26.63	20.75	25.70	26.17	20.75	25.71	26.00
20.75	25.38	26.54	20.50	25.51	26.07	20.50	25.50	25.86
20.50	25.21	26.57	20.25	25.31	25.92	20.25	25.40	25.70
20.25	24.72	26.52	20.00	25.05	25.66	20.00	25.20	25.50
20.00	23.88	26.18	19.75	24.56	25.35	19.75	24.91	25.27
19.75	23.51	25.93	19.50	24.27	25.05	19.50	24.65	25.05
19.50	22.82	25.71	19.25	23.74	24.71	19.25	24.39	24.81
19.25	22.00	25.40	19.00	23.49	24.44	19.00	24.07	24.55
19.00	21.37	25.05	18.75	23.17	24.12	18.75	23.47	24.01
18.75	21.22	24.59	18.50	22.63	23.52	18.50	22.49	23.28
18.50	19.96	24.08	18.25	21.30	22.84	18.25	21.36	22.53
18.25	19.60	23.61	18.00	20.70	22.30	18.00	20.73	22.02
18.00	19.24	23.29	17.75	19.97	21.71	17.75	20.12	21.39
17.75	18.26	23.03	17.50	18.36	21.04	17.50	19.51	20.73
17.50	17.01	22.60	17.25	17.32	20.21	17.25	18.60	20.00
17.25	16.55	22.12	17.00	16.75	19.53	17.00	17.73	19.43
17.00	16.60	21.77	16.75	16.59	19.01	16.75	16.93	18.85
16.75	16.24	21.02	16.50	16.36	18.26	16.50	16.39	18.22
16.50	16.04	20.78	16.25	16.06	17.86	16.25	16.22	17.60
16.25	15.90	19.98	16.00	15.70	17.48	16.00	15.75	16.92

16.00	15.82	19.62	15.75	15.60	17.18	15.75	15.65	16.41
15.75	15.73	19.24	15.50	15.58	16.78	15.50	15.46	16.11
15.50	15.49	18.78	15.25	15.47	16.39	15.25	15.12	15.94
15.25	15.44	18.26	15.00	15.20	16.16	15.00	15.03	15.85
15.00	15.33	17.72	14.75	15.22	16.00	14.75	14.95	15.82
14.75	15.25	17.38	14.50	15.23	15.91	14.50	14.88	15.78
14.50	15.33	17.14	14.25	15.24	15.82	14.25	14.83	15.71
14.25	15.09	16.97	14.00	14.97	15.78	14.00	14.77	15.62
14.00	14.79	16.93	13.75	14.77	15.73	13.75	14.63	15.51
13.75	14.79	16.89	13.50	14.65	15.65	13.50	14.56	15.43
13.50	15.08	16.87	13.25	14.63	15.57	13.25	14.48	15.35
13.25	14.97	16.87	13.00	14.53	15.49	13.00	14.37	15.28
13.00	14.86	16.88	12.75	14.40	15.42	12.75	14.11	15.19
12.75	14.53	16.90	12.50	14.23	15.32	12.50	14.06	15.10
12.50	14.40	16.91	12.25	13.68	15.21	12.25	14.01	14.99
12.25	14.33	16.93	12.00	13.46	15.11	12.00	13.98	14.85
12.00	14.26	16.85	11.75	13.43	15.00	11.75	13.96	14.73
11.75	14.19	16.76	11.50	13.48	14.89	11.50	13.82	14.62
11.50	14.12	16.66	11.25	13.54	14.77	11.25	13.63	14.51
11.25	14.01	16.52	11.00	13.59	14.65	11.00	13.49	14.44
11.00	13.87	16.37	10.75	13.62	14.55	10.75	13.38	14.36
10.75	13.73	16.22	10.50	13.62	14.44	10.50	13.33	14.26
10.50	13.60	16.02	10.25	13.54	14.33	10.25	13.30	14.14
10.25	13.47	15.79	10.00	13.36	14.20	10.00	13.19	14.03
10.00	13.38	15.64	9.75	13.21	14.07	9.75	13.07	13.92
9.75	13.50	15.21	9.50	13.15	13.93	9.50	12.96	13.79
9.50	13.64	15.18	9.25	12.98	13.82	9.25	12.42	13.61
9.25	13.58	15.24	9.00	12.84	13.71	9.00	11.97	13.36
9.00	13.38	15.37	8.75	12.68	13.59	8.75	11.81	13.16
8.75	13.25	15.46	8.50	12.38	13.45	8.50	11.66	13.01
8.50	13.12	15.02	8.25	11.79	13.24	8.25	11.52	12.89
8.25	12.99	14.94	8.00	11.78	13.07	8.00	11.43	12.77
8.00	12.42	14.73	7.75	11.73	12.89	7.75	11.34	12.64
7.75	11.94	14.16	7.50	11.54	12.73	7.50	11.28	12.50
7.50	11.85	14.04	7.25	11.35	12.60	7.25	11.11	12.34
7.25	11.84	13.91	7.00	11.17	12.46	7.00	10.94	12.17
7.00	11.65	13.78	6.75	10.99	12.31	6.75	10.77	11.99
6.75	11.43	13.76	6.50	10.81	12.15	6.50	10.61	11.79
6.50	11.30	13.64	6.25	10.63	11.98	6.25	10.53	11.60
6.25	11.21	13.59	6.00	10.45	11.81	6.00	10.42	11.37
6.00	11.15	13.34	5.75	10.31	11.60	5.75	10.26	11.17
5.75	10.99	13.26	5.50	10.18	11.40	5.50	10.10	10.93
5.50	10.78	13.22	5.25	9.94	11.21	5.25	9.83	10.69
5.25	10.57	12.99	5.00	9.76	11.02	5.00	9.54	10.46
5.00	10.37	12.64	4.75	9.67	10.81	4.75	9.33	10.28
4.75	10.17	12.52	4.50	9.62	10.57	4.50	9.18	10.10
4.50	9.90	12.33	4.25	9.39	10.35	4.25	8.91	9.92
4.25	9.44	12.07	4.00	9.12	10.17	4.00	8.63	9.73
4.00	9.23	11.81	3.75	8.83	9.99	3.75	8.52	9.51

3.75	9.03	11.49	3.50	8.58	9.77	3.50	8.69	9.76
3.50	8.85	11.35	3.25	8.33	9.57	3.25	8.55	9.64
3.25	8.69	11.21	3.00	8.08	9.37	3.00	8.51	9.51
3.00	8.53	11.02	2.75	7.85	9.17	2.75	8.39	9.39
2.75	8.34	10.98	2.50	7.62	8.96	2.50	8.14	9.26
2.50	8.12	10.90	2.25	7.38	8.71	2.25	7.90	9.15
2.25	7.83	10.79	2.00	7.16	8.50	2.00	7.66	9.01
2.00	7.59	10.67	1.75	6.88	8.24	1.75	7.43	8.88
1.75	7.36	10.45	1.50	6.64	7.99	1.50	7.29	8.77
1.50	7.13	10.19	1.25	6.41	7.73	1.25	7.18	8.66
1.25	6.88	9.89	1.00	6.16	7.50	1.00	7.07	8.52
1.00	6.61	9.54	0.75	5.65	7.27	0.75	6.91	8.34
0.75	6.43	9.18	0.50	5.38	7.09	0.50	6.69	8.10
0.50	6.20	8.78	0.25	5.15	6.83	0.25	6.47	7.87
0.25	6.14	8.53	0.00	4.94	6.61	0.00	6.25	7.62
0.00	6.05	8.34	-0.25	4.73	6.37	-0.25	6.04	7.35
-0.25	5.77	8.13	-0.50	4.52	6.14	-0.50	5.83	7.05
-0.50	5.45	8.01	-0.75	4.32	5.85	-0.75	5.68	6.73
-0.75	5.21	7.94	-1.00	3.80	5.60	-1.00	5.09	6.35
-1.00	4.57	7.86	-1.25	3.52	5.33	-1.25	4.73	6.07
-1.25	4.25	7.78	-1.50	3.24	5.05	-1.50	4.59	5.83
-1.50	3.93	7.65	-1.75	2.95	4.70	-1.75	4.45	5.60
-1.75	3.61	7.47	-2.00	2.68	4.50	-2.00	4.31	5.37
-2.00	3.29	7.28	-2.25	2.48	4.33	-2.25	4.16	5.13
-2.25	3.01	7.08	-2.50	2.32	4.13	-2.50	3.71	4.86
-2.50	2.67	6.85	-2.75	2.14	3.82	-2.75	3.47	4.60
-2.75	2.58	6.49	-3.00	1.90	3.55	-3.00	3.29	4.39
-3.00	2.40	5.18	-3.25	1.71	3.27	-3.25	3.13	4.12
-3.25	2.06	4.89	-3.50	1.56	3.02	-3.50	2.93	3.92
-3.50	1.76	4.82	-3.75	1.40	2.82	-3.75	2.73	3.70
-3.75	1.49	4.70	-4.00	1.25	2.59	-4.00	2.53	3.45
-4.00	1.23	4.48	-4.25	1.08	2.34	-4.25	2.32	3.22
-4.25	0.98	4.26	-4.50	0.82	2.07	-4.50	2.10	2.94
-4.50	0.78	4.09	-4.75	0.54	1.81	-4.75	1.89	2.69
-4.75	0.62	3.94	-5.00	0.20	1.53	-5.00	1.61	2.46
-5.00	0.45	3.79	-5.25	-0.35	1.27	-5.25	1.39	2.22
-5.25	0.28	2.89	-5.50	-0.49	0.94	-5.50	1.16	1.98
-5.50	0.09	2.71	-5.75	-0.64	0.66	-5.75	0.95	1.79
-5.75	-0.18	3.05	-6.00	-0.88	0.47	-6.00	0.74	1.60
-6.00	-0.61	2.02	-6.25	-1.12	0.29	-6.25	0.50	1.36
-6.25	-0.85	1.78	-6.50	-1.33	0.07	-6.50	0.24	1.07
-6.50	-1.00	1.56	-6.75	-1.53	-0.24	-6.75	-0.21	0.82
-6.75	-1.60	1.34	-7.00	-1.73	-0.52	-7.00	-0.66	0.52
-7.00	-1.84	1.12	-7.25	-1.92	-0.74	-7.25	-0.78	0.31
-7.25	-1.94	0.87	-7.50	-2.46	-1.01	-7.50	-0.87	0.03
-7.50	-2.12	0.63	-7.75	-2.60	-1.33	-7.75	-0.99	-0.24
-7.75	-2.55	0.38	-8.00	-2.73	-1.63	-8.00	-1.25	-0.54
-8.00	-2.89	0.14	-8.25	-3.09	-1.89	-8.25	-1.74	-0.85
-8.25	-3.14	-0.19	-8.50	-3.47	-2.13	-8.50	-2.01	-1.12

-8.50	-3.24	-0.81	-8.75	-3.77	-2.43	-8.75	-2.17	-1.40
-8.75	-3.34	-1.09	-9.00	-4.08	-2.68	-9.00	-2.42	-1.66
-9.00	-3.53	-1.37	-9.25	-4.39	-3.02	-9.25	-2.61	-1.94
-9.25	-3.97	-1.70	-9.50	-4.66	-3.33	-9.50	-2.84	-2.23
-9.50	-4.51	-2.24	-9.75	-5.01	-3.66	-9.75	-3.17	-2.54
-9.75	-5.05	-2.61	-10.00	-5.30	-4.04	-10.00	-3.53	-2.84
-10.00	-5.29	-2.86	-10.25	-5.54	-4.44	-10.25	-3.88	-3.21
-10.25	-5.39	-3.04	-10.50	-5.77	-4.78	-10.50	-4.22	-3.52
-10.50	-5.52	-3.85	-10.75	-6.55	-5.10	-10.75	-4.55	-3.88
-10.75	-5.78	-4.02	-11.00	-6.74	-5.41	-11.00	-5.01	-4.23
-11.00	-6.10	-4.16	-11.25	-6.95	-5.73	-11.25	-5.54	-4.54
-11.25	-6.41	-4.33	-11.50	-7.12	-6.06	-11.50	-6.03	-4.83
-11.50	-6.72	-4.64	-11.75	-7.31	-6.42	-11.75	-6.06	-5.12
-11.75	-7.03	-5.71	-12.00	-7.78	-6.76	-12.00	-6.04	-5.42
-12.00	-7.32	-5.95	-12.25	-8.20	-7.11	-12.25	-6.48	-5.77
-12.25	-7.61	-6.15	-12.50	-8.57	-7.41	-12.50	-6.92	-6.07
-12.50	-8.15	-6.46	-12.75	-8.94	-7.74	-12.75	-7.35	-6.42
-12.75	-8.77	-6.90	-13.00	-9.30	-8.06	-13.00	-7.64	-6.79
-13.00	-9.04	-7.17	-13.25	-9.72	-8.38	-13.25	-7.87	-7.14
-13.25	-9.30	-7.86	-13.50	-10.06	-8.69	-13.50	-8.20	-7.52
-13.50	-9.56	-8.27	-13.75	-10.38	-9.08	-13.75	-8.53	-7.91
-13.75	-9.82	-8.67	-14.00	-10.48	-9.34	-14.00	-8.86	-8.32
-14.00	-10.08	-8.93	-14.25	-10.91	-9.78	-14.25	-9.24	-8.70
-14.25	-10.45	-9.25	-14.50	-11.53	-10.17	-14.50	-9.64	-9.09
-14.50	-10.96	-9.58	-14.75	-11.62	-10.53	-14.75	-10.12	-9.48
-14.75	-11.20	-9.78	-15.00	-12.32	-10.84	-15.00	-10.39	-9.87
-15.00	-11.45	-9.96	-15.25	-12.63	-11.29	-15.25	-10.67	-10.22
-15.25	-11.92	-10.29	-15.50	-12.84	-11.71	-15.50	-10.96	-10.57
-15.50	-12.20	-10.70	-15.75	-13.05	-12.13	-15.75	-11.35	-10.91
-15.75	-12.46	-10.93	-16.00	-13.40	-12.48	-16.00	-11.75	-11.26
-16.00	-12.80	-11.15	-16.25	-13.61	-12.82	-16.25	-12.15	-11.60
-16.25	-13.38	-11.43	-16.50	-14.01	-13.09	-16.50	-12.45	-11.95
-16.50	-13.66	-11.87	-16.75	-14.27	-13.52	-16.75	-12.91	-12.27
-16.75	-13.93	-12.58	-17.00	-14.53	-13.82	-17.00	-13.27	-12.58
-17.00	-14.19	-12.73	-17.25	-14.78	-14.10	-17.25	-13.53	-12.88
-17.25	-14.45	-13.15	-17.50	-15.19	-14.44	-17.50	-13.75	-13.17
-17.50	-14.72	-13.41	-17.75	-15.44	-14.73	-17.75	-13.97	-13.45
-17.75	-14.98	-13.67	-18.00	-15.66	-14.98	-18.00	-14.22	-13.77
-18.00	-15.47	-13.92	-18.25	-15.95	-15.37	-18.25	-14.66	-14.14
-18.25	-15.84	-14.18	-18.50	-16.31	-15.80	-18.50	-15.13	-14.50
-18.50	-16.12	-14.45	-18.75	-16.82	-16.15	-18.75	-15.35	-14.83
-18.75	-16.29	-14.73	-19.00	-17.08	-16.50	-19.00	-15.57	-15.11
-19.00	-16.55	-15.00	-19.25	-17.38	-16.81	-19.25	-15.80	-15.38
-19.25	-16.86	-15.28	-19.50	-17.63	-17.12	-19.50	-16.08	-15.66
-19.50	-17.16	-15.58	-19.75	-17.91	-17.43	-19.75	-16.43	-15.94
-19.75	-17.38	-15.96	-20.00	-18.16	-17.73	-20.00	-16.68	-16.21
-20.00	-17.67	-16.34	-20.25	-18.56	-18.07	-20.25	-16.97	-16.51
-20.25	-18.03	-16.64	-20.50	-18.85	-18.39	-20.50	-17.25	-16.81
-20.50	-18.46	-16.88	-20.75	-18.97	-18.52	-20.75	-17.76	-17.15

-20.75	-18.64	-17.11	-21.00	N/A	-18.67	-21.00	-18.13	-17.43
-21.00	-18.85	-17.41	-21.25	N/A	0.00	-21.25	0.00	-17.71
-21.25	N/A	-17.75	-21.50	N/A	0.00	-21.50	0.00	-17.80
-21.50	N/A	-18.31	-21.75	N/A	0.00	-21.75	0.00	0.00
-21.75	N/A	-18.85						

Table F3. High-Water statistics for $H/P \approx 0.186$ ($Q \approx 116$ l/s) and with $p = 0.92\ P$ (units in inches).

High-Water Statistics for H/P ≈ 0.186 and *p* = 0.92 *P*		
X	Y Min.	Y Max.
63.25	27.26	27.26
63.00	27.22	27.35
62.75	27.21	27.36
62.50	27.20	27.36
62.25	27.19	27.33
62.00	27.18	27.33
61.75	27.18	27.33
61.50	27.17	27.30
61.25	27.16	27.30
61.00	27.16	27.29
60.75	27.15	27.27
60.50	27.14	27.27
60.25	27.13	27.27
60.00	27.13	27.26
59.75	27.13	27.26
59.50	27.11	27.24
59.25	27.10	27.24
59.00	27.10	27.23
58.75	27.09	27.23
58.50	27.08	27.22
58.25	27.07	27.21
58.00	27.07	27.21
57.75	27.06	27.20
57.50	27.06	27.20
57.25	27.04	27.18
57.00	27.04	27.18
56.75	27.03	27.17
56.50	27.02	27.16
56.25	27.02	27.15
56.00	27.01	27.15
55.75	27.00	27.14
55.50	26.99	27.13
55.25	26.98	27.12
55.00	26.96	27.12
54.75	26.96	27.11

54.50	26.96	27.11
54.25	26.96	27.09
54.00	26.95	27.09
53.75	26.93	27.08
53.50	26.93	27.08
53.25	26.92	27.07
53.00	26.91	27.06
52.75	26.90	27.06
52.50	26.90	27.05
52.25	26.90	27.04
52.00	26.90	27.04
51.75	26.90	27.04
51.50	26.90	27.04
51.25	26.90	27.04
51.00	26.90	27.04
50.75	26.90	27.02
50.50	26.91	27.02
50.25	26.92	27.02
50.00	26.92	27.01
49.75	26.92	27.01
49.50	26.93	27.01
49.25	26.93	27.02
49.00	26.93	27.02
48.75	26.93	27.02
48.50	26.94	27.02
48.25	26.94	27.02
48.00	26.94	27.02
47.75	26.94	27.02
47.50	26.95	27.03
47.25	26.95	27.03
47.00	26.95	27.03
46.75	26.95	27.04
46.50	26.94	27.05
46.25	26.93	27.06
46.00	26.94	27.07
45.75	26.95	27.07
45.50	26.95	27.08
45.25	26.95	27.09
45.00	26.96	27.10
44.75	26.96	27.10
44.50	26.96	27.10
44.25	26.96	27.10
44.00	26.97	27.10
43.75	26.97	27.11
43.50	26.97	27.13
43.25	26.98	27.13
43.00	26.98	27.13
42.75	26.98	27.14
42.50	26.98	27.16

42.25	26.98	27.16
42.00	26.99	27.16
41.75	27.01	27.16
41.50	27.01	27.16
41.25	27.01	27.17
41.00	27.03	27.18
40.75	27.03	27.18
40.50	27.03	27.19
40.25	27.03	27.20
40.00	27.03	27.20
39.75	27.04	27.21
39.50	27.05	27.21
39.25	27.06	27.22
39.00	27.07	27.22
38.75	27.09	27.22
38.50	27.09	27.22
38.25	27.09	27.23
38.00	27.09	27.23
37.75	27.09	27.23
37.50	27.09	27.24
37.25	27.10	27.24
37.00	27.10	27.24
36.75	27.10	27.25
36.50	27.10	27.25
36.25	27.10	27.25
36.00	27.10	27.25
35.75	27.10	27.25
35.50	27.10	27.24
35.25	27.09	27.22
35.00	27.09	27.22
34.75	27.09	27.22
34.50	27.09	27.21
34.25	27.09	27.20
34.00	27.09	27.20
33.75	27.08	27.20
33.50	27.05	27.20
33.25	27.03	27.20
33.00	27.05	27.20
32.75	27.06	27.19
32.50	27.08	27.19
32.25	27.09	27.19
32.00	27.10	27.17
31.75	27.09	27.17
31.50	27.08	27.17
31.25	27.08	27.17
31.00	27.07	27.17
30.75	27.07	27.17
30.50	27.07	27.17
30.25	27.05	27.17

30.00	27.04	27.18
29.75	27.04	27.15
29.50	27.04	27.13
29.25	27.02	27.12
29.00	27.01	27.12
28.75	26.98	27.12
28.50	26.98	27.13
28.25	26.98	27.14
28.00	26.98	27.18
27.75	26.98	27.22
27.50	26.97	27.22
27.25	26.97	27.22
27.00	26.95	27.20
26.75	26.92	27.19
26.50	26.92	27.17
26.25	26.93	27.13
26.00	26.90	27.07
25.75	26.90	27.04
25.50	26.90	27.03
25.25	26.88	27.03
25.00	26.86	27.02
24.75	26.83	27.00
24.50	26.80	27.01
24.25	26.77	27.02
24.00	26.74	27.01
23.75	26.71	27.01
23.50	26.70	27.01
23.25	26.68	26.97
23.00	26.66	26.89
22.75	26.62	26.86
22.50	26.55	26.83
22.25	26.48	26.82
22.00	26.38	26.76
21.75	26.29	26.72
21.50	26.20	26.65
21.25	26.12	26.57
21.00	25.99	26.48
20.75	25.84	26.40
20.50	25.67	26.31
20.25	25.41	26.19
20.00	24.94	26.14
19.75	24.67	26.07
19.50	24.28	25.90
19.25	23.89	25.71
19.00	23.46	25.39
18.75	22.77	24.88
18.50	20.68	24.53
18.25	19.30	23.73
18.00	18.52	23.50

17.75	17.55	22.71
17.50	15.97	21.75
17.25	15.83	21.55
17.00	15.83	21.30
16.75	15.83	20.27
16.50	15.83	19.18
16.25	15.83	18.25
16.00	15.69	17.45
15.75	15.38	17.16
15.50	15.27	17.13
15.25	15.26	17.11
15.00	15.25	16.75
14.75	15.24	16.62
14.50	15.23	16.60
14.25	15.22	16.67
14.00	15.28	16.73
13.75	15.24	16.67
13.50	15.12	16.59
13.25	15.04	16.39
13.00	14.93	16.07
12.75	14.90	16.13
12.50	14.80	16.15
12.25	14.67	16.06
12.00	14.54	15.90
11.75	14.33	15.84
11.50	14.28	15.80
11.25	14.20	15.65
11.00	14.08	15.42
10.75	13.95	15.42
10.50	13.76	15.40
10.25	13.51	15.38
10.00	13.45	15.25
9.75	13.43	15.08
9.50	13.41	14.96
9.25	13.37	14.88
9.00	13.26	14.80
8.75	12.75	14.70
8.50	12.41	14.26
8.25	12.10	14.11
8.00	12.07	14.02
7.75	12.14	13.92
7.50	12.22	13.82
7.25	12.06	13.93
7.00	11.76	13.93
6.75	11.66	13.86
6.50	11.68	13.79
6.25	11.35	13.74
6.00	11.15	13.65
5.75	11.04	13.36

5.50	10.93	13.09
5.25	10.82	13.11
5.00	10.69	13.14
4.75	10.30	13.12
4.50	10.04	13.00
4.25	9.81	12.69
4.00	9.57	12.34
3.75	9.34	12.15
3.50	9.11	11.93
3.25	8.89	11.68
3.00	8.68	11.38
2.75	8.58	11.20
2.50	8.40	11.09
2.25	8.22	10.99
2.00	7.96	10.88
1.75	7.68	10.80
1.50	7.40	10.68
1.25	7.11	10.49
1.00	6.82	10.38
0.75	6.54	10.24
0.50	6.55	10.08
0.25	6.56	9.87
0.00	6.44	9.49
-0.25	6.25	8.80
-0.50	6.07	8.59
-0.75	5.86	8.38
-1.00	5.54	8.16
-1.25	5.35	7.89
-1.50	5.15	7.53
-1.75	4.87	7.17
-2.00	4.59	6.97
-2.25	4.35	6.59
-2.50	4.22	5.70
-2.75	3.95	5.44
-3.00	3.68	5.25
-3.25	3.49	5.18
-3.50	3.32	5.10
-3.75	3.21	4.96
-4.00	2.96	4.78
-4.25	2.43	4.60
-4.50	2.19	4.42
-4.75	2.10	4.19
-5.00	1.89	4.07
-5.25	1.72	3.84
-5.50	1.47	3.64
-5.75	1.25	3.43
-6.00	1.07	3.02
-6.25	0.99	2.61
-6.50	0.74	2.41

-6.75	0.59	2.20
-7.00	0.43	1.99
-7.25	0.24	1.77
-7.50	-0.30	1.48
-7.75	-0.53	1.25
-8.00	-0.71	1.19
-8.25	-1.15	1.11
-8.50	-1.61	1.02
-8.75	-1.76	0.86
-9.00	-1.89	0.63
-9.25	-2.16	0.40
-9.50	-2.38	0.05
-9.75	-2.62	-0.20
-10.00	-2.85	-0.57
-10.25	-3.29	-0.95
-10.50	-3.61	-1.16
-10.75	-3.81	-1.45
-11.00	-4.01	-1.75
-11.25	-4.56	-2.08
-11.50	-5.17	-2.66
-11.75	-5.51	-2.97
-12.00	-6.20	-3.13
-12.25	-6.39	-3.31
-12.50	-6.57	-3.68
-12.75	-6.89	-3.90
-13.00	-7.22	-4.09
-13.25	-7.39	-4.27
-13.50	-7.70	-4.45
-13.75	-8.01	-4.74
-14.00	-8.38	-5.55
-14.25	-8.77	-6.39
-14.50	-9.13	-6.66
-14.75	-9.49	-6.84
-15.00	-9.74	-6.93
-15.25	-10.11	-8.07
-15.50	-10.50	-8.34
-15.75	-10.80	-8.95
-16.00	-11.20	-9.13
-16.25	-11.72	-9.25
-16.50	-12.34	-9.47
-16.75	-12.95	-9.72
-17.00	-13.27	-10.16
-17.25	-13.56	-10.37
-17.50	-13.82	-10.70
-17.75	-14.00	-10.78
-18.00	-14.19	-10.80
-18.25	-14.42	-12.29
-18.50	-14.77	-13.04
-18.75	-15.07	-13.30

-19.00	-15.41	-13.76
-19.25	-15.74	-14.09
-19.50	-16.08	-14.53
-19.75	-16.72	-14.99
-20.00	-17.23	-15.22
-20.25	-17.50	-15.44
-20.50	-17.52	-15.69
-20.75	-17.41	-15.94
-21.00	-17.56	-16.34
-21.25	N/A	-16.79
-21.50	N/A	-17.06
-21.75	N/A	-17.49